Supercapacitor-Assisted Temperature Modification Apparatus (SCATMA) and Fast Supercapacitor Charger

A thesis

submitted in fulfilment

of the requirements for the degree

of

Doctor of Philosophy

in Electronics Engineering

at

The University of Waikato

by

Nicoloy Gurusinghe

THE UNIVERSITY OF
WAIKATO
Te Whare Wānanga o Waikato

2016

Abstract

This thesis presents the design and development of the supercapacitor-assisted "instant" water heating system as well as a new power converter topology to fast charge a supercapacitor bank.

Delayed delivery of hot water in domestic water heating systems wastes over 15 million cubic metres of treated water per annum in New Zealand. The patent pending supercapacitor assisted temperature modification apparatus (SCATMA), solves this problem by using pre-stored supercapacitor energy. These supercapacitors deliver short-term high-power bursts into heater coils placed in the final half meter of pipe connecting the faucet. During a period of less than a minute, 100–200 Wh of energy is released to the heater coil at a rate between 10–20 kW.

Based on the cost constraints of a commercial system and the regulatory authority requirements, a supercapacitor-only solution becomes prohibitively expensive. A review of current state-of-the-art energy storage systems show that no battery chemistry can withstand the associated charge-discharge cycles to reach the expected service life of 5–10 years. While developing the unique two-stage fast supercapacitor charger, a battery-supercapacitor hybrid system was developed for SCATMA as a commercially viable solution for rapid water heating.

Dividing a supercapacitor bank into three parts and circulating them through a 'charge-idle-discharge' sequence was already investigated for the surge resistant uninterrupted power supply. The effectiveness of this technique mandates fast supercapacitor charging. The proposed new charger achieves fast charging by using a high voltage source to overcome the five time constant charging time and a series coupled inductor to charge the capacitor bank by dividing it into two parts. One part is charged using an over-voltaged dc source with capacitor bank terminal voltage monitoring and the other part is charged by the coupled-inductor using the energy stored in the inductor.

This topology is specifically developed for applications with limited energy requirements. Design procedure and results for a 600 W, 2 Wh charger is presented to illustrate the fast charging ability, the inherent power factor correction capability and the scalability of the topology.

Preface

This thesis is submitted in partial fulfilment of the requirements for obtaining the PhD degree at the University of Waikato, New Zealand, power electronics group. The work was carried out during the period from March 2013 until January 2016 and was supervised by A Prof Nihal Kularatna, A Prof Alistair steyn-Ross and A Prof Howell Round. This work was supported by Rinnai New Zealand Ltd through the Ministry of business and innovation grant: "Localised Water Heating".

Listed below are the publications made as part of this project i.e. conference papers, journal papers and patent application. Excluding (1) all the rest is original contributions by the author during the PhD.

(1) N. Kularatna, Fluid temperature modification apparatus,"WO2014/189389 A1, International Patent application PCT/NZ2014/000092.

(2) N. Kularatna, A. Gattuso, N. Gurusinghe, T. Jayasuriya, J. Du Toit, "Pre-stored supercapacitor energy as a solution for burst energy requirements in domestic in-line fast water heating systems, in Proc of IECON 2014,USA, Nov. IEEE, 2014.

(3) N. Gurusinghe, N. Kularatna, D. A. Steyn-Ross, "Essential Physics for "instantaneous" delivery of hot water: SCATMA," in Proc of NZIP 2015, NZ, Jul, 2015.

(4) N. Gurusinghe, N. Kularatna, S. A. Charleston and J. Fernando, "System implementation aspects of supercapacitor based fast in-line water heating system," 2015 IEEE 24th International Symposium on Industrial Electronics (ISIE), Buzios, 2015, pp. 1313-1317.

(5) N. Gurusinghe, N. Kularatna, S. A. Charleston, W. H. Round and J. Fernando, "Hybridisation techniques in Supercapacitor Assisted Temperature Modification Apparatus for inline water heating," in Proc of IECON 2015, JAPAN, Nov. IEEE, 2015.

(6) N. Gurusinghe, N. Kularatna, W. H. Round and D. A. Steyn-Ross "Design approaches for fast supercapacitor chargers for applications like SCATMA, SRUPS in Proc of APEC 2016, USA, Mar. IEEE, 2016.

(7) N. Kularatna, N. Gurusinghe, "Electrical energy charging apparatus," New Zealand Patent application P31578NZ00.

(8) N. Gurusinghe, N. Kularatna, W. H. Round and D. A. Steyn-Ross "Single-stage fast supercapacitor charger with inherent power factor correction for energy limited applications in Proc of IECON 2016, Italy, Sep. IEEE, 2016.

(9) N. Gurusinghe, N. Kularatna, W. H. Round, D. A. Steyn-Ross, "Energy-limited transient-mode fast supercapacitor charger topology," in IEEE Transactions on Power Electronics , vol.PP, no.99, pp.1-1

(10) N. Gurusinghe, N. Kularatna, W. H. Round and D. A. Steyn-Ross "Supercapacitor based special applications leading to the development of a fast supercapacitor charger" to be submitted to IEEE emerging and selected topics in power electronics.

.

Acknowledgements

I wish to acknowledge the support received from all of those who stood by me and helped me throughout this project.

To my supervisory panel

- A Prof Nihal Kularatna
- A Prof Alistair Steyn-Ross
- A Prof Howell Round

My special thanks and appreciation goes to:

- Dr Chi Kit Au
- Prof Jonathan B. Scott

Contents

List of Figures

List of Tables

Acronyms and Abbreviations

ac	alternating current
dc	direct current
DoD	depth of discharge
EMI	electromagnetic interference
ESR	equivalent series resistance
MOSFET	metal-oxide-semiconductor field-effect transistor
PFC	power factor correction
PWM	pulse width modulation
rms	root-mean square
SC	supercapacitor
SCAHDI	supercapacitor-assisted high density inverter
SCALDO	supercapacitor-assisted low-dropout regulator
SCASA	supercapacitor-assisted surge absorber
SCATMA	supercapacitor-assisted temperature modification apparatus
SoC	state of charge
SRUPS	surge resistant uninterrupted power supply
UPS	uninterrupted power supply

Chapter 1

"Instantaneous" Water Heating

1.1 Scope

The scope of this thesis is to present the results obtained in the PhD project "SCATMA and supercapacitor-fast charger" undertaken by the author from March 2013 to January 2016. Most of the scientific findings of this project have been published in the form of peer reviewed conferences and a patent application. The objective of this thesis is to supplement the already published materials by placing them in the context of the overall project to present a complete overview of the work and results obtained.

1.2 Background and Motivation

The power electronic research group at the University of Waikato, New Zealand, is interested in non-traditional applications of supercapacitors (SCs). The inventions developed by this group include

- SCALDO - SC-assisted low-dropout regulator - a high efficient dc–dc converter technique using low dropout regulators [1–3]
- SCASA - SC-assisted surge absorber - a technique developed to absorb power-line surges using SCs [4, 5]
- SRUPS - surge resistant uninterrupted power supply - a batteryless uninterrupted power supply (UPS) technique capable of absorbing power line surges [6]
- SCATMA - SC-assisted temperature modification apparatus - an "instant" liquid flow heating technique based on stored energy [7]
- SCAHDI - SC-assisted high density inverter - a SC technique to improve efficiency and packing density of a high power inverter [8]

SCALDO and SCASA are covered under granted patents [1] and [4] respectively. The initial SCATMA concept was developed in late 2012. This thesis documents the proof-of-concept prototype developed for Rinnai New Zealand Ltd as well as the proposal to improve the value of the product by fast-charging the capacitors using a technique initially introduced for the SRUPS.

1.3 Water Heating Systems

Water heating systems come in two basic types: storage and instantaneous (continuous) flow systems. A variety of energy sources can be used such as electric, gas, solar or wood. All energy sources can be used for hot-water tanks. Following are several storage tank water heating systems used in New Zealand.

- electric hot water cylinders
  An electric element immersed in an insulated water tank heats the stored water. A thermostat is used to set the desired hot-water temperature. Electric hot water cylinders have the cheapest upfront cost but relatively high running cost unless a cheaper night-rate tariff is used. A cylinder big enough to store a days water is required when switching to night rate tariff.
- gas hot water cylinders
  Water stored in a tank is heated by a gas element. For safety reasons a gas hot water cylinder can not be wrapped by an insulation as that could obstruct the air flow and extinguish the flame. Hence the losses are high and relatively expensive to run.
- wetbacks
  A wetback can be used in a house where a wood fire is used for space heating. Wetbacks are generally a supplement to the main water heating system. Wetbacks should be place relatively close to the central hot water cylinder because the natural water circulation through the water jackets by the thermo-siphon effect (hot water rising) has a maximum operation distance.
- solar water heating
  Solar thermal collector panels placed on the roof absorb energy from the sun and transfers that energy to the water stored in the hot water cylinder. During less sunny seasons a boost from electric, gas or wetback is required.
- heat pump water heaters
  Heat pumps use energy from the outdoor air to heat water stored in a storage cylinder. A refrigerant liquid at high pressure absorbs heat from air and evaporates. An electric compressor compresses this refrigerant releasing heat to water. Electricity is used as a means to move heat from air to water. Hence a heat pump water heater is much more efficient than a traditional electric or gas water heater.

Storage water heaters maintain water at a pre-set temperature for use when it is required. Storage tanks are insulated to minimize heat losses. Instantaneous flow systems heat water as it is used, instead of continuously heating a full tank. Hence there is no need for any storage tanks and the losses associated with storage tanks are eliminated. An instantaneous system can run from either electricity or gas.Due to cold water stored in the pipes continuous flow systems tend to waste more water than other types while the

user waits for the water to get hot. This water wastage is important to people on tank water supply or metered water. To address this problem of delayed delivery of hot water most manufacturers slow down the water flow rate to allow enough time for the water to get heated in the heating chamber. As a result a continuous system will supply hot water at a lower pressure than a storage system.

1.4 “Instantaneous” Water Heating Problem

Delayed hot water delivery in domestic water heating systems is a worldwide problem. A typical domestic hot water system will have a delay of around 5–30 s on average depending on the distance of the tap from the central water heater. As a result, cold water stored in buried pipes can waste 0.5–4 L of water each time the hot tap is turned on. Assuming a hot-water tap is used 10 times a day in an average household, there will be an estimated loss of 15000 L annually per house. In New Zealand, this corresponds to over 15 million cubic metres of treated water wasted per year.

There are a few commercial solutions proposed to address this problem. These solutions include

- Under-the-sink tanks [9]
  Under-sink tanks are an alternative option, but they require a mini-tank installed under the sink and a mixer-tap. Hence the solution is expensive and requires regular maintenance. Since the tank maintains the water at a preset temperature regardless of the water at a preset temperature regardless of the water usage, a tank system has poor energy efficiency
- Recirculation systems [10]
  Recirculation system is made up of a closed loop that connects to each hot water usage point, and a pump for recirculating water. These systems cannot be easily retrofitted and the running costs are high.
- Tank-less systems [11–14]
  The tank-less system heats water as it passes through the unit. These systems are also known as point-of-use on-demand systems. This option saves energy as only the water used is heated. However, it requires replacement of the existing mixer-tap and heating system. Further dedicated high current sub circuits need to be wired.

The tank-less system heats water as it passes through the unit. These solutions reduce or eliminate heating delay, but cost several thousand dollars, occupy space and require modifications to plumbing. Hence they are neither convenient nor economical. Under-the-sink tanks and recirculating systems run direct from standard 2.5-kW socket outlet. Since these systems store heated water in some form of a tank at a pre-set temperature, efficiency is low. The heat dissipated by the tank has to be provided by the heater

Table 1.1: Seisco tank-less point-of-use systems performance comparison

Power (kW)	Breaker (A)	Temperature rise (°C) at litres/min 4	6	8
7	30	27	18	14
9	40	34	23	17
14	60/30×2	53	36	27

Table 1.2: Commercial tank-less point-of-use water heater specifications, size and price comparison based on amazon.com

Manufacturer	Model	Power (kW)	Price NZD	Size (mm)
Steibel Eltron tankless point-of-use	mini 6	5.7	260	165×190×85
Seisco supercharger	SC90	9	450	240×190×380
Seisco supercharger	SC140	14	650	240×190×380
Rheem tankless electric water heater	RTE 18	18	700	265×285×85
Rheem tankless electric water heater	RTE 27	27	1040	265×285×85

coils, hence running costs are high. Where as in point-of-use on-demand systems running losses are eliminated. But the downside is the additional dedicated electrical installation. Table 1.2 compares several options available from famous manufacturers and their price range. The market research done by Waikato Link Ltd. showed that the best price for a new "instant" water heater to enter into the NZ market is 400–500 NZD. Table 1.1 summarises the performance of such systems by the American manufacturer Seisco [12]. Figure 1.1 shows how such a system is installed under a bathroom wash basin. These systems can be used as boosters to a whole house tank less or tanked water heating systems or remote application to a cluster of fixtures with considerable delayed hot water delivery. To eliminate the cold water sandwiching effect in low flow draws from airplane, boat or ship lavatory faucets and high efficiency dishwashers. The main drawback of tank-less point-of-use systems is that they require dedicated high-power circuits and at the point of starting of operation, power flickers and other power quality issues may arise. The proposed solution based on SCs will meet similar performances in terms of water flow rate and output water temperature with the installation of a unit with similar volume to the above described commercial units. The main advantage is that by the use of pre-stored energy the new proposed system will overcome the need of dedicated high power circuits. A standard 10 A socket outlet power capability will be sufficient.

Figure 1.1: Wash basin fitted with a Seisco tank-less point-of-use water heater.

1.4.1 Typical Scenario

Since a central water heating system takes 2–4 s to sense and start pumping hot water, the tap will receive that hot water after 5–30 s depending on the proximity of the tap to the central water heater. Therefore the worst-case energy requirement would be to raise the water temperature for 30 s. The total energy required to raise the water temperature by 30°C for 30 s is 504 kJ (140 Wh) at a flow rate of 8 Lmin^{-1}. This energy is equal to the energy required to boil 1.2 L of still water or the energy required to drive an average electric car for 1 km [15]. On the other hand this energy requirement translates to a small annual cost of $\$160$ for an average household, based on the above mentioned hot water tap usage and electrical tariff of $\$0.29$ /kWh .

Though the required energy is manageable, the challenge is the required power. From the above calculations if 150 Wh energy is to be transferred within 30 s it will require an energy delivery at a massive power rating of 18 kW. Therefore the source should be capable of supplying this required power. However, a domestic power supply's maximum capability will be 230 V at 30 A (single phase), and each individual subcircuit would be protected by a 10 A over-current protection device, giving a maximum power delivery capability of 2.3 kW [16].

1.4.2 Requirements

The above power and energy requirement is estimated for the worst case. It indicates that if the required energy is stored in a suitable storage device, then it can be converted into a short-term high-power delivery at the required rate into flowing water, without any additional water tanks, circulation systems or pumps. However, several primary requirements as listed below are essential if such a system is to be acceptable to regulatory authorities.

- Electrical safety and isolation
  Due to safety concerns, a power source over 60 V cannot be utilized because of the low voltage requirements to prevent electrical shock. If mains power is used directly, galvanic isolation via a transformer supplying less than 60 V (rms) may be required as the high-power heater coil is directly in contact with the flowing water [17].
- Domestic installation regulations
  Domestic subcircuits are protected using overcurrent protection devices [16]. The maximum power rating for a domestic subcircuit will be 6.9 kW even if a 30 A dedicated sub-circuit is available. Therefore it is impractical for an existing electrical subcircuit to solely deliver this power.

Due to the above mentioned reasons, if a power level of 18 kW is to be maintained from a source rated at a maximum of 60 V, an average output current of 300 A should flow in the circuit.

1.5 SCATMA Technique

Supercapacitor-assisted temperature modification apparatus (SCATMA), is a patent-pending system developed at the University of Waikato, to overcome the delay of delivery of hot water at water faucets. This system is capable of providing a short-term high-power burst into an in-line heater coil to overcome the delayed delivery of hot water. Therefore, rather than being limited by the maximum power capability of the mains power source, using pre-stored energy the high power demand can be met.

Fundamentally the design is a form of electric kettle whose heating coil extends into a heating element embedded inside the final half-metre of pipe connecting to the sink tap. When comparing an electric kettle with SCATMA, the amount of energy associated is similar but the required power rating can be drastically different based on the duration of the transfer process. Thus the power required to heat a constant flow of water is significantly higher than the power required to obtain the same temperature rise on an equal volume of stationary water in a container within a longer duration. This mandates a form of energy storage to permit short-term delivery of high-output power into a moving fluid. As seen in Table 1.3, the power required for “instantaneous” water heating is beyond

Table 1.3: Typical domestic "instant"-water heating problem specifications

Parameters	minimum	average	maximum
Water flow rate (litres/min)	4	6	8
Delay in centrally heated hot water (s)	5	15	30
Required temperature rise ($^{\circ}C$)	20	30	40
Required energy (Wh)	7.8	52.5	186.7
Required power (kW)	5.6	12.6	22.4

the capability of 230 V/ 10 A socket outlet. To supply this power without violating any of the above mentioned conditions on safety and domestic installation regulations, a solution based on pre-stored energy is required. The simple electrical concept underlying using pre-stored energy for SCATMA is the capability of a voltage source to supply its maximum output power when the load resistance is equal to the source internal resistance. When this condition is satisfied an equal amount of energy is dissipated in the source internal resistance as in the useful load. Therefore by selecting a source which has sufficiently low internal resistance a high power can be delivered to a load with a low loss.

The available energy storage options include electrochemical batteries and SCs. Batteries have high energy density but low power density, while the converse is true for SCs. When selecting an energy storage medium for a fixed-energy high-power requirement such as SCATMA, the following are the major considerations:

- The volume of the stored energy, maximum power capability vs cost per joule
  The source should have a high energy density to be able to fit into the volume available under a kitchen sink, and a high power density to be able to deliver high currents. Neither SCs nor any electrochemical battery chemistry has both high energy density and high power density. On the other hand, when comparing costs, SC energy is more expensive than batteries. One can consider a hybrid system, but because this application has a high peak-to-average power ratio, most automobile hybridization techniques will not work.
- The allowed discharge depth, rate of discharge vs cycle life of the source.
  The ability to deep discharge for high number of cycles will increase the life-time of the energy storage medium. Further, the storage media should be capable of handling high-discharge currents (C-rating) while being deeply discharged without premature performance degradation.

SC's high power density and high maximum cycle count are advantageous for an appplication like SCATMA as seen in Table 1.4. Only SCs have the sufficient discharge times, high output power capability and cycle life capable of powering an instant heater for the expected service life of 10 years. In Chapter 2 the fundamental differences between

Table 1.4: Energy storage devices comparison

Energy storage device	Energy density Wh/L	Power density W/L	Cycle life # cycles	Time constant
Conventional batteries	50–250	150	200–10^3	>1 hour
Conventional capacitors	0.05–5	10^5–10^8	10^5–10^6	<1 ms
Supercapacitors	5–10	10^4–10^5	10^6–10^8	1–5 s

electrochemical and capacitive energy storage are discussed in the light of this application which requires simultaneous high energy and high power: several hundred watt-hours delivered at rate of 10 to 20 kW.

In comparing these energy storage devices, initial tests were carried out to compare the performance of SCs with batteries and high-power transformers with different heating elements and different water flow-rates. This shows SCs are capable of handling the requirements of SCATMA but the low energy density and the present SC price mean that SCs are not the best candidate at this time. An assessment of energy storage media performance and price shows that though SC energy ($/kWh) is expensive, their power ($/kW) is cheap. This opens options for hybridization with cheap batteries: SCs will deliver high currents while the batteries will deliver the continuous average current. After testing and simulating several hard-wired hybrid options, a prototype was made with a series SC lead-acid battery combination. Details of this hybridization technique and results obtained from the prototype design are presented in Chapter 3. This system gives usable but not optimal results, indicating room for improvement.

1.6 Bank Circulation Technique

A typical "instantaneous" water heating system is required to provide high power to a heating element in a 30 s burst, then wait for at least 15 min before having to do this again. During the 15 min duration the energy storage will be replenished at low power as illustrated in Fig. 1.2.

As SCs have a low equivalent series resistance (ESR), they are capable of providing high currents and thus can power a heating coil of a high power rating. But while they have a high capacitance, they do not store very large amounts of energy. So a very large bank of SCs will be required to store the required energy. This would be prohibitively expensive. Therefore as an alternative, a circulating SC bank of smaller capacitor banks as in the Fig. 1.3 is suggested.

Here, at any one time only one of the banks is supplying current to the heater (the load) while another is being recharged. The others are fully charged and are waiting to supply current to the load. When the capacitor that is supplying current is discharged,

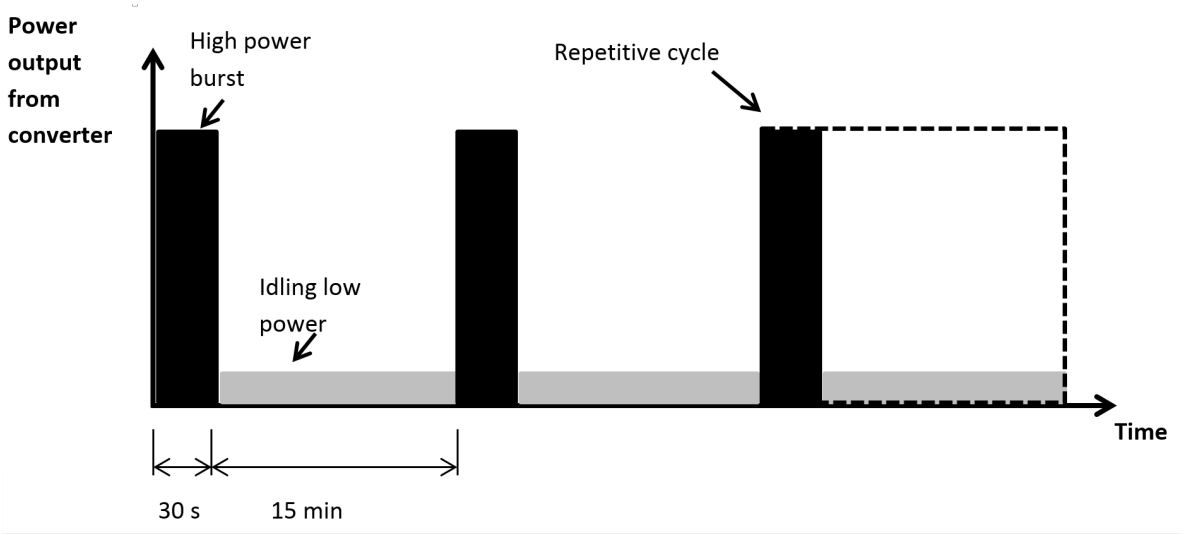

Figure 1.2: The power cycle of SCATMA. It provides a 30 s high-power burst of energy to the heater from a combination of stored energy and energy it extracts from the mains supply through the fast charger. Then over the next 15 minutes, the system is recharged at low power.

the next capacitor is switched in to power the heater and the discharged capacitor is then recharged. To provide the charging current, a fast-charger needs to be developed that

- can provide high power over a short period
- is able to extract as much energy as possible from the mains supply, which will mean over-rating the supply for short periods
- has a low idling power for the 15 min slow recharging

Fig. 1.4 demonstrates how the stored energy is delivered to the load, and the charging and discharging of the capacitor banks in 5 s intervals for an exemplar storage system consisting of three capacitor banks.

This system will not pre-store the total amount of energy required for the application. The remainder of the energy is extracted through the capacitor charger during the 30 s operating interval. Thus it is necessary to recharge the capacitors at high power for a period of time to enable the heater to be further supplied with energy. Recharging the capacitors sufficiently fast is challenging as the high capacitance can lead to long re-charging times. To overcome this, it is anticipated that charging will be done using a much higher voltage than the rated voltage of the capacitor, but for a very short time to avoid damaging the capacitor.

1.7 Fast Capacitor Charger

For the above-mentioned bank-circulation principle to be effective in reducing the amount of pre-stored energy, the capacitor charger should be capable of delivering a significant amount of energy within the high-power burst period of 30 s to 1 min. Compared to a

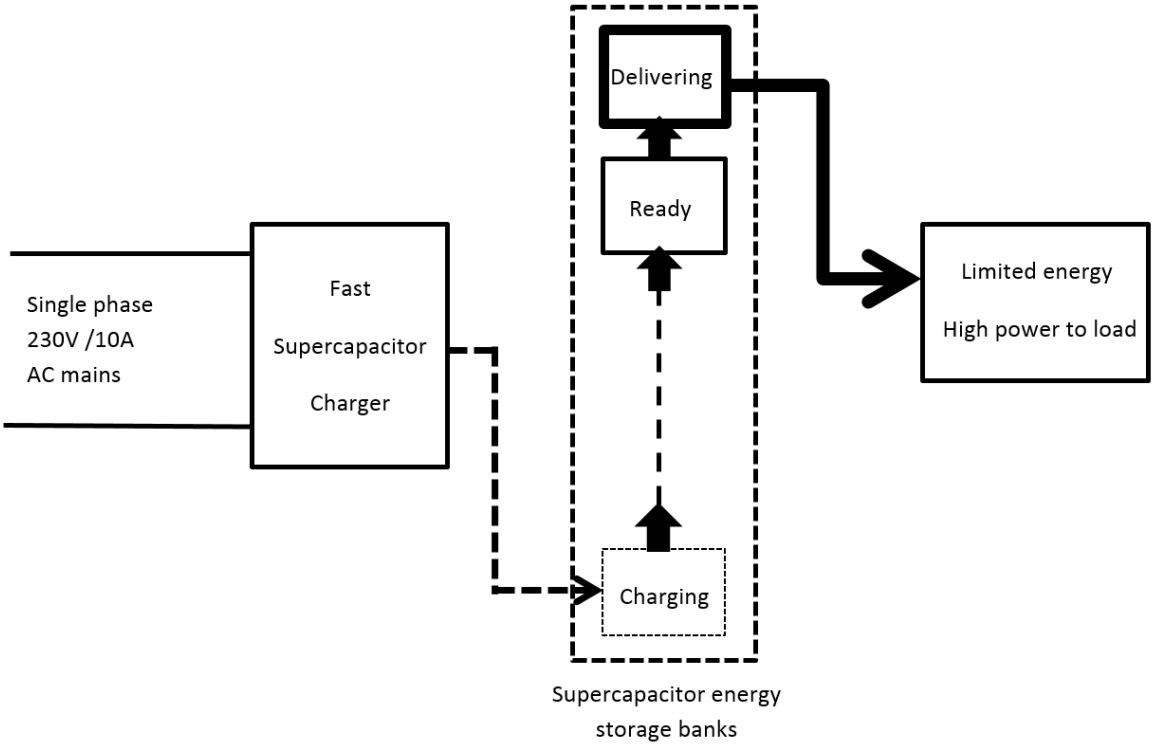

Figure 1.3: Bank circulation technique for limited energy high power applications

battery with an electrochemical potential opposing the charging voltage, a completely depleted SC bank takes five time constants (approximately) to get "fully" charged from an ideal voltage source. The time constant is created by the capacitance and the total loop resistance. To charge a capacitor in five time constants the source should be capable of delivering the maximum current required by the system. In the case of a current source, the total time to charge a capacitor linearly decreases as the current increases. In either case, fast charging requires a high-current-capable source. In comparison to a dc source powering a resistive load continuously, a SC charger can be specified by the maximum charge or energy required by the SC bank. The proposed charger topology is developed for special applications such as SCATMA and SRUPS where fast SC replenishing is paramount. The two major concepts used in this technique are as follows.

- Charging will be done using a much higher voltage than the rated voltage of the SC bank; a terminal voltage monitor coupled to a switch will avoid damaging the capacitor by over-charging.
- When charging a capacitor through a high-voltage charger, the circuit current will not reach zero even when the capacitor reaches its full-charge voltage. Therefore if an inductor is inserted into the charging path, when the capacitor current is extinguished (by the voltage monitoring switch), when the capacitor voltage reaches its rated value there will be energy stored in the series inductor. This inductive energy can be used to charge a secondary capacitor.

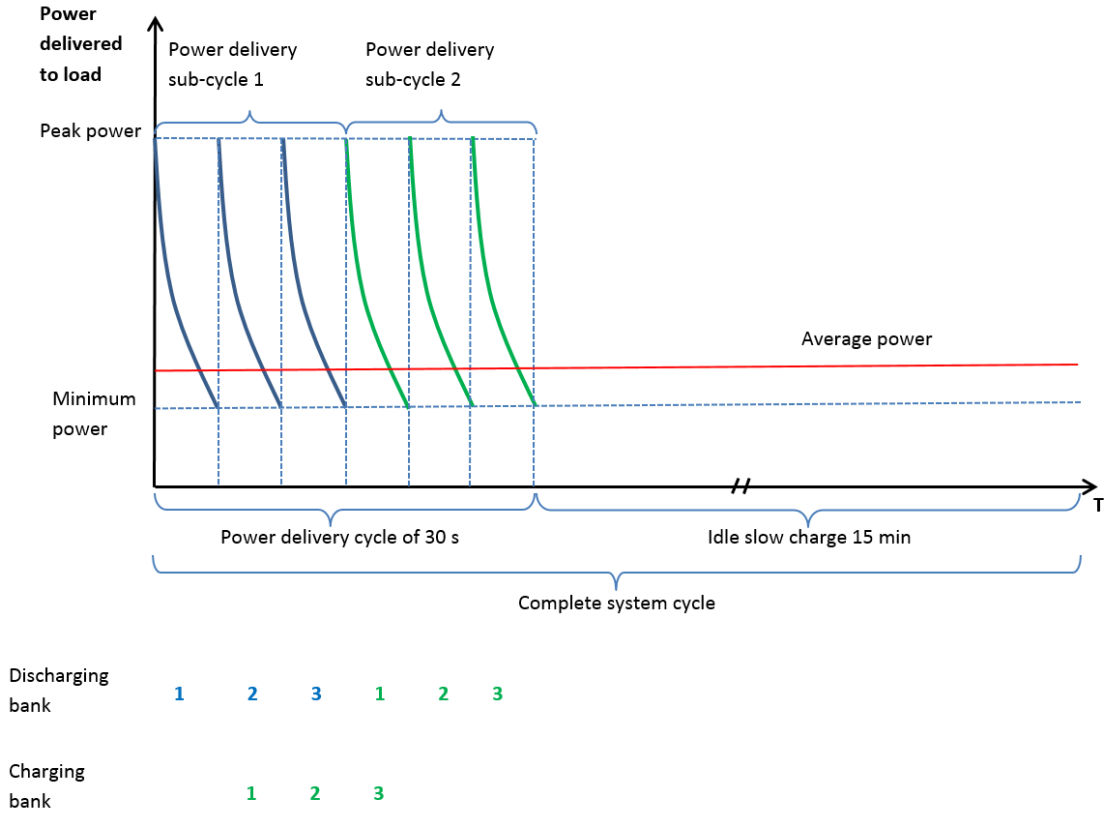

Figure 1.4: Energy delivery to the load and the charging and the discharging of the capacitor banks

1.8 Thesis Structure and Content

The PhD project overview is shown in Fig. 1.5. The structure, organization and content of this PhD thesis is visualized in the flow chart presented in Fig. 1.6.

The published conference papers, journal papers and the patent application cover a broad range of the work performed in this PhD study. Since most of the experimental results are already included in the published material, chapters are organised in such a way to give a step-by-step analysis of the design procedure and how each chapter fits into the "instant" water heating project. The main two parts of the thesis include the SCATMA technique in Chapters 1, 2 and 3, and the fast charger for SCATMA in Chapters 4, 5 and 6. This thesis reflects the same approach adopted for the project, i.e., definition of the objective ⇒ state-of-the-art analysis ⇒ simple fundamental design concept ⇒ initial testing ⇒ detailed design analysis ⇒ prototype design. The intention of this presentation is to present the key engineering concepts involved in the design in a straightforward manner.

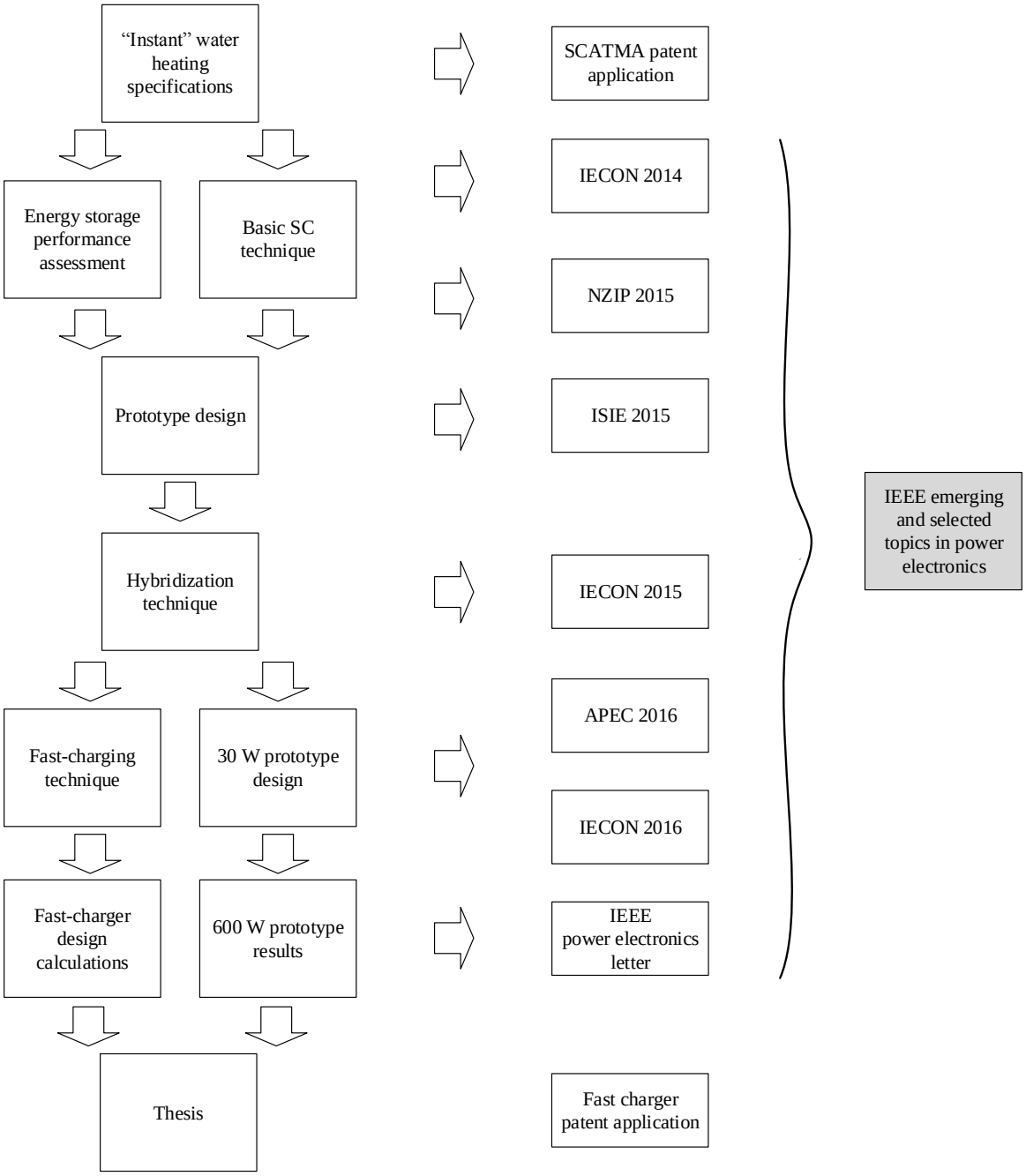

Figure 1.5: PhD project overview of milestones and achievements. Shaded box is the publications still in review.

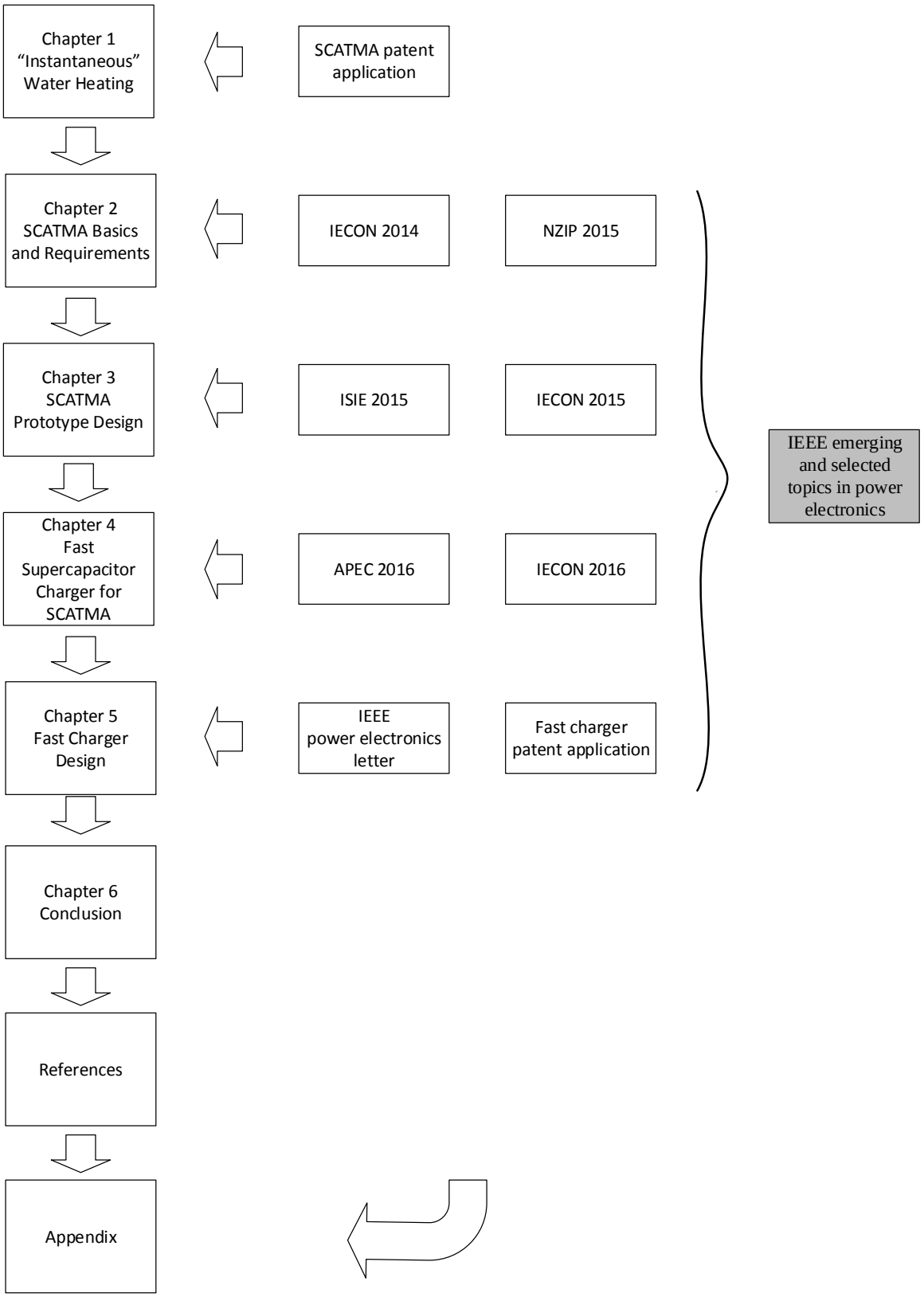

Figure 1.6: PhD thesis structure

Chapter 2

SCATMA Basics and Requirements

This chapter presents the instant water heating problem, the SCATMA solution and the main concerns in selecting an energy storage medium for this application.

2.1 Heating Still and Flowing Water

The amount of energy E [in J] required to raise the temperature of l litres of water inside a perfectly insulated container by $\Delta\theta$ [°C] is

$$E \;=\; \rho l C \Delta\theta \tag{2.1}$$

where ρ is the density of water [$\mathrm{kg\,L^{-1}}$], C is the specific heat capacity of water [$\mathrm{J\,kg^{-1}\,{}^{\circ}C^{-1}}$]. If the temperature rise $\Delta\theta$ is to occur within time ΔT, the required average heating power P can be calculated as

$$P \;=\; \frac{E}{\Delta T} \;=\; \frac{\rho l C \Delta\theta}{\Delta t} \tag{2.2}$$

where no losses are assumed at the source or in the power transfer path. Inserting Eq.(2.1) gives

$$P \;=\; \frac{l}{\Delta t}\rho C \Delta\theta \;=\; Q \rho C \Delta\theta \tag{2.3}$$

where Q is the water flow rate [$\mathrm{Lmin^{-1}}$]. This equation describes heating a flow of water with 100% heat transfer efficiency at the heating element surface.

2.1.1 Electric Kettle Example

Take the static example of a 230 V, 2.3 kW rated 4-litre electric kettle. It takes 9.7 min to raise the temperature of 4 L of water from 20°C room temperature to 100°C. This result follows from Eq. (2.2),

$$2300\ \mathrm{W} \;=\; \frac{(1\ \mathrm{kg\,L^{-1}})(4200\ \mathrm{J\,kg^{-1}\,{}^{\circ}C^{-1}})(80^{\circ}\mathrm{C})}{\Delta t} \quad\Longrightarrow\quad \Delta t \;=\; 9.74\ \mathrm{min} \tag{2.4}$$

If the same power input is applied to water flowing inside a perfectly insulated tube, then the maximum permissible flow rate for the same temperature rise is 0.41 $\mathrm{L\,min^{-1}}$,

$$2300\ \mathrm{W} \;=\; \left(\frac{4\ \mathrm{L}}{9.74\ \mathrm{min}}\right)\rho C\,(80^{\circ}\mathrm{C}) \quad\Longrightarrow\quad Q \;=\; 0.41\ \mathrm{L\,min^{-1}} \tag{2.5}$$

Table 2.1: Typical domestic delayed hot water problem specifications

Parameter	min	avg	max
Water flow rate (Lmin^{-1})	4	8	12
Delay in centrally heated hot water (s)	15	30	60
Power from the wall socket outlet (kW)	2.3	2.3	2.3
Power transfer efficiency (%)	60	70	80

Similarly if the temperature rise is halved to 40°C then the maximum flow rate for the same heater power would be doubled to 0.81 $\mathrm{L\,min}^{-1}$. If the flow rate needs to be increased ten-fold to 8 Lmin^{-1} for the same 40°C temperature rise, then a ten-fold higher power source of 23 kW is required.

2.2 Specifications of SCATMA

In order to compute the power and energy requirements of SCATMA, it is essential to detail the typical tap usage for a domestic kitchen sink or a bathroom wash-basin as seen in Table. 2.1.

A 30 s water flow at a rate of 8 Lmin^{-1} will deliver 4 L of water. The amount of energy required to raise the temperature of this volume of water by 40° C is half the energy required to boil 4 L of water in an electric kettle assuming 20°C room temperature. But according to Eq. (2.3) the average specifications of an instant water heater mean that a power source of 22.4 kW is required. At an average power transfer efficiency of 75% this requires an input power of 30 kW, whereas a 4 litre kettle will operate from the 2.3 kW mains electrical supply.

Though the required energies are comparable, the rates of energy delivery are very different: the energy delivery periods are 30 s and 9 min respectively for an instant water heater and electric kettle. This makes the power requirement of SCATMA almost 10 times of that of an electric kettle. Due to this extreme power requirement and the regulations for domestic wiring subcircuits which limit maximum power each sub-circuit can handle to 2.3 kW, the "instant" water heating problem cannot be solved with a simple connection to mains electrical power. This makes one think of a solution based on pre-stored energy. For electrical energy storage this could be either electrochemical (battery based), electrostatic (capacitor based) or a hybrid battery-capacitor combination.

2.3 Types of Electrochemical Energy Storage

The two main types of electrochemical energy storage are batteries and capacitors as seen in Fig. 2.1. Primary (non-rechargeable) and secondary (rechargeable) batteries store energy in chemical bonds and release (absorb) energy while discharging (charging) according to the reduction-oxidation equations governing the chemicals involved. Thus batteries require mass transfer for energy storage. Popular battery chemistries include lead-acid (Pb-acid), nickel-cadmium (NiCd) and lithium-ion (Li-ion).

Capacitors store energy electrostatically through charge separation in an electric field. Electrochemical capacitors store energy through ion transfer in the electrolyte solution and the electrode material. Since ions travel back and forth between electrolyte and electrode no mass transfer is involved, hence there is no electrochemical wear-out and performance degradation as found in electrochemical batteries. These non-faradaic energy storage device are most popular in the form of symmetric organic electrolyte capacitors. They are called electric double layer capacitors (EDLC), supercapacitors (SC) or ultracapacitors (UC).

2.3.1 Ragone Plot

Performance of energy storage devices can be compared using their energy storage capability and power delivery capability. Ragone plot [19], named after David V. Ragone as seen in Fig. 2.2 is the most convenient tool for this comparison. This is a plot of specific energy [$\mathrm{W\,h\,kg^{-1}}$] vs specific power [$\mathrm{W\,kg^{-1}}$], alternatively a plot of energy density [$\mathrm{W\,h\,L^{-1}}$] vs power density [$\mathrm{W\,L^{-1}}$]. The first type uses energy and power normalised by weight and the latter uses values normalised by volume. These plots are useful for characterising the trade-off between energy storage capacity and power handling capability of

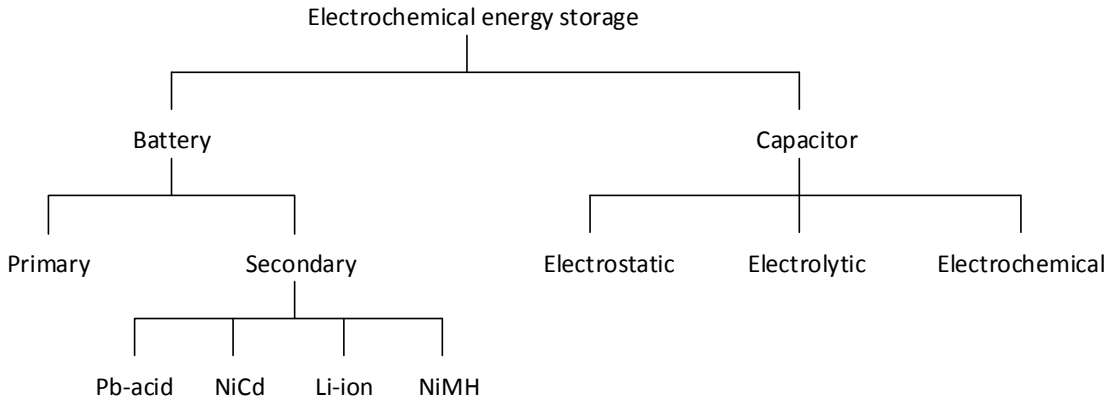

Figure 2.1: Taxonomy of electrochemical energy storage

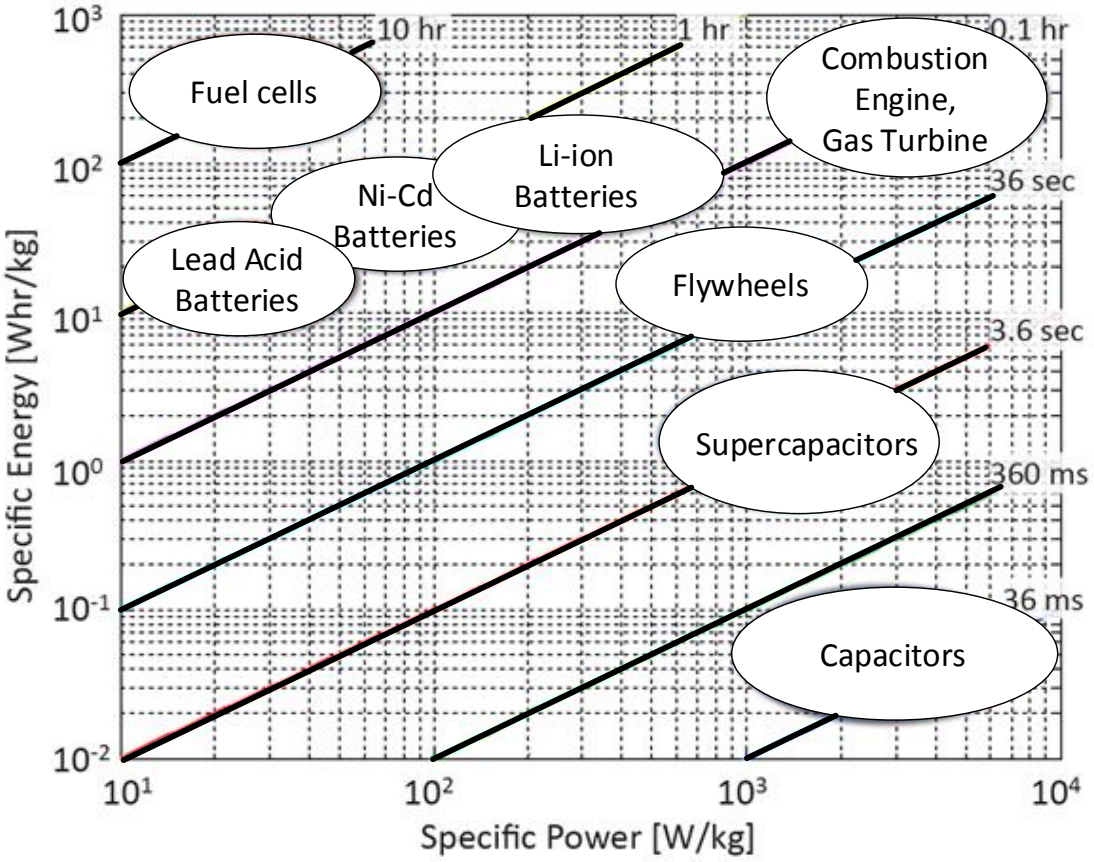

Figure 2.2: Ragone plot of various energy storage/propulsion devices and their "charge" times. Adapted from US Defense Logistics Agency Report [18]

energy storage devices. The vertical axis represents the amount of energy stored and the horizontal axis shows how fast that stored energy can be delivered on to a load.

Conventional capacitors, namely electrolytic, tantalum, mica, ceramic, film capacitors, etc., fit into the lower-right-hand corner of the graph as they cannot store huge amounts of energy per unit volume. They are characterised by the ability to deliver high output currents. Top left hand corner is occupied by all battery chemistries as they store more energy. The main research push in the battery industry is to push these devices diagonally further up this plot achieving high currents and more stored energy.

As seen in Fig. 2.2, ultracapacitors/supercapacitors (SCs) are in the midway between conventional capacitors and batteries. Conventional capacitors are highly power dense and extremely low energy dense, hence they require more volume to store the required energy for a specific application. Therefore conventional batteries would replace conventional capacitors for applications requiring high energy storage, but they lack performance when high discharge currents are required. Since SCs are located between conventional capacitors and batteries, they offer a good compromise in performance and in terms of high output currents and storage capability. This makes SCs an ideal short-term energy

storage option for applications such as wind turbine pitch control systems, vehicle brake energy recovery systems, electric trains, buses and truck traction and starter systems. Further, SCs can be coupled with conventional batteries to deliver extraordinary power and energy performance without having to sacrifice service life. Hybrid electric vehicles and photovoltaic systems are two examples [20].

The sloping lines in Fig. 2.2 indicate the characteristic time constant of these devices. All conventional capacitors have time constants in the milliseconds range whereas all battery chemistries take hours to charge or discharge. This limits the application of each of these extreme devices. SCs at the middle of the graph have seconds-order time constants. They are often used in conjunction with conventional batteries or capacitors to meet the charge/discharge durations of specific applications.

2.3.2 Structure and Significance of Supercapacitors

Though SCs are subject to the electrochemical double-layer effect, their parameters can be adequately approximated using the same equations as all other capacitors [21]. The capacitance (C) of a capacitor is given by,

$$C = \frac{\varepsilon_o \, \varepsilon_r \, A}{d} \tag{2.6}$$

where ε_o is the permittivity of vaccum, ε_r is the relative permittivity of electrolyte, A is the electrode area and d is the distance between the electrodes (the charge separation distance).

SCs have energy storage capability comparable with that of batteries due to the use of porous carbon-based electrodes with typical surface areas between 1 to 2 million $\mathrm{m^2\,kg^{-1}}$ and charge separation distances less than 1 nm. This is achieved through the double-layer construction. These values result in SC capacitances ranging from few farads up to 5000 F. But on the other hand, since the charge separation distance is very small, SC maximum terminal voltages are very low, around 2.7–3.0 V [22, 23].

SCs are electric double layer capacitors: two electrodes immersed in an organic electrolyte separated by a nonconducting layer to separate charges onto each electrode as seen in Fig. 2.3. Since this charge separation process is purely physical (no radox reaction involved), a SC can undergo many more charge-discharge cycles than any other energy storage device, hence they have a high cycle life. Further, this highly reversible physical phenomenon allows for a long shelf life and maintenance-free service life. SCs have a high specific power (cf conventional batteries) and high specific energy (cf conventional capacitors) due to the highly porous activated carbon construction of its electrodes.

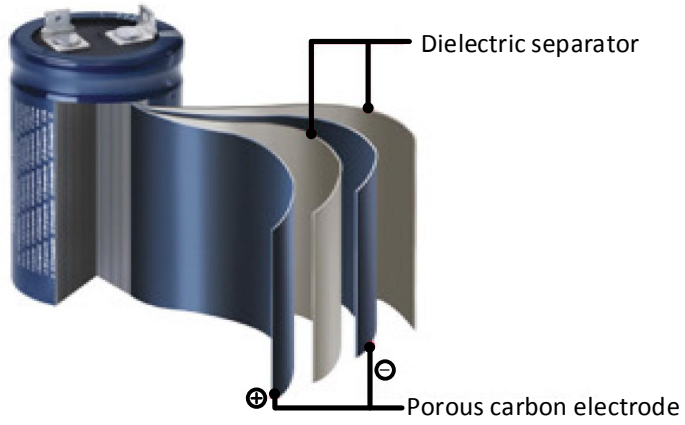

Figure 2.3: Multilayers of a cylindrical LS ultracapacitor

2.3.3 Supercapacitor Equivalent Circuit Models

The behaviour of SCs can be modelled using electric circuit models, mathematical models or non-electric models such as artificial neural networks [24]. Different models have their own advantages and disadvantages. Mathematical models and non-electric models are accurate but do not guarantee an explicit physical meaning in terms of electric circuit components. Electric models are the most convenient form for the electrical engineers for use in simulations. Their performance differs in varying operating conditions, therefore no one model can be used for all operating conditions (e.g., high vs low frequency performance, dc vs surge performance). Hence several more commonly-used electrical equivalent circuit models are discussed below to give an overview.

- **Classical RC model**
  This is the simplest capacitor model. As seen in Fig. 2.4 (a) it has only two components in a single branch. SC ohmic loss is modelled as the equivalent series resistance (ESR) and capacitance (C). The advantage of this model is its simplicity and the primary disadvantage is its inability to model nonlinear characteristics.
- **Parallel branch model**
  This models the SCs nonlinear voltage rise (or fall) observed once charging (or discharging) is stopped. This can be modelled by theoretically large number of parallel RC branches with different time constants. Typical choices of models are two to three branches, depending on the accuracy required, as seen in Fig. 2.4 (b). In a two-branch model, one branch will have a fast response while the other will be slow. This model matches the SCs dynamic behaviour during charge and discharge reflecting changes in internal charge distribution [24].
- **Transmission line model**
  The model of Fig. 2.4 (c) is based on the porous electrode theory developed by de Levie [25]. A transmission line can be used to model a pore in a porous electrode.

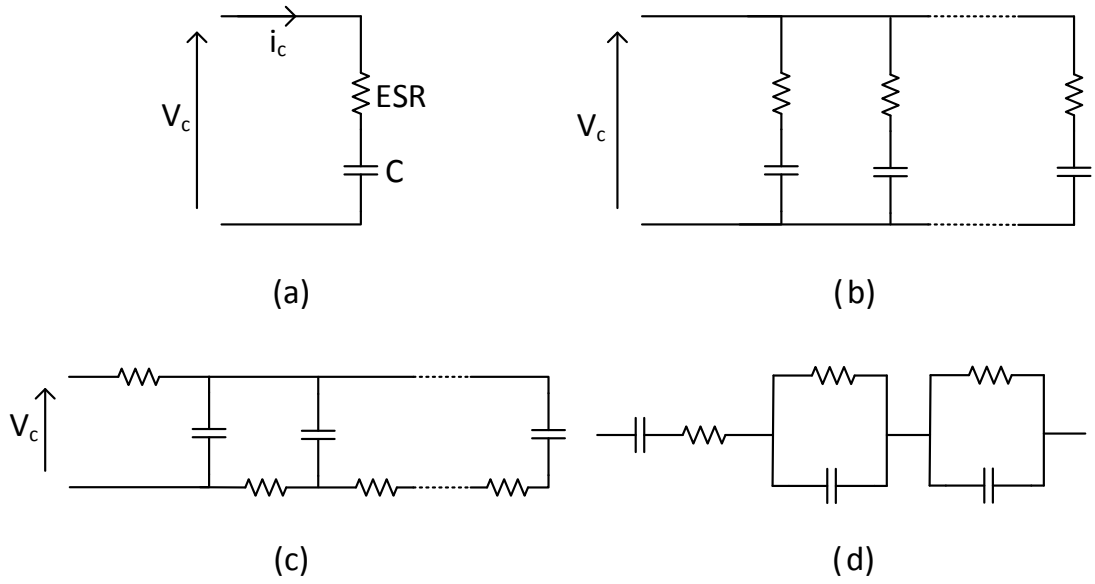

Figure 2.4: Supercapacitor equivalent circuit models (a) classical RC model (b) parallel branch model (c) transmission line model (d) multibranch model

This model captures the distributed double-layer capacitance and the distributed electrolyte resistance. The transmission line model is capable of modelling both dynamic and long-term behaviours.

- **Multibranch model**
  As seen in Fig. 2.4 (d) this model consists of series and parallel branches of *RC* networks [26]. The series branch consists of capacitance and ESR. The parallel *RC* branch represents the SC pore impedance. This model is obtained through impedance spectroscopy testing which measures the impedance over a range of frequencies, thus the frequency response of the system [27].

2.3.4 Ageing of Energy Storage Media

Ageing is affected by the non-reversible reactions happening inside energy storage media. Even electrochemical capacitors become vulnerable to ageing. SC performance degradation is quantified in terms of capacitance loss and increase in internal resistance for the full cell or for each electrode. The main factors affecting ageing are terminal voltage, operating temperature and the current delivered by the device. The following are the key parameters used in comparing the lifetime performance of battery and capacitive energy storage devices.

- **Cycle life**
  Cycle life is defined as the number of deep discharge cycles a storage cell can perform before its capacity is reduced to 80% of its original value [28, 29]. Alternatively, it

can be defined as the number of deep discharge cycles taken to double the internal impedance of the cell. The latter definition is usually applied to higher-power batteries. In actual applications, most energy storage devices are most likely to be subjected to partial discharge cycles of varying depth before being fully recharged. Generally the expected cycle lifetime with shallow discharge cycles is much higher than that with successive deep discharge cycles. As a cell ages it looses its volume of active chemicals leading to a decrease in its energy storage capacity and an increase in internal impedance. This ageing process is continuous. Capacitors do not undergo catastrophic failure at end of life but experience continuous slow deterioration with reducing capacity and increasing internal impedance.
The impressive cycling ability of SCs means that they can undergo millions of deep discharge cycles. This is mainly due to the fact that SCs do not involve any chemical reactions in their energy storage mechanism.

- **Depth of discharge (DoD)**
  Depth of discharge is the amount of energy transferred from a fully-charged energy storage device in to an external circuit until it gets recharged. DoD is an average value based on the actual pattern of power output and recharging. For example, a battery in a car delivers high power when starting the engine but most of the time delivers an average small current for ignition, controls and lights while being continuously recharged. Based on this average DoD, Fig. 2.5 illustrates the expected cycle life of an energy storage device.
  According to the figure, the number of cycles a cell can withstand increases as the discharge becomes shallower. Because of limited cycle life expectancy, most battery chemistries will not tolerate deep cycling. For applications where deep discharging is essential, special chemicals and electrodes should be used to overcome permanent damage. On the contrary, most consumer appliances are recharged at 25–30% of full charge. Most battery chemistries improve cycle life dramatically if the DoD is reduced with the exception of memory effects on NiCd batteries. Memory effects can be reversed by occasional deep discharging. Therefore most battery-based systems are designed to allow a maximum 50% DoD as this offers a balance between the required capacity of the battery vs expected cycle life. The cost of replacement is an important design criterion in designing such a system [30].

- **Temperature effect**
  The chemical reaction or charge separation happening inside all electrochemical energy storage is temperature dependant. The nominal working temperature for most energy storage devices lies in the range 20–30°C. At higher temperatures, chemical reaction speed, and ion and electron mobility increases. As a result internal

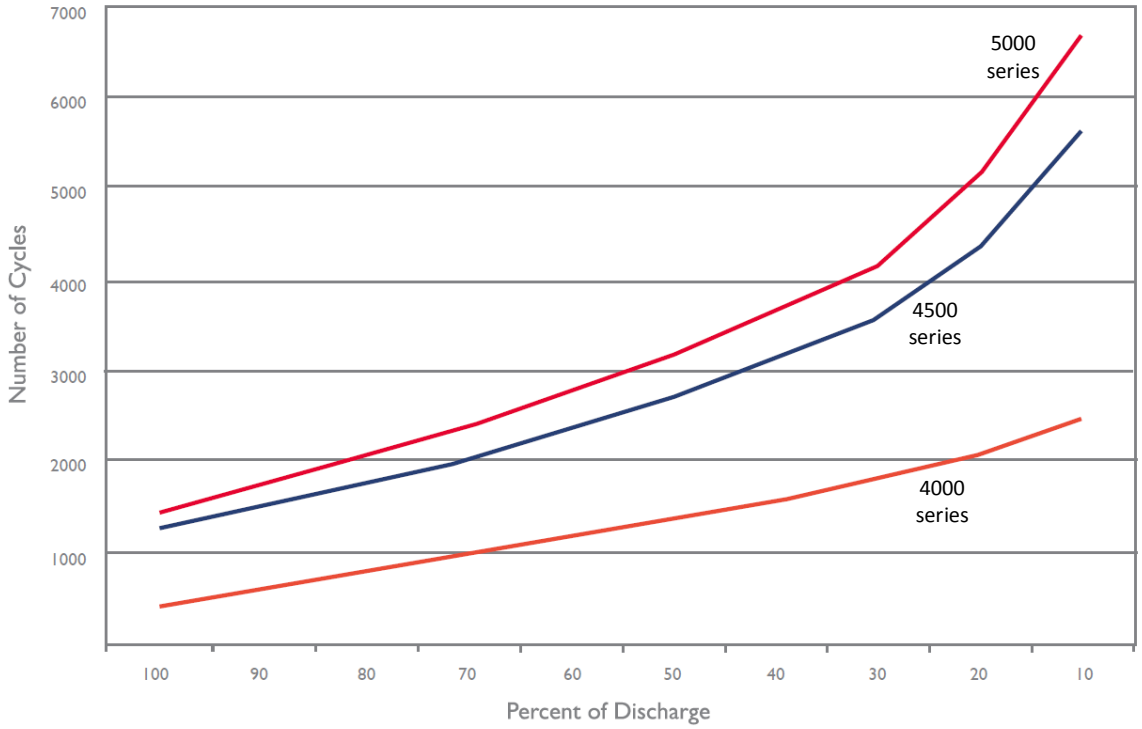

Figure 2.5: Effect of DoD on the cycle life of a battery, for three types of deep discharge batteries from Rolls Battery Engineering [30]. Note the atypical horizontal axis which illustrates the deep discharge capability of the particular battery series.

impedance reduces, hence higher output currents are possible and cell capacity increases. But at extremely high temperatures, electrolytes can evaporate or unwanted chemical reactions may be initiated, causing irreversible damage to the cell. On the other hand, at extra low operating temperatures below the freezing point of most of the electrolytes, performance is impaired by the slow rate of reaction and reduced ion and electron mobility.

Thermal runway can cause catastrophic destruction to a cell as a result of internally generated heat not leaving the cell fast enough. Causes for this could be high output currents increasing I^2R losses in the equivalent series resistance (ESR), high charging currents, or excessive ambient temperature due to poor dissipation of generated surplus heat.

- **Shelf life and calendar life**

  Battery performance deteriorates over time regardless of whether or not it is in active use. Shelf life is the time taken for an inactive battery to drop capacity to 80% of the original value. Similarly, calender life is the time for a battery to lose all of its capacity and become useless while in active use or storage.

  Two main parameters which influence this ageing process are average operating

temperature, and average operating cell voltage. As discussed earlier, higher temperatures will tend to enhance the performance up to a certain upper bound, but beyond that temperature limit the increased rate of harmful chemical reactions or physical processes will degrade cell performance. Further, at higher cell voltages the chemical stress on the electrodes is high and increases the rate of deterioration. Therefore, unless a cell is in active use, it is advised not to maintain the cell voltage at its maximum rated voltage. Based on empirical data for a capacitor with rated voltage, v_r, the operating voltage, v_a, is chosen to be $v_a : 0.8\,v_r < v_a < v_r$ to make the operating voltage dependant life cycle de-rating coefficient, k_v, close to unity.

$$k_v \;=\; \left(\frac{v_a}{v_r}\right)^{-n}$$

The exponent, n, may vary depending on the type of the capacitor, size, rated voltage and terminal type [31].

2.4 Fundamental Single-Loop Circuit Analysis

SCATMA uses a pre-stored energy bank to deliver a high-power boost to the flowing water through a buried coil in the final half-metre of plumbing to a kitchen sink or to a bathroom washbasin tap as seen in Fig. 2.6.

2.4.1 The Basic Loop

The simplified technical concept of SCATMA can be demonstrated as a simple RC loop as in Fig. 2.7. The capacitance C represents the equivalent capacitance of a $p \times q$ capacitor matrix and R_C is the total ESR as given in Eq. (2.7),

$$C \;=\; \frac{c\,p}{q}, \qquad\qquad R_C \;=\; \frac{r_c\,q}{p} \tag{2.7}$$

Each capacitor in the matrix has capacitance c, ESR r_c and a rated voltage v_c. This capacitor bank is connected to a heating element of resistance R_L. If the capacitor bank is initially charged up to V_C, then the varying voltage v_{RL} across the heating element R_L will be,

$$v_{RL} \;=\; \frac{V_C R_L\, e^{-t/C(R_C+R_L)}}{R_C + R_L}. \tag{2.8}$$

If the capacitor stores energy $E(0)$ when fully charged at time $t = 0$, it will discharge to $E(t)$ at time t as given in Eq. (2.9)

$$E(0) \;=\; \frac{CV_C^2}{2}, \qquad E(t) \;=\; \frac{CV_C^2}{2}\,\frac{R_L^2}{(R_C+R_L)^2}\,\exp^{-2t/C(R_C+R_L)} \tag{2.9}$$

Therefore at any given time t, the energy already delivered to the system is

$$E(0) - E(t) \;=\; \frac{CV_C^2}{2}[1 - e^{-2t/C(R_C+R_L)}]. \tag{2.10}$$

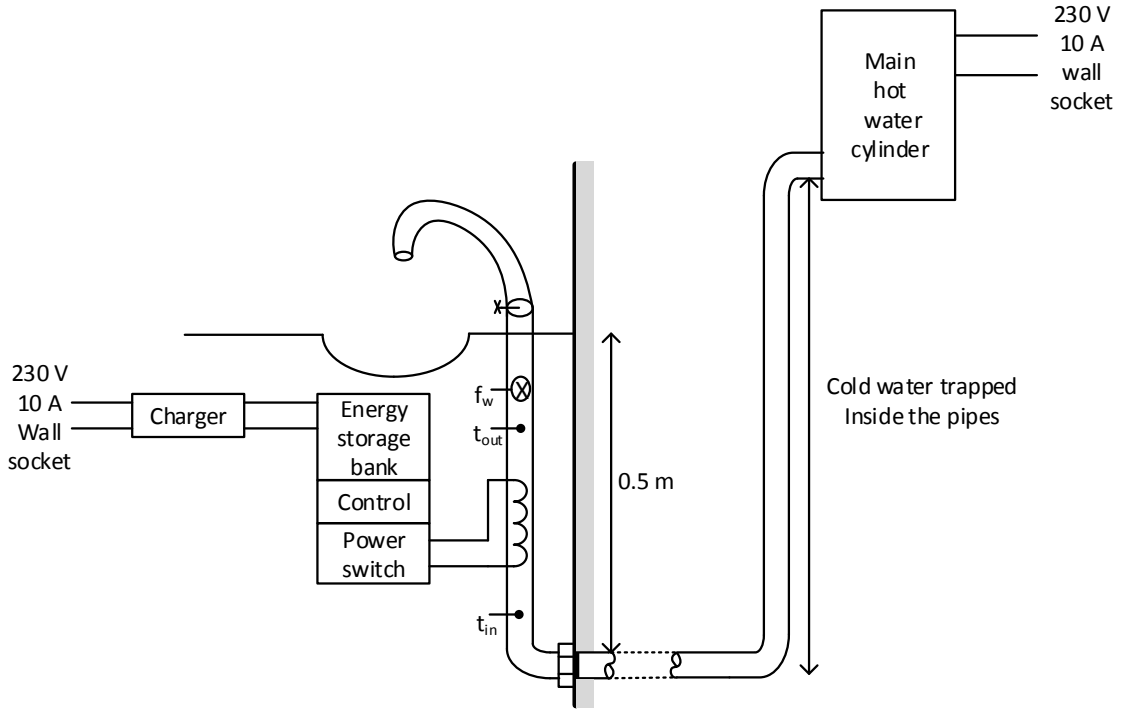

Figure 2.6: A kitchen sink with SCATMA, shows the energy storage bank under the sink with the controller and sensors, and the water trapped inside the pipes connecting to the main water heater.

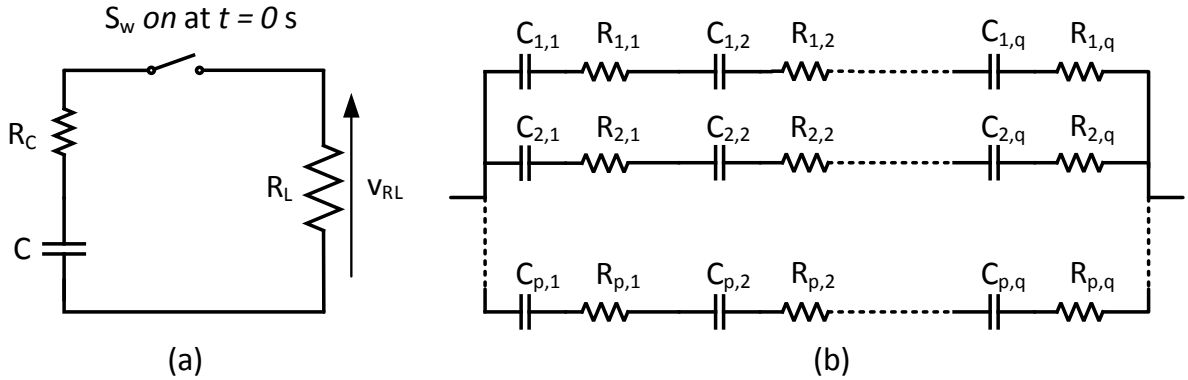

Figure 2.7: Basic RC loop of SCATMA (a) key components, capacitor ESR (R_C), load resistance (R_L) and SC bank (C) (b) equivalent circuit for a $p \times q$ SC bank

The fraction of energy delivered at time t is,

$$e_p(t) \;=\; \frac{E(0) - E(t)}{E(0)} \;=\; 1 - e^{-2t/C(R_C+R_L)} \tag{2.11}$$

For the $p \times q$ SC matrix, the circuit-time constant with the external heating element R_L is,

$$\tau \;=\; (R_C + R_L)C \;=\; \left(\frac{r_c q}{p} + R_L\right)\frac{cp}{q} \;=\; \left(r_c + \frac{pR_L}{q}\right)c \tag{2.12}$$

Figure. 2.8 shows the fraction of energy delivered with time for different capacitor bank sizes into a given resistive heating element. The heating element resistance is much larger than the ESR of the smallest SC bank, so the effect of R_C can be neglected in Eq. (2.11). Within one circuit time constant, all capacitor banks have delivered 86% of their total energy. Therefore if C is chosen to have sufficient energy and R_L to match the operating duration, regardless of SCs' low energy density and lowering terminal voltage during discharge, they are still useful for applications with short duration burst power profiles like SCATMA. This attribute of having seconds-order time constants make SCs an ideal energy storage option for SCATMA as they have a substantial advantage over conventional batteries in terms of power delivery and cycling capability.

SCs as stand alone devices have time-constants (τ_{sc}) in the order of seconds for all capacitor values,

$$\tau_{\text{sc}} \; = \; r_c c \tag{2.13}$$

This is attributed to the chemistry and double layer construction of porous carbon electrodes in SCs.

According to Eq. (2.12) the circuit time-constant is not only dependant on the ESR of the SC bank but it is also dependant on R_L, the external heating element resistance.By tuning the value of R_L both the circuit time constant and the delivered power can be adjusted. For instance, a smaller R_L would allow higher instantaneous currents to be delivered, but this results in a smaller circuit time constant. If R_L is further reduced to the extent that it is comparable with the ESR of the SC bank, the voltage drop across the

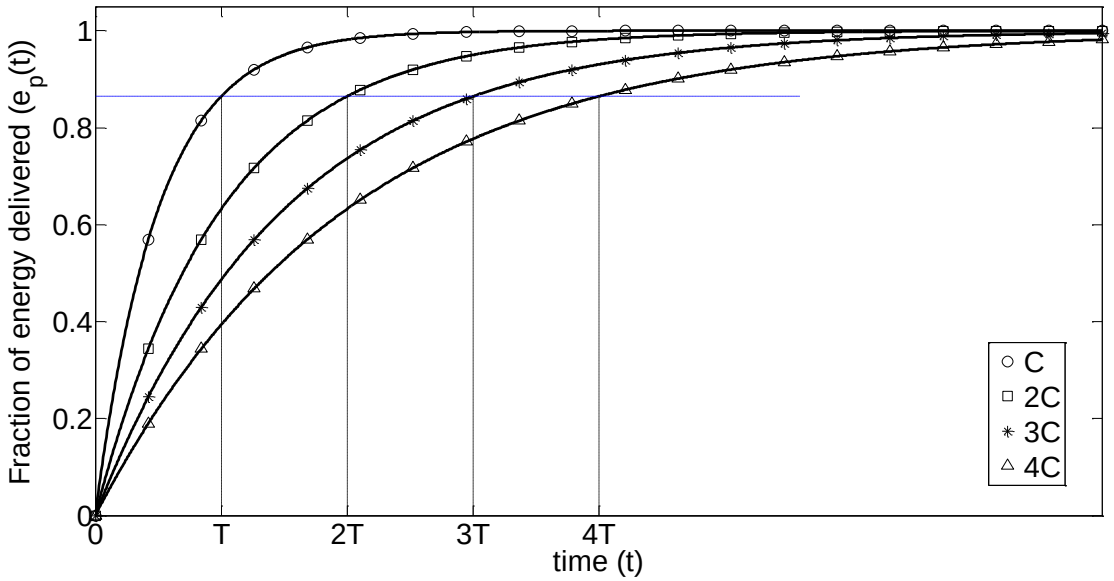

Figure 2.8: Comparison of delivered energy for different capacitor bank sizes. Set $T = CR_L$ assuming R_L is much higher than R_C

ESR becomes appreciable, resulting in increased heating within the capacitor. As a result of this increased operating temperature SC ageing will be accelerated. This motivates to find the condition for optimum power transfer efficiency into R_L.

2.4.2 Power Transfer vs Energy Efficiency

Consider a dc-voltage source with open-circuit voltage V_b and internal resistance of r_b connected to an external resistive load R_L. The power p_{R_L} dissipated in the external load R_L is

$$p_{R_L} = \left(\frac{V_b}{R_L + r_b}\right)^2 R_L. \tag{2.14}$$

which is maximized when

$$\frac{d}{dR_L}\left[\frac{(R_L + r_b)^2}{R_L}\right] = 0 \qquad \Longrightarrow \qquad R_L = r_b$$

$$\Longrightarrow p_{R_L}^{\max} = \frac{V_b^2}{4\, r_b}. \tag{2.15}$$

When the external resistance of the circuit matches the internal source resistance, load power maximized, but an equal amount of energy is dissipated as heat in the source internal resistance, so the energy efficiency is only 50% in this configuration.

Assuming that the load resistance is k times the source internal resistance with$(k > 1)$, the load and internal power dissipations can be written as

$$p_{R_L} = \frac{V_b^2}{(k+1)^2\, r_b}\, k, \qquad p_{r_b} = \frac{V_b^2}{(k+1)^2\, r_b}. \tag{2.16}$$

Hence the ratio of the power dissipation at the load resistance to the source internal resistance is

$$p_{R_L} : p_{r_b} = k : 1 \tag{2.17}$$

Implying an energy efficiency of

$$\eta = \frac{k}{k+1}\, 100\% \tag{2.18}$$

setting $k = 1$ (i.e., $R_L = r_b$) gives $\eta = 50\%$, as expected. To improve efficiency, $R_L > r_b$, corresponding to $k > 1$. For instance, setting $k = 9$ gives an efficiency of 90%. However when k is increased, output power is reduced according to Eq. (2.16). A trade-off between efficiency and output power is needed as high efficiencies result in low output power.

This same principle can be applied to a purely capacitive source. Though the terminal voltage drops with time, when considering a very short time duration, the voltage can be considered as an instantaneous constant voltage source. For every time instant, power can be maximized in the same way as discussed earlier. For a SC bank with a very small internal resistance, the external load resistance should be selected big enough to make

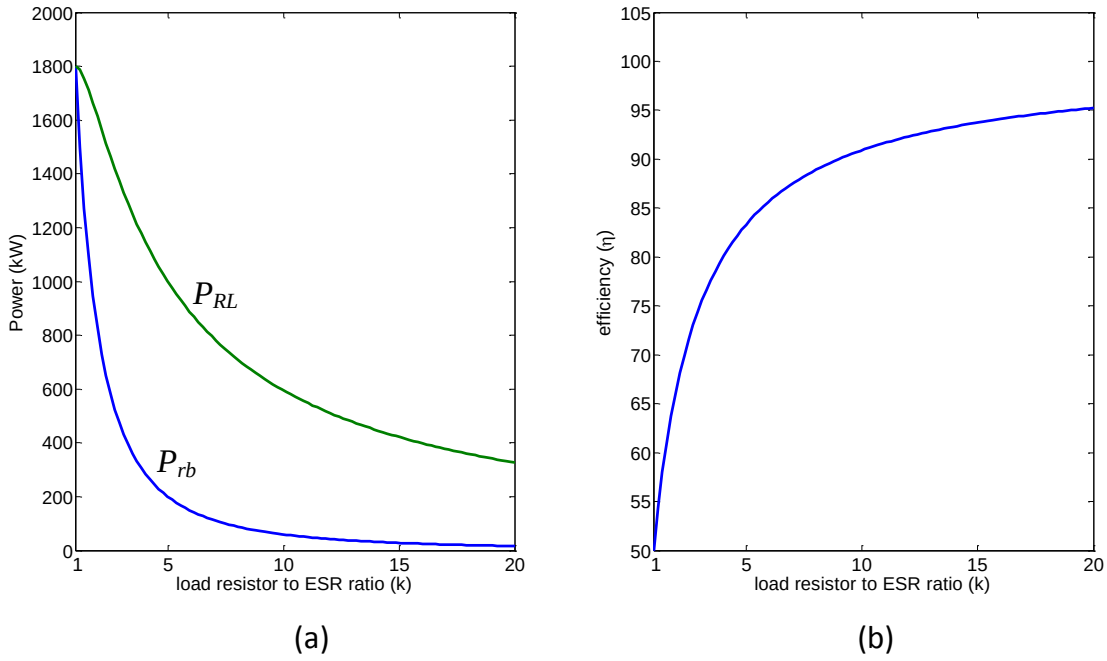

Figure 2.9: Load power, internal power and efficiency variation with resistance ratio k for an example system with $V_b = 12$ V, $r_b = 20$ mΩ and $R_L = 100$ mΩ

sure that the external load dissipates sufficient power and that the SC bank does not get damaged by over-heating. Then if the SC bank is large enough, the combined time constant $C(R_L + R_{\text{ESR}})$ will make sure that though the capacitor voltage keeps decreasing, an average high power can be delivered to the load for one time constant. As long as the power delivery occurs during one time constant of the SC bank, SCs can deliver the necessary energy to the load. SCs have seconds-order time constants and the "instant" water heating application, too, has a power cycle of less than one minute maximum. Given the SC advantages of power density and cycle life, this technology provides a good match for a limited energy, high power application like SCATMA. Further since the load dissipates more power than the power lost in the SC internal resistance, heating of the energy storage medium is not a concern. Hence their is no requirement for a cooling system.

Chapter 3

SCATMA Prototype Design

3.1 Assessment of Capabilities of Energy Sources

Based on the energy and power requirements of SCATMA and regulatory authority safety requirements as discussed in the previous chapters, the following energy sources can be identified as possible options.

3.1.1 Mains Power via 2.5 kW, 250–50 V Transformer

A transformer alone cannot meet the power requirement of "instant" water heating, but can supply a portion of the total required energy. While a 2.5 kW transformer is easy to maintain and meets all the requirements of the regulatory authorities, it is bulky and expensive. At the required power level, even an ac–dc converter running at high frequency would have substantial size and cost. When a transformer supplies continuous high power, heat losses in the windings and the core are unavoidable. Further, when comparing a transformer to a battery or a capacitor, the load does not see purely a voltage source with a minute internal resistance. The transformer secondary winding via which the load is connected will have inductive impedance. Therefore, when the heating element is connected to the secondary winding of the transformer it creates an inductor-resistor circuit in which the current rise is governed by the L/R time constant. Hence the gradual current rise. Further connecting high inductive loads to the mains will require power factor correction which will make the final product more expensive.

3.1.2 Pre-stored Energy in Batteries and Supercapacitors

As noted in Chapter 2, storage devices are classified based on energy and power density ratings. Considering the energy and power requirements of SCATMA should be contained within the space available under a kitchen sink or a bathroom washbasin, it is clear that the storage media should be high power and energy density. This does not match any single-energy storage device presently available in the market. However, SCs and batteries placed at two opposite ends of the Ragone plot can be used for a hybrid solution. Batteries have a constant terminal voltage and high energy density, but have compromised service

life and increased internal resistance when supplying high output currents. In contrast, SCs have superior power density. Compared to batteries, SCs can deliver several hundred times higher currents without any performance or lifetime degradation. The disadvantage of SCs is that their terminal voltage drops as the cell discharges. Hence a suitable control system is needed to regulate for constant power.

3.1.3 Stand-alone Performance Comparison

Given these size, power density, energy density and service-life concerns, each energy storage device was tested using the same heating element and water flow-rate to compare their standalone performance. Figures 3.1 and 3.2 compare the output water temperature generated by a 2.5 kW transformer and a 50-V rated SC bank. Since SC bank voltage decays with discharge, several SC banks were switched with matching delays to obtain a near constant average power for the 30 s period.

When a capacitor C, initially charged to V_C, delivers current into a circuit with an overall time constant τ, the capacitor voltage $v_c(t)$ will be

$$v_c(t) \;=\; V_C \; e^{-t/\tau}. \tag{3.1}$$

After one time constant the capacitor voltage will be

$$v_c(t=\tau) \;=\; V_C \; e^{-1} \simeq 0.37 \; V_C. \tag{3.2}$$

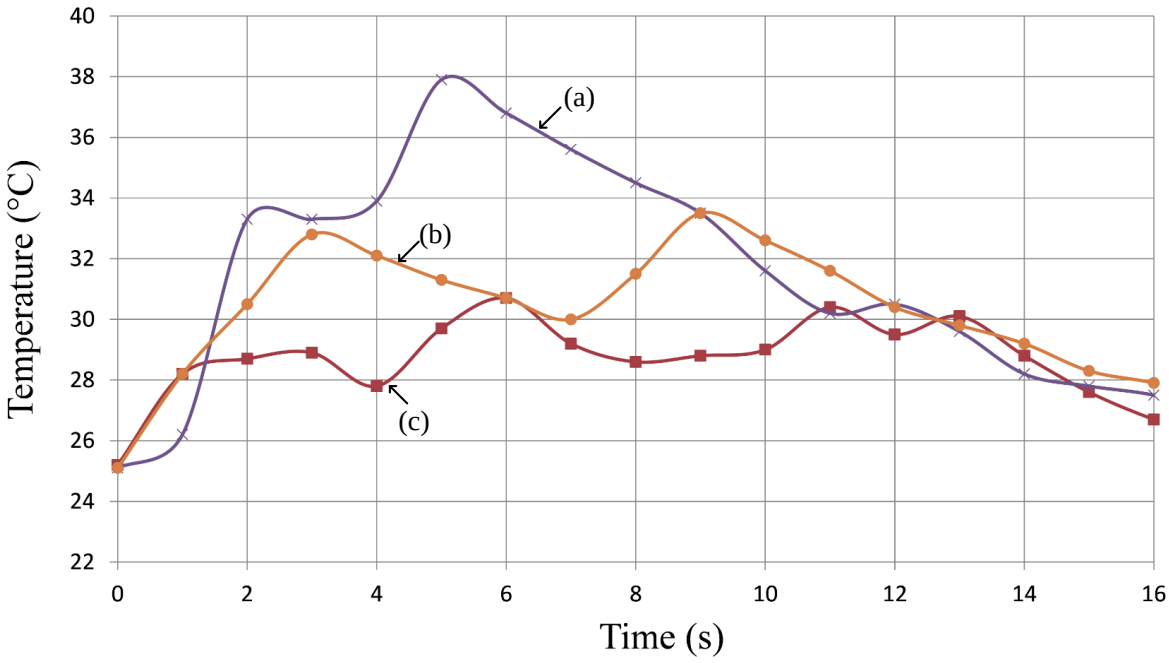

Figure 3.1: Temperature rise versus time of switching three equal size supercapacitor banks in various start up delay sequences. (a) heating element 1 and 2 are switched "on" at the same time then 3 after 3 seconds delay, (b) heating element 1 and 2 are switched "on" at the same time then 3 after 6 seconds delay, and (c) heating element 1, 2 and 3 are switched "on" sequentially with 3 seconds delay.

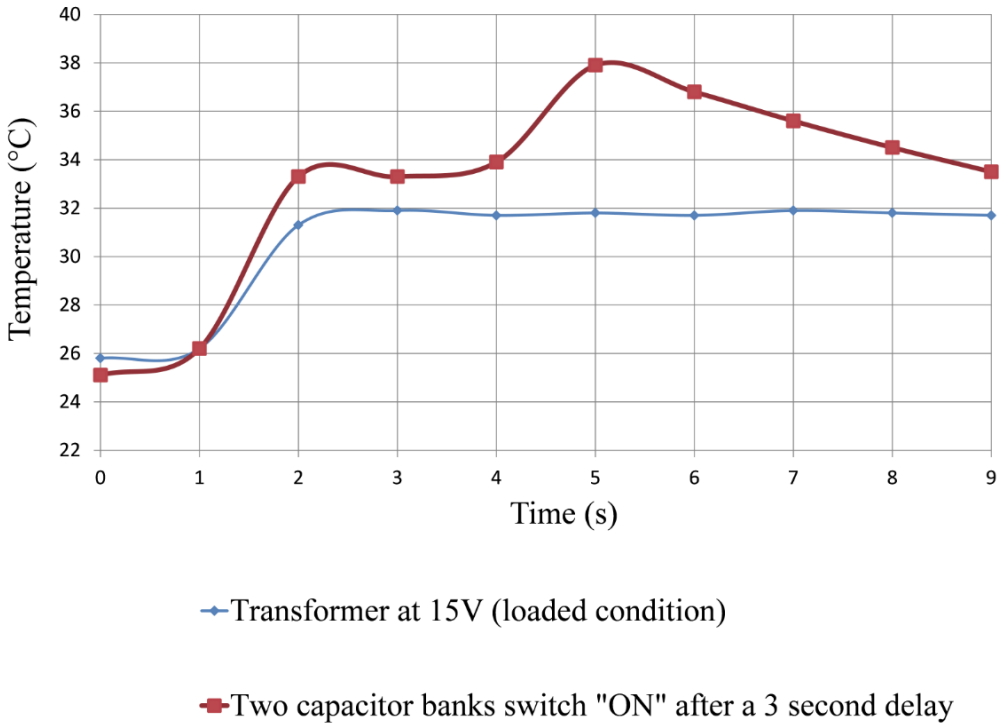

Figure 3.2: Temperature profile comparison between a 2.5kW transformer and SC bank.

Therefore the fraction of energy $f_c(t = \tau)$ remaining in the capacitor after one time constant is

$$f_c(t = \tau) = \frac{E_c(\tau)}{E_c(0)} = e^{-2} \simeq 0.135. \tag{3.3}$$

Where $E_c(0)$ and $E_c(\tau)$ are the energy stored in the capacitor at $t = 0$ and$t = \tau$.

Fig. 3.1 shows the performance of several SCs switched in different delay sequences. These switches were controlled based on the outgoing water temperature to sustain a constant temperature rise. This illustrates the issue of decaying terminal voltage in SCs but the fast temperature rises achieved also highlights the ability of the SCs to control the output temperature. This is due to the low internal resistance of the SCs. Fig. 3.2 shows the continuous power delivery capability of a transformer compared to the decaying power output from a capacitor bank. Though the transformer takes a little longer to reach maximum current (hence the temperature) it can supply continuous power afterwards. The main insight gained through these experiments is that using SC banks allows faster output temperature control due to their higher power density and low ESR. In addition, a transformer's low efficiency due to heating losses, initial current rise delay, cost and size makes the choice less effective for instant water heating.

Further tests were done on SC banks to compare the performance with increasing water flow rates as seen in Fig. 3.3. To establish maximum power transfer capability, coil resistance was doubled and the tests were repeated at different flow rates. It can

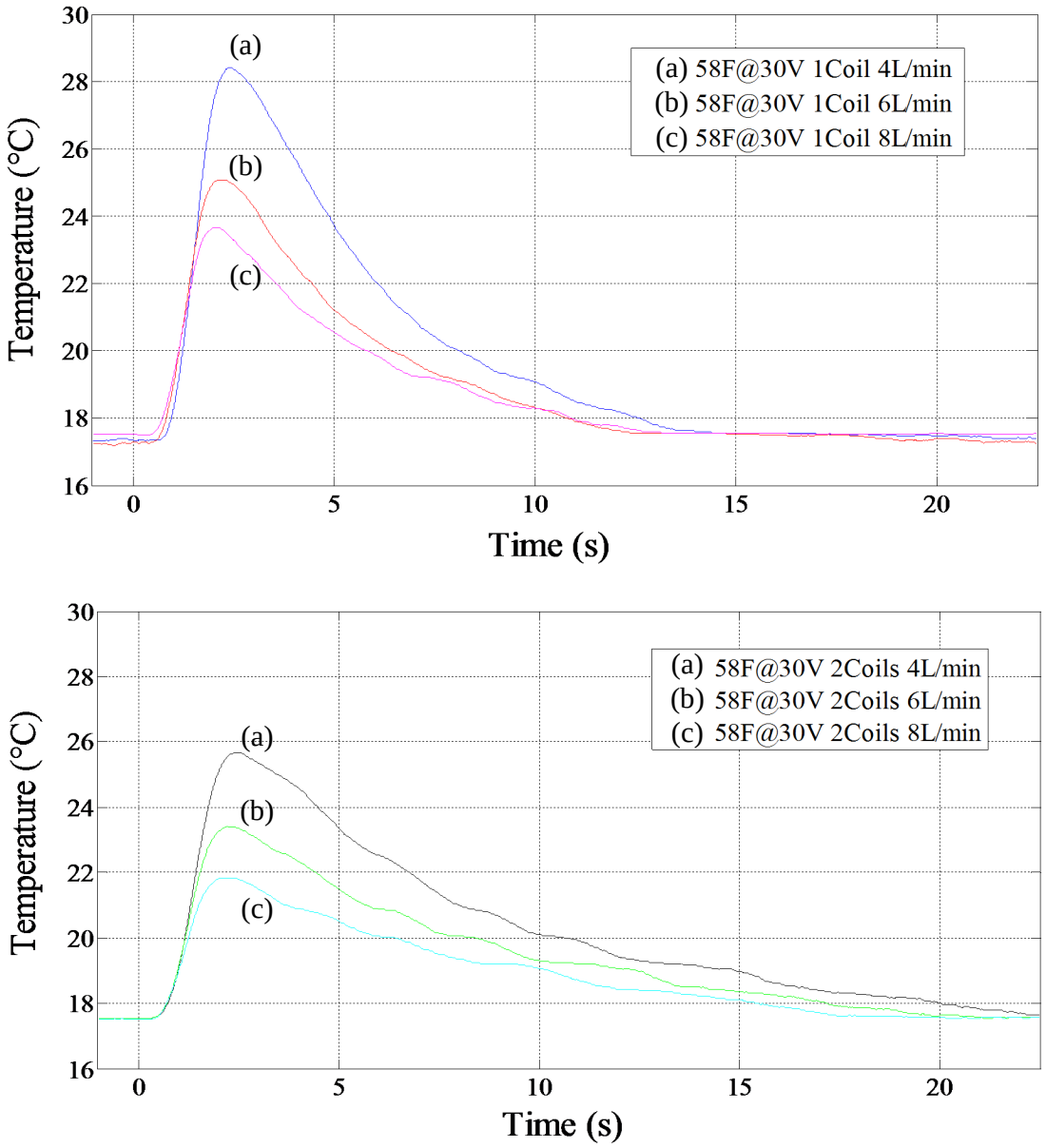

Figure 3.3: The outlet temperature versus time at different flow rates (a) 90 mΩ (b) 180 mΩ, heating coil

be seen that when the coil resistance is doubled, the peak temperature rise drops but the temperature rise is sustained for longer. This gives an indication that with a suitable controller which can set the instantaneous power output to the system by suitable selection of the heating element resistance, performance can be optimized for a specified water flow-rate, required temperature rise and allowed initial delay.

3.1.4 Advantages of a Supercapacitor Solution

The following reasons make a SC based solution better than one with batteries ar transformers.

- The high power requirement of SCATMA can be delivered by SCs without premature ageing.
- Due to the intermittent nature of hot water usage, pre-stored energy can solve the "instant" water heating problem. For instance it takes about 15 min for the water inside plumbing system to release its heat and cool down to room temperature. Therefore the worst case requirement is to supply high power for 20–30 s (based on system specifications) every 15 min. A power rating of less than 1 kW is sufficient to recharge the SC banks in 15 min.
- Since the heater coil delivers continuous high power to the cold water only for a period of less than 30 s, overheating of system components due to parasitic heat losses is minimized. SCs have the advantage of lower internal heating losses as they have very low ESR. The internal losses in terms of I^2R_{ESR} is minimal. For instance, assume a 3000 F cell with 0.25 mΩ discharging at 500 A, the parasitic loss will be 62.5 W. Whereas a 12 V battery with 20 mΩ internal resistance discharging at 100 A will loose 200 W in its ESR.
- Practical delay of delivering hot water in a typical domestic hot water delivery system is in the range of 1–10 s which is a similar duration to the time constants of SC banks with the heating element. SCs naturally have standalone time constants of 1–2 s compared with other capacitor types which are of the order of milliseconds and microseconds. Therefore the proper heater coil resistance choice as given in section 2.4.2 will ensure both the power transfer efficiency and the circuit time constant.

Due to the above mentioned reasons, SCs become the better option for energy storage for "instant" water heating. Despite the power limitations of a 230 V/50 Hz, 10 A mains power, a short-term, nearly-instantaneous power delivery capability can be achieved by using SCs as an energy storage and transfer mechanism.

3.1.5 Implementation Challenges with Supercapacitors

The following challenges need to be addressed when building a SC energy storage.

- Since SCs have low energy density compared to that of the various battery chemistries, other techniques should be considered to reduce the amount of required pre-stored SC energy. For example, hybridisation with cheaper batteries (as discussed in the rest of of this chapter) or supplementing with mains power through a fast SC charging technique (as discussed in Chapter 4) can reduce SC bank size.
- The inline high-power heater coil risks damage if localised boiling occurs in the water flow. This can be solved by two different approaches: (a) optimize the water flow through the heater coil by improving the coil profile and placement; (b) control the power delivered to the heater coil using a pulse width modulation. This control

method should be capable of maintaining the required smooth output temperature profile while avoiding coil damage.

- Sizing the SC bank with cost considerations taking into account the current trends in global prices. At present, the market for SC-driven electric buses is gradually falling and new applications with comparatively smaller energy requirements are emerging in the vehicular industry [32–39]. These include engine start assists, regenerative braking systems and ignition-start-and-go modules; SC prices are expected to halve within the coming 5–10 years [Appendix B.1].
- Managing the initial high currents from the SCs. Since SCs are initially fully charged, when they are connected to a heating element, the instantaneous starting current is in the range of 500–700 A. Though these currents decay during one circuit time-constant, these transient high currents can damage to a MOSFET rated for the average expected current. The absolute maximum current specification for a MOSFET assumes a single high current pulse with a pulse width controlled by the maximum junction temperature. Therefore when selecting a device it should be selected such that its nominal operating current matches or exceeds the instantaneous current rating. Practically, when selecting a switching device it is hard to find such devices with continuous rated currents in the range of 500–700 A. Therefore paralleling of devices is required to share the current between several lower current-rated devices.

3.2 Major Problems to be Solved by an Alternative Energy Storage Scheme

The following are the requirements of an energy storage media to be used in an "instant" water heating application.

High energy density and power density

Due to the limited space under a kitchen sink, the selected energy storage media should have high energy density. Power density should also be high in order to deliver the high currents. As seen from a Ragone plot, neither SCs nor batteries occupy the high energy dense, high power dense, top quadrant of the plot. On the other hand, as batteries and SCs individually excel in their own domains they become candidates for hybridisation.

Depth of discharge vs cycle life

As explained in detail in Chapter 2, DoD and cycle life have a very close relationship for all battery chemistries. SCs, too, show some performance degradation at high-power

deep discharging, but it takes several hundred thousand deep discharge cycles for their capacitance to reduce by 20%. This number of deep discharge cycles will not be reached during the life of the "instant" water heating system. For instance, if the "instant" water heater is triggered ten times each day, then the SC bank will go through $36,500$ deep discharge cycles after 10 years of service. Hence even after ten years of service no discernible performance degradation is expected.

Cost vs size

Batteries with newer chemistries have comparatively high power density and increased energy density and are smaller in size than the conventional chemistries. These newer batteries such as the lithium-based storage devices are much more expensive than a lead acid battery. Therefore a compromise needs to be made weighing up the best battery chemistry against product cost. Since this appliance is intended for commercial sale, an optimum price will be determined from market research. By comparing the current prices and trends in the energy storage market, these newer battery chemistries are prohibitively expensive. The product choice at this price point will be lead-acid batteries.

Energy storage cost

The present high cost of SCs is the major barrier preventing SCs from entering the consumer market. The cost of manufacture is expected to decrease with increased volumes of production thus as more SC applications emerge, it is expected that the SC prices will drop. It is common to express the price of an energy storage device in dollars per kilowatt ($/kW) when power density is the critical selection criterion, and in dollars per watt hour ($/Wh) when comparing energy density.

SCs have a significant advantage over conventional batteries when $/kW prices are compared, whereas batteries have a big advantage in the $/Wh comparison. Since both energy storage devices need to produce the same energy, power and cycle life, the selection criteria are different in each case. When selecting a battery, the critical condition will be the power requirement and cycle life but not the minimum energy requirement since the battery which meets these criteria will store much more energy than the minimum energy requirement. On the other hand, with SCs the size is determined by the minimum energy storage requirement since it can easily satisfy the power and cycle life requirements. Hence a SC solution can be a more optimised solution for an application with high power requirements like SCATMA even though SCs have energy densities 10 times smaller than that of batteries. It is important to highlight the fact that $/kW cost of SCs is about 25% of that of a battery [40].

Table 3.1: Comparison of standalone SC and battery performance based on typical SCATMA power requirements for a heating coil of resistance $R_L = 100$ mΩ

Energy Storage Device	Initial power (kW)	Final power (kW)	Total energy (Wh)	Average power (kW)
SC 300 F, ESR = 10 mΩ,	20.7	2.3	84.2	10.1
New lead acid battery 48 V, ESR = 80 mΩ,	7.1	7.1	59	7.1
Old lead acid battery 48 V, ESR = 400 mΩ,	0.922	0.922	7.7	0.922

3.3 Combining Batteries and Supercapacitors

The fundamental requirements of SCATMA are

- Adequate storage capacity with very high power density and sufficiently high energy density to meet the volume and cost requirements
- Minimum total equivalent series resistance (ESR) of the energy storage bank which does not increase at higher depths of discharge and at higher rates of discharge
- Ability to adjust the time-constant of the heating-coil/SC bank circuit to suit the expected temperature rise and the delay in delivery of hot water in a centrally heated hot water system.

Due to the total amount of energy needed to be pre-stored, a SC-only solution will be too expensive and bulky. But the SC-only solution is more elegant as it requires minimum maintenance with replacements not being expected within the product service life. The choice of battery chemistry for a battery-only solution within the acceptable price range would be lead-acid. Table 3.1 compares the average power delivery capability of a SC bank and a new battery with low internal resistance versus an old battery with increased internal resistance. All the entries are calculated for a load resistance (R_L) of 100 mΩ. The final power and total delivered energy is calculated based on the SCATMA requirement of a 30 s power delivery period. It is evident that a SC bank is capable of delivering a higher average power than a new battery. The last entry shows that as the battery gets cycled, its ability to deliver useful power to the external load reduces drastically as its internal resistance increases. Therefore, considering the effects of cycling and discharge currents associated with SCATMA, a battery-only solution is not practical. As discussed earlier, since neither SCs nor any electrochemical battery chemistry have both high energy density and high power density, and since the application has a low crest factor (peak to rms power ratio), most automobile techniques optimised for pulsed power applications will not be effective.

It is well documented that combining SCs and batteries would significantly reduce the stress on the battery in applications where the batteries are subjected to high current

charge–discharge pulses. A hybrid energy source allows the designer to meet extraordinary application requirements without having to make performance sacrifices. A hybrid system allows components to operate at manufacturers' optimum operating conditions without trade-offs on performance and life. The majority of consumer electronic devices, such as telecommunication products and wireless sensor nodes, can be modelled as pulsed power applications with relatively high peak-to-average power ratios [41,42]. Other commercially significant applications using hybrid solutions include battery assist for vehicle engine starting, and railway and vehicle propulsion systems [43, 44].

In all of these systems, the main driving force for hybridisation is battery deterioration through the increase in internal resistance making the battery incapable of delivering the necessary load power [45,46]. The load demand of SCATMA can be uniquely characterised by its very low peak-to-average power ratio over a 30–60 s period repeated each 15 min at worst case (e.g., 20 kW peak power to 18 kW average power). This is due to the nature of instant water heating requiring continuous high power. Unlike the pulsed-power applications discussed above, this ratio is very high and it spans only few milliseconds to fractional seconds. A typical example is an engine starting battery-assist delivering 500–1500 A only for 50–200 ms. Therefore SCATMA requires hybrid techniques different to the ones used in vehicular applications and portable devices.

3.3.1 Hybridization Options

Battery–SC hybridisation techniques are classified as passive, semi-active, and active [47]. Battery SC passive models mostly use batteries and SCs connected in parallel to the load [41, 48, 49]. This is the best option when size and price are major design criteria as the two following techniques will be more complex and has the added volume of a dc-dc converter and control circuitry. References [50, 51] describe examples of semi-active hybrids employing a DC-DC converter and a control system. The fully active hybrid will attain ultimate performance using two DC-DC converters controlled through each power source [51, 52]. All of these hybrid systems rely on batteries to supply the average power while SCs will provide the dynamic component [41]. Hybridization of SCs with rechargeable batteries can be performed in several different ways. Readily available battery and SC cells can be connected in either of the methods described above or, by analogy, the same approach can be applied at the internal level. Therefore four possible hybridization techniques are available as seen in Fig. 3.4. Further details on hybridisation techniques are described in [53].

If an inexpensive lead-acid battery pack is to be used in developing a hybrid solution to last over 5–8 years (20, 000 cycles) for a commercial product, the DoD of the battery pack should be minimized. Hard-wired passive hybrid is the only option considering the target product cost and available volume for energy storage.

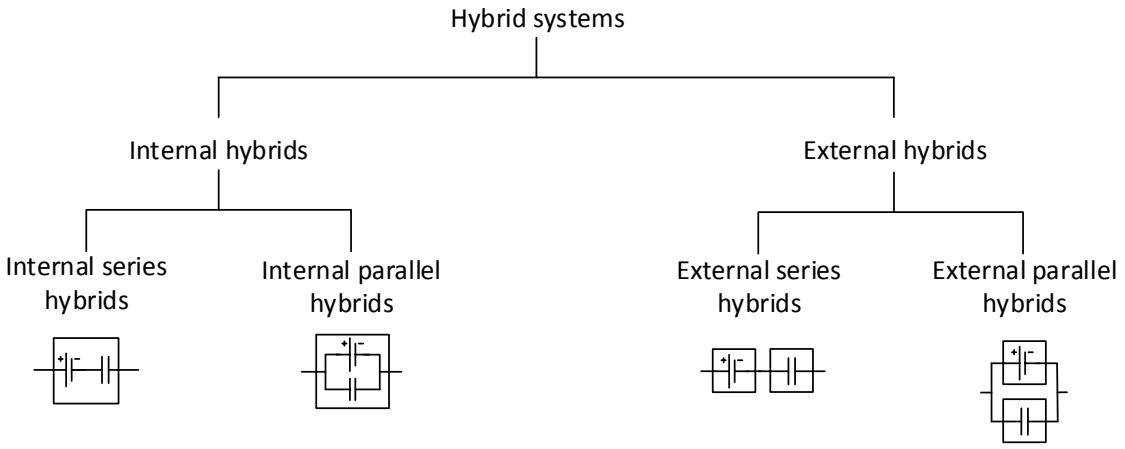

Figure 3.4: Hybridization approaches in supercapacitors and rechargeable batteries

3.3.2 Battery-Supercapacitor Parallel Hybrid

With this option, a SC bank is hard-wired parallel to the battery as shown in Fig. 3.5 so that the entirety the initial high current requirement are supplied via the low equivalent-series-resistance (ESR) SC bank instead of the battery pack. This arrangement saves the battery from supplying high current surges (which could exceed the safe maximum C-rating) in a continuous high power delivery situation. As depicted in Fig. 3.6(a), a parallel battery/SC hybrid supplying a load shows the SC bank initially supplying the total load with a decaying current with the batteries supplying the balance to maintain an output voltage close to DC. An upper bound can be set on the batteries maximum output current (I_{b_op} in Fig. 3.6) to obtain the required cycle life. Therefore the battery should be switched "off" at appropriate times so that the battery does not deliver exceedingly high currents. As shown in Fig. 3.6(b), the "off" state charges the capacitor with a decaying current from the battery. Once the capacitor is charged, the same process repeats for continuous power delivery. The time constants of the "on" and "off" periods can be altered by the capacitor sizing, load resistance and switching period. This shows how the SC and battery currents can vary without exceeding their respective safe limits.

Initial conditions according to Fig. 3.7(a): since the battery and the capacitor are hard wired $v_c(t=0) = V_b$. When switch S_w is "on", the loop equations for the battery and capacitor loops are,

$$V_b - i_b R_b = v_c(t=0) - \frac{1}{C}\int i_c\, dt - i_c R_c = (i_b + i_c) R_L$$

giving

$$i_b(R_b + R_L) + i_c R_L = V_b, \qquad i_b R_b - i_c R_c - \frac{1}{C}\int i_c dt = 0. \tag{3.4}$$

By Laplace transform

$$j_b(R_b + R_L) + j_c R_L = \frac{V_b}{s}, \qquad j_b R_b - j_c(R_c + \frac{1}{Cs}) = 0; \tag{3.5}$$

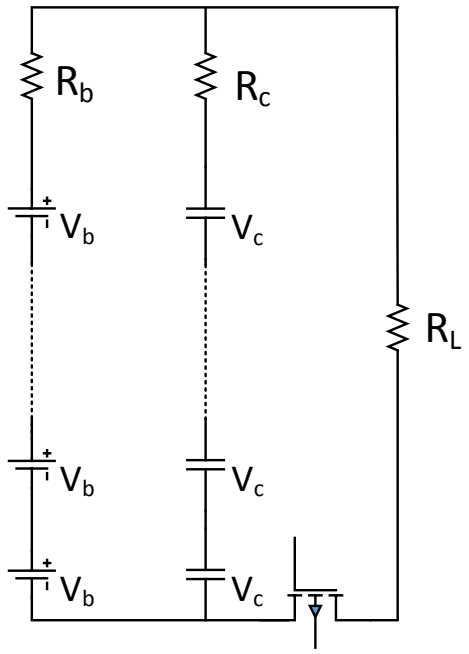

Figure 3.5: Parallel hybrid configured to deliver the total power onto a single load resistor.

where j_b and j_c are $\mathcal{L}(i_b)$ and $\mathcal{L}(i_c)$ respectively. By solving Eq. (3.5) for j_c;

$$j_c = \frac{V_b R_b/s}{R_L R_b + (R_b + R_L)(R_c + 1/Cs)} = \frac{DC}{A} \frac{1}{s + B/A} \tag{3.6}$$

where

$$\begin{aligned} D &= V_b R_b, \\ A &= C[R_L R_b + (R_b + R_L)R_c], \\ B &= R_b + R_L. \end{aligned}$$

By inverse Laplace transform;

$$i_c(t) = \frac{DC}{A} e^{-Bt/A} \tag{3.7}$$

and substituting in Eq. (3.4)

$$i_b(t) = \frac{V_b}{B} - \frac{DC}{AB} R_L e^{-Bt/A}. \tag{3.8}$$

It is note worthy that the ratio DC/A is independent of capacitance, meaning that maximum current delivered from the system is independent of the capacitance of the capacitor bank. Though there is a connection between R_c and C, the effect of that variation can only be predicted from datasheet values. The exponential decay term is inversely proportional to capacitance, which results in larger capacitors being able to sustain higher

currents for longer periods of time. Switch S_w should be turned off when i_b reaches its maximum safe operating current I_{b_op}. This value is based on the maximum DOD and C-rating for a given battery to reach the required cycle life.

When 'S_w' is off, capacitor and battery are connected in parallel as seen in Fig. 3.7(b). The loop equation will be,

$$V_b - iR_b \;=\; v_c + iR_c + \frac{1}{C}\int_0^t i \;\; dt. \tag{3.9}$$

Based on the duration of the "on" cycle, the value of v_c will change. The main difference between the "on" and "off" cycles is the direction of the current through the capacitor. In terms of voltage v_{12} this can be expressed as,

$$v_{12}^{\text{on}} \;=\; v_c - iR_c, \qquad v_{12}^{\text{off}} \;=\; v_c + iR_c \tag{3.10}$$

Therefore according to Fig. 3.6(b) when the "off" cycle starts, the battery will have a decaying current until the capacitor is fully charged. This imposes an uncontrolled parameter onto the circuit because the "off" time is directly controlled through the capacitor size, parasitic resistance and "on"-time duration.

Advantages and disadvantages:

- Initial high currents are delivered from the SCs rather than from the batteries
- SCs do not get fully discharged, therefore the bank size is larger than optimal

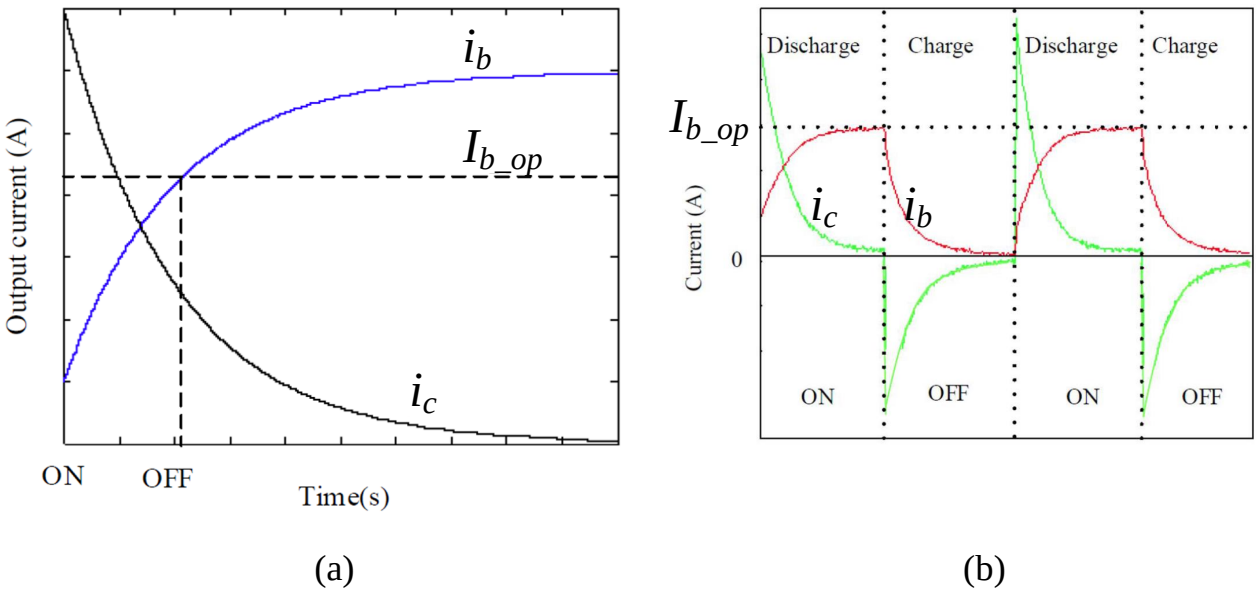

Figure 3.6: Parallel hybrid current profiles (a) expanded view of a single cycle beyond off time; showing I_{b_op}. (b) switching cycles, on duration controlled by I_{b_op}.

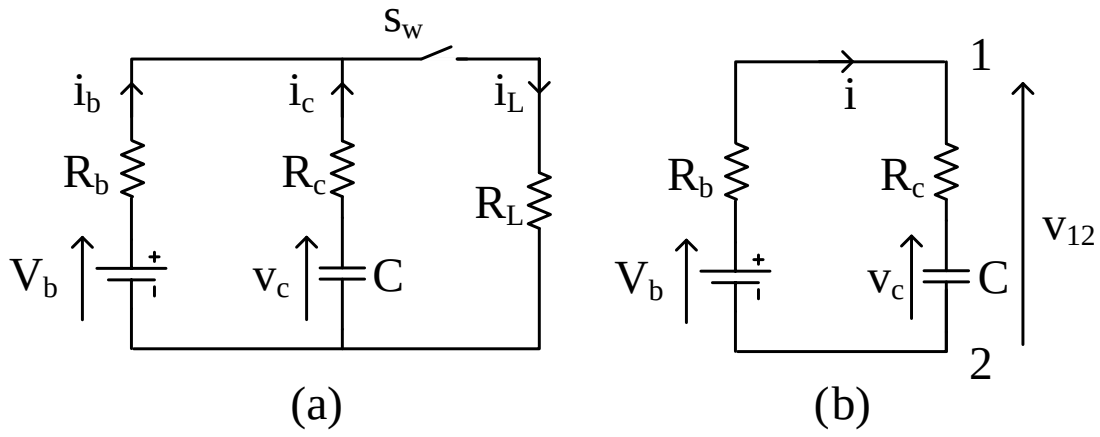

Figure 3.7: Parallel-hybrid equivalent circuit; (a) switch S_w closes when $t = 0$ s, (b) "off" state equivalent circuit

- In the "off" cycle, the charging rate is governed by the "on" duration. This is limited by the battery's safe rate of discharge Therefore the battery's C-rating governs the allowed "on" time, hence the ripple in the output current

3.3.3 Battery/Supercapacitor Series Hybrid

The problem identified in the battery/SC parallel hybrid was the inability to discharge the SCs fully. To overcome this issue and to gain more control over the output current while being hard wired, the series/capacitor hybrid arrangement is examined. As seen in Fig. 3.8, the battery is connected in series with a SC to allow the SC to be fully discharged.

The Thévenin equivalent circuit for S_{w1} during the "on" period is shown in Fig. 3.9. The equivalent loop resistance (R_{th}) and circuit time constant (τ) can be written as

$$R_{\text{th}} = \frac{R_b}{m} + nR_c + R_L, \qquad \tau = \frac{C}{n}R_{\text{th}} \tag{3.11}$$

Advantages and disadvantages of this system are:

- Several batteries can be used in parallel to share the current and reduce the risk of premature battery failure
- Using several SC banks in series with a battery allows a high output current to be maintained for a longer duration, and gives more output control
- Batteries have to deliver all of the high output currents; this is a disadvantage

3.4 Implementation of a Prototype System

3.4.1 Implementation

Given the advantage of a series-hybrid configuration in Fig. 3.8, the first implementation and related tests were carried out based on the simplified block diagram of Fig. 3.10.

The energy storage system consists of the batteries and the SCs in a series configuration. This is controlled by a switching system consisting of metal-oxide-semiconductor field-effect transistor (MOSFET) power switches as well as their drivers. The stored energy is fed into a coil, which directly heats the water. The power stage of the system is shown in Fig. 3.8, with the possibility of several batteries in parallel, to share the required current demand from the heater coils. This then branches into individual SC banks which power the resistance coils for water heating.

A microprocessor-based control system was developed to switch the MOSFETs based on the output water temperature. In the initial trials a temperature rise of 20°C within 10 s was attempted as in Fig. 3.11(a). Using this trapezoidal temperature profile, the total energy requirement is reduced compared to a rectangular one with a sustained constant output temperature. From the point of view of the end user, the gradual temperature rise will feel more pleasant than a sudden temperature rise. The gradual dip after the first

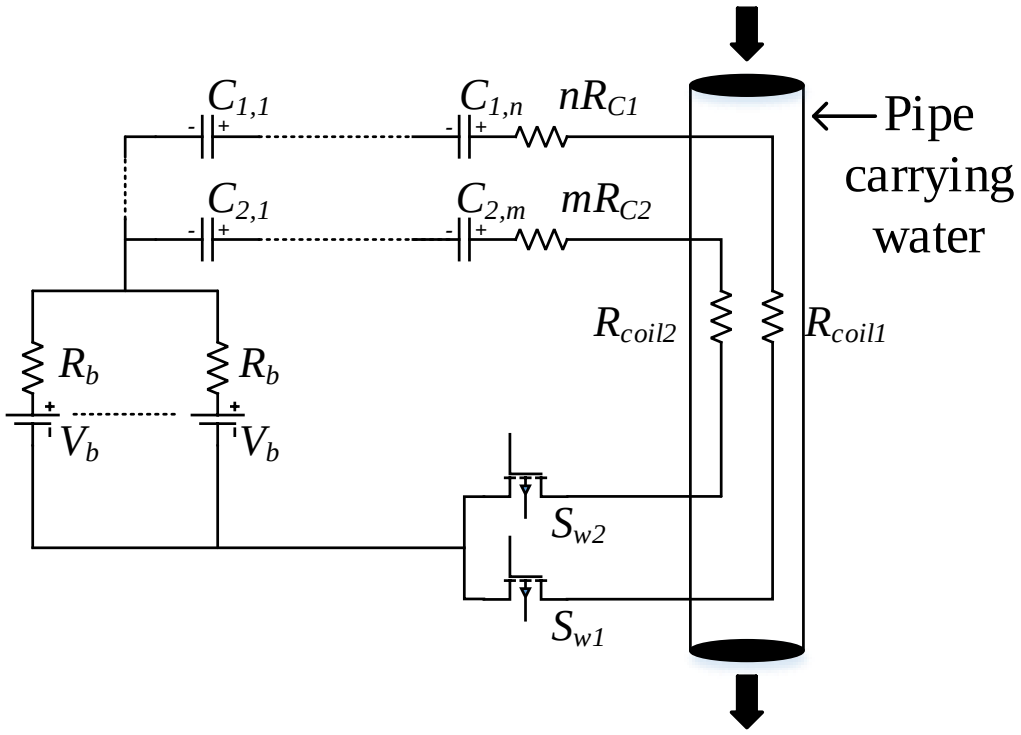

Figure 3.8: Series-hybrid arrangement, capable of dividing the total load into two load resistances buried inside a water tube.

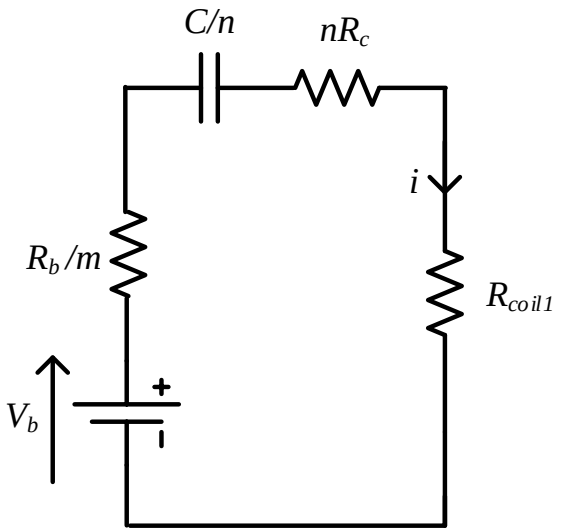

Figure 3.9: Series-hybrid equivalent circuit with m identical parallel batteries and n identical SCs when S_{w1} is on

20 s will not be felt as the main water heater is expected to start pumping hot water by this time.

As seen in the previous discussion, on the series-hybrid system, one of the major concerns is that the SCs can get charged in the opposite direction by the battery current. Therefore the voltages of the SCs are monitored, so they can be safely switched off without being reversed charged. While monitoring the battery voltage, the rise-time of the temperature can be adjusted to be longer or shorter than 10 seconds. However to achieve a shorter rise time than 10 seconds, the power output of the storage banks needs be increased. In a final system, this will require a trade-off between energy costs in power, and customer preference for prompt heating.

The final decrease is modelled linearly at this initial stage of testing, as the test setup does not currently have a delayed mains hot-water supply. The target temperature was initially set to 40°C, as this was still hot to the touch for testing, as well as being in the middle of the specification range.

3.4.2 Final System Integration

The configuration tested at this stage first used four, 12 V, 12 Ah lead-acid batteries placed in parallel. These are standard automotive batteries and the cheapest option in terms of cost per joule. The use of four batteries was to reduce the current drawn from

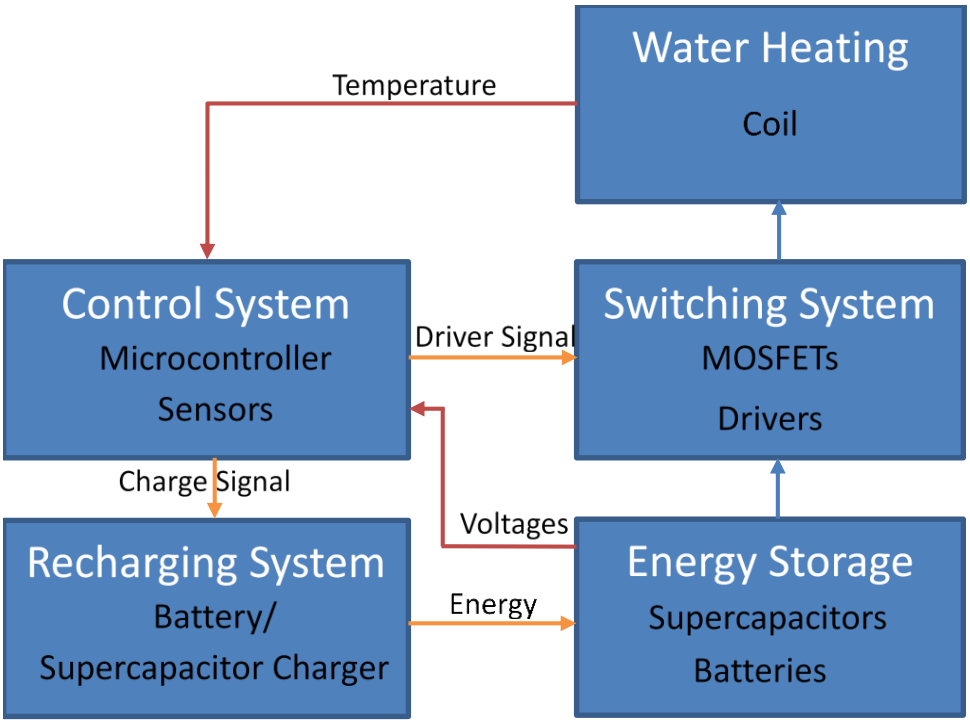

Figure 3.10: Simplified block diagram of the series-hybrid system

each battery, and to keep the DoD at a reasonable value such that the estimated battery lifetime will surpass the 5 year limit. A single heater coil of 100 mΩ was used initially with a SC bank of approximately 187 F for a flow rate of 6 litres per minute.

Fig. 3.11(b) depicts the results of this test using the maximum energy of the hybrid system, switching off before the SCs begin reverse charging. The system was switched at 90 % duty cycle, and a frequency of 30 Hz. This is the fastest rise time achievable from the hybrid system, with an overall temperature rise of about 35 °C. As seen in Fig. 3.11(b), energy transfer was initiated at 3.5 s from the start, to accommodate the delays associated with temperature and flow sensors.

It can be seen that within approximately 2 s, the temperature rises from approximately $\sim 20°C$, up to approximately $\sim 55°C$. This temperature rise matches those in the target specifications, however it is unable to sustain this temperature due to the inadequacy of stored energy in the SC bank.

In the next test, the control system was implemented using proportional-integral (PI) control to achieve the temperature profile of Fig. 3.11(a) with the results shown in Fig. 3.11(c). Fig. 3.11(c) shows that the target is followed relatively closely. The temperature error could be further reduced with optimisation of the control system, however this is probably not necessary, as a faucet user will not be able to sense the temperature corrections. The SCs run out of energy halfway through the decline phase, hence the temperature drops back to the mains cold temperature before completing the 30 s cycle.

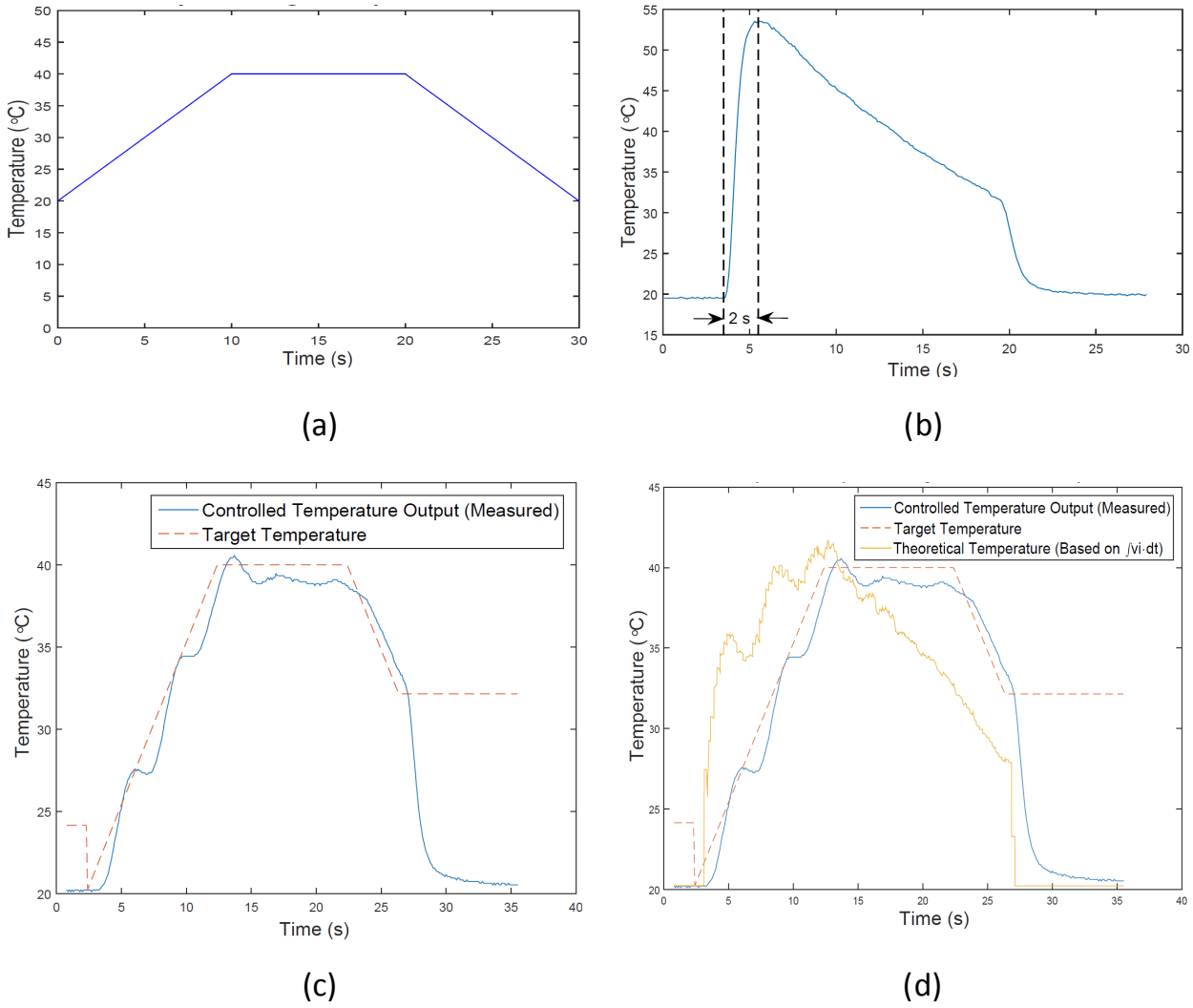

Figure 3.11: Prototype system control, (a) Temperature profile used in initial testing with a 10 s temperature rise followed by a 10 s of constant temperature and the final 10 s temperature rise decay (b)Temperature profile running at 90 % duty cycle for a full discharge of the series-hybrid energy storage system (c) Measured controlled faucet temperature output, with target (d) Controlled faucet temperature output, with target and theoretical temperature rise based on voltage, current and flow rate measurements

Further testing is required, adding more SCs to energize the entire duration, as well as increasing target temperatures to meet possible worst case specifications.

Because the test setup measures both the voltages and the currents in the power stage of the system, the total power delivered to the coil can be calculated. This can be used along with the measurement of the flow rate to calculate the theoretical temperature rise. Fig. 3.11(d) depicts the target temperature profile, theoretical temperature rise and the practical results. Appendix [B.2] gives more details on the control system design by Sean A. Charleston.

Chapter 4

Fast Supercapacitor Charger for SCATMA

4.1 Fast Charging Requirement in SCATMA

As described in previous chapters, "instant" water heating requires stored energy that can be delivered at a fast rate. The hybrid solution based on a SC/battery series-hybrid arrangement as described in Chapter 3 has the major drawback that the size of the required energy storage is too big. Compared with SCs, batteries have a very short cycle life (one million deep discharge cycles for SCs vs a maximum of 1000–2000 for batteries [54]). From a marketing point of view, having batteries which will ultimately require replacement regardless of the best design is undesirable. If a solution can be found using only SCs, consuming minimal space and within the cost limitations of the product, that will lay a solid foundation for a reliable product. This reliability comes from the fact that SCs should not require replacement for at least 15 years, given the average hot water usage of a house. In addition, SCs being service free will ensure the product is of "install and forget" kind required by customers. This idea is well supported by SC market research results which shows SC prices are expected to drop by half within five years as the automotive industry starts using SCs for engine start assists, brake energy recovery systems, and ignition start and go systems [33, 55, 56]. Though the prices will relax, a significant increase in SC energy density is not expected as the energy density gap between SCs and batteries are separated by a factor of 10–20 [57]. Therefore the solution for SCATMA should be one which reduces the total amount of pre-stored energy.

4.1.1 Energy Balance

Based on the average specifications of "instant" water heating, 100–150 Wh of energy is required for the 30 s period of operation. A SC bank providing up to 50 Wh is feasible based on cost and size. Possible options for the rest of the energy requirement are

1. to draw more than 10 A from the mains supply for a short period of time without overloading the wiring or tripping the protective circuit breaker. For example, an ABB miniature circuit breaker S201PR-K10, a 240 VAC, 10 A rated supplemental

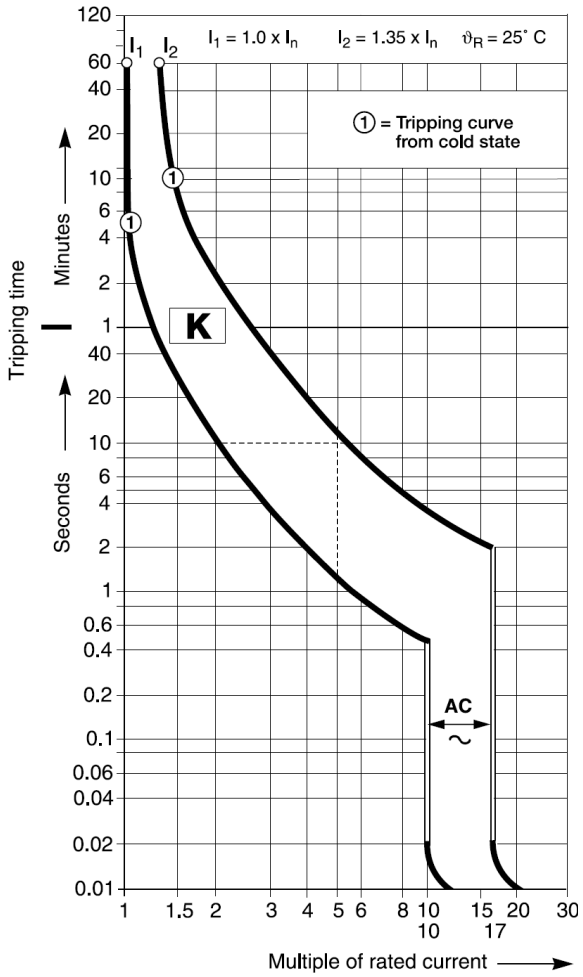

Figure 4.1: ABB miniature circuit breakers S200 series tripping characteristic K, UL1077 supplementary protection standards [58]

protector, is designed to pass five times the nominal 10 A current for 10 s without tripping. This allows a maximum of 11.5 kW to be accessed as illustrated in dotted lines in Fig. 4.1.

2. to draw the nominal 2.3 kW from the mains supply. This can be used for the time after the mains supply has had its 10 A supply exceeded by the previous option.
3. to store energy by a cheaper alternative than SCs (such as a battery). Such a store can have a lower power density but a higher energy density than SCs.

According to option one, if a special protection device designed to allow higher in-rush currents during system start up is used, a maximum power of 11.5 kW for 10 s and 2.3 kW for the remaining 20 s can be drawn from the mains supply. This is a total energy of (11.5 kW×10 s) + (2.3 kW×20 s) = 32 Wh + 13 Wh = 45 Wh. Based on 150 Wh total energy this is equivalent to 30% of the total energy requirement. In the case of not having the option of laying a dedicated high-in-rush current subcircuit for a specific household, then the mains can supply up to 2.3 kW×30 s = 19.2 Wh, which is 12.8% of the needed total energy.

Given the availability of these options the problem lies in how this energy can be delivered to the load with galvanic isolation and at the required 15–18 kW average power level. For both of these conditions to be satisfied, a SC bank circulation technique first proposed for surge resistant uninterrupted power supply (SRUPS) [6, 59] is used.

4.1.2 SRUPS

The SRUPS is an UPS technique developed to withstand short power outages of several ac mains cycles up to a few hundred milliseconds. The advantage of this technique is that the inverter runs online and is continuously fed by a circulating capacitor bank as seen in Fig. 4.2(a). At a given instant, a bank partitioned into three has one bank supplying the load while another is fully charged and ready to deliver and the third bank is being charged. Through this circulating principle, and by using an on-line inverter, galvanic isolation is achieved. This is advantageous for UPS surge resistance. At all times the mains supply is never directly connected to the load. The load will be fed from a separate SC bank while the mains is charging another SC bank. Any incoming transient voltage spike in the mains supply will be safely absorbed by the SC being charged. This ability of SCs to absorb high voltage transients without any damage was shown in [60].

This technique provides a new way of using SCs in the middle of an UPS where the SCs are used as both an energy storage medium and a surge absorbing element, providing an enhanced level of surge protection to the connected loads. This technique can be developed to a fully versatile topology to eliminate the requirement of a battery pack for short-term ac mains power blackouts.

4.1.3 Bank Circulation

The bank circulation technique can be used in any high-power application where the load power requirement is higher than that provided by the mains supply. Therefore rather than relying purely on prestored energy, the amount of prestored energy can be reduced by supplementing with mains energy through a circulating bank. A circulating SC bank may consist of as many SC banks as required, each in one of the three above-mentioned states. The bank circulation technique divides the total energy storage requirement among several storage banks in order to reduce the per-bank pre-stored energy. Depending on the amount of energy each bank stores, the system may be required to circulate for several cycles during the course of operation. The optimum choice of SC bank size and number of cycles required to deliver a predetermined quantity of energy will

- minimize the leftover energy at the end of the process
- make sure the required constant power output is maintained throughout the period of operation

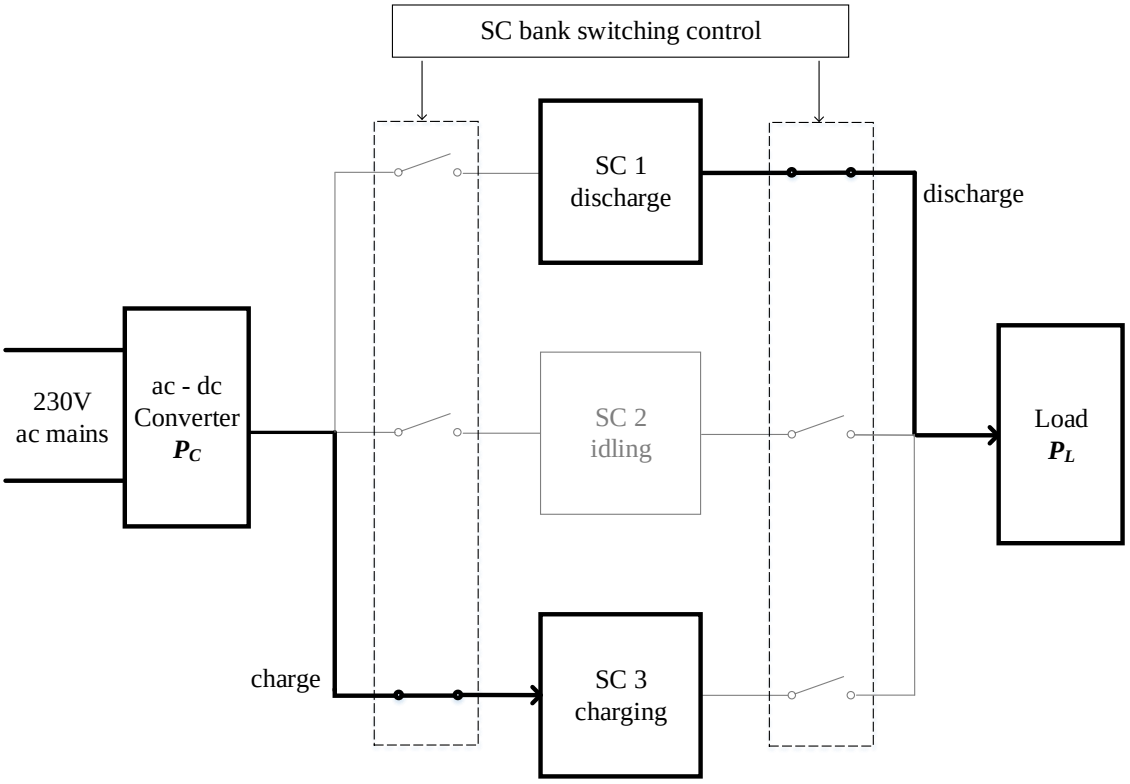

Figure 4.2: Bank circulation technique (a) A three-bank example of the bank circulating technique. The load will be an inverter in the case of SRUPS and a resistive high power heater coil for SCATMA. (b) Generalised scheme of operation for n SC banks circulating for m cycles [6]

In the most generalised case, the ac-dc converter in Fig. 4.2(a) has a power rating of P_C while the load power is P_L, where $P_C < P_L$. Consider the energy storage system shown in Fig. 4.2(b) with n banks operating for m cycles for a period of time T. The energy balance for the system (assuming no switching losses) will be the addition of the total pre-stored energy and the total energy supplied from the charger to the system during the period of operation. Since SCs have very low ESR, if the load resistance is chosen large enough to achieve a higher efficiency according to Eq. (2.18), losses in capacitor discharging can be neglected. According to Eq. (2.11), after one time-constant each SC bank will have delivered 86% of its total energy. When n SC banks are operating for m cycles during time period, T, assuming each bank is allocated equal time ΔT to discharge within each cycle,

$$\Delta T \;=\; \frac{T}{mn}. \tag{4.1}$$

Similarly for charging, each bank will be allocated the same interval ΔT per cycle. This will allow an amount of energy E to be replenished during the ΔT period,

$$E \;=\; \frac{P_C T}{mn} \tag{4.2}$$

During time T a single bank will be replenished $(m-1)$ times, resulting in energy replenishment $(m-1)E$ into a single bank. Including this replenished energy, each capacitor bank will take τ time to discharge 86% of its total energy. Thus

$$\tau \;=\; \frac{[E_C + \frac{(m-1)}{mn} P_C T]\, 0.86}{P_L} \tag{4.3}$$

According to Eq. (4.1) if each bank is given the same discharge time then

$$\tau \;=\; m\,\Delta T \;=\; \frac{T}{n}. \tag{4.4}$$

Substituting in Eq. (4.3),

$$nE_C + P_C T \frac{m}{m-1} = \frac{P_L T}{0.86} \tag{4.5}$$

For each capacitor bank, the circuit time-constant with the load resistance should match the total available discharge time for each bank. Therefore if R_L is the load resistance and R_c is the ESR of the SC bank,

$$C(R_L + R_c) \;=\; \frac{T}{n}. \tag{4.6}$$

According to Eq. (2.18), for a resistive load, if the load resistor is selected to be nine times the capacitor internal resistance, 90% efficiency can be obtained. Hence

$$10\; CR_c \;=\; \frac{T}{n} \quad \Longrightarrow \quad n \;=\; \frac{T}{10\tau}. \tag{4.7}$$

where $\tau \;=\; CR_c$ is the time constant of the SC bank. Independent of the number of rows and columns in a capacitor matrix, the stand-alone bank time constant will be the individual cell time constant as given in Eq. (2.7). For SCs, this time constant value is between 0.6–0.9 s as seen in Table. 4.1. Therefore, on average, τ can be selected to be 0.8. Thus

$$n \;=\; \frac{T}{8}. \tag{4.8}$$

By using Eqs. (4.5) and (4.8), the optimal n and m can be obtained for a given P_C, P_L and T. For example, consider delivering an average power, P_L, of 15 kW to water flowing at 6 Lmin^{-1} to a kitchen tap for $T \;=\; 30$ s with 50 V SC banks in a SCATMA setup. Let the charger power, P_C, be 2.3 kW (the rms power from a 10 A domestic socket

Table 4.1: Maxwell technologies D-cell and K2 series supercapacitor stand-alone time constant based on datasheet nominal capacitance and ESR values

Capacity (F)	ESR (Ω)	Time constant (s)
310	2.2	0.7
350	3.2	1.1
650	0.8	0.5
1200	0.58	0.7
1500	0.47	0.7
2000	0.35	0.7
3000	0.29	0.9

outlet). According to Eq. (4.5), n is chosen to be $30 \div 8 \approx 4$. From Eq. (4.8), C and m are related as

$$4\left(\frac{1}{2}C\ 50^2\right) + 2500\ \frac{m}{m-1}\ 30\ =\ \frac{(15000)(30)}{0.86}. \tag{4.9}$$

By choosing a value for m, C can be obtained as seen in Fig. 4.3. As seen in the figure, the reduction in the bank capacity is minimal for high m. Therefore choosing m to be 4 is a good compromise. When $m\ =\ 4$, $C\ =\ 93.4$ F. For a $p \times q$ capacitor matrix, if each capacitor has capacitance c, by equating the bank voltage and capacitance separately to the specified SC bank voltage and to the obtained C value

$$2.7\ q\ =\ 50\ \text{V}\quad \text{and}\quad \frac{cp}{q}\ =\ 93.4\ \text{F}\ \Longrightarrow\quad q \approx 19\quad \text{and}\quad p\ =\ \frac{1775}{c} \tag{4.10}$$

Based on the individual cell capacity the number of rows will change. For instance, if 650 F cells are chosen, $p\ =\ 3$ rows are required to obtain the correct bank capacity.

4.1.4 Specification for the Charger

The charger required for these applications should overcome the five time-constant charging duration and will be required to deliver only a limited amount of energy. In the case of SCATMA, the operating time will be 30 s to 1 min and in SRUPS, the UPS action is only required for several ac mains cycles, i.e., 20–30 ms. For this sort of fast charging, the converter which feeds the capacitor banks should be able to supply a high current. Since SCs have low ESR they can be discharged very fast. When charging, the low ESR presents almost a dead short circuit to the charger causing the charger to limit its current to the maximum available from the charger. SC chargers are described in the literature, but none of those cater for the special needs of these applications because:

- All available chargers are developed to cater to storage systems of just several joules where the maximum instantaneous current possible is still a few amperes [61–63]

- All approaches have assumed a constant-current/constant-power charging profile with the assumption that the maximum constant charge current is determined by the capacitor ESR
- All chargers are designed for continuous power transfer and pay more attention to charging a capacitor fully rather than paying attention to limited energy transfer at high power to partly replenish a capacitor
- The energy context of available chargers is not comparable with that of SRUPS or SCATMA.

The literature usually deals with continuous power delivery with application-specific requirements on power levels, ripple affordability, efficiency, EMI and power density [64–66]. In contrast, for this specific application the requirements are quite different. The storage banks need to be charged at a higher power rate but still the required energy is finite. The design considerations are

- The charger can charge a capacitor in less time than the traditional five time-constants rule of thumb
- The converter must deliver a finite amount of energy within a limited time
- The thermal management requirements of the converter components can be relaxed because high power is delivered only for a finite period of time and with an adequate rest period for component heat recovery

Given these requirements the topology developed uses a higher source voltage to overcome the five time-constant charging rule, and a coupled inductor technique to quickly replenish the SC bank by dividing it into two parts.

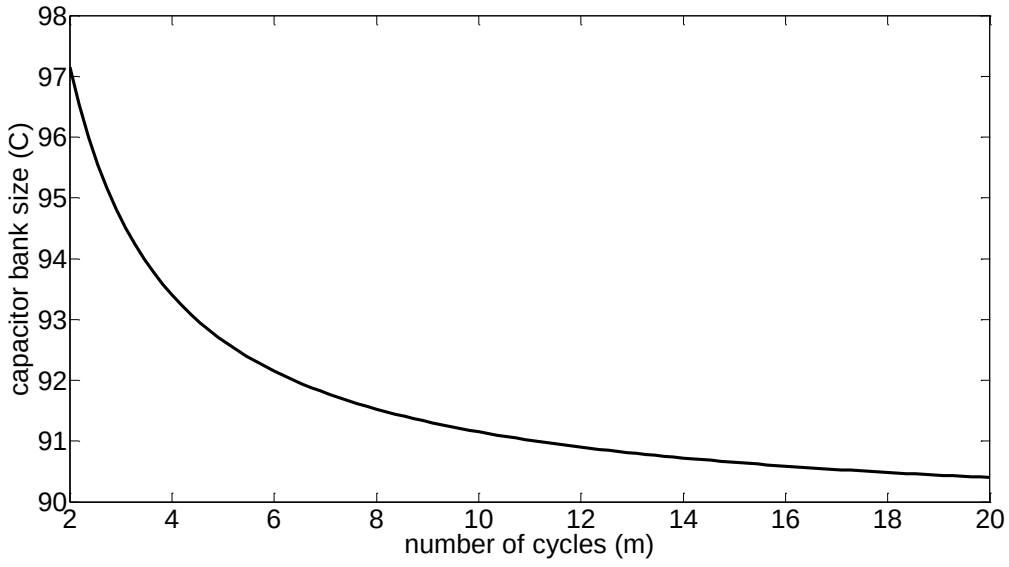

Figure 4.3: Solution for the capacitor bank size variation with increasing number of cycles for the SCATMA application

4.2 Capacitor Charging

A capacitor charger can be uniquely characterised by the associated charge or (number of coulombs) it needs to pump into the capacitor. In normal practice, capacitor charging is done using either a current-limited voltage source or by a current source. The main difference between capacitor charging and supplying power to a resistive load is that the resistive load will take a constant current according to the supplied voltage. Hence a continuous power is consumed by the load. But a capacitor will vary its current and voltage based on its state of charge. One can think of a capacitor as a variable voltage source in series with a resistance. The varying voltage will be the capacitor voltage and the series resistance is the capacitor ESR. When a voltage source is connected to a fully discharged capacitor, the initial current through the circuit I_0 will be

$$I_0 \;=\; \frac{V_s}{R_s + R_{\mathrm{ESR}}} \tag{4.11}$$

where V_s is the open circuit voltage of the voltage source and R_s is the source internal resistance. For a practical example, if a 12 V lead-acid battery with 20 mΩ internal resistance is connected to a string of five 3000 F, 2.7 V SCs with 0.3 mΩ ESR, through thick-gauge copper wire with minimal resistance, the initial current through the circuit will be

$$I_0 \;=\; \frac{12\ \mathrm{V}}{20\ \mathrm{m\Omega} + 0.3 \times 5\ \mathrm{m\Omega}} \;=\; 558\ \mathrm{A}.$$

The initial current is very similar to the battery short circuit current because the capacitor ESR is very small when compared with the internal resistance of the battery (13 times smaller). Using a current-controlled voltage source for capacitor charging will overcome this issue of drawing an initial high current from the source by setting the maximum current I to the maximum capability of the source. The power P_{cc} delivered from a current limited voltage source in capacitor charging will be

$$P_{cc}(t) \;=\; I v_c(t) \tag{4.12}$$

where $v_c(t)$ is the varying voltage across the charging capacitor. Though the charging current is fixed, since the capacitor voltage varies from 0 V to the full charge voltage, the output power will also vary depending on the capacitor voltage. With an ideal voltage source a fully discharged capacitor (C) takes five RC time-constants to effectively reach its full charge, where R is the total resistance of the charging loop. For a current source with maximum current rating of I, the time to charge will be CV_C/I. Based on the previous two relationships, the capacitor charging time is dependant on circuit parameters for a voltage source and on the source current limit for a current source. The following section details several combinations of source voltages and currents for charging a capacitor, and investigates how a capacitor can be charged faster by using a current-limited voltage source, set at a multiple of the capacitor-rated voltage, to fast charge the capacitor.

4.2.1 Capacitor Charging Methods

This section compares the time taken by four differently configured voltage sources to fully charge a capacitor up to its rated voltage (V_c) starting from zero.

1. Voltage source at capacitor-rated voltage with no current limit

   This is the typical textbook case for charging a capacitor from a voltage source. Capacitor voltage $v(t)$ and current $i(t)$ will be

   $$v(t) \;=\; V_c(1 - e^{-t/\tau}), \quad i(t) \;=\; \frac{V_c}{R} e^{-t/\tau} \tag{4.13}$$

   where $\tau \;=\; RC$ is the circuit time-constant. Capacitor voltage $v(t)$ reaches $0.993V_c$ after five time constants. For the capacitor to be charged at this rate the source should be capable of supplying the maximum current of V_c/R. Fig. 4.4, case (1) illustrates the voltage and current plots.

2. Voltage source at capacitor rated voltage with current limit I

   Most practical capacitor chargers will be of this nature. Since they are unable to deliver the high currents, they will operate in constant-current mode until the current requirement of the circuit goes below I or, equivalently, until the capacitor is charged up to $V_c - IR$. The constant current charging duration t_{I} will be

   $$t_{\mathrm{I}} \;=\; \frac{C}{I}(V_c - IR). \tag{4.14}$$

   Voltage across the capacitor during this period will be

   $$v_{\mathrm{I}} \;=\; \frac{It}{c}. \tag{4.15}$$

   After t_{I}, the capacitor will follow an exponentially decaying current until the capacitor is fully charged. At $t \;=\; t^*$, the capacitor voltage will be $V_c - IR_L$ on a non-current limited charging curve, hence

   $$t^* \;=\; -RC \;\ln\left[1 - \frac{V_c - IR}{V_c}\right] \;=\; RC \;\ln\left[\frac{V_c}{IR}\right] \tag{4.16}$$

   Capacitor voltage and current during this period will be

   $$v \;=\; V_c(1 - e^{-t'/\tau}) \;=\; \frac{V_c}{R}\, e^{-t'/\tau} \tag{4.17}$$

   $$\text{where } t' \;=\; t - t_{\mathrm{I}} + t^*$$

   These voltage and current curves are shown in Fig. 4.4, case (2). The total time taken to fully (99.3%) charge the capacitor is

   $$T_2 \;=\; t_{\mathrm{I}} + (5RC - t^*) \;=\; \frac{C}{I}(V_c - IR) + 5RC - RC \ln\left[\frac{V_c}{IR}\right] \tag{4.18}$$

$$\implies T_2 = \frac{CV_c}{I} + 4RC + RC\ln\left[\frac{IR}{V_c}\right] \tag{4.19}$$

3. Voltage source at m ($m > 1$) times the capacitor-rated voltage with no maximum current limit

   The voltage and current curves for this charging method are shown in Fig. 4.4, case (5). Capacitor voltage and the current will be

$$v(t) = mV_c(1 - e^{-t/\tau}), \quad i(t) = \frac{mV_c}{R}e^{-t/\tau} \tag{4.20}$$

   Time taken for the capacitor voltage to reach V_c is T_3

$$V_c = mV_c(1 - e^{-T_3/\tau}) \tag{4.21}$$

$$T_3 = \tau\ln\left[\frac{m}{m-1}\right] \tag{4.22}$$

   This time can only be achieved if the source can supply mV_c/R initial current. In comparison with case (1), the start-up current is m times higher. Another important point in this charging scheme is that, even when the capacitor reaches its full charge voltage, the circuit current is non-zero. Therefore a capacitor terminal voltage monitoring circuit and a switch are required to extinguish the charging current once the capacitor reaches full charge.

4. Voltage source at m times the capacitor rated voltage with current limit I

   In this charging scheme, the value of source factor (m) should be higher than a critical value m^* to ensure that the capacitor will get charged from a continuous current until it reaches its rated voltage V_c

$$mV_c - IR > V_c \quad \implies \quad m > 1 + \frac{IR}{V_c} = m^* \tag{4.23}$$

   There are two cases to consider
   (a) When $1 < m < m^*$

   The source voltage is lower than the critical source factor m^*. The charging profile is not a continuous current. When the capacitor voltage is equal to $mV_c - IR$, at time $t_1 = \frac{C}{I}(mV_c - IR)$, the charging profile will change from a constant current to a decaying current until the capacitor is fully charged. The time taken from the

change-over point until the capacitor reaches its full voltage can be calculated in a similar way to case (2). The time taken to charge the capacitor to V_c if the source is not current limited is

$$RC \ln \left[\frac{m}{m-1} \right]. \tag{4.24}$$

The time at which the change-over occurs from constant current to a decaying current with non-current-limited charging is

$$t^* \;=\; RC \ln \left[\frac{mV_c}{IR} \right]. \tag{4.25}$$

Therefore the current-limited source will supply a decaying charging current for a time

$$RC \ln \left[\frac{m}{m-1} \right] - RC \ln \left[\frac{mV_c}{IR} \right] \;=\; RC \ln \left[\frac{IR}{V_c(m-1)} \right]. \tag{4.26}$$

Hence the total time taken to charge the capacitor is

$$T_4 \;=\; \frac{C}{I} mV_c + RC + RC \ln \left[\frac{IR}{V_c(m-1)} \right]. \tag{4.27}$$

The source will supply continuous current I for time t_I. The voltage across the capacitor during this period will be

$$v_{\mathrm{I}} \;=\; \frac{It}{C}. \tag{4.28}$$

The current and voltage after t_{I} will be

$$v(t) \;=\; mV_c(1 - e^{-t'/\tau}), \quad i(t) \;=\; \frac{mV_c}{R}\, e^{-t'/\tau} \tag{4.29}$$

$$\text{where } \; t' \;=\; t - t_{\mathrm{I}} + t^*. \tag{4.30}$$

Reduction in charging time compared to case (2) from Eqs. (4.19) and (4.27),

$$\Delta T_1 \;=\; T_2 - T_4 \;=\; \frac{CV_c}{I}(1-m) + 5RC + RC \ln(m-1) \tag{4.31}$$

(b) When $m > m^*$

The capacitor will continue to be charged by the continuous current I until it is fully charged

$$T_5 \;=\; \frac{CV_c}{I} \tag{4.32}$$

The capacitor voltage will rise linearly according to

$$v(t) \;=\; \frac{I}{C}\, t \tag{4.33}$$

The reduction in charging time compared to case (2) from Eqs. (4.19) and (4.32) is

$$\Delta T_2 \;=\; T_2 - T_5 \;=\; 4RC + RC \ln \left[\frac{IR}{V_c} \right] \tag{4.34}$$

In Fig. 4.4, cases 3 & 4 are for the critical value $m = m^*$ with two different charging currents. The increase in charging current causes a linear decrease in charging time since the charger voltage is at the critical value. If the charger voltage was not at (or beyond) this critical value, the charging time reduction will not be as effective. For example, for a 30 A rated charger with $m = 1.2$, the charging time will be 80.7 s.

Table 4.3 compares the different charging times taken by each source to charge a capacitor and the maximum current required for a 100 F, 10 V SC bank with a total path resistance of $R = 250$ mΩ. By comparing the second and the last rows, a 53% charging time reduction is achieved by using a higher-voltage-rated source even with the same current rating of 15 A. The shortest charging time is achieved by using a voltage source at 20 V ($m = 2$) with no current limit. This requires the source to be capable of delivering 80 A at start up, so this charging scheme becomes less practical. In summary it is seen that even with the same current limit a source with a voltage higher than the capacitor rated voltage will charge a capacitor faster than a source with the capacitor rated voltage. This is seen in Fig. 4.4 cases (3) and (4).

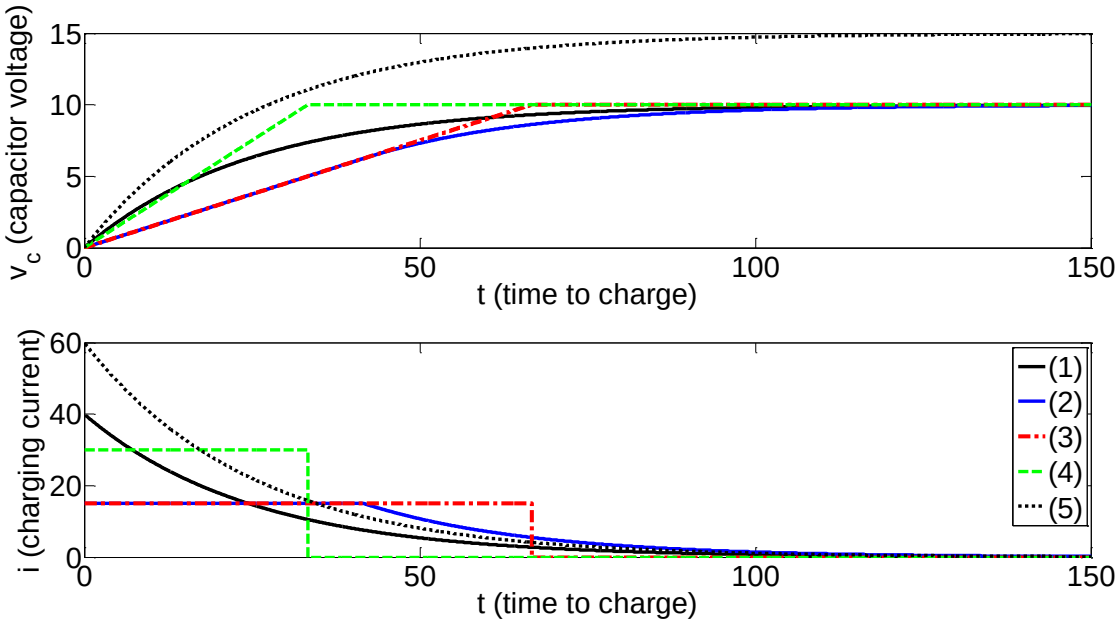

Figure 4.4: Capacitor charging methods, current and voltage profiles. A comparison for a 100 F, 10 V SC bank with 250 mΩ path resistance. (1) $m = 1$, $I = 40$ A (2) $m = 1$, $I = 15$ A (3) $m = m^*$, $I = 15$ A (4) $m = m^*$, $I = 30$ A (5) $m = 1.5$, $I = 60$ A

Table 4.2: Comparison of capacitor charger types

Charging source type	Time to charge (s)	$I_{\max}$ (A)
V_c source with no current limit	$5CR$	V_c/R
V_c source with I current limit	$CV_c/I + 4RC + RC\ln(IR/V_c)$	I
mV_c source with no current limit	$RC\ln[m/(m-1)]$	mV_c/R
mV_c source with I current limit ($m < m^*$)	$mCV_c/I + RC + RC\ln[IR/V_c(m-1)]$	I
mV_c source with I current limit ($m \geq m^*$)	CV_c/I	I

4.3 Charging a Capacitor with a High Voltage

4.3.1 Basics of Charging a Capacitor

The previous section looked at several different ways of charging a capacitor. When the capacitor to be charged is a big SC bank, the task of charging becomes more challenging. Depending on the size of the SC bank, the energy requirement of a SC bank can be comparable to a battery. Due to the absence of an electrochemical potential in a discharged SC, the currents drawn will be high. Using a current-limited source will overcome this initial high current issue. When using a voltage source rated at a voltage higher than the capacitor working voltage, this constant current charging can be made faster. This section will look at the basic principle of charging a capacitor via a resistive path; this will be compared with charging via an inductive-resisive path in the next section. This comparison will consider the time taken to fully charge the capacitor and the efficiency of the charging process.

The general scenario of capacitor charging required in SCATMA and SRUPS is the subject of the analysis. It is based on a source voltage higher than the capacitor rated voltage . This source is to recharge a partially discharged capacitor to its rated voltage. Previously it was seen that a capacitor will deliver 86% of its total stored energy within

Table 4.3: Capacitor charger types comparison for a 100 F, 10 V SC bank with $R = 250$ mΩ. Current limit is kept blank for sources which can deliver much higher currents than required. For the 4^{th} and 5^{th} rows $m^* = 1.375$

Source factor m	Current limit I	Time to charge (s)	$I_{\max}$ (A)
1		125	40
1	15	142.1	15
1.5		27.4	60
$1.2 < m^*$	15	116.7	15
$m^* < 1.4$	15	66.6	15

one circuit time-constant. The reduced capacitor terminal voltage after the first time-constant will result in low output power. Therefore in most applications where capacitors are used, they are only allowed to be partially discharged hence the analysis will consider charging a partially discharged capacitor.

As seen in Fig. 4.5 for a capacitor C rated at V_c terminal voltage, a high voltage source of mV_c (source factor $m > 1$) is used to charge the capacitor from nV_c (start factor n with $n < 1$) to V_c through the lumped resistance R which represents the addition of the source internal resistance, path resistance and the capacitor ESR.

If q represents charge, a fully charged capacitor holding charge Q for voltage V_c will have charge nQ at the beginning of the charging process. The total amount of energy stored in the capacitor E_C when charged from nV_c (charge nQ) to V_c (charge Q) will be the work done on the electric field of the capacitor

$$E_C = \int_{nQ}^{Q} v_c \, dq \tag{4.35}$$

Since $q = Cv_c$ this can be rewritten as

$$E_C = \frac{1}{C}\int_{nQ}^{Q} q \, dq = \frac{Q^2}{2C}(1 - n^2). \tag{4.36}$$

If the capacitor takes time T to be fully charged, from the circuit loop equation the value for T can be solved as follows

$$\begin{aligned} mV_c &= i(t)R + v_c(t) \\ &= i(t)R + nV_c + \frac{1}{C}\int i(t)\, dt \end{aligned} \tag{4.37}$$

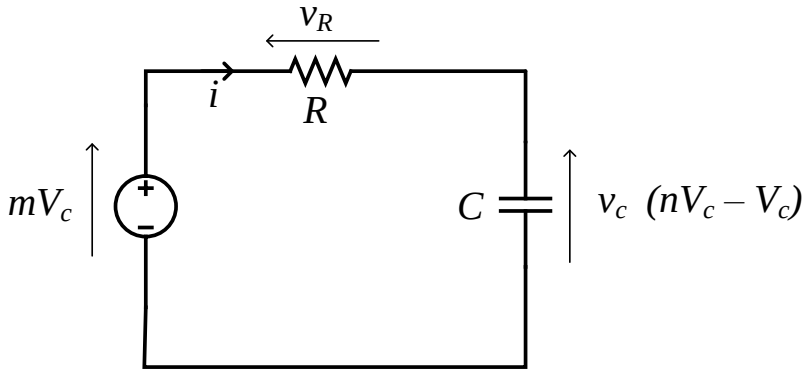

Figure 4.5: Charging a partially discharged capacitor from a high voltage source through a purely resistive path

By Laplace transform, where s is complex frequency and $I(s) \equiv \mathcal{L}\, i(t)$

$$\begin{aligned} \frac{mV_c}{s} &= I(s)R + \frac{nV_c}{s} + \frac{1}{Cs}I(s) \\ \implies I(s) &= \frac{(m-n)}{RCs+1}CV_c \\ &= (m-n)\frac{V_c}{R}\,\frac{1}{s+\frac{1}{RC}} \end{aligned} \tag{4.38}$$

By the inverse Laplace transform,

$$i(t) = (m-n)\frac{V_c}{R}e^{-t/RC}. \tag{4.39}$$

Substituting in Eq. (4.37),

$$v_c(t) = mV_c - (m-n)V_c e^{-t/RC}, \tag{4.40}$$

and as at time T, $\quad v_c(t) = V_c$,

$$T = RC\,\ln\left(\frac{m-n}{m-1}\right). \tag{4.41}$$

When the capacitor is charged from nV_c to V_c, the amount of energy, E_R, lost in the lumped resistance R is

$$\begin{aligned} E_R &= \int_0^T i^2(t)R\,dt \\ &= \int_0^T (m-n)^2\frac{V_c^2}{R}\,e^{-2t/RC}\,dt \\ &= \frac{1}{2}CV_c^2(1-n)(2m-n-1) \\ &= \frac{Q^2}{2C}(1-n)(2m-n-1) \end{aligned} \tag{4.42}$$

The efficiency of charging increases when the capacitor stores more energy than that lost in the resistor. Therefore $E_C - E_R$ should be positive

$$E_C - E_R = \frac{Q^2}{C}(1-n)(1+n-m) = \frac{Q^2}{C}(1-m-n^2+mn). \tag{4.43}$$

Given the ranges for m and n

$$m > 1,\ 0 < n < 1 \quad \Leftrightarrow \quad \forall n,\ 1-n > 0 \text{ and } 1+n < 2 \tag{4.44}$$

Then for efficient charging

$$E_C - E_R > 0 \implies (1+n) - m > 0 \tag{4.45}$$

$$\implies m < (1+n) < 2 \tag{4.46}$$

$$\Leftrightarrow m < 2 \tag{4.47}$$

Table 4.4: Charging a capacitor from a voltage source at capacitor rated voltage through a resistive path.

Start factor n	Capacitor energy E_C	Resistive loss E_R	$E_C - E_R$
0	$\frac{Q^2}{2C}$	$\frac{Q^2}{2C}$	0
n	$\frac{Q^2}{2C}(1-n^2)$	$\frac{Q^2}{2C}(1-n)^2$	$\frac{Q^2}{C}n(1-n)$

Further for optimum performance $E_C - E_R$ should be maximised. For this the first derivative of $E_C - E_R$ should be zero.

$$\frac{\partial}{\partial n}(E_C - E_R) = 0 \quad \Longrightarrow \quad -2n + m = 0 \quad \Longrightarrow m = 2n \tag{4.48}$$

$$\frac{\partial}{\partial m}(E_C - E_R) = 0 \quad \Longrightarrow \quad n - 1 = 0 \quad \Longrightarrow \quad n = 1 \tag{4.49}$$

Here, $n = 1$ represents a capacitor not discharged, so there will not be any effective energy transfer occurring. Hence it is practically unimportant. The optimum will be when $m = 2n$. Since $n < 1$, this will meet the previous condition of $m < 2$ as well. Two special scenarios within this generalised charging scheme are illustrated in Table 4.4. The first scenario is for charging a capacitor fully discharged from a voltage source at the capacitor rated voltage. This method loses the same amount of energy as stored in the capacitor in the lumped resistor irrespective of the value of the total resistance of the charging path. The second scenario is charging a partially discharged capacitor from a voltage source at the capacitor rated voltage. The losses are dependant on the start factor n and they vary as seen in Fig. 4.6. For the scenario depicted in Fig. 4.6, the best charging efficiency is achieved when $E_C - E_R$ maximises. That is when the first derivative of $E_C - E_R$ with respect to n becomes zero:

$$\frac{d}{dn}[n(1-n)] = 0 \quad \Longrightarrow \quad n = \frac{1}{2}. \tag{4.50}$$

At this n value, the capacitor will store $0.75\frac{Q^2}{2C}$ energy and the resistor will lose $0.56\frac{Q^2}{2C}$ energy. Normalized by the capacitor total energy storage, $\frac{Q^2}{2C}$, this is equal to 75% and 56% respectively at the capacitor and the resistor.

Fig. 4.7 shows experimental results obtained to verify the reduction in charging time by charging a capacitor with a high-current power supply with terminal voltage m times the capacitor rated voltage. As the source voltage increases, the maximum current capability should also increase to achieve this advantage. When using a voltage higher than the capacitor rated voltage to charge a capacitor, a terminal voltage monitoring switch should be used to avoid capacitor overcharge.

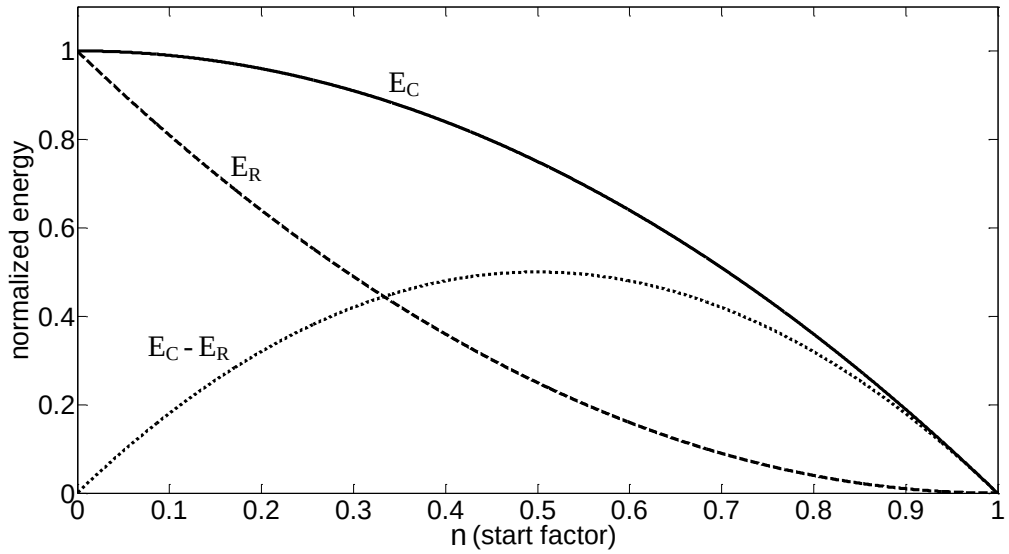

Figure 4.6: Efficiency of charging a capacitor in a resistive path. All energy values are normalized by $Q^2/2C$

Fig. 4.8 illustrates that charging time reduction (ΔT) achieved by using a charger voltage m times higher, increases with higher charging current values and higher source factors (i.e. higher charger voltages). ΔT is calculated by subtracting T_{mV_c} (the time taken by the mV_c source) from T_{V_c} (the time taken by the V_c source) with the same current limit:

$$\Delta T = T_{V_c} - T_{mV_c}. \tag{4.51}$$

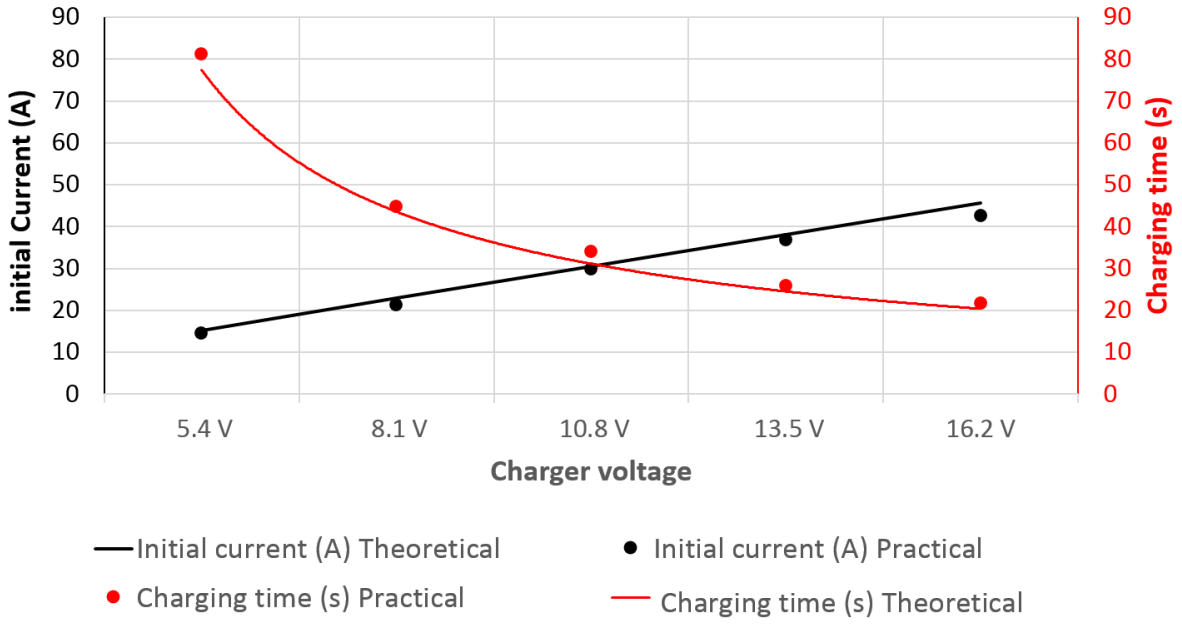

Figure 4.7: Charging time improvement and initial charging current variation of high voltage charging with terminal voltage monitoring for a 310 F, 2.7 V capacitor

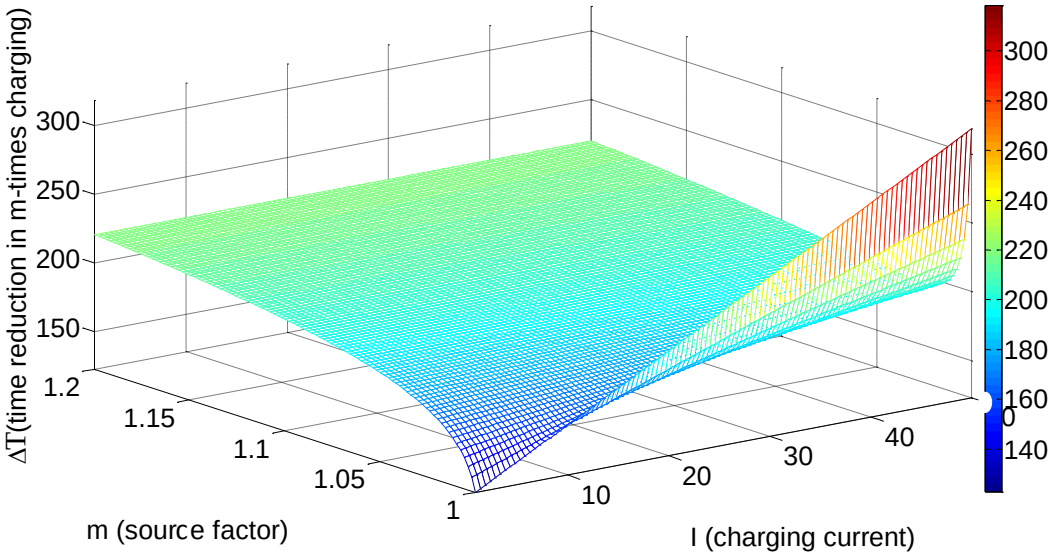

Figure 4.8: Charging time improvement of high voltage charging with terminal voltage monitoring for a 310 F, 2.7 V capacitor

The following section examines the case when the charging path becomes inductive. When the charging source voltage is higher than the capacitor rated voltage, even when the capacitor is fully charged the circuit current is nonzero. Therefore if the charging path is strongly inductive, inductive energy $\frac{1}{2}Li^2$ will be stored in the inductor. By creating a secondary capacitor charging path to use this energy, the overall charging efficiency can be improved. Further, by having a series inductor in the charging path, the initial current rise will be controlled by the inductor.

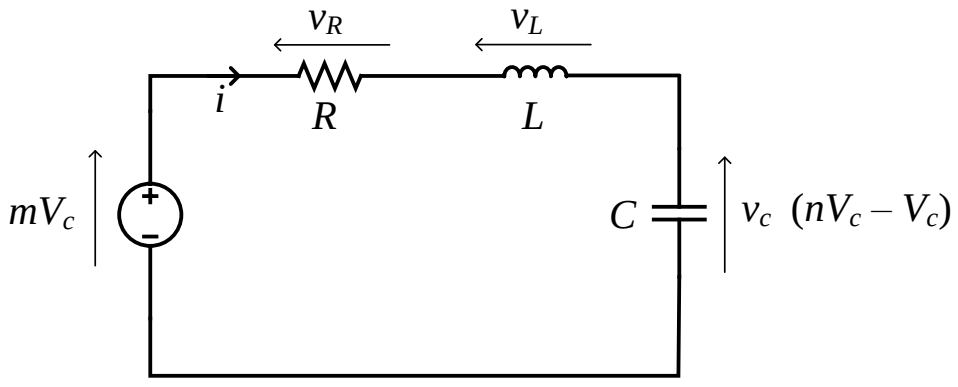

Figure 4.9: Charging a partially discharged capacitor from a high voltage through an inductive path

4.3.2 Charging a Capacitor Through an Inductive Path

A series inductor, L, is added to the circuit to model an inductive charging path. Consider a partially discharged capacitor being charged from nV_c with source factor $(n < 1)$ to V_c from voltage source mV_c with m and n having the same definitions as the previous section.

Applying Kirchoff's voltage law to the loop

$$mV_c \;=\; v_R(t) + v_L(t) + v_C(t) \tag{4.52}$$

$$mV_c \;=\; i(t)R + L\frac{di(t)}{dt} + nV_c + \frac{1}{C}\int_0^t i(t)dt \tag{4.53}$$

By Laplace transform

$$\frac{mV_c}{s} \;=\; I(s)R + LsI(s) + \frac{nV_c}{s} + \frac{1}{Cs}I(s) \tag{4.54}$$

where s is complex frequency and $I(s) \equiv \mathcal{L}i(t)$. Solving for $I(s)$

$$I(s) \;=\; (m-n)\,\frac{V_c}{L}\,\frac{1}{\left[s+\frac{R}{2L}\right]^2 + \left[\sqrt{\frac{4L-R^2C}{4L^2C}}\right]^2} \tag{4.55}$$

According to Eq. (4.55), the current response will depend on the size of the inductor. Depending on the sign of the square root term (based on L), one of three different current responses will occur.

Case 1: Underdamped oscillations $(L > R^2C/4)$

Circuit resistance is small compared to the inductor and the capacitor, alternatively a large inductor.

$$i_1(t) \;=\; 2(m-n)V_c\;\sqrt{\frac{C}{4L-R^2C}}\;\;e^{-Rt/2L}\;\;\sin\left[\sqrt{\frac{4L-R^2C}{4L^2C}}\;\;t\right]. \tag{4.56}$$

The response for the underdamped system is a decaying sine wave as seen in Fig. 4.10(a).

Case 2: Critically damped oscillations $(L \;=\; L_{\text{crit}} \;=\; R^2C/4)$

At this critical inductor value the circuit current response will be,

$$i_2(t) \;=\; \frac{4}{R^2C}\,(m-n)V_c\;t\;e^{-2t/RC} \tag{4.57}$$

The response for the critically-damped system is seen in Fig. 4.10(b).

Case 3: Over damped oscillations $(L < R^2C/4)$

Circuit resistance is large compared to the inductor and the capacitor, alternatively a smaller inductor.

$$i_3(t) \;=\; 2(m-n)V_c \sqrt{\frac{C}{R^2C-4L}}\;\; e^{-Rt/2L}\;\; \sinh\left[\sqrt{\frac{R^2C-4L}{4L^2C}}\;\; t\right] \tag{4.58}$$

The under-damped system response is shown in Fig. 4.10(c).

The case 3 current rise is the fastest, when the inductance is the smallest. Since the intention of this analysis is to find the fastest charging method and compare its efficiency with a RL system, the overdamped response will be the choice.

Similar to an RL system the energy stored in the capacitor will be the same as given in Eq. (4.36),

$$E_C \;=\; \frac{Q^2}{2C}(1-n^2). \tag{4.59}$$

To find the amount of energy stored in the inductor and the energy lost in the resistor when the capacitor is fully charged, first the time taken by the capacitor to fully charge should be calculated. If the source is capable of delivering the high currents required and the source runs continuously, then the time T taken can be obtained as follows:

$$v_c(t) \;=\; nV_c + \frac{1}{C}\int_0^t i(t)dt \tag{4.60}$$

If $v_c(t \;=\; T) \;=\; V_c$

$$v_c(T) \;=\; V_c \;=\; nV_c + \frac{1}{C}\int_0^T i(t)dt. \tag{4.61}$$

When the capacitor reaches full charge the energy stored in the inductor E_L and the energy lost in the resistor E_R can be calculated as:

$$E_L \;=\; \frac{1}{2}LI^2, \qquad E_R \;=\; R\int_0^T \; i^2(t)\; dt \tag{4.62}$$

where $I \;=\; i(t \;=\; T)$. Because these equation cannot be solved analytically, an ordinary differential equation solver in MATLAB is used to find a numerical solution for the T-time to charge. Hence the E_L and E_R can be obtained. Appendix D gives more details of the simulation. Fig. 4.11 shows the simulation results for charging time, energy stored in the inductor and energy lost in the resistor. With higher source factors, the charging time has reduced as expected. As m increases, resistive losses increase due to the high currents. Meanwhile, a higher source voltage has increased the energy stored in the inductor when the capacitor is fully charged. Hence by selecting a bigger inductor the resistive heating losses can be minimised.

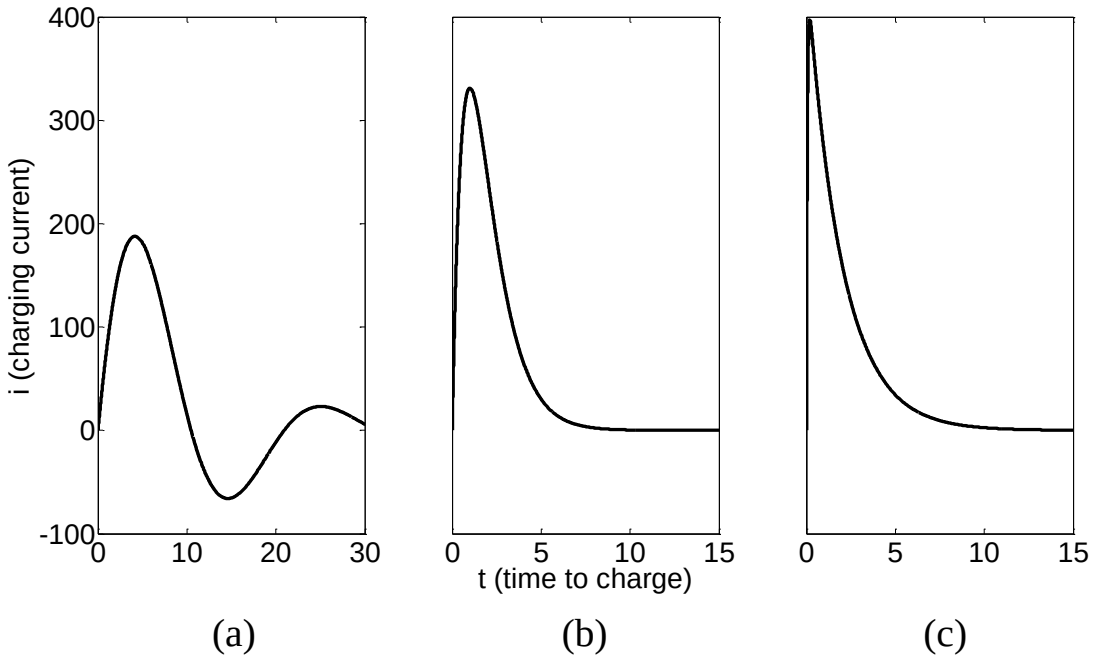

Figure 4.10: The three current responses of a RLC system. (a) underdamped, (b) critically damped and (c) overdamped. e.g., $R = 40$ mΩ, $C = 50$ F, $m = 2$, $n = 0.5$, $V_c = 12$ V, $L_{\text{critical}} = R^2C/4$, $L_{\text{over}} = 10L_{\text{crit}}$, $L_{\text{under}} = 0.1L_{\text{critical}}$

4.3.3 RC vs RLC Charging Efficiency

MATLAB simulations on high voltage charging were used to compare the efficiency of an RC charging scheme with an RLC scheme with a series inductor in the charging path controlling rate of current rise. Fig. 4.12 compares the percentage energy loss of an RC system and an RLC system charging the same capacitor with the same path resistance. The source factor, m, is varied for charging a partly discharged capacitor from nV_c to Vc where $n < 1$. Percentage energy loss ($\%E_{loss}$) is calculated based on energy loss in the resistor (E_R), energy stored in the inductor (E_L) and capacitor (E_c). E_L is zero for the RC system

$$\%E_{loss} = \frac{E_R}{E_R + E_c + E_L} \times 100\% \tag{4.63}$$

Values for E_R, E_c and E_L were solved numerically using MATLAB to obtain efficiencies. Based on these results, a charger topology which is capable of reusing the energy stored in the inductor (to charge another part of the same capacitor bank) will always perform better than an RC charging scheme. From Fig. 4.12 it is seen that an RLC system becomes more efficient as the source factor increases. This is mainly due to the increase in the stored energy in the inductor when using a higher source voltage. By using a suitable technique which can reuse the stored energy in the inductor, these efficiency gains can be achieved. The use of the high voltage source and the series inductor reduces the charging time and improves overall charging efficiency.

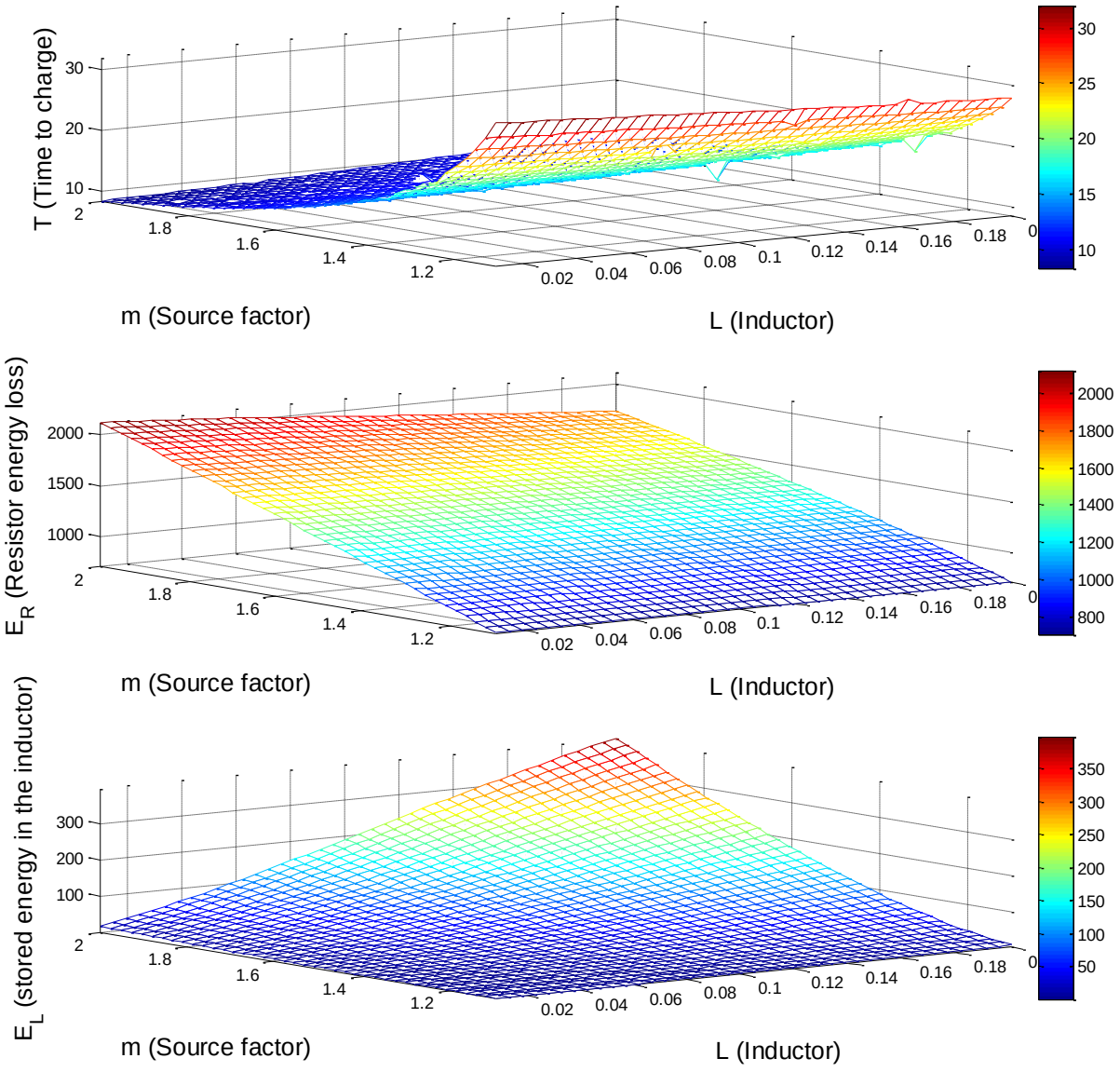

Figure 4.11: Charging a capacitor through an inductive path. $V_c = 2.7$ V, $R = 50$ mΩ, $C = 310$ F and $n = 0.3$

4.3.4 Practicalities of a Real World Switched-mode Converter With a Series RLC Arrangement

For the case of a switching converter with a series RLC arrangement, the same simulation can be extended with the following simplifications:

- If the operating frequency is high enough to avoid inductor L saturation then the current rise Δi through the inductor for a constant source voltage of V during the time duration Δt can be calculated using the linear equation

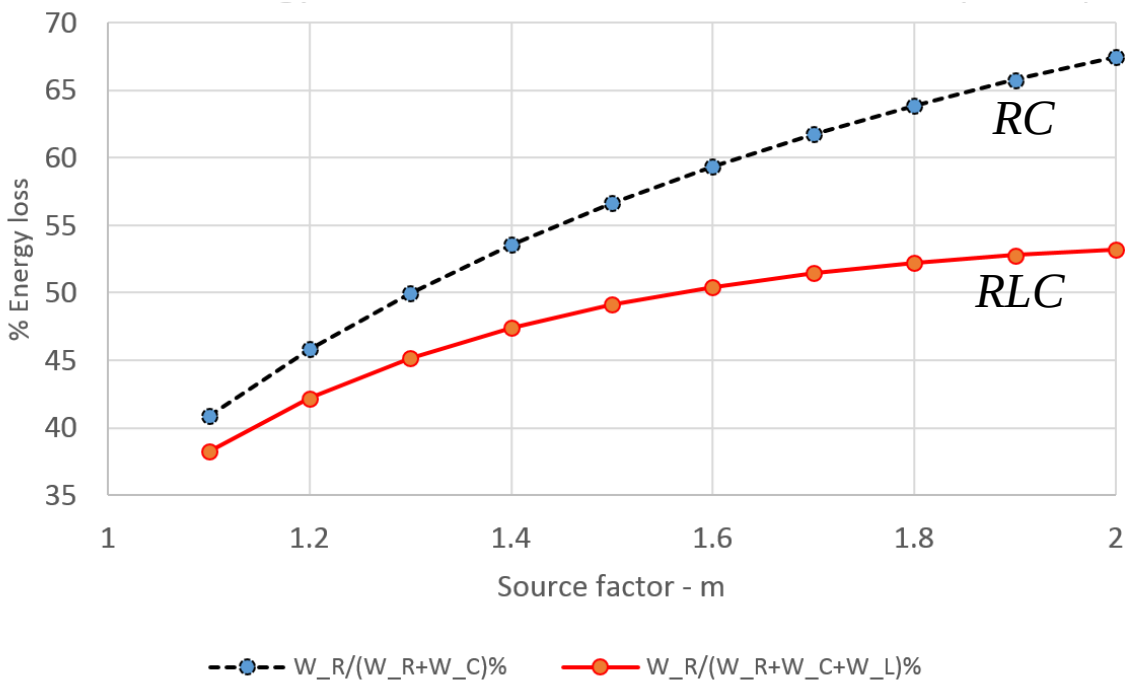

Figure 4.12: Efficiency improvement of a RLC system over a RC system for m-times charging ($C = 310$ F, $L = 2$ mH, $R = 50$ mΩ, $V_C = 2.7$V, $n = 0.3$)

$$V = L\frac{\Delta i}{\Delta t}$$

- If the source factor is large enough then the effect of the start factor can be neglected. particularly in the case if using the mains voltage (230 V) to charge a low voltage ($<$ 50 V) SC bank
- The energy stored in the inductor during the "on" time is emptied during the "off" time. In this way it can be assured that at the beginning of each switching cycle the inductor magnetic field will be fully relaxed

From the first assumption stated above, if the series RLC circuit is switching at a frequency f_{sw} with a fixed 50% "on" time (for simplicity) then the circuit current will rise to a maximum current I:

$$mV_c = L\frac{I}{\frac{1}{2}\frac{1}{f_{sw}}} \qquad \Longrightarrow \qquad I = \frac{mV_c}{2Lf_{sw}} \tag{4.64}$$

where m is the source factor and V_c is the capacitor rated voltage. To calculate the percentage energy loss of this system, using Eq. (4.63) for a single switching cycle would be sufficient due to the assumption that the inductor is fully relaxed at the end of each switching cycle. The equation for the "on" time current rise will be

$$i(t) = 2If_{sw}t \tag{4.65}$$

The energy stored in the inductor can be calculated as

$$E_L \;=\; \frac{1}{2}LI^2 \;=\; \frac{m^2\,V_c^2}{8\,L\,f_{sw}^2} \tag{4.66}$$

The energy lost in the inductor during a single switching cycle "on" time can be calculated based on the area under the instantaneous resistive power dissipation curve ($i^2(t)R$)

$$E_R \;=\; \int_0^{1/2f_{sw}} 4I^2 f_{sw}^2 R t^2\,dt \;=\; \frac{I^2R}{6f_{sw}} \;=\; \frac{m^2V_c^2R}{24L^2f_{sw}^3} \tag{4.67}$$

Similarly the energy stored in the capacitor at the end of the "on" time can be calculated based on the area under the current curve

$$E_C \;=\; \frac{1}{2}\left[\frac{1}{2}\frac{1}{2f_{sw}}I\right]^2\frac{1}{C} \;=\; \frac{m^2\,V_c^2}{128\,L^2\,C\,f_{sw}^3} \tag{4.68}$$

During the "off" cycle, the energy stored in the inductor is used to charge another similar size capacitor through a total path resistance, R. Assume a perfect-coupled inductor used to transfer the stored energy in the inductor has a turns ration of $n:1 (n>1)$. During the "off" cycle the current through the second capacitor will ramp down to zero starting with nI. Hence the resistive energy loss in the secondary capacitor charging path, E_{Rs}, can be calculated in a similar way to the E_R calculation as

$$E_{Rs} \;=\; \frac{m^2V_c^2Rn^2}{24L^2f_{sw}^3} \tag{4.69}$$

Based on these expressions the theoretical converter efficiency, η, can be calculated as,

$$\eta \;=\; \left[1-\frac{E_R+E_{Rs}}{E_C+E_R+E_L}\right]100\% \tag{4.70}$$

This equation was simulated in MATLAB for a power converter operating from the 230 V mains at 20 kHz to charge two 360 F, 25 V SC banks. The series inductor is 2 mH and both capacitor charging paths are assumed to have the same total loop resistance of 50 mΩ. When the transformer turns ratio, n, is varied from 1–10, the theoretical efficiency varies from 99.9% to 94.1% assuming a lossless coupled inductor. Results are shown in Fig. 4.13. This theoretical simulation was done for a real world application of SCATMA where 150 Wh is stored in two 25 V SC banks.

Based on the above observation of charging a capacitor in an RLC arrangement through a switching converter it can be concluded that a good transformer design with low leakage and core loss is essential for achieving high efficiency. The main advantage of a switching RLC system over an RC system is that resistive energy losses are reduced since the circuit current is not allowed to rise beyond a certain value dictated by the inductor size.

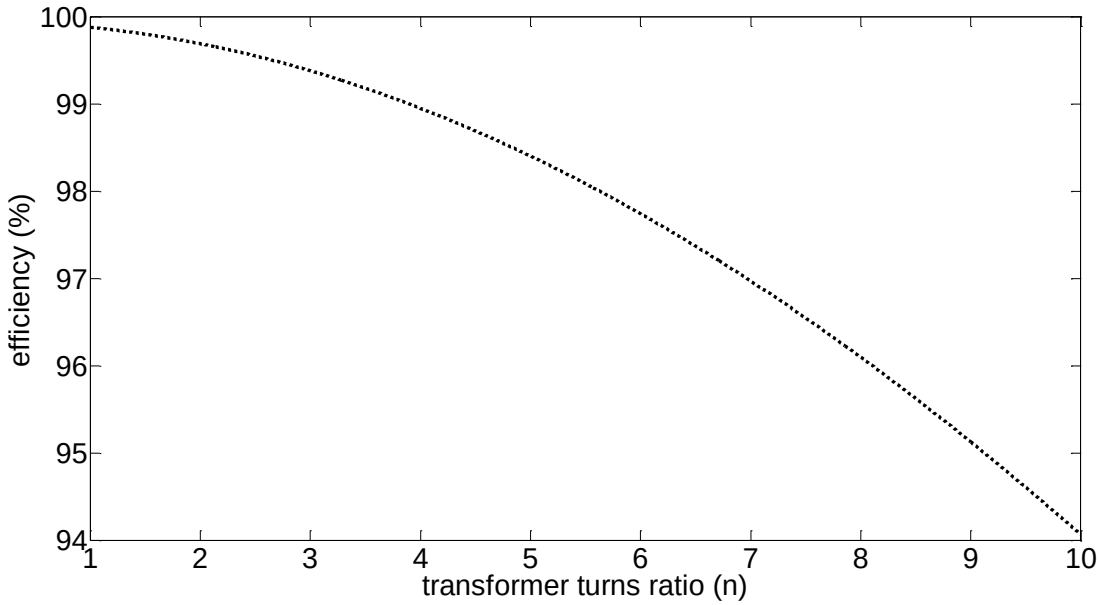

Figure 4.13: Theoretical efficiency of a switching power converter with an inductive energy reusing scheme. ($V_c = 25$ V, $m = 10, C = 360$ F, $f_{sw} = 20$ kHz, $L = 2$ mH and $R = 50$ mΩ)

4.3.5 Fast and Efficient Capacitor Charging technique

In SCATMA, SRUPS or other short-duration high-power applications which use SCs for energy storage, can use a fast charger to either reduce the amount of pre-stored energy or to improve the SC charging efficiency. Several applications where high-power limited-energy is used are described below.

- Portable nail guns

  A nail gun is not a tool essentially designed for continuous use. A SC-based nail gun can use a fast charger to reduce the duration between two nailing operations.
- 1–2 cup boiling-hot water dispensers

  A refrigerator with this facility can use a fast SC charger to reduce the amount of pre-stored energy and to reduce the time between two successive uses.
- High-efficient washing machines

  At the beginning of a washing cycle, to quickly dissolve the detergent an "instant" water boiler can be made using SCs. By using a fast SC charger the amount of pre-stored energy in SCs can be reduced.
- Sink-waste crushers

  These systems will only operate for a short duration at high power. Efficiency of such a system can be improved by using pre-stored SC energy to drive a dc motor. A fast charger can reduce the amount of pre-stored energy.

- Cargo-tow tractors

  For electric tow tractors at airports to reduce the SC bank recharging time

It was observed in the previous section on capacitor charging, that by using a higher source voltage than the capacitor rated voltage, a capacitor can be charged in less than five time constants. This argument is true for even current limited sources as seen in Table 4.3. When using a higher source voltage for charging a capacitor, charging should be extinguished by sensing the capacitor terminal voltage to avoid overcharging. On the other hand when charging a fully discharged capacitor from a voltage source rated at the capacitor maximum operating voltage, a similar amount of energy to that stored in the capacitor is lost in the loop resistance. When a higher source voltage is used in an *RC* arrangement, the resistor loss will further increase as seen in Fig. 4.12. In most SC energy storage applications, SCs are not allowed to deep discharge to improve the SCs' service life. When charging a partially discharged capacitor up to its rated voltage, the charging efficiency is improved by the reduction in the initial charging current.

To reach a higher efficiency when using a higher source voltage to charge a capacitor, an inductor can be added in series to the capacitor. The introduction of the inductor will alter the circuit in two ways,

- The inductor will dictate the initial current rise through the capacitor. Hence controlling the losses caused by the initial high charging currents.
- The series inductor will store energy while charging the capacitor. When the charging is extinguished, there will be energy stored in the inductor. By reusing this stored energy to charge another part of the capacitor bank, charging efficiency can be improved.

In the case of a switching converter, the energy stored in the inductor can be repeatedly reused through a coupled inductor to charge another part of the same capacitor bank. This will require the energy storage to be a SC bank with a tapping for a third connection. Theoretical simulations of a lossless switch and a perfect coupled inductor reaches close to 99% efficiency for a typical SCATMA-supercapacitor recharging. This efficiency improvement is a result of the addition of the series inductor. In an *RLC* set up part of the energy lost in the resistor of an *RC* system is reused as useful energy by transferring the stored energy in the inductor to charge another part of the same capacitor bank. By using a clever arrangement of the inductor and the capacitor bank this efficiency gain can be realised.

Chapter 5

Fast Charger Design

It was seen in Chapter 4 that the fast charging requirement of applications like SCATMA and SRUPS is unique. The bank circulation technique offers an elegant solution with a SC bank acting as an interface between the high power load and the low power charger. By using a minimum amount of pre-stored energy, the complete system is capable of sustaining the high power required by the load. To assure proper functioning, the charger should not be restricted by the five time-constant charging time barrier. When the SC bank to be charged becomes larger, the circuit time constant increases. Given the fact that SCATMA and SRUPS [6, 7] utilise SC banks of 20–200 Wh capacity, the associated circuit time constants will easily reach 0.5–1 min, comparable with the operating time duration of an instant water heater or an UPS.

A current-limited higher voltage source can fully charge a capacitor faster than a voltage source that matches the capacitor maximum dc voltage rating. A high-voltage charger mandates terminal voltage monitoring circuitry coupled to a disconnect switch to avoid overcharging. Using an in-line inductor improves overall charging efficiency because the energy stored in the inductor can be utilised to charge another capacitor or a part of the same capacitor bank.

The new topology facilitates fast-charging of a SC bank by using a higher supply voltage connected via a series inductor. This design allows to

- combine the two capacitor banks to obtain a single tapped capacitor bank (3 wires)
- use direct-rectified ac mains as the high voltage input power source to the converter
- do an energy limited design since both the target applications of the charger have limited energy in the capacitor banks
- reduce the component count to improve efficiency and reduce cost

5.1 The Topology

A converter which can operate directly from the ac mains doesnot require use of a smoothing capacitor at the dc bus. But even without a bulk capacitor, the converter should be capable of controlling the input current so that adequate power factor correction (PFC) is achieved. The main advantage of not having a smoothing capacitor is that it will reduce

the size of the converter as the bulk capacitor is the biggest component in modern power converters (however a small capacitor is still required to filter out switching noise). An inductor is placed in series to one part of the capacitor bank to control the rate of current rise through the circuit. To extract the energy stored in the series inductor, a coupled inductor configuration should be used (Fig. 5.1). The second inductor is wound on the same magnetic core but the two inductors should not conduct at the same time. This allows the source to store energy in the series inductor during the sw_1 "on" period. Only when the current through the series inductor is extinguished (sw_1 turns "off") should the coupled inductor start conducting. In this way the energy stored in the series inductor during one part of the cycle is transferred to the coupled inductor during the other part of the cycle.

The intended application does not require the charger to operate continuously. Therefore the bulky and expensive magnetic components can be designed taking an aggressive thermal management approach since in both fast charging applications sufficient cooling-off time is available between consecutive activation cycles as seen in Fig. 1.2. In SCATMA there is typically a 15-min gap between each 30 to 60 seconds of high power delivery, and in SRUPS the operation is rated only for several mains ac cycles, therefore it has a maximum run time of 50–100 ms, for the examples used in [6, 7].

As shown in Section 4.2, for a given current limit, current limit a higher voltage source can charge a capacitor faster than a source rated at the capacitor working voltage. When charging a capacitor from a higher voltage source, even when the capacitor becomes fully

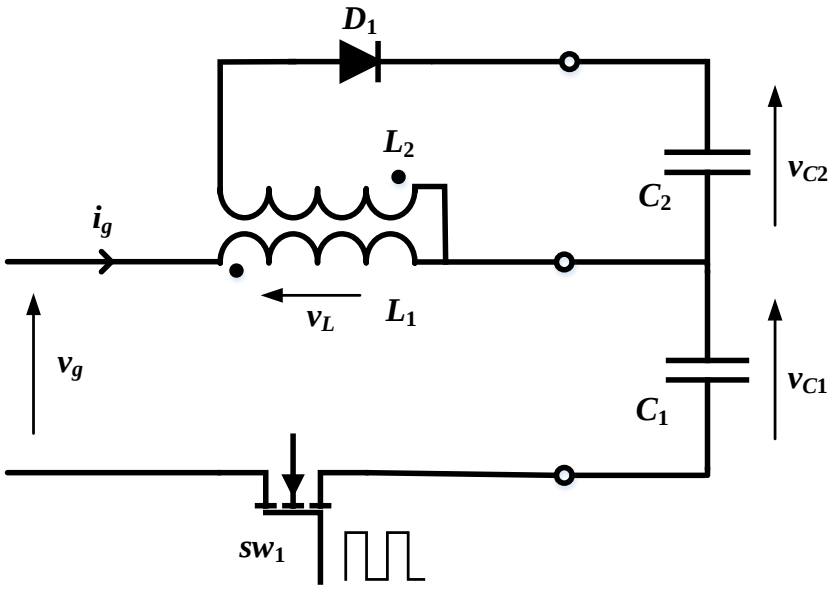

Figure 5.1: The basic coupled inductor topology connected to a centre-tapped capacitor bank. L_1 is the series inductor and L_2 is the coupled inductor

charged, the current through the circuit will not decay to zero. Hence a capacitor terminal voltage monitoring circuit coupled to a switch is required to extinguish charging.

In Section 4.3.3 it was seen that charging a capacitor through a series inductor is more efficient than a purely resistive path. Also it was seen that when the current through the circuit is limited using a high-frequency switching scheme, the efficiency can be further increased. The topology proposed incorporates all these aspects to construct a fast charger suitable for both SCATMA and SRUPS applications.

The proposed technique is shown in Fig. 5.1. The topology utilises a coupled inductor to charge the capacitor bank partitioned in two (C_1 and C_2). The converter can be directly fed with full-wave rectified mains voltage. The two parts of the capacitor bank work as two separate capacitors in the operation of the converter as there are no ground loops formed through any component parasitics to discharge one capacitor bank to the other. The circuit has two states of operation based on whether the switch sw_1 is "on" or "off". This technique takes advantage of both a higher voltage source and access to the energy stored in an inductor.

The current paths in the two states of operation are shown in Fig. 5.2. Here the coupled inductor is modelled as an ideal transformer with a magnetizing inductance similar to the transformer of a fly-back converter. Parasitics present in a practical transformer, like the leakage inductance (l_p), winding resistance (r_p), and core losses (R_C) (eddy current losses and hysteresis losses), are excluded from the model for simplicity and clarity. A complete equivalent circuit of a transformer with all the parasitics referred to the primary is shown in Fig. 5.3.

In the circuit shown in Fig. 5.2, the magnetising inductance, L_m, of the transformer primary placed in series with the charging path of C_1 stores energy during the "on" period.

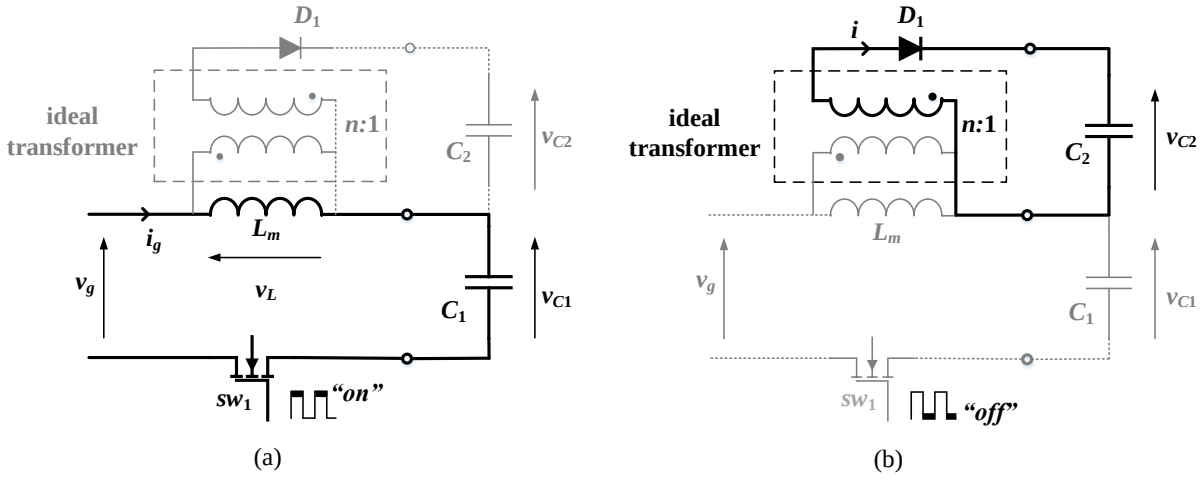

Figure 5.2: Topological equivalent circuit of Fig. 5.1. The coupled inductor is modelled as an ideal transformer in parallel with the magnetizing inductance. (a) ON state (b) OFF state. Current path in each state is indicated with thicker lines.

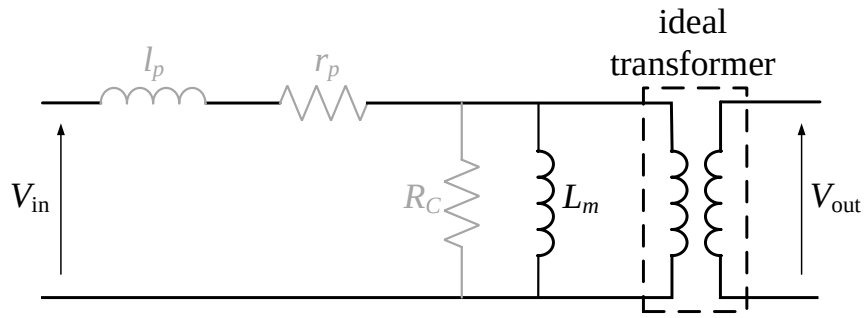

Figure 5.3: Equivalent circuit of a practical transformer including all parasitic elements. The elements shown in thicker lines are the components used for the modelling.

The charging path through L_m and C_1 will be referred to as the primary current loop. Since the secondary coil is wound with reverse polarity to block the diode during the "on" period, it keeps the secondary capacitor C_2 isolated from feeding back to the inductor. During this period, while the input stores energy in the inductor, the primary capacitor C_1 will be charged. During the "off" period the energy stored in the magnetic field of L_m is released from the secondary winding through the forward biased diode to charge C_2; the primary capacitor will not discharge as there is no closed loop in the primary path. Even the parasitic MOSFET body diode, which is antiparallel to the MOSFET drain-source junction (as seen in Fig. 5.4), will not get forward biased as the voltage difference between C_1 and v_g is very high (maximum voltage of a SCATMA bank is 50 V for safety and SRUPS runs from a 15–24 V storage).

Since v_g is the value of the rectified ac mains, energy transfer may occur close to mains zero crossing when the induced voltage in the transformer secondary is insufficient to keep the diode reverse biased. The effect of that on the overall operation can be neglected as the energy available to be transferred near the zero crossing is negligible.

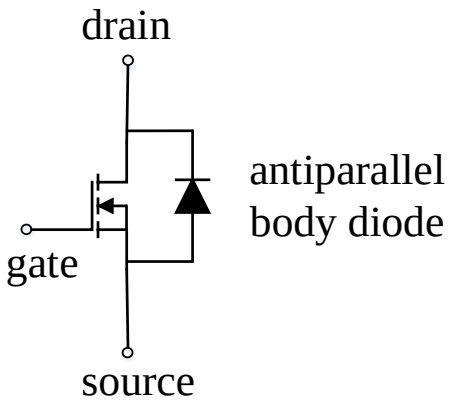

Figure 5.4: Parasitic elements present in practical MOSFET: antiparallel body diode

With the rectified ac mains used as the input voltage source, the capacitor voltages should be continuously monitored to avoid overcharging. The pulse width modulated (PWM) control signal will ensure that both capacitors charge at the same rate and will provide power factor correction without using an extra choke. Further, since a part of the capacitor to be charged is always connected in series with the line voltage, a buffer capacitor is not required. The low parts count of the design helps to reduce the total cost.

Since the converter operation is extinguished once capacitors C_1 and C_2 are fully charged, a steady state of operation is not reached. Hence the converter always operates in transient mode. Being driven by the rectified mains voltage, the resulting input current waveform peak envelope will be a fullwave rectified sine. The following section generates the required timing relationships for the control signal.

5.1.1 Converter Analysis

As seen in Fig. 5.5, the converter switches at frequency $F_s = 1/T_s$ with "on" time t_{on}, and "off" time, t_{off}. During the first subinterval $(0 - t_{\text{on}})$, when the primary MOSFET (sw) is switched "on", the circuit reduces to Fig. 5.2(a). The voltage across the inductor L_m, will be

$$v_L(t) \;=\; v_g(t) - v_{C1}(t). \tag{5.1}$$

The corresponding current rise in the inductor is dependant on the mains voltage as seen in Fig. 5.6.

During the second subinterval $(t_{\text{on}} - T_s)$ the primary MOSFET is switched "off", and the diode conducts. The equivalent circuit is shown in Fig. 5.2 (b). The voltage across L_m will be

$$v_L(t) \;=\; -nv_{C2}(t). \tag{5.2}$$

In transition mode of operation shown in Fig. 5.6, the inductor current will return to zero at the end of each switching cycle. Hence the net change in the inductor current is zero. From the definition of an inductor

$$v_L(t) \;=\; L\frac{di(t)}{dt} \tag{5.3}$$

By integrating over one complete switching cycle (0–T_s)

$$i_L(T_s) - i_L(0) \;=\; \frac{1}{L}\int_0^{T_s} v_L(t)dt \;=\; 0 \tag{5.4}$$

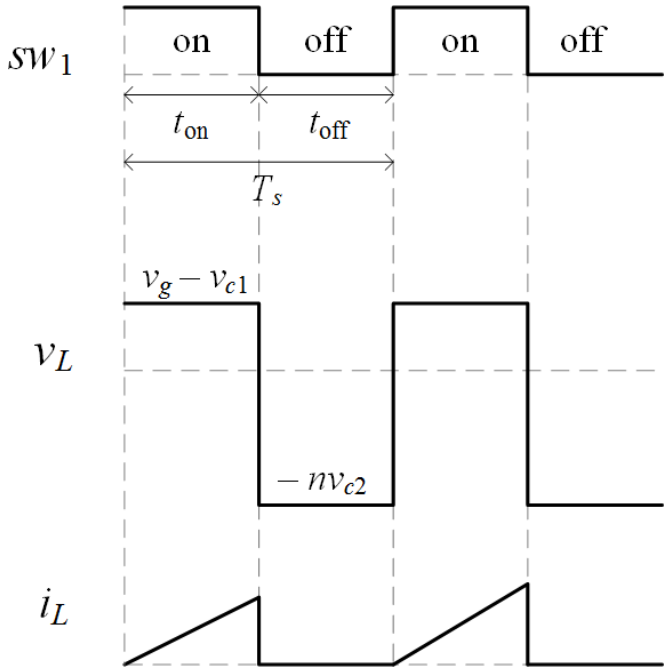

Figure 5.5: Inductor voltage and current in the two states of operation

Hence the volt-second sum of the inductor during one complete switching cycle should be zero. Applying this principle of volt-second balance to the inductor L_m

$$[v_g(t) - v_{C1}(t)]\, t_{\text{on}} + [-nv_{C2}(t)]\, t_{\text{off}} \;=\; 0$$

$$D \;=\; \frac{t_{\text{on}}}{t_{\text{on}} + t_{\text{off}}}$$

$$\Longrightarrow \qquad D \;=\; \frac{n\, v_{c2}(t)}{v_g(t) + n\, v_{c2}(t) - v_{c1}(t)} \tag{5.5}$$

Since the samples of v_{C1}, v_{C2} and v_g are slow-varying (50 Hz) quantities in comparison to the kilohertz switching frequency of the converter, the instantaneous values can be considered as short-term fixed values for the converter operation.

Consider the special case of C_1 and C_2 being equal; this corresponds to having a capacitor bank with two equal-sized partitions. To balance the rate of charge of the two capacitor banks, the capacitor voltages should rise at the same rate. Therefore the switching PWM duty should be maintained to have

$$v_{C1}(t) \;=\; v_{C2}(t) \;=\; v(t). \tag{5.6}$$

Further when the two capacitors are equal in size, to obtain the advantage of faster charging from a higher source voltage, both capacitors should see the same source voltage, hence $n \;=\; 1$. Revising Eq. (5.5) for the special case gives

$$D \;=\; \frac{v(t)}{v_g(t)}. \tag{5.7}$$

Therefore to ensure that both portions of the capacitor bank are charged at the same rate, both capacitor voltage and input voltage should be monitored.

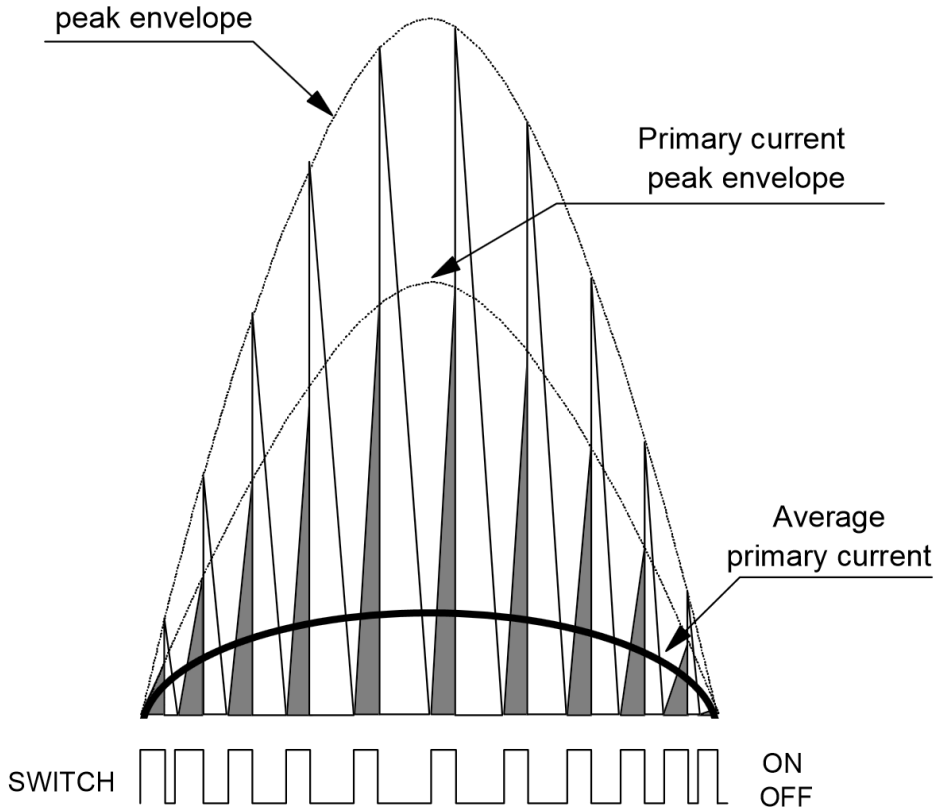

Figure 5.6: Current waveforms in transition mode of operation. The triangular primary current flows only during the "on" time, as illustrated by the shaded triangles. Source [67]

5.1.2 Transformer Design Process

A transformer arranged as shown in Fig. 5.7 will act as the coupled inductor in the converter topology. Since the converter topology avoids having the two transformer windings conduct at the same time, this transformer will operate as two coupled inductors.

Transformer design involves several steps:

- selecting core material and geometry
- determining maximum peak power density
- selecting core size
- selecting primary and secondary winding turns ratio, number of turns and wire gauge
- calculating the air gap necessary to achieve the desired inductance

Based on the design requirements, several parameters for the transformer need to be calculated. The maximum primary inductance $L_m^{\max}$ can be calculated as follows

$$L_m \;=\; v_g \,\frac{D}{f_s \Delta i_g} \tag{5.8}$$

To achieve maximum inductance set

$$L_m^{\max} \;=\; V_g^{\max} \,\frac{D}{f_s^{\min} I_g^{\max}}. \tag{5.9}$$

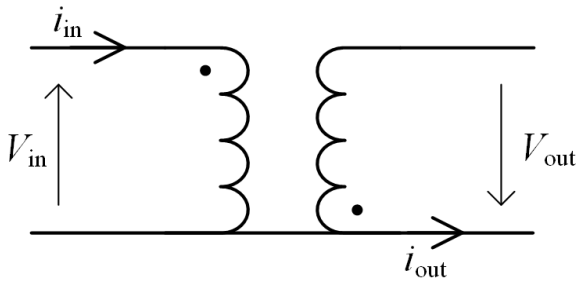

Figure 5.7: A two-winding transformer with inverse series connection will work as a coupled inductor in the converter topology

For $V_g^{\max}$, Δi_g will be $I_g^{\max}$. $D = 0.5$ can be selected as a general point of reference for the design calculations. $I_g^{\max}$ will be calculated based on this condition. Suppose that i_g is limited by the sub-circuit over-current protection device with a fusing rating of $I_g^{\rm rms}$. According to Fig. 5.8 the relationship between $I_g^{\rm rms}$ and $I_g^{\max}$ can be obtained as follows:

$$\begin{aligned} I_g^{\rm rms} &= \sqrt{\frac{1}{T_s}\int_0^{T_s/2} i_g^2(t)\,dt} \\ &= \sqrt{\frac{1}{T_s}\int_0^{T_s/2} \left[\frac{I_g^{\max}}{T_s/2}\right]^2 t^2\,dt} \\ &= \frac{1}{\sqrt{6}}\, I_g^{\max}. \end{aligned} \tag{5.10}$$

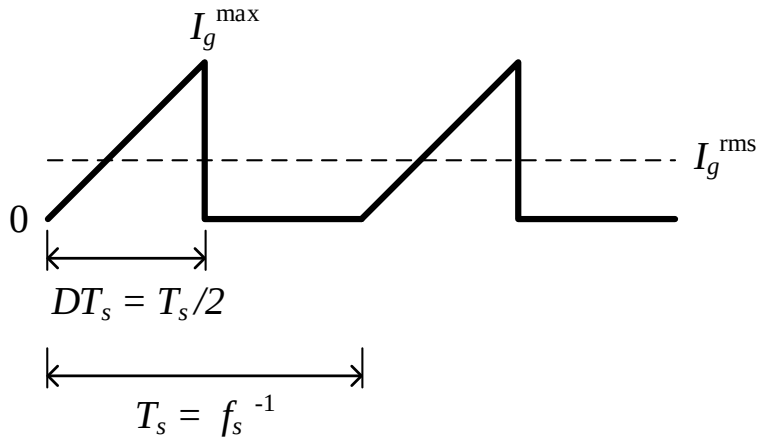

Figure 5.8: Peak input current to RMS input current relationship for a 50% duty switching waveform.

5.1.3 Core Material Selection

Transformer core material selection needs to take into consideration the following key parameters

- switching frequency
- operating flux density
- resulting core losses
- operating temperature

The maximum power available for the transformer is limited by the power capability of the wall socket outlet. A core size can be selected based on the power handling capability of the core. By setting the lowest frequency of operation as high as possible, the size of the transformer can be minimized. Operating temperature rise is caused by the core losses in the magnetic core and copper losses in the winding wire. Core losses include hysteresis losses and eddy current losses. Hysteresis losses are a function of core flux swing and operating frequency. The hysteresis loop area represents the energy loss and the power depends on how many times the loop is traversed, thus it is directly dependent on frequency. For a gapped core, the high reluctance air gap can cause localised high heating in the windings around the air gap [68]. Hysteresis loss is independent of the input voltage or the load current.

Core eddy current loss, on the other hand, is a function of the volts per turn applied to the winding, and the duty cycle. The core flux will see the core as a single turn secondary and therefore the eddy current losses in the core are primarily I^2R losses based on the core resistance reflected to the primary by turns ratio squared. Copper losses include the copper wire resistance, the proximity effect and the skin effect when the transformer is operating at a higher frequency. In a solid conductor at high frequencies, a major part of the total current will flow through the outer layer of the conductor. This will effectively reduce the cross sectional area of the wire, increasing the resistance and hence the losses. The proximity effect is caused by the presence of transverse fields. Due to the magnetic fields generated by nearby conductors, current will flow in other undesirable patterns (loops or localised concentrated areas) [69].

For all the following calculations, Magnetics Inc's transformer design guide and their datasheets are used as reference. Ferrite magnetic materials are designed to have core losses within a specific operating temperature range. Fig. 5.9 shows the core losses for different materials for a range of operating temperatures. It can be seen that the F material offers the lowest losses in the temperature range from room temperature to 40°C.

As seen in Fig. 5.10, for each material based on the operating frequency of the converter, the maximum flux density the core can handle would vary. Switching frequency of the converter may be dependent on many other limitations dictated by the individual

characteristics of other components. To limit the core losses to a moderate level (40°C approximate core temperature rise), choosing a core loss density of 100 mW/cm^3 is a good base reference [70]. Using the curves shown in Fig. 5.10, the maximum flux density the core can operate at a given frequency can be obtained while maintaining a 100 mW/cm^3 core loss density. From the curves, the F magnetic material has the highest flux density in the 20–100 kHz frequency range.

Based on the previous discussion referring to Magnetics ferrite products; F, P and R magnetic materials offer the lowest core losses and the highest saturation flux density. Therefore these materials are the choice for high power, high temperature applications.

5.1.4 Core Geometry Selection

Fig. 5.11 shows the range of magnetic core shapes available from Magnetics Inc. The required ferrite geometry will vary in shape and size depending on the application specifications. The choice of the core geometry depends on the following parameters:

- core cost
- bobbin cost
- winding cost
- winding flexibility
- assembly
- mounting flexibility
- heat dissipation
- shielding

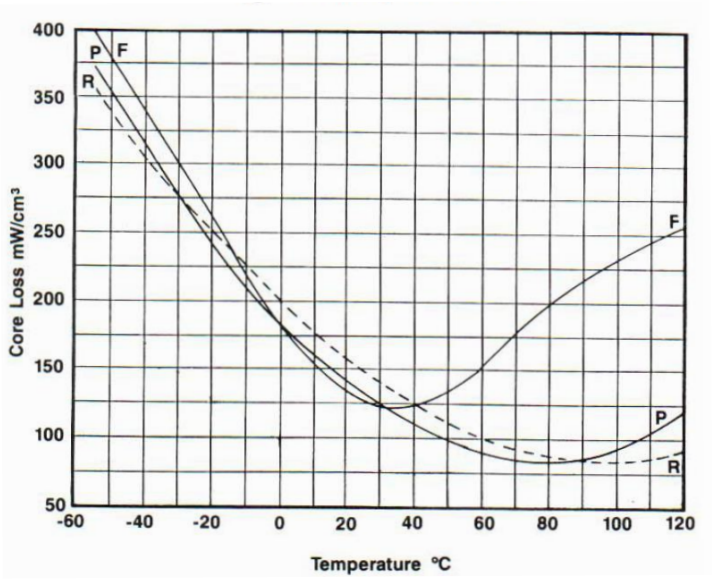

Figure 5.9: Core loss variation of F, P and R ferrite materials with temperature at 100 kHz for fixed 10 μT flux density [70].

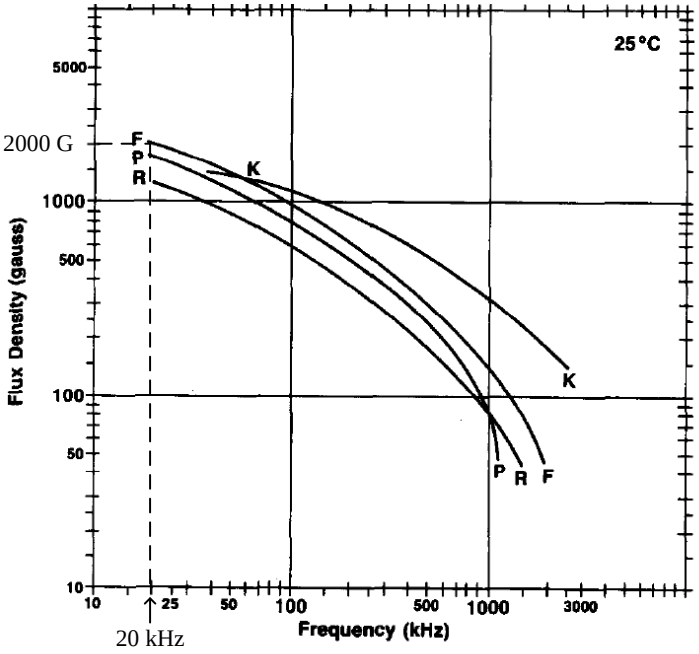

Figure 5.10: Maximum usable flux density variation F, P, R and K ferrite materials with frequency for a constant core loss of 100 mW/cm^3 [70]. 1 G = 10^{-2} μT

Toroids are the most economical solution as they do not require a bobbin or any assembly accessories. Pot core would cover the whole winding with the core material, shielding the coil from picking up any electromagnetic interference (EMI) from the surrounding circuits. Due to the shape of the pot cores, these are more expensive than a similar power rated core of other geometries and not many sizes suitable for high power applications are readily available from manufacturers. RM cores are similar to pot cores and they have a further reduced printed circuit board footprint. EP cores have round centre posts and the winding is completely surrounded by the core material. EC, ETD, EER and ER core are shapes between E cores and pot cores. They provide wide openings on each side for winding large diameter wires (litz wire) and copper tape. Better air circulation through the cores will keep the assembly cooler. E cores are the most common and they are readily available in many sizes from different manufacturers. E cores are less expensive than a pot core and the simple bobbin style makes winding easier.However, they do not offer self shielding like a pot core. For building a proof-of-concept prototype, using an E core is adequate.

5.1.5 Core Size Selection

Available core window area, W_a, and effective core cross-sectional area, A_c, are two important physical parameters of a core in deciding its power handling capability. W_a and A_c for an E core are shown in Fig. 5.12. The power handling capability of a transformer core can be determined by the $W_a\,A_c$ product. For a square wave excitation of a winding [71],

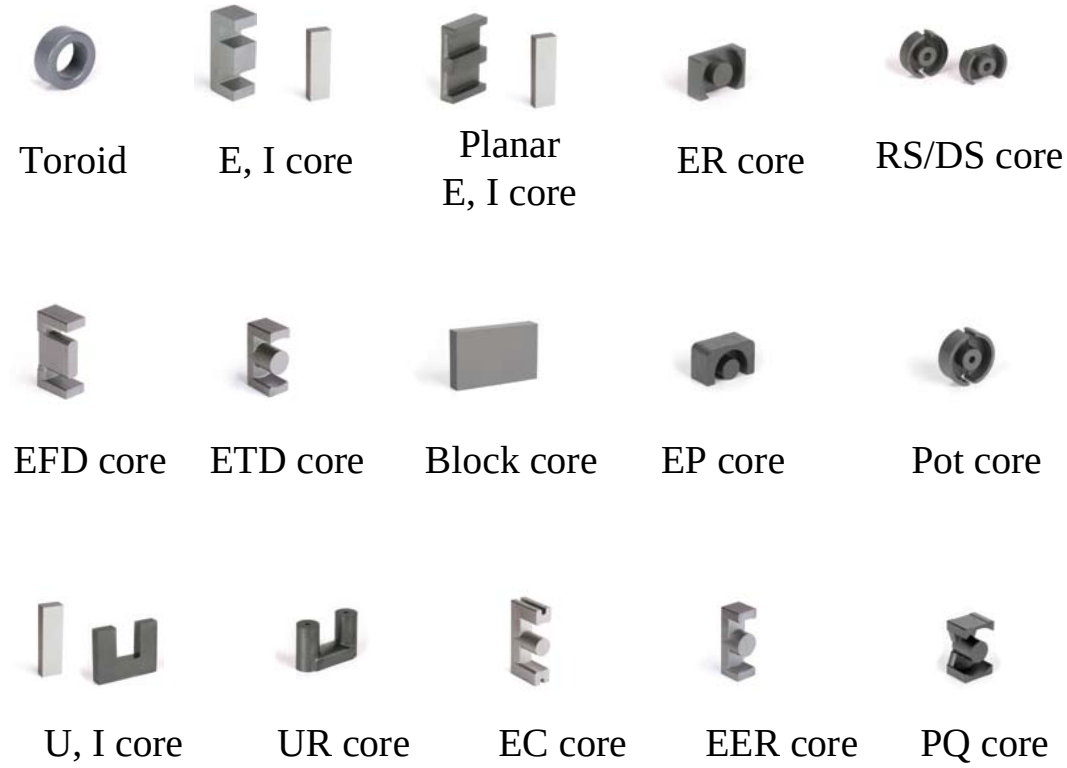

Figure 5.11: Ferrite core shapes from 2013 Magnetics ferrite cores catalogue.

$$V = 4\,B\,A_c\,N\,f \times 10^{-8} \tag{5.11}$$

where V is the rms voltage (V), B is the flux density (G), A_c is the core area (cm^2), N is the number of turns and f is the operating frequency (Hz). The utilisation of window area by the winding is called the winding factor K. This can be calculated using the wire

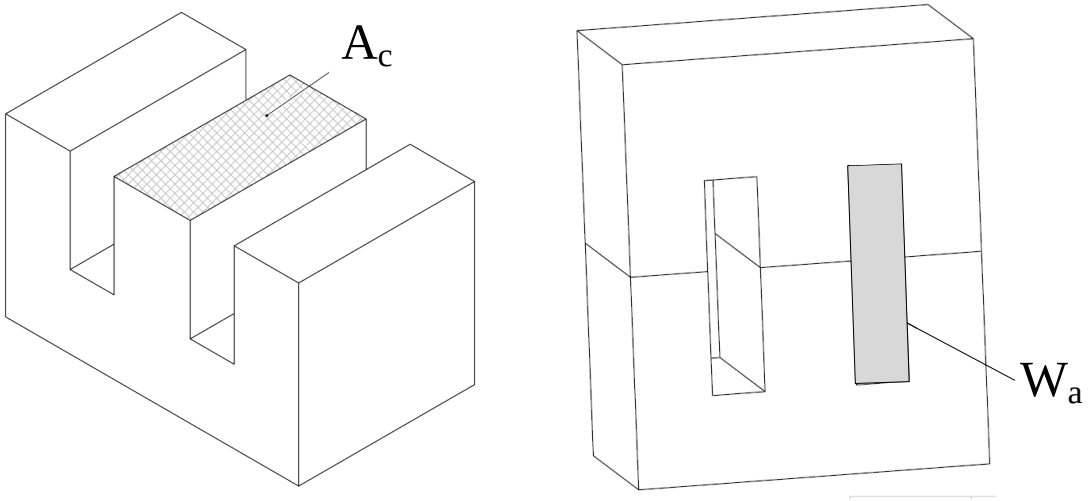

Figure 5.12: Window area and effective cross-sectional area of an E core.

area (cm^2), A_w, as follows

$$K = \frac{N A_w}{W_a} \tag{5.12}$$

Another important parameter when choosing a transformer for a power converter is the current capacity of the wires, C_w. Depending upon the allowed temperature rise, C_w is chosen. For transient applications where the rated power is only delivered for a brief period of time, the choice of C_w can be aggressive. C_w is defined using the input current I as

$$C_w = \frac{A_w}{I}. \tag{5.13}$$

Solving for W_a by substituting A_w from Eq. (5.13) into Eq. (5.12) gives

$$W_a = \frac{N I C_w}{K}. \tag{5.14}$$

Combining Eq. (5.14) and A_c from Eq. (5.11), the $W_a A_c$ product can be calculated as

$$\begin{aligned} W_a A_c &= \frac{V \times 10^8}{4 B N f} \frac{N I C_w}{K} \\ &= \frac{P_{\text{in}} C_w \times 10^8}{4 B f K} \end{aligned} \tag{5.15}$$

where $P_{\text{in}} = V I$ is the input power. For a square wave excitation and for E-U-I and pot cores, $C_w = 5.07 \times 10^{-3}$ cm^2/A and $K = 0.7$. To minimize wire losses and core size, the winding factor should be as high as possible. In practice, the use of round section enamelled wire will leave free space between windings. Use of litz wire with twisted, multiple insulated strands will further reduce the winding factor. Using copper tape will increase K as the gap between two layers is only the thickness of the insulator.

As seen in Fig. 5.13, in the proposed topology the unipolar pulses cause the flux in the core to increase and when the pulse is "off" the energy stored in the core is supplied through the secondary winding. The converter needs the transformer to act as an energy storage device as well as provide normal transformer action. In the transient mode of operation for the maximum core utilization, the minimum flux in the core will approach zero. Therefore the maximum flux swing, B, for Eq. (5.15) can be selected to be half the maximum allowed flux density of the core at the given operating frequency. Once the area product $W_a A_c$ is calculated, a suitable transformer can be selected from the area product distributions available from core manufacturers (see sample tables in Appendix C).

5.1.6 Primary and Secondary Winding

Once the core is selected, the next step is to calculate the number of turns for the primary and the secondary. If the turns ratio n is known primary turns (N_p), secondary

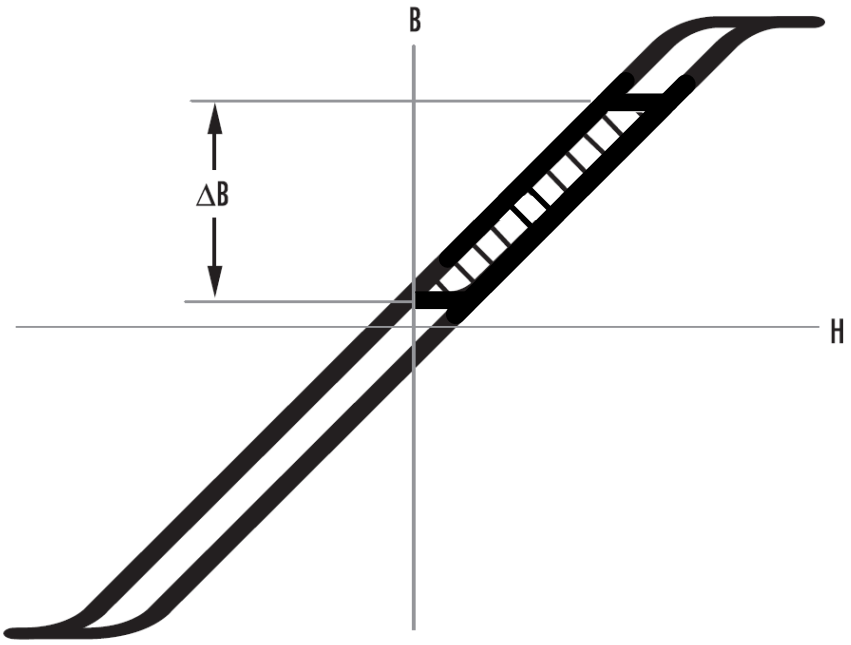

Figure 5.13: Hysteresis loop for a magnetic core operating only in the first quadrant of the B-H curve.

turns N_s and primary and secondary wire areas A_{wp} and A_{ws} can be obtained from Eqs. (5.11) and (5.12) as

$$N_p = \frac{V \times 10^8}{4\ B\ A_c\ f}, \quad N_s = \frac{N_p}{n} \tag{5.16}$$

$$K\,W_a = N_p A_{wp} + N_s A_{ws}. \tag{5.17}$$

5.1.7 Transformer Air Gap

As mentioned earlier, this power converter topology uses the transformer for normal transformer operation as well as for energy storage in the core, similar to the case of a flyback converter. To be an effective energy storage device the core must not saturate, hence an air gap is created to increase the reluctance of the core and control the current rise through the core. In an ordinary inductor the core material guides the magnetic flux lines all the way around the windings. Like a resistor controlling the current through a resistive circuit, an air gap in a magnetic core will control the excessive flux produced by the high current in the winding. In analogy to a resistor in an electric circuit, the air gap provides the extra reluctance required. The reluctance of the air gap, R_g, and the reluctance of the ferrite material, R_f, can be expressed as

$$R_g = \frac{L_g}{\mu_0\, A_c} \quad \text{and} \quad R_f = \frac{L_e}{\mu_0\, \mu_r\, A_c} \tag{5.18}$$

where L_g is the gap length (in cm), L_e is the effective core magnetic path length (in cm), μ_0 is the permeability of free space and μ_r is the relative permeability of the ferrite core

material. From here it can be seen that since μ_r is a higher value, the air gap is the main contributor to the overall reluctance. Because of this, most of the energy is stored in the magnetic field within the air gap. It is general practice to equate the total energy stored in the inductor to the energy stored in the air gap.

To calculate the required air gap, first the relative permeability of the ungapped core must be calculated [72].

$$\mu_r \;=\; \frac{A_L\, L_e}{0.4\pi\, A_c \times 10} \tag{5.19}$$

Using these parameters, the gap length can now be calculated as in Eq. (5.20). The industry practice is to mill the gap only in the centre leg of the core. However, for small developments or prototypes, half the gap calculated below can be produced by using insulating material of suitable thickness

$$L_g \;=\; \left[\frac{0.4\,\pi\, N_p^2\, A_c}{100\, L_m} - \frac{L_e}{\mu_r}\right]. \tag{5.20}$$

5.1.8 Example Transformer Design

As marked on Fig. 5.10 at the lowest operating frequency of 20 kHz (as explained earlier, this frequency is set as the minimum operating frequency of the converter to minimize the size of the transformer) up to 100 kHz, F material is the choice with the highest flux density capability. But from Fig. 5.9, F material's core losses increase with temperature for temperatures beyond 30°C. Since the transformer design is based on a transient operation (until the capacitors are charged) the core material need not run at a very low temperature. Hence the core temperature can be allowed to rise 40–60°C beyond the room temperature. Given this reason the best material choice based on the thermal characteristics curve would be the P material. Referring back to Fig. 5.10, P material too can hold a maximum flux density of around 1600 G. Therefore the P material is chosen since it does not have a big effect on the maximum flux the core can handle.

The shape is selected as E, since EMI is not a main concern at this stage of the design, for ease of prototyping (manufacturing the gapped leg) and a variety of E core sizes being readily available off the shelf from many core vendors. The choice of an E core shape supports the material choice as the shape would allow more heat to be dissipated rapidly than an enclosed core type like a pot core.

From Eqs. (5.9) and (5.10) the required maximum primary inductance can be calculated for 230 V ac mains with 2.3 kW RMS input power ($I_g^{\mathrm{rms}} = 10$ A),

$$L_m^{\max} \;=\; 230\sqrt{2}\,\frac{0.5}{20\text{ kHz}\;10\sqrt{6}\text{ A}} \;=\; 332\;\mu\text{H}. \tag{5.21}$$

The maximum allowed flux swing in the core as seen from Fig. 5.13 is half the maximum flux capability of the core. Now from Eq. (5.15) the area product of the required core can be calculated as follows:

$$W_a\, A_c \;=\; \frac{2.3\ \text{kW}\,(5.07\times10^{-3})\ \text{cm}^2\text{A}^{-1}\,10^8}{\left[4\ \times\ \frac{1600}{2}\right]\ \text{G}\,20\ \text{kHz}\ \times 0.7} \;=\; 26.02\ \text{cm}^4.$$

From Magnetics Inc's 2013 magnetics catalogue [73], choosing the E core 46527EE with area product of 24 cm^4 and from the power handling chart in Appendix C, it is seen that the core can handle a power of 2 kW at 20 kHz, and up to 8.75 kW at 250 kHz. From core data the following parameters are extracted: $A_L = 9200$ mH/1000 turns, $l_e = 147$ mm and $A_c = 540\ \text{mm}^2$. The dimensions of the core are $65 \times 32 \times 27$ mm.

The next step is to calculate the turns ratios for the two main windings as well as for all other bias windings. In the practical implementation, two bias windings were used for the drivers and the controller. Since the currents drawn by these windings are negligible calculations are not included. Since both partitions of the capacitor need to be charged at the same rate it is advantageous to choose a one-to-one transformer turns ratio as the secondary side will also be charged from the same high voltage. From Eq. (5.16) the primary and secondary number of turns will be

$$N_p \;=\; N_s \;=\; \frac{230\ \times 10^8}{4\times 800\ G\ \times\ \frac{540}{10^2}\ \times\ 20\ \text{kHz}} \approx 66\ \text{turns}.$$

The wire thickness can be obtained from Eq. (5.17),

$$0.7\ \times\ \frac{25.4\ \text{cm}^4}{5.4\ \text{cm}^2} \;=\; 2\times 66\times A_w$$

$$A_w \;=\; 2.4\ \text{mm}^2$$

13 AWG wire with cross-sectional area of 2.62 mm^2 and diameter 1.8 mm is chosen. For this size of conductor to carry the current without an increase in the copper loss, the skin depth of copper at the operating frequency should be higher than the radius of the conductor. This happens due to the phenomenon of skin effect: when a conductor carries alternating current, the current density towards the surface of the conductor tends to increase, thus reducing the effective conductor cross-sectional area, hence increasing the resistivity of the conductor. The skin depth, δ, of the conductor can be calculated using

$$\delta \;=\; \sqrt{\frac{\rho}{\pi\, f\, \mu_0\, \mu_r}} \tag{5.22}$$

where ρ is the resistivity of the medium in Ωm. The skin depth of copper at 20 kHz will be

$$\delta_{20k} \;=\; \sqrt{\frac{1.68\times10^{-8}\ \Omega\text{m}}{\pi\ \times\ 20\ \text{kHz}\ \times\ (4\pi\times10^{-7})\ \text{Hm}^{-1}\ \times\ 0.99}} \;=\; 0.46\ \text{mm}.$$

Based on this value, the minimum diameter of the wire should be at least 1 mm. Therefore the maximum wire thickness that can be used is a 1.02 mm diameter, 18 AWG copper wire. For the current density to be no more than what was calculated earlier, the number of strands used from this thinner wire should be more than one. By equating the current density, I', of the previous calculated wire to the new, the required number of strands, m, can be obtained:

$$I' = \frac{I}{A_w} = \frac{I}{A_w^{'} m} \qquad \Longrightarrow \qquad A_w = A_w^{'} m \tag{5.23}$$

where A_w is the area of the wire obtained (13 AWG) from the transformer winding factor equation in Eq. (5.17) and $A_w^{'}$ is the maximum wire area selected (18 AWG) based on the skin depth calculation. By substituting the numbers in the equation above

$$2.4 \text{ mm}^2 = 1.02 \text{ mm}^2 \times m \qquad \Longrightarrow \qquad m = 2.$$

$m = 2$ would be an aggressive choice but based on the transient nature of the application, even if the transformer windings get heated up there will be ample time left between two charging cycles to cool the transformer through natural convection.

The next step would be the calculation of the required air gap to avoid core saturation. Using Eq. 5.19 the relative permeability of the core can be calculated as follows:

$$\mu_r = \frac{9200 \text{ mH/1000turns} \times 14.7 \text{ cm}}{0.4\pi \times 5.4 \text{ cm}^2 \times 10} = 1992.9.$$

Based on this value the gap length can be calculated using Eq. 5.20:

$$L_g = \frac{0.4\pi \times 66^2 \times 5.4 \text{ cm}^2}{100 \times 332 \ \mu\text{H}} - \frac{14.7 \text{ cm}}{1992.9} \approx 0.88 \text{ mm}.$$

This is the required length of the gap to be grounded at the middle leg. For ease of manufacturing a non-magnetic material of half the required thickness was placed at the two outside legs to effectively obtain the same gap. A summary of the calculated transformer parameters is given in Table 5.1.

5.1.9 Transformer Measurements for Leakage Inductance

Leakage inductance is a result of the uncoupled self inductance of a transformer coil. These inductances cause voltage spikes in the primary side switching device. Snubber circuits are required to clamp these high voltages and degrade the voltage regulation in power supplies [74]. Transformer inductance measurements are given below for the 600 W transformer built using TDK EE80/38/20 ferrite core. According to Eq. (5.9), the calculated transformer primary and secondary inductance (using a 1:1 turn ratio) is

$$L_1 = 325 \times \frac{0.5}{20 \text{ kHz} \times \sqrt{6} \cdot \frac{600 \text{ W}}{230 \text{ V}}} = 1.27 \text{ mH}.$$

Table 5.1: Details of the transformer for a 2.3 kW converter

Parameter	Value
Frequency range	20–200 kHz
Operating temperature	40–80°C
Magnetics Inc. part number	46527EE
Magnetic material type	P
Core shape	EE
Maximum primary inductance, $L_m^{\max}$	332 μH
Area product	24 cm^4
A_L	9200 mH/1000 turns
Effective path length, L_e	147 mm
Effective cross sectional area, A_c	540 mm^2
Dimensions	$65 \times 32 \times 27$ mm
Primary turns, N_p	66 turns
Secondary turns, N_s	66 turns
Wire gauge	18 AWG
Number of strands, m	2
Gap length at the outside legs	0.44 mm

The following measurements for the transformer configurations shown in Fig. 5.14 were carried out to obtain the leakage inductance, l_p, mutual inductance, M, and coupling coefficient, k. All tests were carried out using an RLC meter at 20 kHz. As seen in Fig. 5.3, the core loss R_C is represented as a parallel resistor to the magnetising inductance L_m. When using an RLC meter to measure the transformer primary impedance, the measurement will be expressed as an equivalent series RL network. This will convert the parallel core loss resistance into an additional series resistor added to the winding resistance. The short-circuit test will provide the primary leakage when the primary is measured shorting the secondary as shown in Fig. 5.14(c). The series and inverse series inductor connection arrangements shown in Figure 5.14(d) and (e) are used to obtain the transformer mutual inductance and the coupling coefficient. For the series and inverse

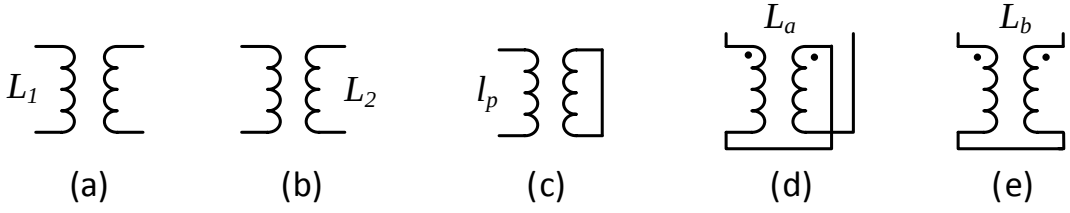

Figure 5.14: Measurement of transformer inductances: (a) primary inductance (b) secondary inductance (c) leakage inductance (d) series connection inductance (e) inverse series connection inductance

Table 5.2: Experimental measurements for transformer leakage

Parameter	Value
Primary inductance, L_1	1.26 mH
Secondary inductance, L_2	1.48 mH
Leakage inductance, l_p	19.9 μH
Series inductance, L_a	5.47 mH
Inverse series inductance, L_b	31.21 μH

series arrangements the following expressions can be written:

$$L_a = L_1 + L_2 + 2M, \tag{5.24}$$

$$L_b = L_1 - L_2 - 2M. \tag{5.25}$$

By solving these two equations:

$$L_1 + L_2 = \frac{L_a + L_b}{2} \quad \text{and} \quad M = \frac{L_a - L_b}{4}. \tag{5.26}$$

The coupling coefficient (k) can be found using the equation

$$k = \sqrt{\frac{M^2}{L_1 L_2}}. \tag{5.27}$$

Practical measurements obtained are listed in Table. 5.2. Hence $L_1 + L_2 = 1.26 + 1.48$ mH $= 2.74$ mH. $L_1 + L_2$ can be obtained using L_a and L_b according to Eq. 5.26.

$$L_1 + L_2 = \frac{5.47 + 0.031}{2} \text{ mH} = 2.75 \text{ mH}.$$

Mutual inductance can be calculated from Eq. 5.26

$$M = \frac{5.47 - 0.031}{4} \text{ mH} = 1.36 \text{ mH}.$$

The coupling coefficient calculated according to Eq. (5.27)

$$k = \sqrt{\frac{1.36^2}{1.26 \times 1.48}} \implies k = 0.995.$$

The experimental values will further reduce when the measurements are carried out at a higher frequency or with a square wave excitation (due to the presence of parasitic winding capacitance being more prevalent high frequency harmonics).

5.2 Simulation and Experimental Results

5.2.1 Ideal Component Simulations

All simulations on the power converter were done using LTspice. The aim of this was to find the best matching component for the secondary switch and to analyse the effects of

parasitics present in components, mainly the effect of MOSFET body diode and transformer leakage inductance. Later the simulated system which has the closest resemblance to the actual converter experimental waveforms was used to run simulations for input PFC. The fast fourier transform of the input current was used to analyse the harmonic content present at the input. Further, the simulations were used to estimate the charging time to calculate an equivalent charging current which will be discussed later in Section 5.2.4. These measurements can be used to compare the performance of this charger topology with already available conventional chargers.

5.2.2 Primary and Secondary Switch Options

The secondary side switch should operate 90° out of phase with the primary side switch. To obtain more control over the secondary "on" time, a controlled MOSFET switch could be used in the secondary loop. The current waveforms when a controlled MOSFET is used is shown in Fig. 5.15(a). The first cycle corresponds to a primary "on" time. As seen in Fig. 5.3, the antiparallel body diode of the secondary side MOSFET will get forward biased during the on cycle. Hence a negative current flows from C_2 discharging it. Hence the operation cannot be controlled as intended by using two 90° out of phase MOSFET gate control signals. It can easily be shown that the parasitic component which causes this operation failure is the MOSFET body diode by simulating an ideal switch for the secondary side with an antiparallel body diode. The results are the same for a system with a secondary MOSFET and a system with an antiparallel diode to the secondary ideal switch as seen in Fig. 5.15(c). Fig. 5.15(b) is the current waveforms with two ideal switches. The current waveforms for a secondary diode is seen in Fig. 5.15(d). The system with a secondary diode gives similar results to that of an ideal switch.

During the "off" period, the forward voltage v_d across the MOSFET body diode as shown in fig. 5.16 will be

$$v_d = v_{C1} - nv_{C2} - v_g \tag{5.28}$$

For the body diode to conduct $v_g > 0.7$ V. The worst case will be near the mains voltage zero crossings where $V_g \to 0$. For a centre-tapped capacitor bank with $n = 1$, if both the capacitors are getting charged at the same rate the body diode will not conduct. Hence a MOSFET is capable of switching the primary side of the converter without discharging the capacitors.

5.2.3 Transformer Leakage

A practical transformer cannot be realised with perfect coupling. The coupling coefficient, k, represents the degree of magnetic coupling between the two windings wound on the

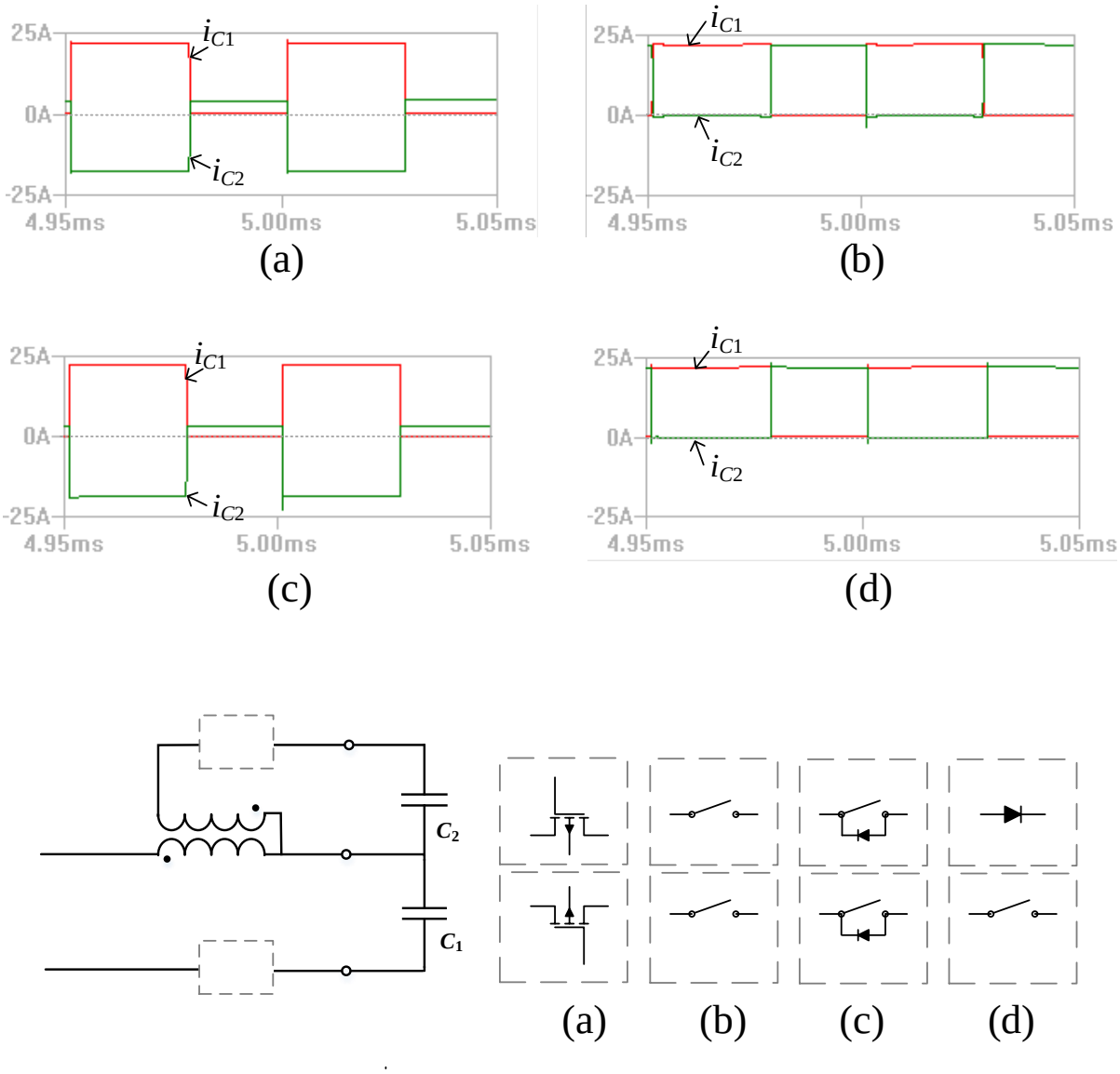

Figure 5.15: Spice simulated primary and secondary capacitor currents with the corresponding switch arrangements. (a) with a MOSFET as the secondary switch, (b) two ideal switches, (c) two ideal switches with an antiparallel diode to the secondary switch and (d) primary ideal switch and a secondary diode.

same magnetic core. Due to leakage inductance the coupling coefficient of a practical transformer will be in the range from 0.95 - 0.98 [75].

As seen in Fig. 5.17(b), the leakage inductances present in the transformer primary and secondary will change the secondary current shape compared to the ideal case. The ideal case (closely resembled by a low leakage transformer) is shown in Fig. 5.17(a). During t_0–t_1 the primary capacitor current rises through the magnetizing inductance l_m. Once the primary switch is turned "off", the stored energy in the magnetic field will cause a current through the forward biased secondary diode into C_2. When the converter operates

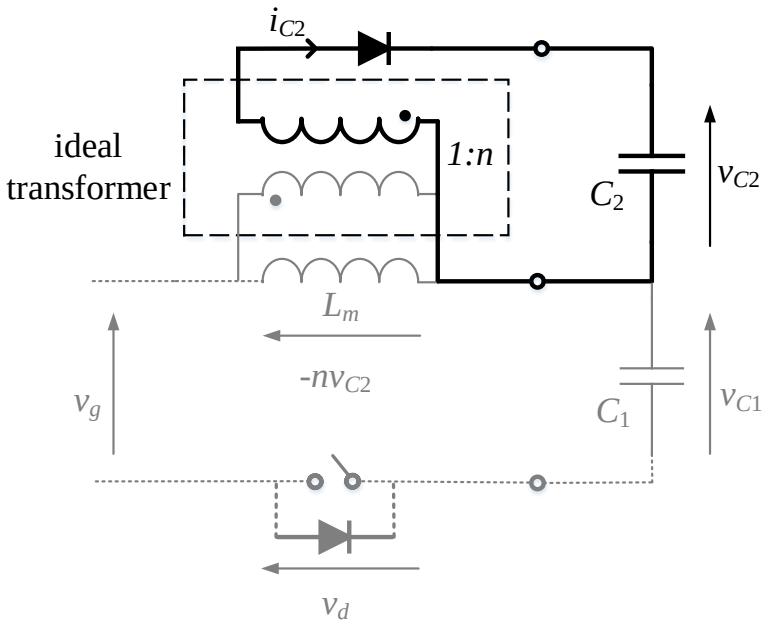

Figure 5.16: Equivalent circuit for the "off" state of operation.

in the transition mode of operation the MOSFET will be turned "on" by sensing i_{C2} zero crossing.

With the presence of leakage inductance, at t_0' when the primary MOSFET switches "on", the secondary diode should get reverse biased and the secondary should stop conducting. But due to the uncoupled energy stored in the secondary leakage inductance, $l_{\text{leak-s}}$, secondary current will decay through the diode onto C_2. In this way the energy stored in $l_{\text{leak-s}}$, is also used to charge the capacitor bank.

During the MOSFET "off" period, t_1'–t^* when the MOSFET is switched "off", the uncoupled-energy stored in the primary-leakage inductance $l_{\text{leak-p}}$, will dissipate the stored energy into the snubber. The snubber current, i_{snub} will cause a reflected current in the secondary through transformer action in the opposite direction, hence a rising current instead of a falling current. After t^*, once the leakage is completely dissipated onto the snubber, the secondary will conduct the maximum current according to the secondary loop resistance during the period t^*–t_2'. The 1:1 turns ratio was selected as to charge both the capacitors at the same rate. As seen in Fig. 5.17(a), if a higher n value is selected the secondary current during the "off" state will drop faster.Figure 5.18 compares the experimental results for the 600 W, 1:1 prototype transformer with a small 30 W, 17:1 low-leakage flyback transformer TP07074 by Power Integrations [76]. This is a mass-scale produced part for other applications with very low leakage.

Further when the two windings are loosely coupled the current drawn from the supply will reduce. Fig. 5.19 shows the reduction in current when the coupling coefficient is reduced from 0.95 to 0.9 with all other circuit parameters held the same.

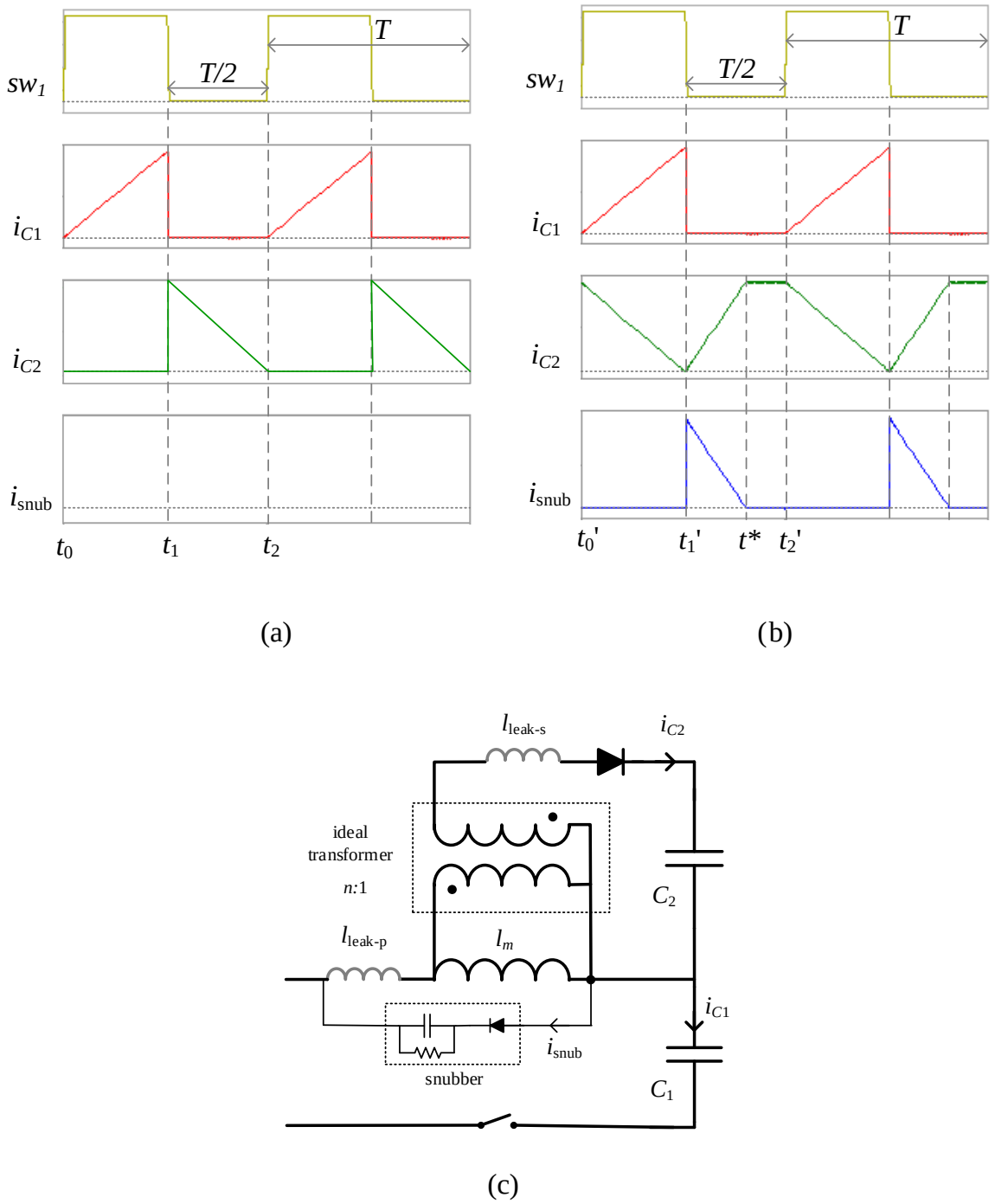

Figure 5.17: Effect of leakage inductance on the converter operation (a) converter current waveforms with no leakage inductance and $n = 17$ (b) converter current waveforms with leakage inductance and $n = 1$ (c) equivalent circuit of the converter with primary and secondary leakage inductances, $l_{\text{leak-p}}$ and $l_{\text{leak-s}}$

5.2.4 Equivalent Charging Current

The following discussion is based on the converter implemented according to Fig. 5.20, with a snubber circuit across the primary winding to protect the MOSFET.

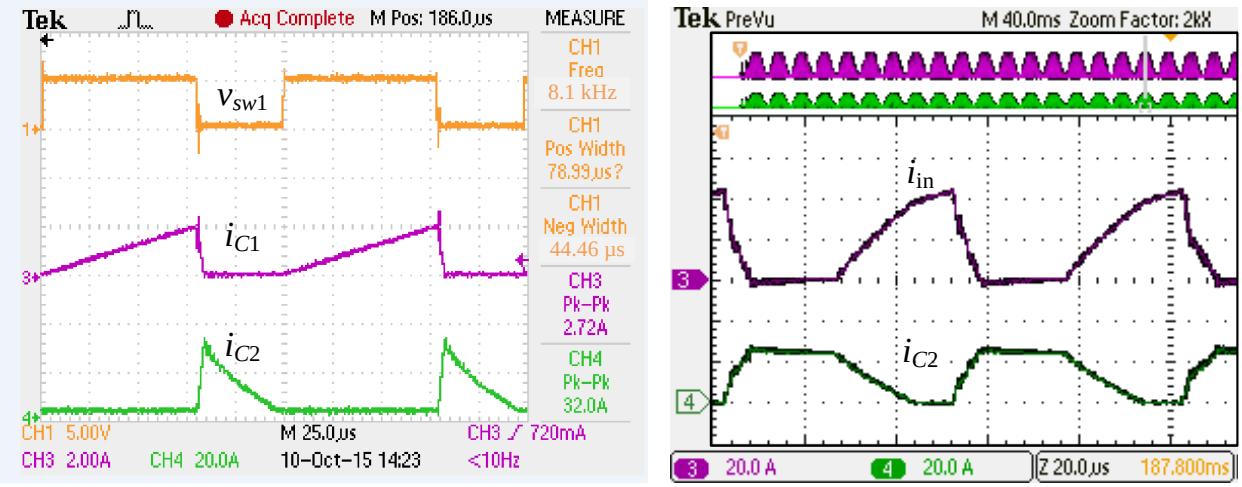

(a) (b)

Figure 5.18: Experimental results for leakage effect (a) using a low-leakage, commercial, 30 W flyback transformer with 17:1 turns ratio (b) using the 600 W prototype transformer with 1:1 turns ratio. $i_{\text{in}} = i_{C1} + i_{\text{snub}}$

As seen previously, in most practical cases (sources with a maximum current limit) the rate at which a capacitor can be charged depends on the current rating of the power source. To compare the performance of the proposed technique with available chargers, an equivalent charging current, I_{eq}, should be calculated. Since this converter is directly fed by the full wave rectified mains source as seen in Fig. 5.21, the input current wave form (similarly the capacitor charging current waveform as the capacitor is in series) will have a sinusoidal peak-current envelope as seen in Fig. 5.22. Therefore rather than comparing the power rating of the charger, the equivalent charging current is more meaningful in specifying this type of a charger i.e., if energy E is to be stored in a capacitor C with a ΔV_C terminal voltage rise within ΔT time, then the equivalent charging current I will

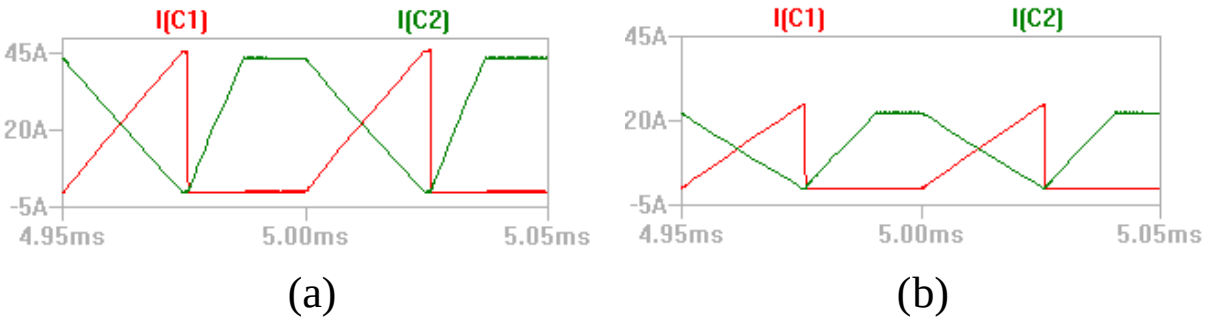

(a) (b)

Figure 5.19: Effect of coupling on the input current (a) $k = 0.95$, (b) $k = 0.9$

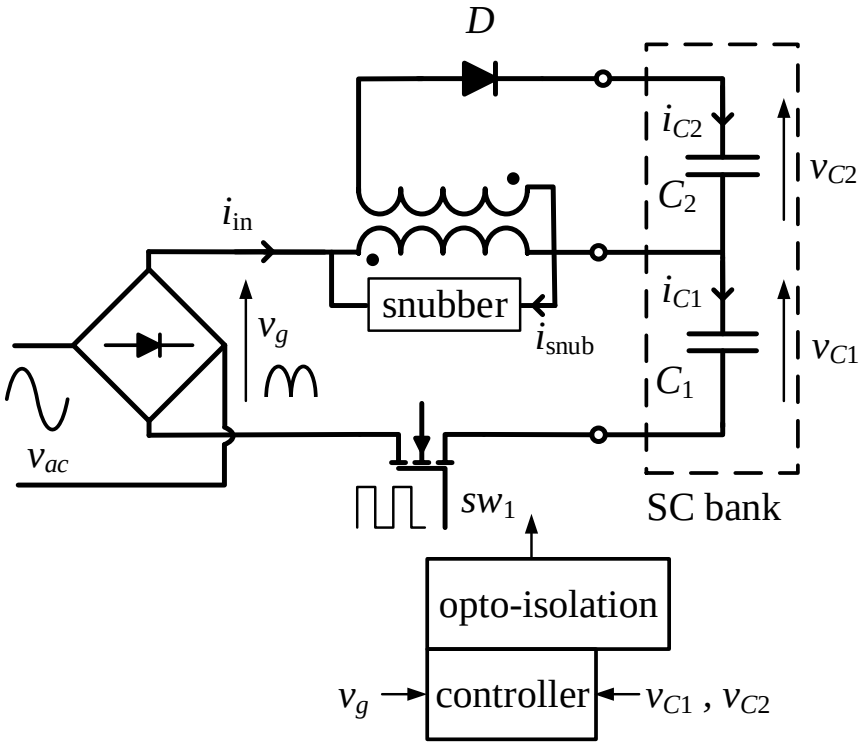

Figure 5.20: The experimental setup of the complete system

be

$$I = \frac{2E}{\Delta T\, V_C}. \tag{5.29}$$

Similarly, based on the total charge transferred into the capacitor, the equivalent charging current can be calculated as

$$I_{\text{eq}} = \frac{C\Delta V}{\Delta T}. \tag{5.30}$$

$C\Delta V$ is the amount of charge transferred into the capacitor. This total charge should be equal to the total area under the current curves of the two capacitors. Since both capacitor currents have sinusoidal peak envelopes, an analytical estimate for the equivalent charging current can be obtained by measuring only the two envelope peak current values (maximum value within one sine envelope: I_{p2} and I_{p1} as marked in Fig. 5.22). The generalised wave shapes for the current through C_1 and C_2 are shown in Fig. 5.17 for 50% fixed duty with T switching period.

Neglecting the snubber losses, the area under the primary and the secondary current curves A_1 and A_2 for the switching cycle with the maximum current, can be calculated as

$$A_1 \;=\; \frac{1}{2}\,\frac{T}{2}\,I_{p1} \;=\; \frac{I_{p1}}{4}\,T \quad \text{and} \quad A_2 \;=\; \frac{1}{2}\left[T + \frac{T}{2}\right] I_{p2} \;=\; \frac{3I_{p2}}{4}\,T \tag{5.31}$$

As seen in Eq. 5.31, the areas are proportional to the peak current values. Hence the envelope of the individual cycle areas will also fit into a sinusoidal envelope. Using the time average definition on a fullwave rectified sinusoid $i(t) \;=\; I_p|\sin(\theta)|$ where I_p is the

peak of the sinusoidal waveform, the average value I_{avg} can be calculated as

$$I_{avg} = \frac{1}{\pi/2}\int_0^{\pi/2} I_p \sin(\theta)\, d\theta = \frac{2}{\pi} I_p \tag{5.32}$$

From the average definition, the area under the curve will be $I_{\text{avg}} \times \Delta T$. By applying this to Eq. (5.31), and equating the total area under one of the sinusoidal current envelopes to the total charge Q

$$Q = \frac{I_{p1}}{4}\frac{2}{\pi} + \frac{3\, I_{p2}}{4}\frac{2}{\pi}. \tag{5.33}$$

By substituting Q in Eq. (5.30) for $C\Delta T$, the equivalent charging current can be obtained as

$$I_{\text{eq}} = \frac{I_{p1}}{2\pi} + \frac{3\, I_{p2}}{2\pi}. \tag{5.34}$$

Fig. 5.23 shows the simulation results for charging a capacitor bank partitioned into two. Based on the results from Eq. (5.30),

$$I_{\text{eq}} = \frac{0.52\ \text{F} \times (11.53\ \text{V} + 4.84\ \text{V})}{600\ \text{ms}} = 14.18\ \text{A}$$

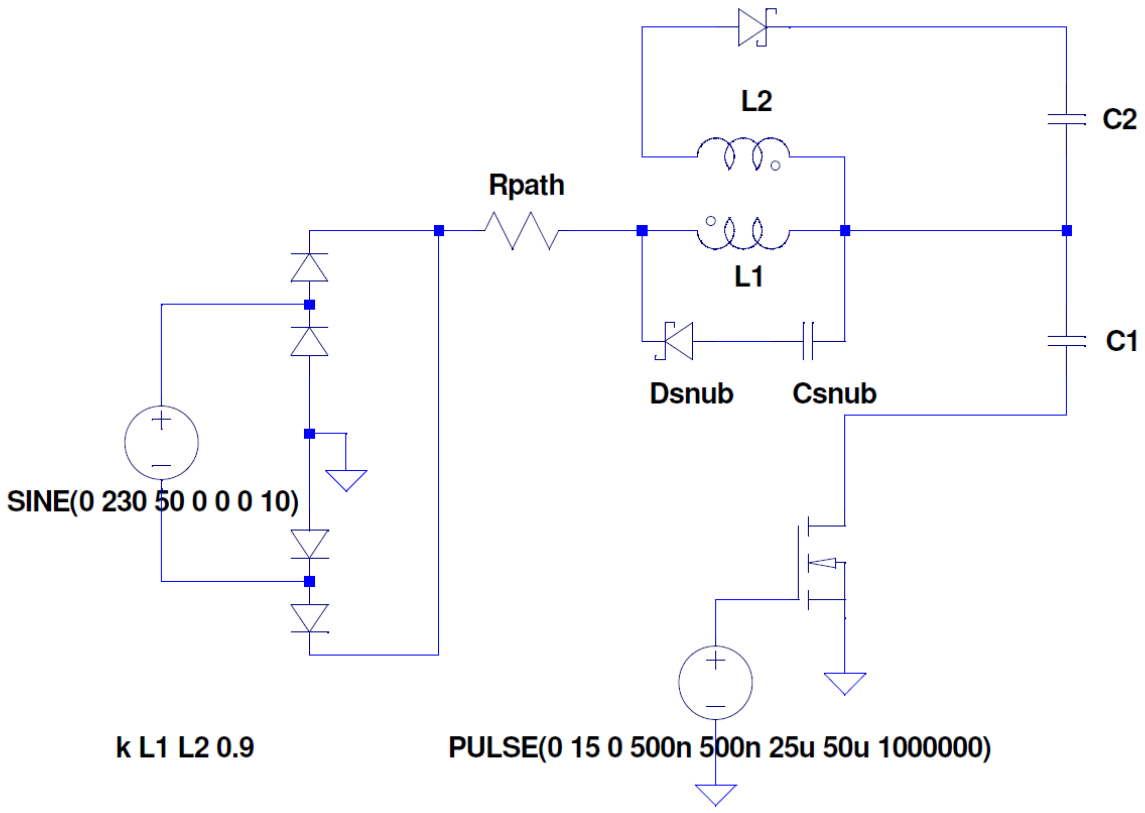

Figure 5.21: The simulated circuit for the fast charger topology. The rectified mains source directly feeds the converter, a single MOSFET switch controls the switching and a Schottky diode for the secondary.

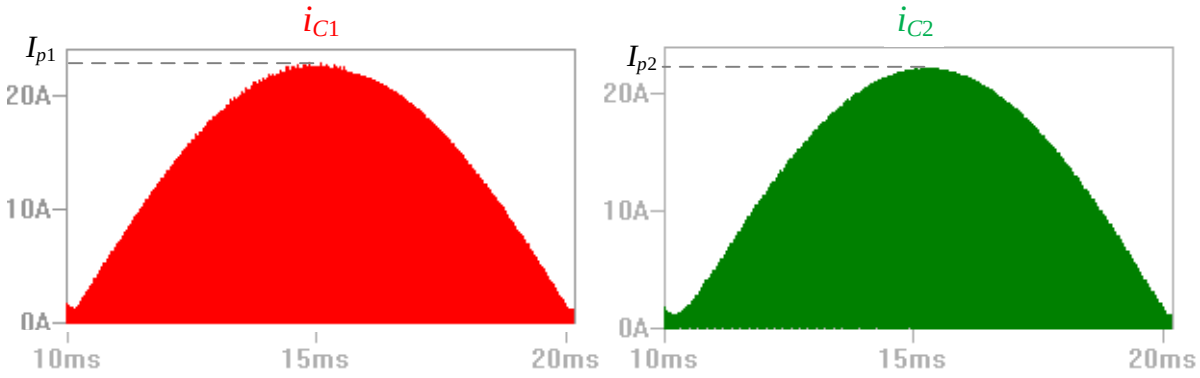

Figure 5.22: Converter current waveforms: primary capacitor current (i_{C1}) and secondary capacitor current (i_{C2})

From Eq. 5.34

$$I_{eq} = \frac{24.8 \text{ A}}{2\pi} + \frac{3 \times 22.4 \text{ A}}{2\pi} = 14.6 \text{ A}$$

The percentage mismatch for simulated results is 2.8%.

Fig. 5.24 shows the experimental results for charging a SC bank partitioned into two. From the figure $I_{p1} = 45$ A and $I_{p2} = 28$ A. After 8.76 s the two SC voltages rise by 0.8 V and 0.82 V. Based on these results from Eq. 5.30

$$I_{\text{eq}} = \frac{650/6 \text{ F} \times (0.8 \text{ V} + 0.82 \text{ V})}{8.76 \text{ s}} = 20.03 \text{ A},$$

and from Eq. (5.34)

$$I_{\text{eq}} = \frac{45 \text{ A}}{2\pi} + \frac{3 \times 28 \text{ A}}{2\pi} = 20.53 \text{ A}.$$

The percentage mismatch of 2.4% can be attributed to the current and time measurement errors. Table 5.3 summarises the calculated I_{eq} values from Eqs. (5.30) and (5.34) based

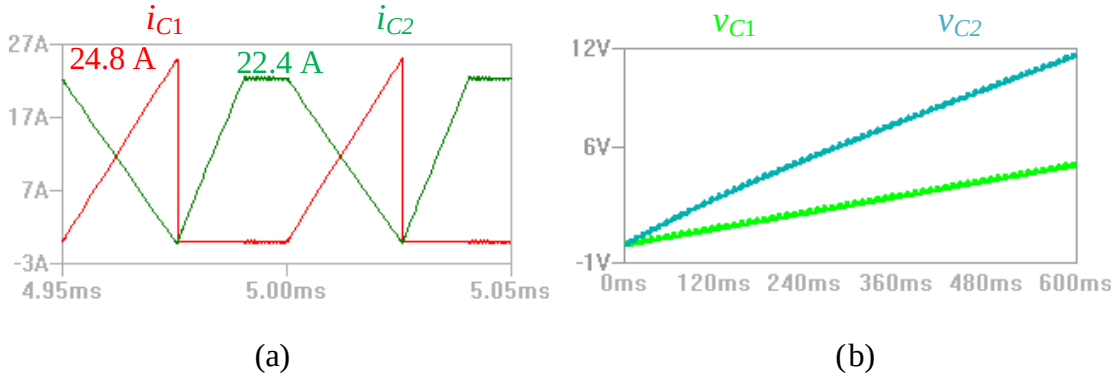

Figure 5.23: Simulation for charging two 0.52 F capacitor banks. (a) expanded view of capacitor current (b) capacitor charging voltage profile

Table 5.3: Comparison of Eq. (5.30) and Eq. (5.34) for Simulation and experimental results

	Simulation	**Experimental**
Time average Eq. (5.30)	$[650/6 \text{ F}(1.3 \text{ V} + 0.82 \text{ V})]/10 \text{ s}$ $= 22.97$ A	$[650/6 \text{ F} \times (0.94 \text{ V} + 0.91 \text{ V})]/10 \text{ s}$ $= 20.04$ A
Analytical Eq. (5.34)	$44.25 \text{ A}/2\pi + (3 \times 29.7 \text{ A})/2\pi$ $= 21.22$ A	$45 \text{ A}/2\pi + (3 \times 28 \text{ A})/2\pi$ $= 20.53$ A
% mismatch	-7.6	2.4

on simulation and experimental results as per Fig. 5.25. This confirms the consistency of Eq. (5.34) for both simulated and experimental results.

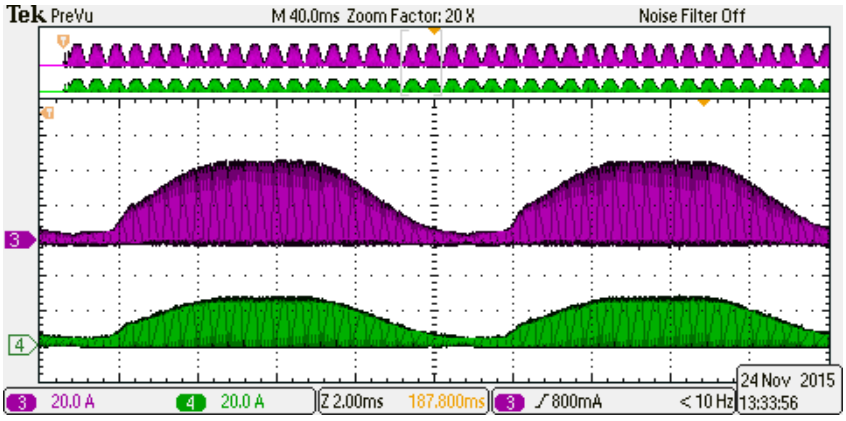

(a)

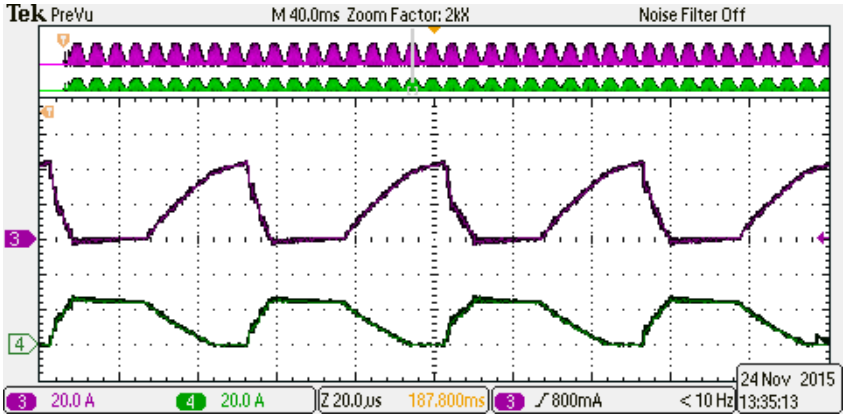

(b)

Figure 5.24: Experimental results for charging two 650 F×6 SC banks. CH 3 - i_{in} and CH 4 - i_{c2} (a) two mains half cycles (b) expanded view for three switching cycles

5.2.5 Converter Efficiency

It was seen in Section 4.3.4 that by introducing an inductor into an RC charging circuit the efficiency can be improved by reusing the stored energy in the inductor. Without the insertion of the inductor an RC circuit will waste energy in the total loop resistance. This can be as bad as 50% of the total energy when charging a capacitor form a voltage source at capacitor rated voltage. The advantage of the series-inductor energy reusing scheme can reach very high theoretical efficiencies as shown in Fig. 4.13. These theoretical simulations assume a perfect coupled inductor and an ideal switch. In a real world implementation efficiency losses may occur at the switching stage: mosfet conduction, switching and snubber losses, and the coupled inductor: leakage and core losses. This section analyses ways to quantify snubber losses and overall converter efficiency based on real world current and voltage measurements.

The converter efficiency can be estimated based on the peak-source voltage, v_{p1}, the peak-source current, i_{p1}, and capacitor final voltages, v_{c1} and v_{c2} using a sinusoidal-average estimation as follows. The peak average power, $p_{\text{avg}}^{\max}$, for a 50% duty converter operating at frequency, f_{sw}, is

$$p_{\text{avg}}^{\max} \;=\; \frac{\frac{1}{2}\,\frac{1}{2f_{sw}}\,v_{p1}\,i_{p1}}{\frac{1}{f_{sw}}} \;=\; \frac{v_{p1}\,i_{p1}}{4} \tag{5.35}$$

Hence the average-input power curve, $p_{\text{avg}}(t)$, can be expressed as,

$$p_{\text{avg}}(t) \;=\; \frac{v_{p1}\,i_{p1}}{4}\sin(2\pi f_{\text{main}}t) \tag{5.36}$$

where f_{main} is the mains supply frequency. Now using Eq. (5.32), the dc average input power, p_{in} can be calculated as

$$p_{\text{in}} \;=\; \frac{v_{p1}\,i_{p1}}{4}\frac{2}{\pi} \;=\; \frac{v_{p1}\,i_{p1}}{2\pi} \tag{5.37}$$

When charging a two fully discharged capacitors of capacitance, C, for time, T, the energy stored in the capacitor, E_C will be,

$$E_C \;=\; \frac{1}{2}C\left(v_{c1}^2 + v_{c2}^2\right) \tag{5.38}$$

For the charging period, T, the power-converter efficiency, η can be calculated based on Eqs.(5.37) and (5.38) as,

$$\eta \;=\; \frac{E_C}{p_{\text{in}}T}\,100\% \tag{5.39}$$

Based on the simulated and experimental results for charging a 650 F×6 SC bank as seen in Fig. 5.25, the calculated efficiency values are around 40%. This lower efficiency is due to various loss components in the circuit. Snubber loss, mosfet switching loss, transformer losses and secondary diode loss.

Using the same sinusoidal-average estimation, the average snubber loss, P_{snub}, can be estimated as in Eq. (5.40)

$$P_{\text{snub}} = \frac{2}{\pi}\left(\frac{1}{2} L_{\text{leak}} I_{p1}^2\right) f_s = \frac{L_{\text{leak}} I_{p1}^2 f_s}{\pi} \tag{5.40}$$

For the experimental set-up with 19.9 μH leakage inductance, L_{leak}, the snubber loss, $P_{\text{snub}} = 19.9\ \mu\text{H} \times 45\ \text{A}^2 \times 20\ \text{kHz}/\pi = 256$ W. In the work presented, snubber optimization and efficiency improvement was not a prime consideration, since this was only a proof of concept circuit prototype. A careful transformer design to reduce leakage inductance and a lossless snubber arrangement can reduce the loss.

5.3 Power Factor Correction

Power factor is defined as the ratio of real power (watts) to apparent power (VA) where the real power is the average, over a cycle, of the instantaneous product of current and voltage, and the apparent power is the product of the rms value of current and the rms value of voltage. If both current and voltage are sinusoidal and in phase, the power factor is 1.0 [78, 79].

PFC reshapes the current drawn from the mains to sinusoidal and aligns it with the source voltage. This shaping and aligning maximizes the real power available from the mains [77]. In Europe and Japan, all electrical equipment consuming 75 W or more must comply with the IEC61000-3-2 standards as seen in Fig. 5.26. To achieve appreciable PFC, input current waveform harmonics beyond the 3$^{\text{rd}}$ should be less than -20 dB.

5.3.1 PFC Ability of the Topology

To achieve PFC, the converter topology does not require the use of an additional choke. When the converter operates in transient mode as shown in Fig. 5.6, it uses a constant on-time control. This mode of control dictates the controller to sense the transformer secondary current zero crossing in order to trigger the next switching cycle [80]. Therefore, during the 50 Hz ac mains cycle the "off" time will vary, resulting in a varying operating frequency.

In order to generate the relationships governing the transient mode of operation with power factor correction, the following conditions are assumed:

- The line voltage is perfectly sinusoidal and the bridge rectifier is ideal, thus the voltage at the converter input is rectified sinusoidal

$$v_g(t) = V_p|\sin(2\pi f_l t)|. \tag{5.41}$$

  where V_p is the peak line voltage and f_l is the line frequency

- The two inductors are perfectly coupled hence there is no leakage
- The secondary side diode is ideal with zero forward voltage drop
- The converter operates in transition mode, i.e., the boundary between continuous and discontinuous inductor current mode

During the "on" time, from the primary current loop

$$v_g(t) \;=\; v_L(t) + v_{C1}(t). \tag{5.42}$$

From the secondary loop, the diode will have a reverse bias of $nv_L + v_{C2}$. This voltage will always be greater than the junction voltage (for a practical diode), therefore a secondary current will not flow (assuming reverse breakthrough is not reached). Further, both the intended applications start charging a capacitor bank that is only partially discharged, hence the reverse bias voltage is guaranteed to be negative even close to the mains zero crossing. From the primary current loop, the "on" time of the control signal is

$$T_{\text{on}} = \frac{L_m i_g(t)}{v_g(t) - v_{C1}(t)} \tag{5.43}$$

According to the first assumption, to obtain a power factor corrected input, the primary current should have a rectified sinusoidal envelope.

$$i_g(t) \;=\; I_p|\sin(2\pi f_l t)|. \tag{5.44}$$

where I_p is the peak current allowed by the source. For the two perfectly coupled inductors the secondary current would be according to the primary to secondary winding ratio n, hence the secondary current $i_s(t) \;=\; n\, i_g(t)$.

During the off time, the secondary side diode conducts. The voltage across the inductor secondary would be v_{C2} as the diode is assumed to be ideal. $n\, v_{C2}$ is the reflected voltage (v_r) on the primary coil during the off period. Therefore the MOSFET's body diode should be capable of handling a peak inverse voltage of $v_r + v_g$.

Similar to Eq.(5.43), the off time $T_{0\text{ff}}$ will be

$$T_{off} = \frac{L_m}{n^2}\,\frac{n\, i_g(t)}{v_{C2}(t)} = \frac{L_m i_g(t)}{n\, v_{C2}(t)} \tag{5.45}$$

For PWM control, the duty cycle D is defined as the ratio of the "on" time to the switching period

$$D \;=\; \frac{T_{\text{on}}}{T_{\text{on}} + T_{\text{off}}}. \tag{5.46}$$

Since the system works in the transition mode, the sum of "on" and "off" times should be equal to the period of the switching signal. By substituting from Eqs. (5.43) and (5.45)

$$D \;=\; \frac{n\, v_{c2}(t)}{v_g(t) + n\, v_{c2}(t) - v_{c1}(t)} \tag{5.47}$$

If the two parts of the capacitor bank are equal, for a constant rate of charge $v_{C1}(t) = v_{C2}(t) = v$, then according to Eq. (5.47) the duty cycle, D, will be

$$D = \frac{nv}{V_P|\sin(2\pi f_L t)| + v(n-1)}. \tag{5.48}$$

The duty cycle, D, will vary with the instantaneous line voltage. The switching frequency f_{sw} will also vary with the line voltage.

$$\begin{aligned} f_{sw} &= \frac{1}{T_{\text{ON}} + T_{\text{OFF}}} \\ \text{when} \quad v_{C1}(t) &= v_{C2}(t) = v \\ f_{sw} &= \frac{nv\,(v_g - v)}{L_m\, i_g\,[v_g + (n-1)\,v]}. \end{aligned} \tag{5.49}$$

To minimize the size of the actual transformer, a minimum frequency higher than 15–20 kHz is selected. In a practical setup the parasitics involved in the MOSFET switching will not allow the switches to follow the ideal relationships for on and off times in Eqs. (5.43) and (5.45). This will effect the performance around the zero crossing but does not affect performance since there is very little energy transfer close to the zero crossing point. As illustrated in an exaggerated form in Fig. (5.6), the switching waveform will hold a constant "on" time while the "off" time is changed to match the peak current determined by the instantaneous line voltage. During each mains half-cycle the input current peak $i_{\text{peak}}(t)$ varies with the instantaneous line voltage according to

$$i_{\text{peak}}(t) = I_{\text{peak}}|\sin(2\pi f_L t)| \tag{5.50}$$

where I_{peak} is the maximum allowed line current.

5.3.2 Simulation and Experimental Results for PFC

Figure 5.27 shows the simulated results of the FFT of the input current waveform. According to the figure the harmonic amplitude for the 3$^{\text{rd}}$ and beyond are lower than -20 dB. This result is achieved with the MOSFET switching kept fixed at 20 kHz with 50% duty. These results show that this converter technique inherits PFC qualities since it can obtain results within the standards even without using any special dedicated technique for PFC.

Figure 5.28 shows the experimental results obtained for the FFT of the input current waveform. As seen in Fig. 5.28(a), the mains current drops to zero during every switching cycle, hence the coloured sinusoidal envelope rather than a sinusoidal outline (which will be normal for a technique using a bulk capacitor). The FFT of the input current waveform matches with the simulation results since all harmonics amplitudes including and beyond the third harmonic are lower than -25 dB. According to both simulation and experimental

results, the −20 dB limit can be reached without employing any special PFC control techniques; this implies that the converter topology has inherent PFC capability. Thus by employing a dedicated PFC control technique much improved results are expected.

5.4 The Complete Circuit

An overview of the prototype converter implemented based on the transformer measured in Section 5.1.9 including all ancillary circuit blocks is given in the block diagram in Fig. 5.29. It shows the main control block and the separate control signals. Optocouplers are used to obtain galvanic isolation between the SC voltage measurements and the controller, and to obtain isolation from the controller to the MOSFET gate driver. The MOSFET used should be a high current capable, N-channel device which can operate beyond the peak ac mains voltage. The secondary side diode should be a high current capable Schottky diode for fast on and off times. The complete fast charger with closed loop control is shown in Fig. 5.30. Further details and the microcontroller coding is provided in Appendix E. The converter interface to the SC bank is via three wires for positive, negative and centre tap. The main advantage in terms of component size is that the design is energy limited, hence need not have components with continuous power capability. For instance, the transformer used for this prototype will go beyond the intended operating temperature of the device (according to the magnetic material selection based on the operating temperature range) when operated at the maximum current to deliver 4 Wh, which is sufficient energy to charge a 310 F×12 SC bank. This was due to the selection of an aggressive current density for the windings to make the transformer size smaller. For these reasons, energy losses will increase once the thermal threshold is exceeded. After careful transformer design and component selection, this converter topology can accommodate any energy requirement at the maximum current available from the mains supply. The New Zealand provisional patent filed for this technique to fast charge a SC bank is given in Appendix A.2

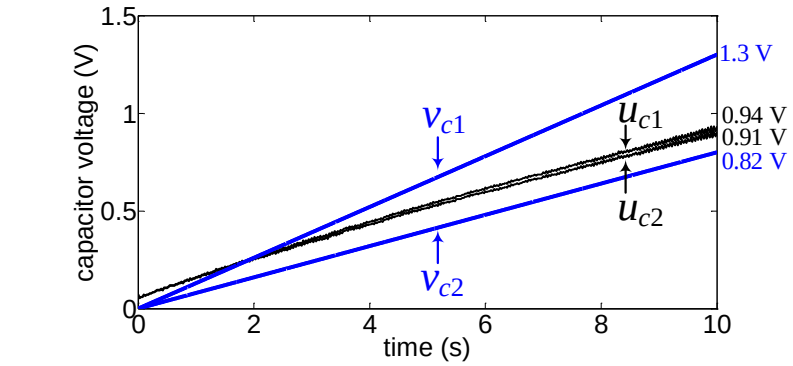

(a)

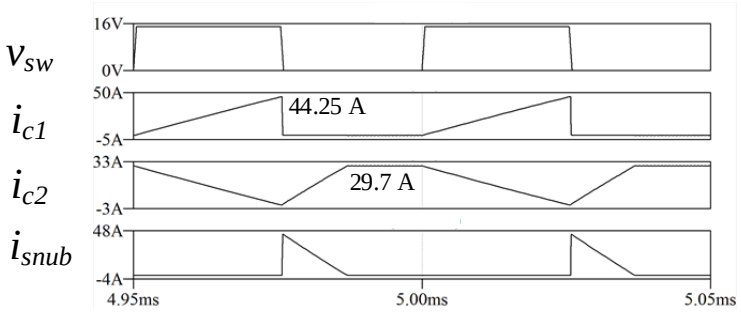

(b)

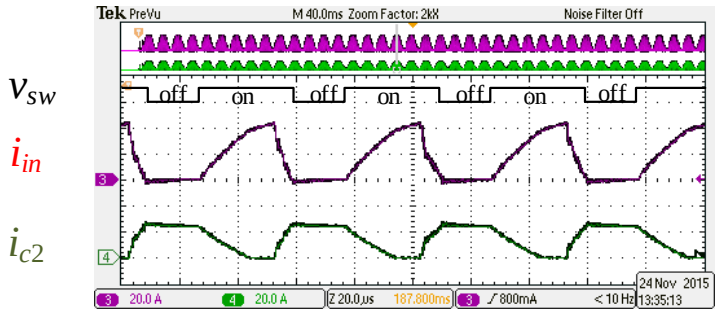

(c)

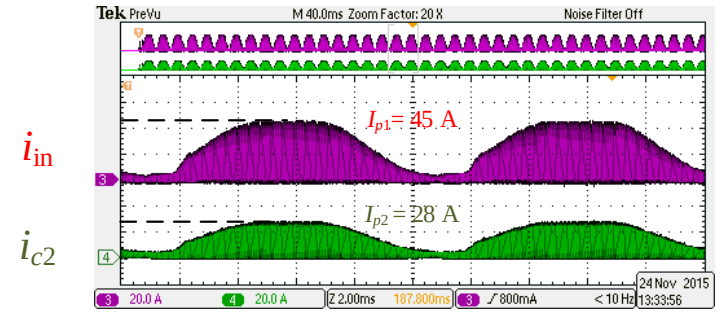

(d)

Figure 5.25: Simulation and experimental results for a 10 s test charging two 3 Wh, 650 F × 6, 16.2 V in series SC banks using a transformer with 0.9 coupling coefficient and 1:1 turns ratio. Switching at 20 kHz with 50% fixed duty. (a) simulated (v_{c1} and v_{c2}) and experimental (u_{c1} and u_{c2}) capacitor voltage rises (b) simulated current waveforms at the center of the 50 Hz sinusoidal envelope (c) and (d): experimental current waveforms, scale 20 A/div

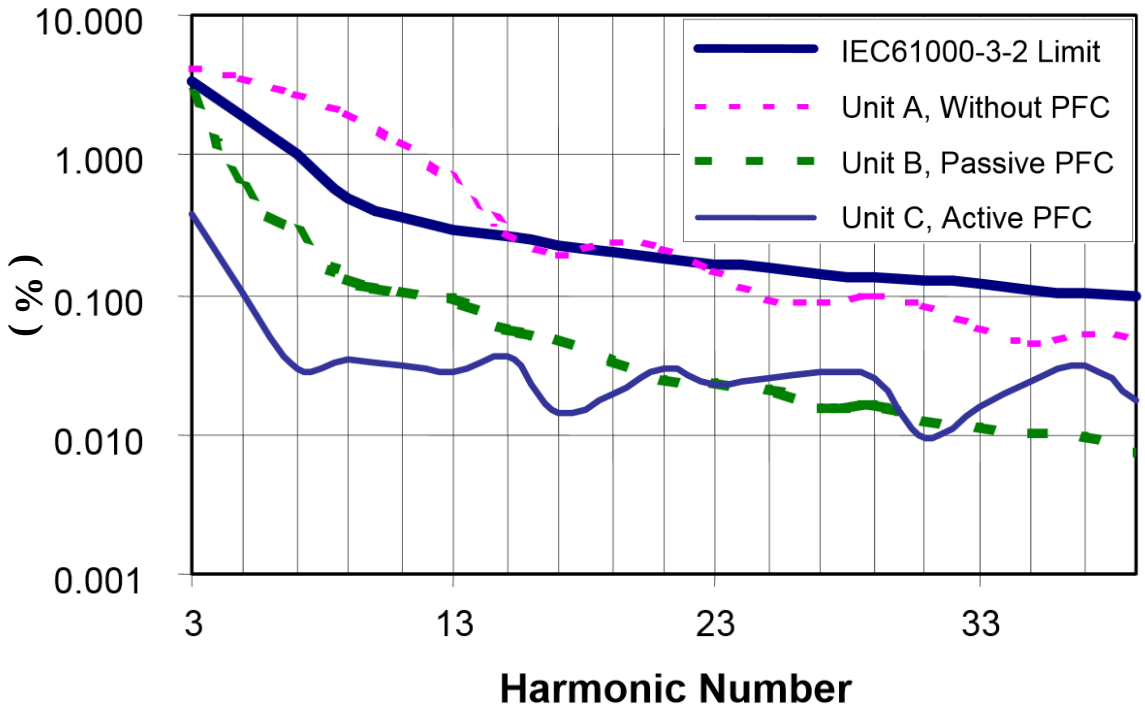

Figure 5.26: Input harmonics percentage for three computer power supplies relative to IEC61000-3-2 Limits [77]

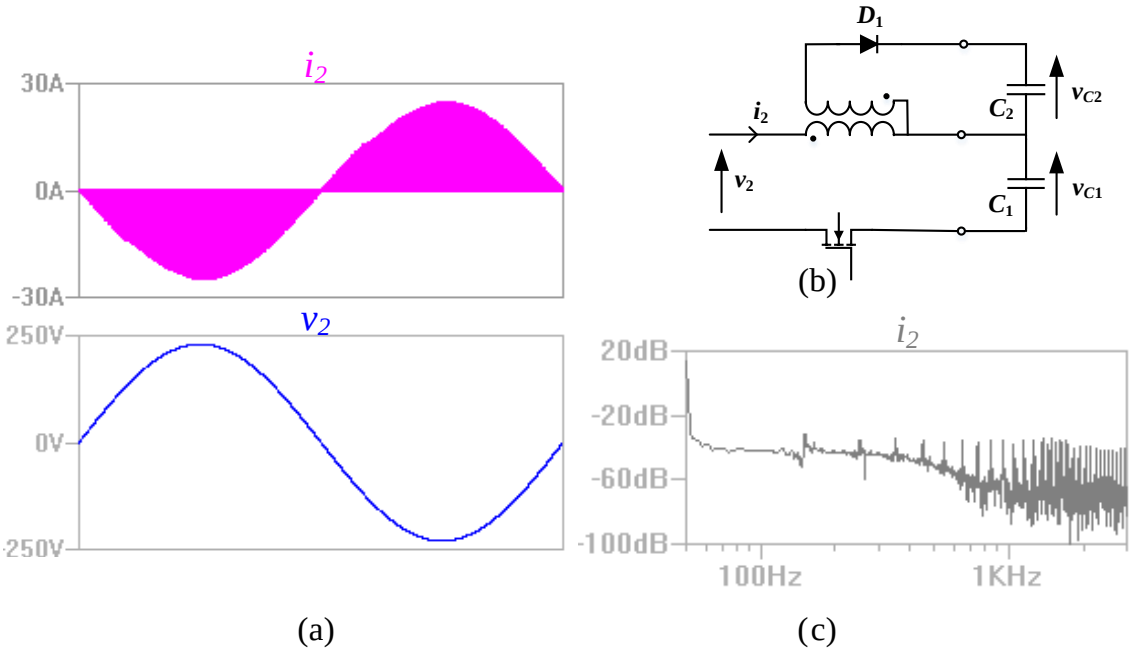

Figure 5.27: Simulation results for PFC. (a) input voltage and current waveforms (b) v_2 is the input source voltage and i_2 and (b) FFT of the input current waveform

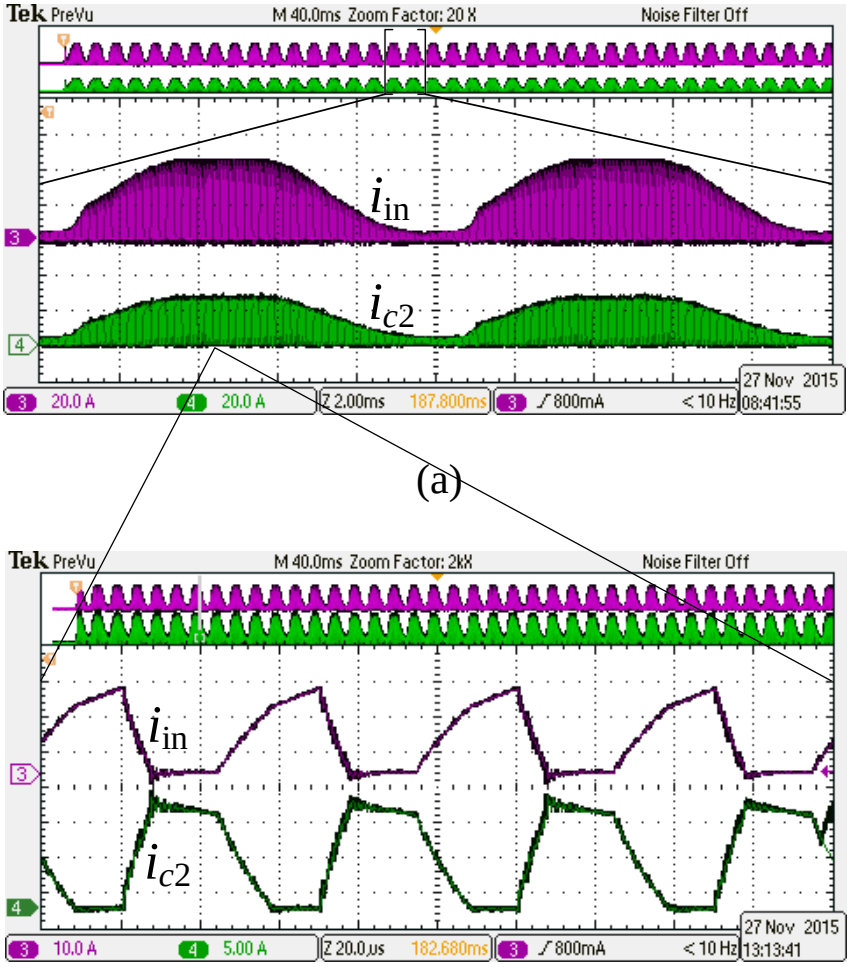

Figure 5.28: Experimental results for PFC. (a) A single ac mains cycle of the primary and secondary currents (b) expanded view of the primary and secondary currents (c) FFT of the current drawn from the mains (addition of the primary capacitor current and the snubber current) CH 3 - $i_{\text{in}} = i_{C1} + i_{\text{snub}}$ and CH 4 - i_{c2}.

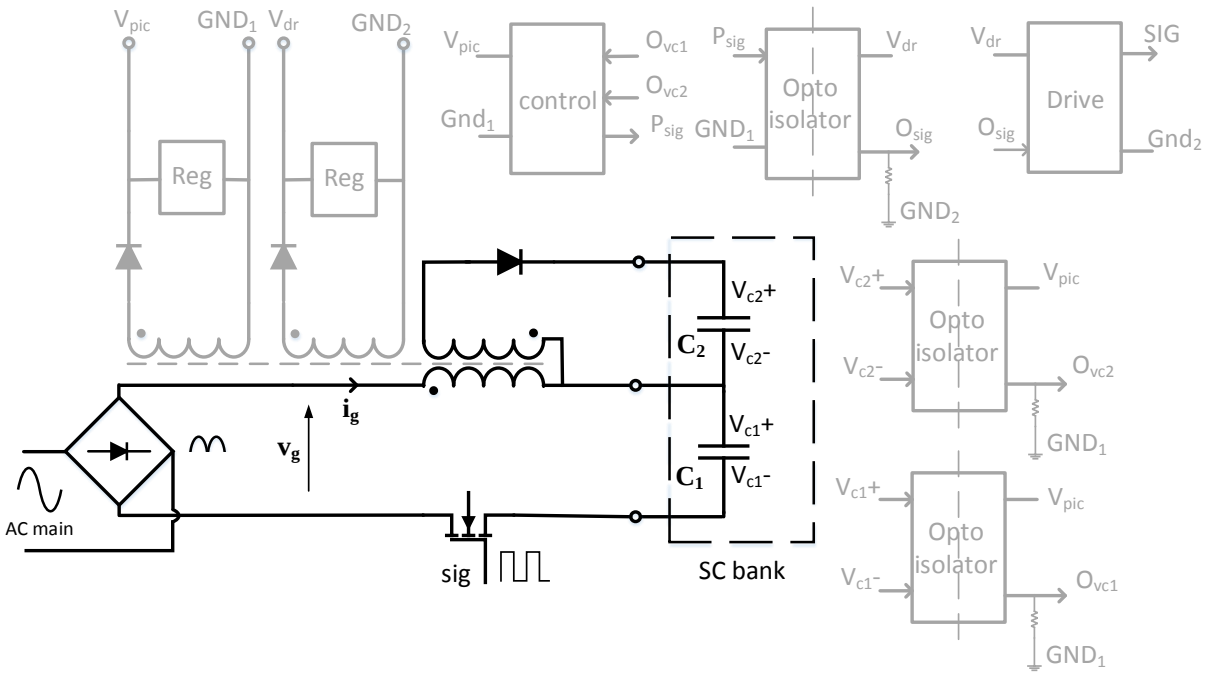

Figure 5.29: The overall circuit with integrated controls for charging C1 and C2 at the same rate. The converter is directly fed by the fullwave rectified mains without using any buffer capacitors.

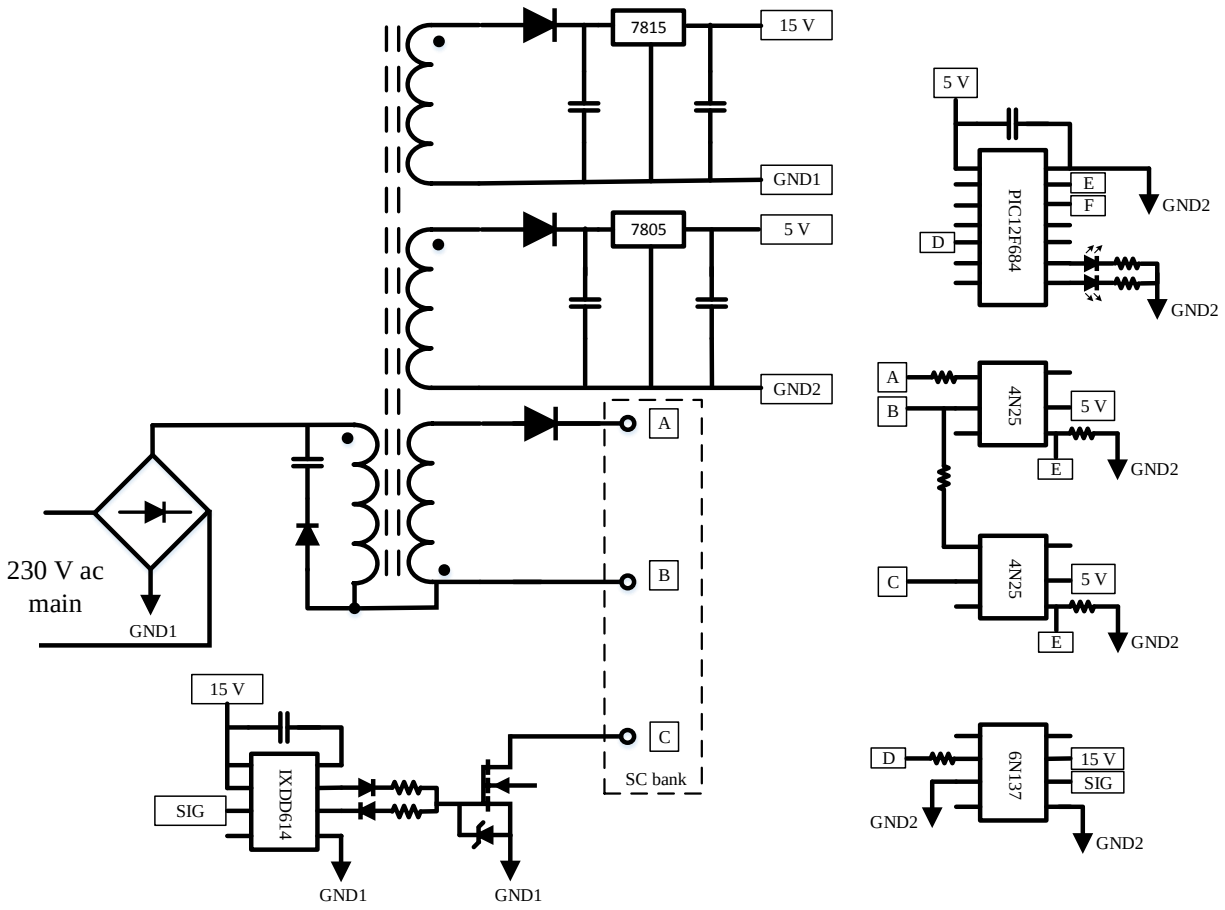

Figure 5.30: The complete circuit of the fast charger with closed-loop control to avoid capacitor overcharging.

Chapter 6

Conclusions and Future Work

6.1 Summary and Conclusion

Analysis of the "instantaneous" water heating problem revealed the specifications for SCATMA

- High power is required for a short duration resulting in a limited energy content
- Power source should be high in both power and energy density
- Power source should have galvanic isolation from the mains supply
- Input power available from the mains is limited by safety regulations.

To fulfill the above specifications, the solution should use pre-stored energy. State-of-the-art energy storage media are not capable of meeting these requirements because

- There is no energy storage medium which has the high energy density and the high power density required
- Even SC, the only technology capable of handling the required high output power and cycle life, have very low energy densities and the cost per joule is still too high though the cost per kilowatt is low
- All battery chemistries undergo premature ageing in stand-alone operation at the required power level

Having identified pre-stored energy as the only solution, and having regard to the limitations of each device, the closest practical implementation is a hybridization of SCs with batteries. A hybrid configuration combines the high energy density of batteries with the high power density of SCs to meet the specifications. Several hybrid solutions were analysed. A prototype was built based on the new battery-SC series-hybrid system. Based on the results of this system the following conclusions can be made

- A series hybrid system can meet the temperature rise, power and energy requirements of "instant" water heating
- The cycle life of the batteries can be managed by reducing the depth of discharge and the discharge rate by paralleling multiple low-capacity batteries
- The size of the energy storage, even in the form of a hybrid system, is still beyond the affordable cost for a commercial implementation and the available volume under a kitchen sink

Based on these conclusions, for a SCATMA system to be commercialized, the amount of pre-stored energy in SCs should be reduced. A similar challenge (high power and limited energy) was addressed by the SRUPS research team. The bank circulation technique in SRUPS was analysed for more generalised high-power limited-energy applications which revealed that the optimum number of SC banks and bank circulation cycles required can be found analytically. The optimum choice will minimize the energy remaining at the end of the operating cycle and ensure constant output power during the period of operation.

For this circulation technique to be effective in reducing the pre-stored SC energy, the system mandates that the capacitors to be charged at the maximum capability of the mains power source. Hence the requirement for a fast charger. A comparison of available charging mechanisms shows that a capacitor can be charged faster using a higher voltage source (a voltage higher than the capacitor working voltage), than when using a voltage source that matches the capacitor rated voltage, even with the same maximum constant current limit. To obtain fast charging the source voltage should be higher than a critical source voltage value dependent on the charger current limit and the charging path resistance.

The main goal of this charging process is fast replenishing of the capacitors during the operating cycle of the bank circulation. Therefore in the analysis, time to charge is paramount. The comparison between RC and RLC circuits shows that

- When a capacitor is charged through a resistor, at high voltages the energy loss in the resistor increases due to higher initial charging currents
- The optimum charging efficiency in an RC system is obtained by choosing the source voltage to match the allowed depth of discharge
- In an RLC circuit the use of a series inductor improves charging efficiency if the energy stored in the inductor can be reused.

Based on the above results, a novel converter topology for fast capacitor charging was implemented using a coupled inductor which allows

- A high voltage source in the form of a full-wave rectified ac mains to be used directly to feed the converter
- Elimination of the conventional dc bus bulk capacitor required for PFC
- The capacitor bank to be charged at a higher equivalent current by partitioning the SC bank into two parts
- To store energy in the series inductor while the capacitor is getting charged
- The stored energy in the inductor to charge the second part of the capacitor bank

This method requires capacitor voltage monitoring to avoid overcharging. The converter works in transient mode and PFC is achieved without using any additional components. Simulation and experimental results on the prototype design suggest

- The equivalent charging rate can be calculated based on the primary and secondary peak currents
- The design is energy limited based on the transformer design and component selection
- The converter design has inherent transient mode power factor correction capability

6.2 Future Work

The battery storage configuration requires more investigation. Tests need to be done to investigate how much energy is being used per battery, for each water heating cycle. The total drain per day can then be calculated, along with the depth of discharge. Accelerated cycle life testing of the energy storage media should be performed on a typical SCATMA system to analyse the performance of the storage media under typical household hot water usage.

At the time of this project, hybrid SCs with 2.5–2.7 times more energy density than electric double layer SCs were not introduced into the market. At the time of the project completion hybrid SCs are commercially available from manufacturers like Samwha capacitors Inc. [81]. Instead of the activated carbon electrodes they use a lithium titanate anode and a standard activated carbon cathode to improve the energy density of the hybrid energy storage device. Table 6.1 compares the new devices with the already available SCs and Li-ion batteries. New hybrid SCs store more energy while the peralty on power density is very minute. Based on the current market prices, a hybrid-SC SCATMA solution for typical wash basin will cost around 600 NZD to store the required 100 Wh. This is well within the target NZ market price for an "instant" water heater given the ability of a fast charger to reduce the total energy storage requirement. Further the size of the energy storage to store 100 Wh based on Samwha 7500 F, 2.85 V hybrid SC is also comparable with commercial solutions listed in Table 1.2. The 7500 F capacitor has a specific energy of 50126 mm^3/Wh, hence the required volume to store 100 Wh is 5×10^6 mm^3. This volume will fit into a size 250 mm×250 mm×80 mm.

Table 6.1: Comparison of electric double layer capacitors, hybrid supercapacitors and lithium-ion batteries

Item	Supercapacitors	Hybrid capacitors	Li-ion batteries
Energy density (Wh/kg)	3–6	7–14	20–100
Power density (W/kg)	2000- 6000	2000–3000	100–300
Cycle life	>500000	>50000	<1000
Cost/kWh (NZD)	10000–10500	6000–6500	550–650

More research and investigation is required around the coil/element at the water interface. Optimising the coil shape, size and material could greatly reduce the initial inefficiencies in the circuit. This would result in a lower energy requirement, as well as an inherent reduction in the rise time of the temperature (moving from the current 10 seconds, to the target 2–4 seconds).

Additional research and development effort is required to incorporate the suggested fast charger and a circulating SC bank into a SCATMA system to reduce the amount of pre-stored energy. A complete controller with protection circuitry needs to be developed and demonstrated.

To obtain maximum allowable power from the mains supply, several fast chargers should be interleaved. This may be implemented using several magnetic cores or by using a special switching arrangement to interleave the several primary and secondary windings wound on the same magnetic core.

More detailed research is required to implement the proven PFC method into the fast charger. EMI and power quality issues should be studied prior to the implementation of this fast charger as a commercial solution to "instant" water heating.

Appendix A

Patent Applications

A.1 SCATMA Patent

N. Kularatna, Fluid temperature modification apparatus,"WO2014/189389 A1, International Patent application PCT/NZ2014/000092.

(12) INTERNATIONAL APPLICATION PUBLISHED UNDER THE PATENT COOPERATION TREATY (PCT)

(19) World Intellectual Property Organization
International Bureau

(43) International Publication Date
27 November 2014 (27.11.2014)

WIPO | PCT

(10) International Publication Number
WO 2014/189389 A1

(51) International Patent Classification:
F24H 9/20 (2006.01) *F24H 1/10* (2006.01)

(21) International Application Number:
PCT/NZ2014/000092

(22) International Filing Date:
21 May 2014 (21.05.2014)

(25) Filing Language: English

(26) Publication Language: English

(30) Priority Data:
610789 21 May 2013 (21.05.2013) NZ

(71) Applicant: **UNIVERSITY OF WAIKATO** [NZ/NZ]; Hillcrest Road (no number), Hamilton, 3216 (NZ).

(72) Inventor: **KULARATNA, Alythwela Domingo Vithanage Nihal**; 29 Langdale Court, Huntington, Hamilton, 3210 (NZ).

(74) Agents: **MURPHY, Simon John** et al.; Level 10, 21 Queen Street, Auckland, 1010 (NZ).

(81) Designated States *(unless otherwise indicated, for every kind of national protection available)*: AE, AG, AL, AM, AO, AT, AU, AZ, BA, BB, BG, BH, BN, BR, BW, BY, BZ, CA, CH, CL, CN, CO, CR, CU, CZ, DE, DK, DM, DO, DZ, EC, EE, EG, ES, FI, GB, GD, GE, GH, GM, GT, HN, HR, HU, ID, IL, IN, IR, IS, JP, KE, KG, KN, KP, KR, KZ, LA, LC, LK, LR, LS, LT, LU, LY, MA, MD, ME, MG, MK, MN, MW, MX, MY, MZ, NA, NG, NI, NO, NZ, OM, PA, PE, PG, PH, PL, PT, QA, RO, RS, RU, RW, SA, SC, SD, SE, SG, SK, SL, SM, ST, SV, SY, TH, TJ, TM, TN, TR, TT, TZ, UA, UG, US, UZ, VC, VN, ZA, ZM, ZW.

(84) Designated States *(unless otherwise indicated, for every kind of regional protection available)*: ARIPO (BW, GH, GM, KE, LR, LS, MW, MZ, NA, RW, SD, SL, SZ, TZ, UG, ZM, ZW), Eurasian (AM, AZ, BY, KG, KZ, RU, TJ, TM), European (AL, AT, BE, BG, CH, CY, CZ, DE, DK, EE, ES, FI, FR, GB, GR, HR, HU, IE, IS, IT, LT, LU, LV, MC, MK, MT, NL, NO, PL, PT, RO, RS, SE, SI, SK, SM, TR), OAPI (BF, BJ, CF, CG, CI, CM, GA, GN, GQ, GW, KM, ML, MR, NE, SN, TD, TG).

Declarations under Rule 4.17:

— *of inventorship (Rule 4.17(iv))*

Published:

— *with international search report (Art. 21(3))*

— *before the expiration of the time limit for amending the claims and to be republished in the event of receipt of amendments (Rule 48.2(h))*

(54) Title: FLUID TEMPERATURE MODIFICATION APPARATUS

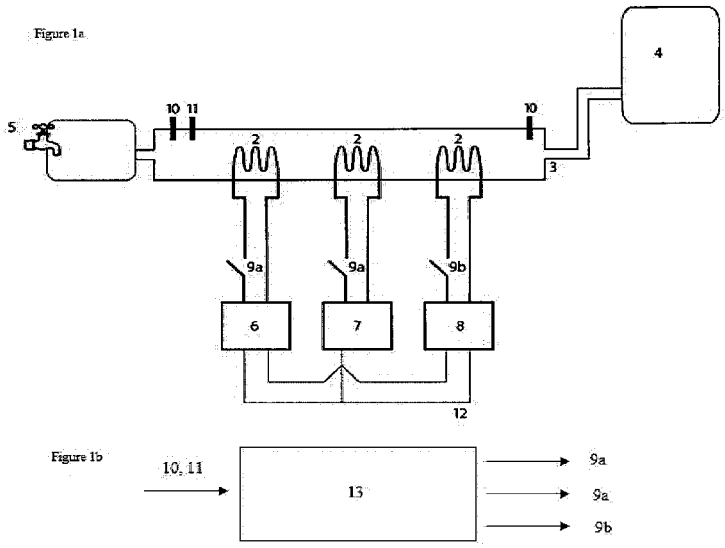

(57) Abstract: In one aspect the invention provides a fluid temperature modification apparatus which includes at least one temperature modification element associated with a fluid conduit. This temperature modification element or elements are located adjacent to an outlet of the fluid conduit. The apparatus also includes at least one energy storage capacitor, and at least one trigger switch which when operated connects one or more energy storage capacitors to a temperature modification element. The operation of a trigger switch at least partially discharges at least one energy storage capacitor to energise a temperature modification element which modifies the temperature of fluid in the conduit adjacent to the outlet port of the conduit.

WO 2014/189389 A1

FLUID TEMPERATURE MODIFICATION APPARATUS

Field of the Invention

This invention relates to a fluid temperature modification apparatus. In a preferred embodiment the invention may be arranged to deliver hot water from a hot water supply tap without a user having to wait for cold water to be flushed out of a hot water supply line.

Background of the Invention

Plumbing and fluid conduit based systems have been developed to allow fluid to be distributed to various points inside a structure. These systems can be used to distribute a range of fluids from a supply reservoir or a connection to a utility supply network. In a variety of instances the temperature of these fluids may need to be adjusted before they can be used in a desired application.

Central fluid heating or cooling systems plumbed into supply lines can adjust the temperature of a fluid prior to delivery. However these systems will leave sections of supply line between outlet ports and the temperature treatment system holding fluid, and the fluid within ultimately ends up at the ambient environmental temperature. The fluid within these sections of supply line will need to be flushed out before fluid at a desirable temperature is available at an outlet.

This approach will result in the fluid at ambient temperature being wasted, with wastage accumulating to significant volumes both over time and within supply networks having multiple fluid outlets serviced by a single temperature treatment system.

For example, in houses and apartment blocks hot water can be delivered to multiple outlet taps from a central tank of heated water. Water users who turn on hot water delivery taps will typically have to run the tap for 5-40 seconds to flush out water at the ambient temperature. The entire volume of

water trapped in the plumbing between the tap and central hot water tank will need to be flushed out and is generally allowed to run down a drain.

This wastage of water is a concern to both householders and water supply utilities. Furthermore, householders find it inconvenient to have to wait for cold water to be flushed out of a tap before they have hot water delivered.

To combat this problem it would be possible to install additional heating or cooling systems adjacent to an outlet port or tap. However, in these buildings electrical energy is generally delivered by alternating current ("AC"). These AC systems generally run at either 230V at 50Hz or 110-120V at 60Hz. Having AC power supplied to electrical components in the vicinity of fluids such as water can create safety issues, and these problems are normally addressed by using a transformer isolated power converter to provide galvanic isolation and convert the available AC power into a direct current supply.

Although transformer isolated technology and associated circuitry can allow AC or DC current to be supplied safely the vicinity of a fluid outlet tap, the internal construction of the transformer places significant restrictions on how quickly energising current can be supplied to an associated heating coil. In particular, transformers are not able to supply a high enough energising current quickly enough for users wishing to have immediate access to hot water.

A similar situation is applicable with heating or cooling systems powered by existing electrical battery technology. The relatively high internal resistance of existing batteries limits their capacity to supply instantaneous high power, with the internal resistance of the battery also increasing as it is discharged. Additionally, battery lifetime will be limited by the requirement for repeated high power discharge cycles.

It would therefore be of advantage to have an improved fluid temperature modification apparatus which addressed any or all of the above issues, or at least provided the public with an alternative choice. In particular it would be of advantage to have an apparatus which could modify the temperature of fluid stored in the supply line prior to the fluid reaching the delivery outlet

from a central temperature treatment system. An additional advantage would be the ease of installation of such a device, enabling plumbers to retrofit into existing fluid supply lines. It would also be of advantage in domestic applications to have an apparatus which could almost instantly deliver hot water from a hot water tap without a user having to wait for cold water to be flushed out of a hot water supply line.

Disclosure of the Invention

According to one aspect of the present invention there is provided a fluid temperature modification apparatus which includes

at least one temperature modification element associated with a fluid conduit, said temperature modification element being located adjacent to an outlet of said fluid conduit, and
at least one energy storage capacitor, and
at least one trigger switch which when operated connects one or more energy storage capacitors to a temperature modification element,

wherein the operation of a trigger switch at least partially discharges at least one energy storage capacitor to energise a temperature modification element which modifies the temperature of fluid in the conduit adjacent to the outlet port of the conduit.

According to a further aspect of the present invention there is provided a fluid temperature modification apparatus substantially as described above wherein a trigger switch is associated with a bank of energy storage capacitors and a temperature modification element.

According to a further aspect of the present invention there is provided a fluid temperature modification apparatus substantially as described above which includes a plurality of trigger switches, two or more of said trigger switches each being connected to a separate bank of energy storage capacitors.

According to yet another aspect of the present invention there is provided a fluid temperature modification apparatus substantially as described above

which includes a plurality of temperature modification elements, with one of a plurality of trigger switches being associated with each temperature modification element.

According to a further aspect of the present invention there is provided a fluid temperature modification apparatus substantially as described above wherein said at least one temperature modification element is energised by a transformer isolated power converter and associated electronic sub-systems providing a supply of direct current (DC) electrical energy from an alternating current (AC) source.

According to another aspect of the present invention there is provided a fluid temperature modification apparatus substantially as described above which includes an activation sensor adapted to issue a signal which indicates when the outlet of the conduit has been opened.

Preferably an activation sensor can be formed from a flow rate sensor.

According to a further aspect of the present invention there is provided a fluid temperature modification apparatus substantially as described above which includes a controller arranged to receive said indicative activation signal from the activation sensor and to issue at least one control signal to at least one trigger switch to operate said trigger switch or switches based on the received activation signal.

According to a yet further aspect of the present invention there is provided a fluid temperature modification apparatus substantially as described above which also includes
an inlet temperature sensor arranged to provide a signal indicative of the temperature of fluid entering the fluid conduit, and
a controller arranged to receive said indicative temperature signal from an inlet temperature sensor and to issue at least one control signal to at least one trigger switch to operate said trigger switch or switches

According to yet another aspect of the present invention there is provided a fluid temperature modification apparatus substantially as described above which also includes

an inlet temperature sensor arranged to measure the stored fluid temperature, and
an output temperature sensor arranged to provide a signal indicative of the temperature of fluid leaving a fluid conduit outlet, and
a controller arranged to receive said indicative temperature signal from the temperature sensors and to issue at least one control signal to at least one trigger switch to operate said trigger switch or switches based on at least in part the received indicative temperature signals.

Preferably the controller is arranged to issue at least one control signal to operate said trigger switch or switches based on a combination of an indication of conduit fluid flow rate provided by an activation sensor and the received indicative temperature signals received from the inlet and outlet temperature sensors.

The present invention is arranged to provide a temperature modification apparatus used in conjunction with a fluid conduit. The invention is to be located adjacent to an outlet of this fluid conduit and is to be used to modify the temperature of fluid stored in the supply conduit to facilitate prompt delivery of fluid at or near a desired temperature.

Those skilled in the art will appreciate that conduits have a significantly greater length than diameter and are usually closed by a terminating valve or similar component. The conduits with which the present invention are employed will therefore immediately allow for the delivery of fluids once a user has made a demand for these fluids.

In a preferred embodiment the invention may be used in a domestic hot water heating application. In this application the fluid to be modified is water at ambient temperatures which is located in a section of plumbing conduit which runs between a central hot water supply system and an outlet hot water tap. In such embodiments the invention includes at least one temperature modification element located in contact or association with a section of plumbing conduit which extends from a wall or similar structure and which terminates in a hot water outlet such as a hot water tap.

In other embodiments the invention may be used to heat or cool other types of fluids in a variety of applications. For example in alternate applications the invention may be used to heat raw material fluids which are employed in a production process and are delivered via conduit from a main reservoir. In yet other embodiments the invention may – for example – be used to cool beverages delivered via supply lines in public bars.

Reference throughout this specification will in the main be made to the invention being used to heat water in a domestic hot water supply application. However those skilled in the art will obviously appreciate that the invention may be used in other applications and reference to the above should in no way be seen as limiting.

The invention includes at least one temperature modification element which – when energised – is arranged to heat or cool fluid contained within a conduit. As referenced above, in a preferred embodiment a temperature modification element may be arranged to heat water in a section of conduit adjacent to a hot water tap.

In such preferred embodiments a temperature modification element may be formed by an electrically energised heating coil sited inside a conduit and in direct contact with water or other fluid to be heated. A heating coil can be supplied with an electrical current so that the coils electrical resistance will result in the heating of water in the conduit.

In other embodiments however a temperature modification element may be arranged to cool fluid within a conduit. For example, in one alternative embodiment the invention may implement temperature modification elements in the form of thermo-electronic cooling devices which incorporate at least one Peltier junction.

Reference throughout this specification will however be made to a temperature modification element being formed from a heating coil, although those skilled in the art will appreciate that other components may be employed in various alternative embodiments.

In a preferred embodiment the invention includes a plurality of temperature modification elements. Each temperature modification element may be energised by at least one capacitor, and in preferable embodiments energised by a bank of capacitors.

In some embodiments a temperature modification element may be energised by two or more banks of capacitors. For example, in one potential embodiment the invention may include a fast discharge capacitor bank and a high storage capacitor bank, each of the fast discharge and high storage capacitor banks being connected to a separate trigger switch.

Preferably in such embodiments the trigger switch connected to the fast discharge capacitor bank is closed to energise a temperature modification element once the opening of the outlet of the conduit has been detected. In such embodiments the trigger switch connected to the high storage capacitor bank can be closed to energise a temperature modification element after the at least partial depletion of the fast discharge capacitor bank.

In yet other embodiments a temperature modification element may be energised by a transformer isolated power converter and associated electronic sub-systems providing a supply of DC electrical energy from an AC source. In such embodiments the trigger switch can be closed to energise a temperature modification element at substantially the same time as said one or more energy storage capacitors are used to energise a temperature modification element.

Reference throughout this speciation has also been made to the invention employing a transformer isolated power converter and associated electronic sub-systems in various roles in a number of embodiments. Those skilled in the art will appreciate that this component may take a range of forms from a traditional large stand-alone transformer through to small integral high frequency ferrite or similar components which can perform in the same function.

Furthermore, in one particular embodiment the invention may be implemented by a combination of three separate heating coils - each energised respectively by a fast discharge capacitor bank, a high storage

capacity capacitor bank, and a transformer isolated power converter providing a supply of DC electrical energy from an AC source.

The invention employs at least one energy storage capacitor which is at least partially discharged to energise at least one temperature modification element.

In a preferred embodiment the invention may employ large capacitors provided by electrical double layer capacitors. These EDL or electrical double layer capacitors are also known as super capacitors, ultra-capacitors, pseudo capacitors or cap-batteries.

EDL capacitors have a high capacitance giving these components and their associated circuitry high relative time constants. Due to the nature of their construction and size, EDL capacitors have relatively large energy storage capacity and can be discharged at a high rate of power.

Reference throughout this specification will also be made to the invention employing large capacitors formed from or provided by EDL capacitors. However those skilled in the art will appreciate that the present invention may also be implemented through other forms of suitable capacitors.

According to one aspect of the invention there is provided a trigger switch used to connect a temperature modification element to a source of energy such as a capacitor bank, or a DC current supply provided by a transformer isolated power converter. Trigger switches associated with either or both of an energy source or temperature modification element can allow a variety of energy supply configurations to be developed.

For example in embodiments where the invention is used to implement a fast discharge capacitor bank and a high-capacity capacitor bank, the fast discharge bank can be discharged to a heating coil as soon as the opening of the conduit outlet is confirmed. A temperature sensor provided by the invention can determine whether the fluid leaving the outlet has been heated enough. After a threshold time since opening of the outlet, if the fluid leaving the outlet requires further heating a trigger switch associated with a high-capacity capacitor bank may be activated.

As indicated above in various embodiments the invention may provide a temperature modification element energised by an AC or DC supply derived from a transformer isolated power converter. The temperature modification element energised by the power converter may also be connected to a trigger switch. The energisation of this temperature modification element can then be triggered at the same time as the outlet opens and in parallel with the temperature modification element energised by a fast discharge capacitor bank or high-capacity capacitor bank.

In a variety of embodiments a trigger switch may be deployed or located within a fluid conduit and adjacent to a temperature modification element. This arrangement of the invention also allows any waste heat generated by the operation of the switch to be delivered to fluid present in the conduit. In a number of such embodiments trigger switches may be implemented using solid state transistor or similar semiconductor based switches which can be submerged in the fluid held by a conduit and still function effectively.

Preferably in embodiments where the invention provides a temperature modification element energised by a DC supply derived from a transformer isolated power converter, these same energy supply connections can be used to recharge the capacitor or capacitors used by the invention.
In some embodiments of the invention at least one temperature modification element may be energised by a battery providing a supply of DC electrical energy. Batteries can provide an alternative source of electrical energy which can complement the energy discharge characteristics of the capacitors used with the invention.

Preferably in such embodiments the trigger switch associated with the battery is closed to energise a temperature modification element at substantially the same time as said one or more energy storage capacitors are used to energise a temperature modification element. This approach caters for the limited power capability of battery systems, allowing capacitors to energise a temperature modification element immediately, with a battery providing a further energy source prior to the capacitors being fully discharged.

In some embodiments the trigger switch associated with a battery can be closed in a periodic or repeating fashion to establish a duty cycle for the battery connection in some circumstances. For example in some cases a pulse width modulation connection scheme may be employed in conjunction with a battery trigger switch to vary the heating or cooling contribution provided by the battery. The effective duty cycle of this triggering signal may for example be modified depending on the predicted energy demands currently being placed on the invention.

In a preferred embodiment the invention may include a capacitor recharge circuit configured to recharge one or more at least partially discharged capacitor banks at the same time as one or more charged capacitor banks are being discharged. This capacitor recharge circuit can therefore allow different members of the same bank of capacitors to be recharged while other members of an alternative charged bank are being discharged.

In a preferred embodiment the invention may also include a controller. This controller may be implemented through any appropriate programmable device, but in a preferred embodiment may be provided by a programmable microprocessor.

The controller may be connected to at least one temperature sensor – referred to as an outlet temperature sensor – which is capable of providing an indication of the temperature of fluid leaving the outlet of the conduit. In additional embodiments the controller may be connected to a further temperature sensor – referred to as an inlet temperature sensor – which is capable of providing an indication of the temperature of fluid stored in a supply conduit.

In a further preferred embodiment the invention may also incorporate an activation sensor capable of confirming that the outlet of the conduit has been opened. For example, in one embodiment this activation sensor may be formed by a fluid pressure or flow sensor capable of signalling to the controller that the outlet has been opened.

In a preferred embodiment an activation sensor may be implemented by a flow rate sensor arranged to measure or indicate the rate at which fluid is

moving through the conduit associated with the invention. In addition to detecting when the conduit has been opened, these flow rate measurements – in combination with a measurement of inlet and outlet fluid temperature – may be used to calculate the energy demand currently required of the invention.

The controller may also be programmed to issue activation signals to trigger switches. The controller may be programmed to monitor the performance of the invention and modify the connections of the trigger switches accordingly. As indicated above in some embodiments the controller may be able to calculate or estimate the energy demands currently required of the invention. The controller may control the selection of particular trigger switches and the activation times for these trigger switches based on these energy demands.

In addition in some embodiments this controller may also use the signals or information provided by an outlet and/or inlet temperature sensor(s) to modify the behaviour of the invention. In particular the temperature of water provided by the outlet may be monitored by the controller for safety reasons to ensure that the temperature of the water supplied does not exceed a safe temperature value.

In yet other instances the temperature reading provided by an inlet temperature sensor can give an indication of the temperature of fluid travelling through the conduit and towards the remaining components of the invention. If the temperature sensed by the inlet temperature sensor meet that required from the operation of the invention, the invention may be deactivated.

Those skilled in the art will also appreciate that a controller provided in conjunction with the invention may also receive input signals from sensors other than just flow rate or temperature sensors. Depending on the application in which the invention is employed additional sensor input derived control parameters may be considered by the controller in determining a switching program for the invention's trigger switch or switches.

The present invention may therefore provide many potential advantages over the prior art, or in the least providing the public with an alternative choice.

The invention may be used to almost immediately raise or lower the temperature of a fluid leaving a conduit.

In a preferred embodiment this is achieved by activating a set of heating coils powered by a combination of large capacitor banks and an AC or DC current supply from a transformer isolated power converter or a derived DC power supply. The discharge characteristics of the capacitors used can rapidly supply significant energy to a heating coil by suitably adjusting the heating coil characteristics combined with capacitor bank characteristics.

Different configurations of capacitor banks may also be employed in situations where heating or cooling needs to be conducted over longer periods of time. In these instances a high-capacity capacitor bank may be used to energise a heating coil after a fast discharge capacitor bank has been significantly discharged.

In various embodiments the controller may allow for the independent automatic operation and intelligent control of the temperature modification apparatus provided. Manual user inputs are not required to adjust the activation and behaviour of the invention for it to function effectively and efficiently. The invention can also perform to promptly heat or cool fluids where the energy demands placed on it vary significantly and unpredictably. For example, in the case of domestic hot water supply applications the invention can perform effectively irrespective of whether hot water is required for a 10 section period, or for the duration of a shower. In embodiments where multiple trigger switches and energy sources are provided the controller may determine and execute a switching program which allows for the prompt and preferably immediate delivery of fluids at the correct temperature.

In addition in embodiments where inlet temperature values are sensed a controller provided with the invention may disable its operation if it determines that fluid at the correct temperature is currently being delivered

through the conduit involved. In embodiments where the temperature of fluid provided at the outlet of the conduit is monitored, the operation of the invention may also be disabled if the sensed temperature is outside of a safe operational range.

Brief description of the drawing

Additional and further aspects of the present invention will be apparent to the reader from the following descriptive embodiment with reference to the accompanying drawing in which:

- Figures 1a and 1b provide a representative sketch of a fluid temperature modification apparatus 1 as provided in a preferred embodiment, and
- Figure 2 shows the steps executed within a switching control algorithm executed by the controller used in accordance with a further embodiment of the invention.

Further aspects of the invention will become apparent from the following description of the invention which is given by way of example only of a particular embodiment.

Best modes for carrying out the invention

Figures 1a and 1b provide a representative sketch of a fluid temperature modification apparatus 1 as provided in a preferred embodiment. Figure 1a shows the elements of the invention associated with a conduit, and figure 1b illustrates the inputs and outputs of a controller as used in the embodiment shown.

The apparatus 1 includes three temperature modification elements implemented by heating coils 2.

These heating coils are located in the interior of a conduit, which is provided in this embodiment by a domestic hot water supply line 3.

The hot water supply line 3 is supplied with hot water originating from a boiler tank 4. The boiler tank 4 is centrally located within the building housing the apparatus and is arranged to feed a large number of hot water supply lines.

Without the operation of the invention hot water could not be rapidly delivered to a user operating a hot water outlet tap 5 connected to the hot water supply line 3. The user of the tap 5 will need to wait for the hot water from the boiler 4 to flush out the intervening ambient temperature water currently held in the hot water line 3.

Each of the heating coils 2 are connected to an energy supply system in the form of either a fast discharge large capacitor bank 6, a high-capacity large capacitor bank 7, or a transformer isolated power converter 8. In other embodiments the AC powered isolation transformer many alternatively be provided by, or combined with a battery based energy supply system.

In this embodiment the fast discharge bank 6 will have an energy storage capacity lower than the high capacity bank 7, but will take much less time to recharge back to a full charge.

Each of the fast discharge 6, high-capacity 7 or transformer isolated power converter 8 energy sources are connected to its own dedicated heating coil 2.

Interrupting the connection of the energy source of each heating coil 2 is a trigger switch 9. The operation of the trigger switch is controlled by a microprocessor 13 (as shown in figure 1b) provided with inlet and outlet fluid temperature readings from inlet and outlet temperature sensors 10, which are sited in combination with a fluid pressure/ flow sensor 11. These sensors can detect whether the hot water tap 5 has been opened from a measured flow rate value, the temperature of the water leaving the hot water tap, and the temperature of the water travelling from a remote hot water supply tank.

The controller is also capable of sending a similar form of control signal to recharging connections 12 made between the capacitor banks 6, 7 and the

isolation transformer 8. These connections are used to recharge each capacitor bank from the AC power source associated with the transformer isolated power converter 8 in periods with low demand for hot water.

The temperature and pressure/flow sensors 10, 11 provide performance information to the controller which can adjust the connections made by each capacitor bank trigger switch 9a or inductor trigger switch 9b. The controller can implement various combinations of capacitor bank and transformer energy supply connections to raise the outlet water temperature above a threshold temperature in the minimum period of time required to achieve this.

For example, after a period of low demand for hot water, the first use of the invention will result in hot water being present in the conduit, where this water has a temperature above or near a threshold temperature. Subsequent openings of the tap in the short term will only need this water to be heated slightly.

In this environment of increased frequency of demand the fast capacitor bank will re-charge quickly in the periods available between tap openings. The high capacity bank may not need to be connected to its heating coil in these circumstances, allowing it to recharge un-interrupted from the transformer isolated power converter 8.

The input information provided to the controller can also be used to modify the behaviour of the invention in a number of additional way. For example in the embodiment shown, if a signal provided by the flow sensor indicated the fluid flow rate has dropped to zero with the hot water tap being closed, all the trigger switches 9a, 9a, 9b can be opened by the controller. Furthermore, if the inlet temperature sensor 11 indicates that hot water from the hot water supply tank has now reached the hot water tap, again all the trigger switches 9a, 9a, 9b can be opened by the controller.

The tables below summarise the key variables that the electronic control unit or controller used in the embodiment of figure 1 independently assesses to quantify the energy to be delivered. Table 1 and 2 are specific to the

prompt delivery of hot water to taps in domestic households, while Table 3 considers energy requirements in alternative applications.

Table 1: Key dependencies

Variable	Notes
Required outlet temperature	Likely to be fixed between 40°C and 55°C
Inlet temperature	Dependent on season (i.e. could be 1°C in winter vs. 18°C in summer in New Zealand)
Flow rate	Variable across households; however, likely to be between 5 and 8L/min
Volume to be heated	Dependent on length of pipe run between main water heater and outlet; however, likely to be between 2 and 4L

5

Table 2: Potential use cases within the domestic delayed hot water application

	Req. Outlet Temp. (°C)	Inlet Temp (°C)	Flow Rate (L/min)	Volume (L)	Power (kW)	Energy Required (Wh)
Scenario 1	40	18	5	2	7.5	50
Scenario 2	55	1	8	4	30	250

Table 3: Potential future water heating applications

Application	Req. Outlet Temp. (°C)	Inlet Temp (°C)	Flow Rate (L/min)	Volume (L)	Power (kW)	Energy Required (Wh)
Alternative to gas califont	45	10	6	10	14.5	400
Alternative to under-sink tank	45	10	6	25	14.5	1000
Alternative to boiling tank	100	10	6	25	37.5	2600
Alternative to	45	10	6	120	14.5	4850

gas / electric main water heating system						

As indicated above Table 2 illustrates how the inlet water temperature and measured water flow rate is assessed to determine the energy required to deliver hot water promptly in this application. This determination of specific on-demand energy expenditure is used as an input parameter to a switching control algorithm executed by the controller.

Figure 2 shows the steps executed within a switching control algorithm executed by the controller used in accordance with a further embodiment of the invention. In this embodiment the invention is provided with an equivalent implementation to the embodiment discussed with respect to figures 1a, 1b, other than being provided with an additional energy source in the form of a battery.

At step A of this algorithm a test is made of the measured flow rate of water travelling through a hot water supply conduit. If no water flow is detected the controller deems that the hot water tap terminating the conduit is closed, causing the algorithm to wait until water flow is detected.

Step B is executed once water flows is detected to test whether the temperature of water sensed by a water inlet temperature sensor is less than a target temperature to be delivered. If the temperature of the water in the conduit is at or higher than the target temperature the algorithm loops back to step A. Step C is executed if the inlet water temperature is below the target temperature.

At step C the controller closes the trigger switch of a fast discharge capacitor bank and closes the trigger switch of the transformer isolated power converter. The controller then waits for a period of five seconds before moving on to step D.

At step D the controller again tests for water flow in the conduit, at step E tests the inlet water temperature, and at step F tests the outlet water

temperature. If there is no water flowing in the conduit, if the inlet water temperature is up to the target temperature, or if the outlet water temperature is up to the target temperature then step G is executed. At step G all open trigger switches are closed and the algorithm loops back to step A.

If none of these conditions are met then step H is executed. At step H the trigger switch of the fast discharge capacitor bank is opened and this capacitor bank is connected to a recharge circuit. Also at step H the trigger switch of a high-capacity capacitor bank is closed, and the trigger switch of a battery based energy supply is activated with a low duty cycle pulse width modulated trigger signal. The controller then waits for a period of five seconds before executing step I.

At step I the controller again tests for water flow in the conduit, at step J tests the inlet water temperature, and at step K tests the outlet water temperature. If there is no water flowing in the conduit, if the inlet water temperature is up to the target temperature, or if the outlet water temperature is up to the target temperature then step L is executed. At step L all open trigger switches are closed and the algorithm loops back to step A.

If none of these conditions are met then step M is executed. At step M the trigger switch of the battery based energy supply is activated with a high duty cycle pulse width modulated trigger signal. The controller then waits for a period of five seconds before executing step N.

At step N the controller again tests for water flow in the conduit, at step O tests the inlet water temperature, and at step P tests the outlet water temperature. If there is no water flowing in the conduit, if the inlet water temperature is up to the target temperature, or if the outlet water temperature is up to the target temperature then step Q is executed. At step Q all open trigger switches are closed and the algorithm loops back to step A.

If none of these conditions are met then step R is executed. At step R the trigger switch of high-capacity capacitor bank is opened and this capacitor bank is connected to a recharge circuit. The battery is then connected

continuously, and the outlet temperature is tested until it reaches the target temperature. Once this occurs the closed battery and transformer isolated power converter trigger switches are opened, the battery is connected to a recharging circuit, and the algorithm loops back to step A.

In the preceding description and the following claims the word "comprise" or equivalent variations thereof is used in an inclusive sense to specify the presence of the stated feature or features. This term does not preclude the presence or addition of further features in various embodiments.

It is to be understood that the present invention is not limited to the embodiments described herein and further and additional embodiments within the spirit and scope of the invention will be apparent to the skilled reader from the examples illustrated with reference to the drawings. In particular, the invention may reside in any combination of features described herein, or may reside in alternative embodiments or combinations of these features with known equivalents to given features. Modifications and variations of the example embodiments of the invention discussed above will be apparent to those skilled in the art and may be made without departure of the scope of the invention as defined in the appended claims.

What we claim is:

1. A fluid temperature modification apparatus which includes at least one temperature modification element associated with a fluid conduit, said temperature modification element being located adjacent to an outlet of said fluid conduit, and
at least one energy storage capacitor, and
at least one trigger switch which when operated connects one or more energy storage capacitors to a temperature modification element,
wherein the operation of a trigger switch at least partially discharges at least one energy storage capacitor to energise a temperature modification element which modifies the temperature of fluid in the conduit adjacent to the outlet port of the conduit.

2. A fluid temperature modification apparatus as claimed in claim 1 wherein a trigger switch is associated with a bank of energy storage capacitors and a temperature modification element.

3. A fluid temperature modification apparatus as claimed in claim 1 which includes a plurality of trigger switches, two or more of said trigger switches each being connected to a separate bank of energy storage capacitors.

4. A fluid temperature modification apparatus as claimed in claim 1 which includes a plurality of temperature modification elements, with one of a plurality of trigger switches being associated with each temperature modification element.

5. A fluid temperature modification apparatus as claimed in claim 1 which includes an activation sensor adapted to issue a signal which indicates when the outlet of the conduit has been opened.

6. A fluid temperature modification apparatus as claimed in claim 5 which includes an activation sensor formed from a flow rate sensor.

7. A fluid temperature modification apparatus as claimed in claim 5 which includes a controller arranged to receive said indicative activation signal from the activation sensor and to issue at least one control signal to at least

one trigger switch to operate said trigger switch or switches based on the received activation signal.

8. A fluid temperature modification apparatus as claimed in claim 7 which includes an inlet temperature sensor arranged to provide to the controller a signal indicative of the temperature of fluid leaving a fluid conduit.

9. A fluid temperature modification apparatus as claimed in claim 8 which includes an outlet temperature sensor arranged to provide to the controller a signal indicative of the temperature of fluid present in the conduit.

10. A fluid temperature modification apparatus as claimed in claim 9 wherein the controller is arranged to issue at least one control signal to at least one trigger switch to operate said trigger switch or switches based on at least in part the received indicative temperature signals.

11. A fluid temperature modification apparatus as claimed in claim 10 wherein the controller is arranged to issue at least one control signal to operate said trigger switch or switches based on a combination of an indication of conduit fluid flow rate provided by an activation sensor and the received indicative temperature signals received from the inlet and outlet temperature sensors.

12. A fluid temperature modification apparatus as claimed in claim 1 wherein said at least one temperature modification element is located in contact with a section of water plumbing conduit which terminates in a hot water outlet.

13. A fluid temperature modification apparatus as claimed in claim 12 wherein the water plumbing conduit terminates in a hot water outlet tap.

14. A fluid temperature modification apparatus as claimed in claim 1 wherein a temperature modification element is formed by an electrically energised heating coil sited inside a conduit.

15. A fluid temperature modification apparatus as claimed in claim 1 wherein a temperature modification element is formed a thermo-electronic cooling device which incorporates at least one Peltier junction.

17. A fluid temperature modification apparatus as claimed in claim 1 which includes a capacitor recharge circuit configured to recharge one or more at least partially discharged capacitors banks at the same time as one or more charged capacitor banks are being discharged.

18. A fluid temperature modification apparatus as claimed in claim 1 wherein a temperature modification element is energised by two or more banks of capacitors.

19. A fluid temperature modification apparatus as claimed in claim 1 which includes a fast discharge capacitor bank and a high storage capacitor bank, each of the fast discharge and high storage capacitor banks being connected to a separate trigger switch.

20. A fluid temperature modification apparatus as claimed in claim 19 wherein the trigger switch connected to the fast discharge capacitor bank is closed to energise a temperature modification element once the opening of the outlet of the conduit has been detected.

21. A fluid temperature modification apparatus as claimed in claim 20 wherein the trigger switch connected to the high storage capacitor bank is closed to energise a temperature modification element after the at least partial depletion of the fast discharge capacitor bank.

22. A fluid temperature modification apparatus as claimed in claim 1 wherein an energy storage capacitor is provided by electrical double layer capacitor

23. A fluid temperature modification apparatus as claimed in claim 1 wherein a trigger switch is implemented using a solid state semiconductor switch submerged in the fluid held by a conduit.

24. A fluid temperature modification apparatus as claimed in claim 1 wherein said at least one temperature modification element is energised by a transformer isolated power converter and associated electronic sub-systems providing a supply of DC electrical energy from an AC source.

25. A fluid temperature modification apparatus as claimed in claim 24 wherein DC electrical energy supplied by the transformer isolated power converter is used to re-charge the one or more energy storage capacitors.

26. A fluid temperature modification apparatus as claimed in claim 24 wherein the trigger switch associated with the transformer isolated power converter is closed to energise a temperature modification element at substantially the same time as said one or more energy storage capacitors are used to energise a temperature modification element.

27. A fluid temperature modification apparatus as claimed in claim 1 wherein said at least one temperature modification element is energised by a battery providing a supply of DC electrical energy.

28. A fluid temperature modification apparatus as claimed in claim 27 wherein the trigger switch associated with the battery is closed to energise a temperature modification element at substantially the same time as said one or more energy storage capacitors are used to energise a temperature modification element.

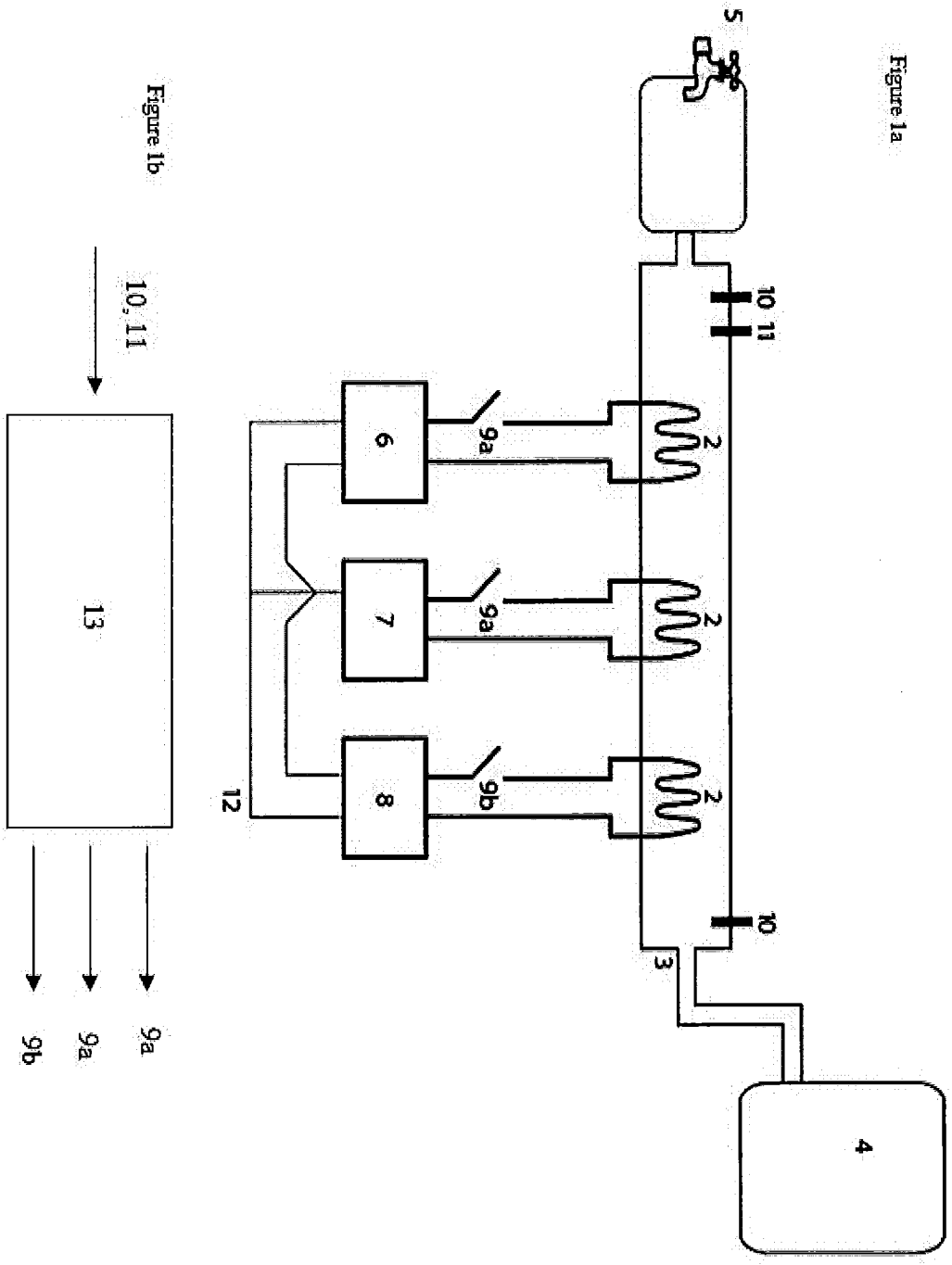

Figure 1a

Figure 1b

Figure 2

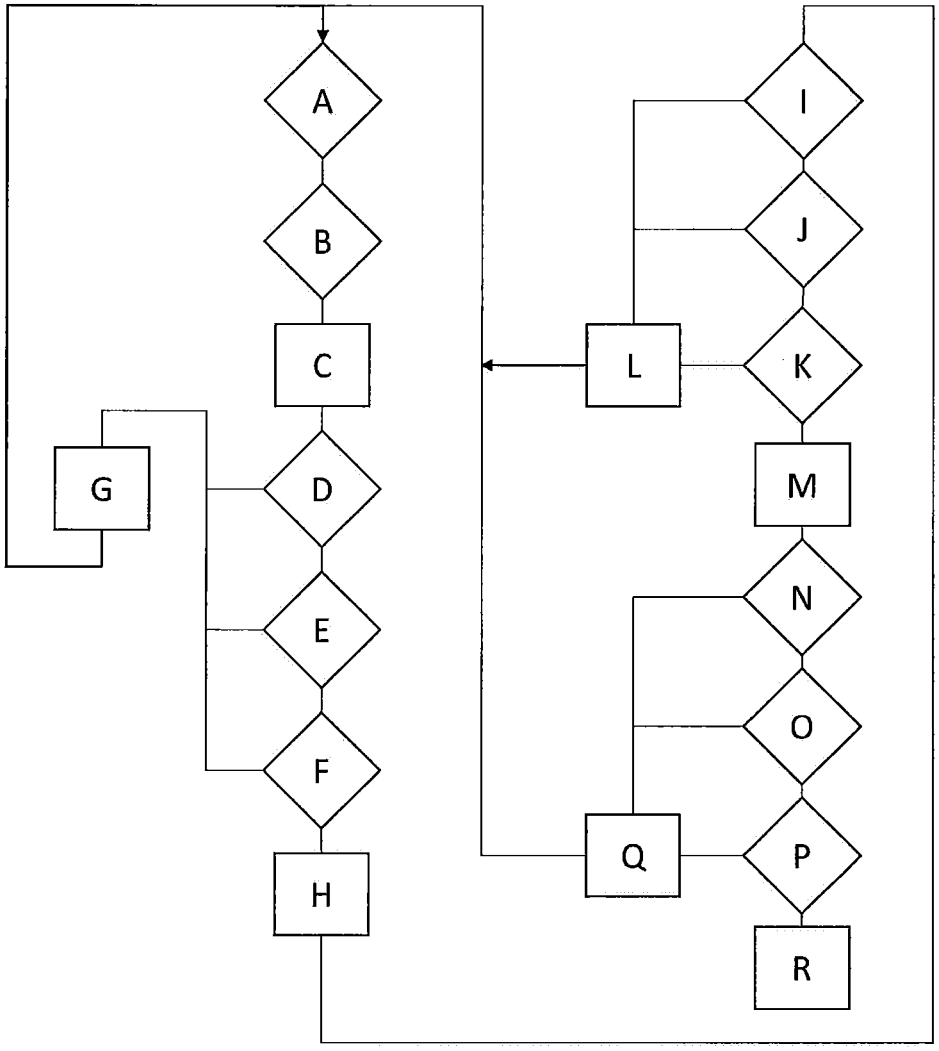

INTERNATIONAL SEARCH REPORT

International application No.
PCT/NZ2014/000092

A. CLASSIFICATION OF SUBJECT MATTER

F24H 9/20(2006.01)i, F24H 1/10(2006.01)i

According to International Patent Classification (IPC) or to both national classification and IPC

B. FIELDS SEARCHED

Minimum documentation searched (classification system followed by classification symbols)
F24H 9/20; F24H 1/22; F24H 1/00; F28G 9/00; F24H 1/10; G07F 13/00; F23N 5/00; F23N 5/14

Documentation searched other than minimum documentation to the extent that such documents are included in the fields searched
Korean utility models and applications for utility models
Japanese utility models and applications for utility models

Electronic data base consulted during the international search (name of data base and, where practicable, search terms used)
eKOMPASS(KIPO internal) & keywords: fluid, temperture modification, conduit, energy storage, capacitor, and trigger switch

C. DOCUMENTS CONSIDERED TO BE RELEVANT

Category*	Citation of document, with indication, where appropriate, of the relevant passages	Relevant to claim No.
X	JP 2008-025913 A (POWER SYSTEM:K.K.) 07 February 2008 See paragraphs [0037]-[0050],[0056]-[0059] and figures 1-4.	1-2,12,14-15,18,22,27-28
Y		5-11,13
A		3-4,17,19-21,23-26
Y	JP 08-159552 A (HARMAN CO., LTD.) 21 June 1996 See paragraphs [0020],[0026] and figure 1.	5-11,13
A	EP 1344993 A2 (ACQUADRO, PAOLO et al.) 17 September 2003 See page 2, line 11 - page 3, line 6, page 4, lines 12-16 and figures 1-2.	1-15,17-28
A	JP 2004-233028 A (NORITZ CORP.) 19 August 2004 See abstract, paragraphs [0039]-[0060] and figure 4.	1-15,17-28
A	JP 61-015099 A (NORITSU CO., LTD.) 23 January 1986 See page 1, right column, line 5 - page 2, lower right column, line 14 and figures 1-2.	1-15,17-28

☐ Further documents are listed in the continuation of Box C.

☒ See patent family annex.

* Special categories of cited documents:
"A" document defining the general state of the art which is not considered to be of particular relevance
"E" earlier application or patent but published on or after the international filing date
"L" document which may throw doubts on priority claim(s) or which is cited to establish the publication date of another citation or other special reason (as specified)
"O" document referring to an oral disclosure, use, exhibition or other means
"P" document published prior to the international filing date but later than the priority date claimed
"T" later document published after the international filing date or priority date and not in conflict with the application but cited to understand the principle or theory underlying the invention
"X" document of particular relevance; the claimed invention cannot be considered novel or cannot be considered to involve an inventive step when the document is taken alone
"Y" document of particular relevance; the claimed invention cannot be considered to involve an inventive step when the document is combined with one or more other such documents,such combination being obvious to a person skilled in the art
"&" document member of the same patent family

Date of the actual completion of the international search	Date of mailing of the international search report
21 October 2014 (21.10.2014)	**22 October 2014 (22.10.2014)**

Name and mailing address of the ISA/KR
International Application Division
Korean Intellectual Property Office
189 Cheongsa-ro, Seo-gu, Daejeon Metropolitan City, 302-701, Republic of Korea
Facsimile No. +82-42-472-7140

Authorized officer
OH, Jae Min
Telephone No. +82-42-481-8731

INTERNATIONAL SEARCH REPORT

Information on patent family members

International application No.
PCT/NZ2014/000092

Patent document cited in search report	Publication date	Patent family member(s)	Publication date
JP 2008-025913 A	07/02/2008	None	
JP 08-159552 A	21/06/1996	None	
EP 1344993 A2	17/09/2003	EP 1344993 A3	17/12/2003
		IT MI20020563 A1	15/09/2003
		IT MI20020563 D0	15/03/2002
JP 2004-233028 A	19/08/2004	JP 03991898 B2	17/10/2007
		JP 03994899 B2	24/10/2007
		JP 2004-233029 A	19/08/2004
JP 61-015099 A	23/01/1986	None	

A.2 Fast Charger Patent

N. Kularatna, N. Gurusinghe, "Electrical energy charging apparatus," New Zealand provisional Patent application P31578NZ00, 13 Nov 2015.

PROVISIONAL SPECIFICATION

Electrical Energy Charging Apparatus

We, The University of Waikato of Hillcrest Road (no number), Hamilton, New Zealand, a body existing by virtue of the University of Waikato Act 1963, do hereby declare this invention described in the following statement to be true:

ELECTRICAL ENERGY CHARGING APPARATUS

Technical Field

This invention relates to an electrical energy charging apparatus. In preferred embodiments the invention may be configured to provide a fast charging circuit to be used in combination with super capacitor based energy storage systems.

Background art

Electrical systems which incorporate their own integral energy storage structures are becoming increasingly widespread.

Portable electrical devices such as digital cameras or smart phones generally integrate some form of energy storage structure in the form of a battery.

Electric cars incorporating chemical batteries are also seen as an environmentally friendly transport option and are becoming more popular with consumers.

Super capacitor based energy storage systems have also been used in applications such as the on demand heating or cooling of fluid flows. For example, PCT patent publication number WO2014/189389 describes a super capacitor based fluid temperature modification system which employs banks of energy storing super capacitors to power electrically driven heating or cooling elements.

In these various applications there is a demand for an electrical recharging facility which is able to replenish the energy delivered by these forms of energy storage structures. In applications where users expect immediate service – such as with vehicles or domestic hot water delivery systems – there is also a demand for a recharging circuit which will rapidly recharge depleted energy in a storage system.

This rapid charging requirement is difficult to meet with batteries which have high energy densities, and with super capacitors where high time constants make for slow recharging times.

It would therefore be of advantage to have available improvements in the field of electrical energy recharging circuits which could assist in these applications. In particular it would be of advantage to have an improved fast recharge circuit available for chemical batteries or super capacitors.

Disclosure of Invention

According to one aspect of the present invention there is provided an electrical energy charging apparatus configured to recharge two or more at least partially discharged energy storage structures, the apparatus including
an electrical energy supply configured to supply a charging electrical current with a voltage greater than the maximum rated voltage of at least one of the energy storage structures to be recharged, and
a primary inductor connected to a first energy storage structure and configured to receive charging electrical current from the electrical energy supply, and
a secondary inductor mutually coupled to the primary inductor and connected to a second energy storage structure to deliver a charging electrical current to the second energy storage structure, the charging current delivered by the secondary inductor being induced in the secondary inductor by changes in electrical current travelling in the primary inductor, and
a terminal voltage sensor associated with the first energy storage structure, and
a control element connected to the terminal voltage measurement sensor and configured to connect and disconnect the supply of charging electrical current delivered by the electrical energy supply,
the control element disconnecting the electrical energy supply charging current when the terminal voltage measurement sensor indicates that the first energy storage structure is at a voltage greater than the maximum rated voltage of the first energy storage structure.

According to one aspect of the present invention there is provided an electrical energy charging apparatus substantially as described above wherein the control element is arranged to repeatedly connect and disconnect the supply of charging electrical current to the primary inductor to induce a charging current in the secondary inductor which is delivered to the second energy storage structure.

The present invention provides an electrical energy charging apparatus. This apparatus allows the electrical energy stored in a number of electrical energy storage structures to be replenished when depleted.

A variety of different forms or types of energy storage structures may be recharged in accordance with the present invention. For example, in various embodiments the invention may be adapted to recharge chemical battery systems. In yet other embodiments the invention may be employed to recharge super capacitors which are configured or arranged to perform an energy storage role. Those skilled in the art will appreciate that the present invention has a range of applications and may be used with a variety of electrical energy storage systems.

Reference in general throughout this specification will be made to the invention recharging an energy storage structure, although those skilled in the art should appreciate that such a structure per se may be composed from a number of cells or elements connected together. For example, in various embodiments an energy structure storage structure may be formed from a battery composed of a number of cells - whereas in other embodiments such a structure may be formed from a bank or sub-bank of super capacitors.

Reference in general throughout this specification will be made to the invention concurrently recharging two separate energy storage structures at the same time. However those skilled in the art will appreciate that other modifications or reconfigurations of the invention are also possible to charge multiple sets or pairs of energy storage structures and references to the recharging of two structures only should no way be seen as limiting.

Reference throughout this specification will be made to the invention being used to recharge a bank of energy storing super capacitors where this bank is partitioned into two sub-banks, each sub-bank defining one of the energy storage structures referenced above. Again however those skilled in the art will appreciate that other arrangements of various types of energy storage structures may also be recharged in accordance with the present invention.

The invention includes an electrical energy supply which is configured to supply a charging current to other components of the invention. This

charging electrical current has a relatively high voltage and specifically is provided with a voltage greater than the maximum rated voltage of at least one of the super capacitors to be recharged. In a further preferred embodiment the supply voltage may be greater than the rated voltage of all of the super capacitors to be recharged by the invention. Those skilled in the art will understand that the term rated voltage means the voltage specified by the manufacturer of the component which if exceeded could result in damage to the component. This rated voltage may also be higher or lower for different types of energy storage structures or different arrangements of these storage structures.

The invention includes a primary inductor which receives the charging electrical current provided by the electrical energy supply. This primary inductor is also connected to a first energy storage structure to be recharged, being in a preferred embodiment a first super capacitor bank partition. The connection scheme employed in conjunction with a primary inductor may also vary in a range of embodiments. For example, in some embodiments the primary inductor may be connected directly to the supply and also to the first super capacitor partition. In other embodiments intervening components – such as, for example, electrical resistors – may be interposed between these connections. These connection schemes therefore allow for the delivery of the relatively high voltage charging current provided by the supply to the first super capacitor partition and through the primary inductor. The first super capacitor partition will therefore be exposed to the high voltage charging current of the supply to recharge its super capacitor elements.

The invention includes a secondary inductor which is mutually coupled to the primary inductor. The mutual coupling of these two inductors therefore ensures that a secondary charging current is induced within the secondary inductor when there are changes in the electrical current flowing through the first conductor. The secondary inductor is also connected to a second energy storage structure, or in a preferred embodiment a second super capacitor bank partition. Again the connection scheme employed with the second super capacitor bank partition and secondary inductor may vary, being either a direct connection or an indirect connection through additional components interposed between these elements. This connection arrangement allows for the supply of the secondary charging current induced in the secondary inductor to the second super capacitor bank partition.

The invention includes a terminal voltage sensor associated with the first super capacitor bank partition. This sensor is employed to determine or measure the voltage between the terminals of the partition and therefore whether the partition voltage has exceeded the rated voltage which could result in damage to the components of the partition.

The invention includes a control element, formed in preferred embodiments by a microprocessor. This controlling microprocessor can be programmed to receive a terminal voltage sensor output signal and also to connect and disconnect the supply of charging electrical current delivered by the electrical energy supply. The microprocessor can therefore be used to monitor the terminal voltage of the first super capacitor partition as this voltage increases with the application of the charging current from the supply. Charging of the first super capacitor partition can then be halted once its terminal voltage reaches the rated voltage of its components.

The microprocessor can also be programmed to repeatedly connect and disconnect the charging current delivered by the supply to induce the secondary charging current within the secondary inductor to recharge the second super capacitor bank partition. In further preferred embodiments this microprocessor controller can be programmed to repeatedly switch in and out the supply charging current to recharge the second super capacitor partition while also preventing overvoltage charging of the first super capacitor partition.

In a further preferred embodiment the switching duty cycle implemented by the control element may be configured to perform a power factor correction role. In such embodiments the number of components normally required to effect a power factor correction may be dispensed with. For example, in various preferred embodiments where super capacitors are being recharged, buffer capacitors need not be provided as a capacitor bank partition is always connected in series with the supply. Extra boost chokes are also not required for power factor correction as the primary inductor is connected in series with the supply.

The present invention may provide many potential advantages in respect of the charging of a variety of energy storage structures.

The invention allows for the safe application of high voltage charging current to energy storage components which would normally exceed the

rated voltage of these components. Terminal voltage monitoring sensors can ensure that the operation of the invention is controlled to prevent damage to such components during charging operations.

The invention also performs efficiently to concurrently charge two or potentially more energy storage structures at the same time, utilising charging currents induced in a secondary inductor to recharge a second energy storage structure.

The circuit arrangement provided by the invention and in particular its use of primary and secondary inductors can also result and reductions in the number of components normally required for a charging circuit, eliminating the need for buffer passages or boost chokes.

Brief description of the drawings

An example embodiment of the invention is now discussed with reference to the drawings in which:

Figure 1 provides a schematic circuit diagram of an electrical energy charging apparatus circuit configured to recharge two super capacitor bank partitions in a preferred embodiment, and

Figure 2 shows plots of charging current amplitude over time for the charging current supplied to the first super capacitor bank partition C1 and the second super capacitor bank partition C2 illustrated with respect to figure 1.

Best modes for carrying out the Invention

Figure 1 provides a schematic circuit diagram of an electrical energy charging apparatus circuit configured to recharge two super capacitor bank partitions in a preferred embodiment.

This circuit is configured to recharge a first super capacitor bank partition C1 and a second super capacitor bank partition C2.

An electrical energy supply V_{in} is provided to supply a charging electrical current with a voltage greater than the maximum rated voltage of both of the bank partitions C1, C2.

A primary inductor L1 is connected to the first capacitor bank partition C1 as well as to the supply V_{in} to receive the charging electrical current it provides.

A secondary inductor L2 is mutually coupled to the primary inductor L1 and also connected to the second supercapacitor bank partition C2. The bank partition C2 and secondary inductor L2 are connected by an intervening switch element, although in other embodiments various forms of current direction control elements – such as a diode for example – may also be provided at this point. These connections allow the bank partition C2 to receive charging electrical current induced in the secondary inductor by changes in electrical current travelling in the primary inductor.

The apparatus includes a terminal voltage sensor (not shown) associated with the first capacitor bank partition C1 which measures its terminal voltage $V_{C1.}$

The apparatus also includes a control element formed in this embodiment by a microprocessor (not shown). This microprocessor is connected to the terminal voltage measurement sensor and configured to connect and disconnect the supply of charging electrical current delivered by the electrical energy supply $V_{in.}$

The controlling microprocessor is programmed to disconnecting the electrical energy supply charging current when the terminal voltage measurement sensor indicates that the first super capacitor bank partition C1 is at a voltage greater than its maximum rated voltage.

As is shown more clearly by the current over time plots of figure 2 the controlling microprocessor is programmed to repeatedly connect and disconnect the supply of charging electrical current to the primary inductor L1 to induce a charging current in the secondary inductor L2. As seen by the first plot for L1 current the capacitor bank C1 is repeatedly supplied with a high voltage charging current which then stops after a short interval. The change in current flows experienced by inductor L1 then induces the second charging current shown in the second plot for the inductor L2 current to charge the second capacitor bank partition C2. This process is repeated over time to charge both the first C1 and second C2 capacitor bank partitions.

The charging process is then terminated once the terminal voltage V_{C1} is equal to the rated voltage of the first capacitor bank partition C1.

It is to be understood that the present invention is not limited to the embodiments described herein and further and additional embodiments within the spirit and scope of the invention will be apparent to the skilled reader from the examples illustrated with reference to the drawings. In particular, the invention may reside in any combination of features described herein, or may reside in alternative embodiments or combinations of these features with known equivalents to given features. Modifications and variations of the example embodiments of the invention discussed above will be apparent to those skilled in the art and may be made without departure of the scope of the invention.

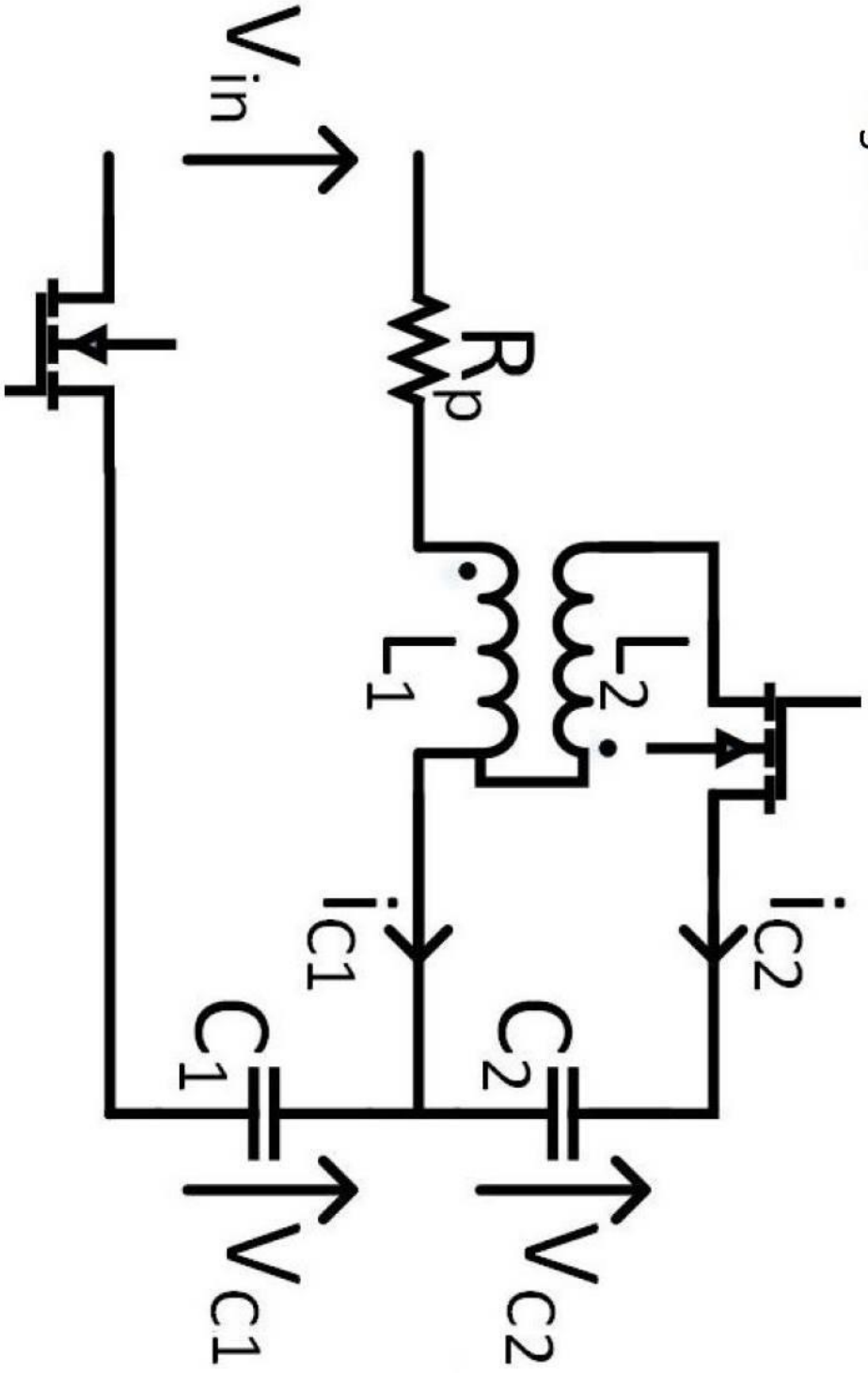

Figure 1

5

Figure 2

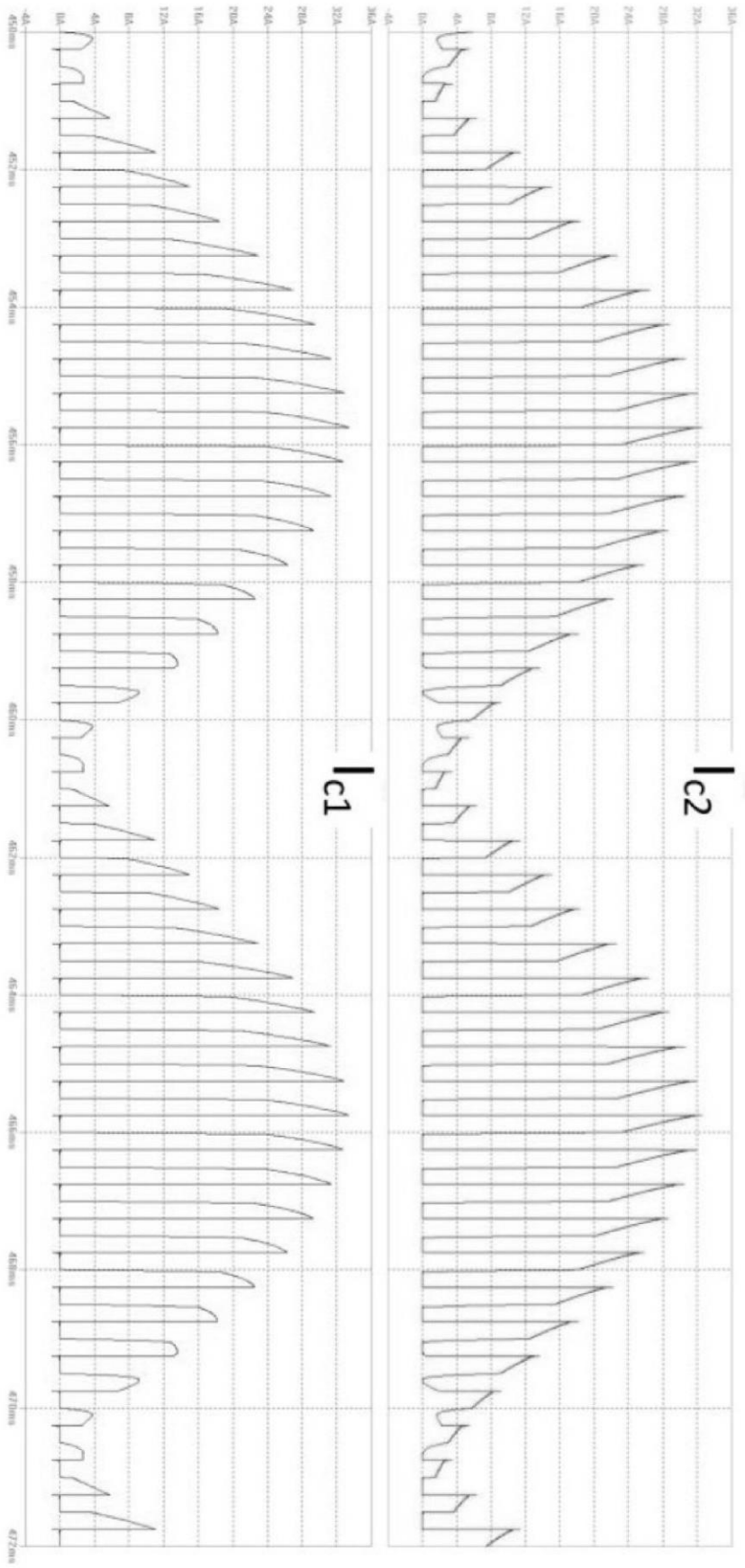

Appendix B

"Localised Water Heating" Project Reports

B.1 Energy Storage Cost Estimation

ENERGY STORAGE COST ESTIMATION
TARGET SYSTEM VOLTAGE = 48-60V
TARGET COMPONENT COST = LESS THAN $200

Variables Expected to Affect Total Component Costs		
Variable	**Notes**	**Controllable**
Volume discounting		N
Exchange rate		N
Supercap price trends	Expected to be 0.5 c per F within 5 years	N
Supercap capacitance	When using SC in combination with batteries,	Y
Flow rate	Regulating flow will decrease total energy	Y
Rapid SC-SC charging	Developments in the pipeline - 3 year PhD	Y

Variables Expected to Affect Battery Lifetime		
Variable	**Notes**	**Controllable**
Depth of discharge from battery	Greater discharge from battery will decrease energy requirements from the supercaps; trade	Y
Battery size	Doubling battery size will reduce depth of	Y
Supercap capacitance	Reducing capacitance will require greater battery	Y

Exchange Rate		
	US	**NZ**
US-NZ	1	1.21

Supercapacitor Price Trends	
Cost per farad after 5 years ($)	0.005

Component Costs						
Unit		**Supplier**	**Volume**	**Price Per Unit (USD)**	**Price Per Unit (NZD)**	**Price Per Unit in 5 years (NZD)**
Voltage (V)	***Capacitance (F)***					
16 V	58F x 6 module	LS Mtron	100	$60	$72.60	
			1 million	$44	$53.24	
2.7V	650	LS Mtron	100	$18.30	$22.14	$3.25
			1 million	$13.47	$16.30	
2.7V	1200	LS Mtron	100	$28.00	$33.88	$6.00
			1 million	$17.33	$20.97	
2.7V	1200	Maxwell	100	$56.20	$68.00	$6.00
2.7V	1500	LS Mtron	100	$32.00	$38.72	$7.50
			1 million	$18.83	$22.78	
2.7V	3000	LS Mtron	100	$40.00	$48.40	
			5,000	$36.00	$43.56	$15.00
			1 million	$26.57	$32.15	

Total Component Cost for Various Energy Storage Configurations					
SUPERCAPACITOR			**TOTAL COMPONENT COST (NZD)**		
Supplier	**Unit**	**Number**	**Current**	**In 5 Years**	**% of Current Cost after 5 years**
LS Mtron @ 100 unit pricing	58F x 6 module / 16 V	8	$580.80		
LS Mtron @ 1M unit pricing	58F x 6 module / 16 V	8	$425.92		
LS Mtron @ 100 unit pricing	650F / 2.7V	24	$439.20	$78.00	17.76%
LS Mtron @ 1M unit pricing	650F / 2.7V	24	$391.17	$78.00	/
LS Mtron @ 100 unit pricing	1200F / 2.7V	24	$813.12	$144.00	17.71%
LS Mtron @ 1M unit pricing	1200F / 2.7V	24	$503.26	$144.00	/
LS Mtron @ 100 unit pricing	1500F / 2.7V	24	$929.28	$180.00	19.37%
LS Mtron @ 1M unit pricing	1500F / 2.7V	24	$546.82	$180.00	/
LS Mtron @ 100 unit pricing	3000F / 2.7 V	24	$1,161.60	$360.00	30.99%
LS Mtron @ 1M unit pricing	3000F / 2.7 V	24	$771.59	$360.00	/

B.2 Localised Water Heating Project Report

This report was written on 15 Dec 2014 for Rinnai NZ ltd as the final project update. This includes details on the control circuit tuning done by Sean A. Charleston.

Localised Water Heating

Project Update – 15/12/14

Key Specifications

- Flow Rate: 5 L/min – 8 L/min
- Delivered Water Temperature: $55\ ^{\circ}C$ maximum
- Rise time: 2 – 4 seconds

Energy Storage System

- A number of energy storage configurations were investigated at the beginning of the project.
- It was decided that a combination of batteries and supercapacitors was the ideal configuration.
    - The benefits of a hybrid system arise from the fact that supercapacitors have poor energy density (energy stored per unit volume), with a high power density (delivered power per unit volume). The result is that in a supercapacitor only system, a large number of supercapacitors would be required to store the required energy, which is not feasible with the current price and size of supercapacitors.
    - Batteries lie on the other end of the spectrum, with a high energy density, but a low power density.
    - The solution of a hybrid configuration then arises, where the high energy density of the batteries is combined with the high power density of the supercapacitors to meet the specifications.
- Two hybrid configurations were tested; a parallel and series configuration.
    - In the parallel configuration, the supercapacitor takes the burden of the initial high current, while the batteries current slowly ramps up (Figure 1).
        - The main disadvantage lies in the fact that the capacitor bank does not use all of its stored power, resulting in wasted energy (voltage across supercapacitor battery parallel circuit must stay the same; the battery voltage governs the supercapacitor bank voltage, meaning the supercapacitor bank cannot be discharged to 0 V). A secondary disadvantage is that the battery should be switched before the high, damaging currents are reached. This adds an additional restriction in the cycle configuration, which could result in reduced battery life.
    - In the series configuration, both the supercapacitors and the batteries share the same current output (Figure 2)
        - The advantage of this configuration arises in the fact that the entire supercapacitor energy can be output, reducing the battery energy storage requirements.
        - The main disadvantages arise in the fact that care needs to be taken to not reverse-charge the capacitor bank. This is currently managed by monitoring the supercapacitor bank voltage and electronically switching off before it reaches 0 V. We would expect that the final electronic system would have a similar cut off mechanism.

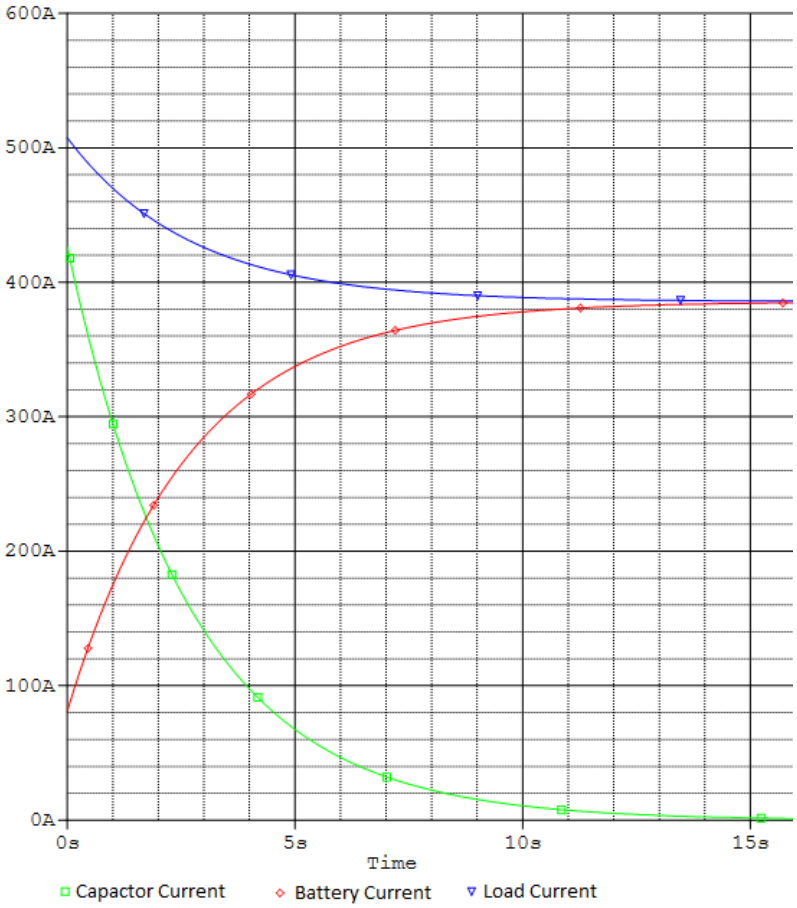

Figure 1: Hybrid-Parallel Battery Capacitor Configuration Current Outputs

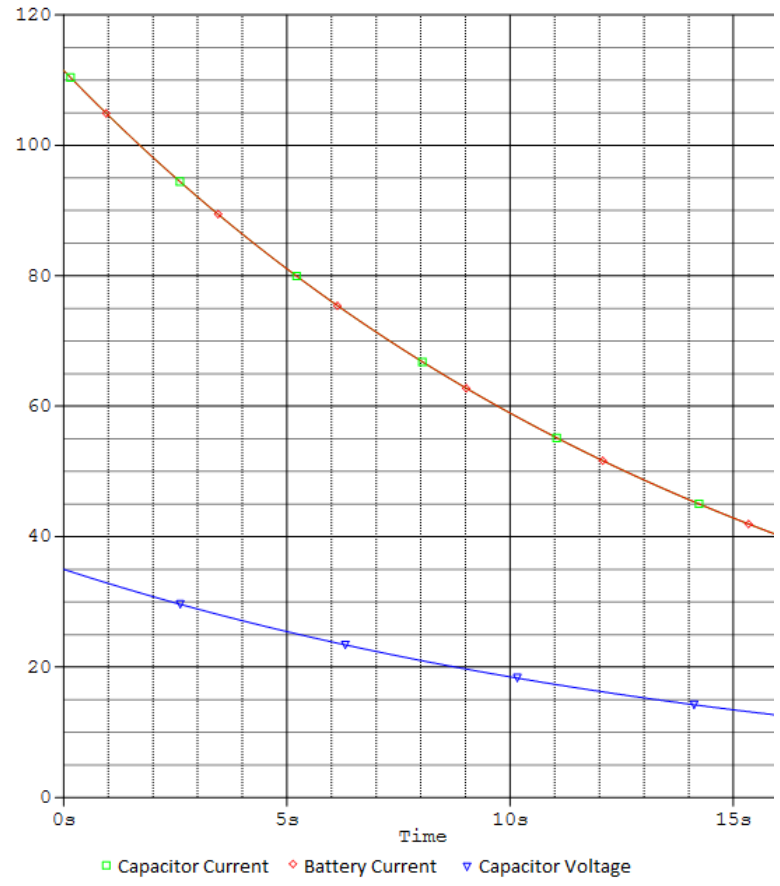

Figure 2: Hybrid- Series Battery Capacitor Configuration Current and Voltage Outputs

Recharging Subsystem

- A recharging subsystem has been developed, which consists of a compact supercapacitor recharger, along with a battery recharger.
- The supercapacitor recharger runs after each 30 second hot water cycle, and takes approximately 15 minutes.
- The battery charger is able to be run overnight, and can take anywhere from 10 minutes to hours, depending on the amount of discharge.
    - Further testing is going to take place, to determine the amount of discharge that occurs on the batteries per cycle, along with how that changes the lifetime of the batteries.

Semiconductor Switching Module

- High power switches (MOSFETS) are required, in order to switch the high currents required to heat the coil. These switches need to operate rapidly, so that a pulse width modulated (PWM) signal can be used to manipulate the average power delivered (and hence average temperature).
- The chosen MOSFETS are capable of switch up to 500 Amperes, with a low on resistance ($1.6\ m\Omega$).
- A system has then been designed, with safely drives these MOSFETS, at the correct rates to not damage any electronics.
    - The frequency currently used is $30\ \mathrm{Hz}$, which can have a duty cycle of up to 90%. This is an important factor, as it effects how rapidly the control subsystem can respond to changes in the temperature. A high frequency is usually desirable, however $30\ \mathrm{Hz}$ is fast enough for this application.

Heating Element

- Only a small investigation has been taken into the heating element. A number of resistances have been simulated, with $100\ m\Omega$ being optimal in theory.
- A coil is currently used as the interface to the water. Further investigation would be required to find an optimal configuration for heat transfer to water, which would improve the overall system efficiency.
    - This could involve investigation into an element with fins etc. Other considerations could be in how the water flows over the element (i.e. turbulent vs laminar flow).
    - A secondary consideration is that in New Zealand, the mains water supply is earthed. Investigation is required to see if having a charged coil in contact with the water supply is in breach of any safety standards. One solution in this case would be to investigate using an insulated coil/element.

Control Subsystem

- A large electronic setup has been built around the control of the system. The first stage of this was to develop a sensor interface. Currently, the temperature is being measured at three points, as well as the flow rate. The voltages and currents are also being measured at

all points in the system, for testing purposes (a number of these sensors would be unnecessary in a final solution)

- These sensors then interface to a small microcontroller (ATMEGA 328p). These sensors are monitored, then passed into a number of other functions. One of the components of this test rig is a serial interface to a PC. This allows the data to be analysed on the computer (again this would be unnecessary in a final solution).
- The final stage is the control system itself. This system controls how the energy output responds to changes in the temperature.
    - Currently, a proportional-integral (PI) controller is being used. This allows the system to respond to differences between the desired temperature and the current output temperature.
    - The current target is a linear rise in temperature over 10 seconds (to reach the target), followed by a sustain of the target temperature for 10 seconds. Finally, the system linearly decreases in temperature for 10 seconds, under the assumption that the mains hot water would start to come in. This means that the mains hot water is working in combination with the energy from the supercapacitor bank (until the mains temperature reaches its maximum), to maintain the target temperature.
    - The system operates purely on the output of the temperature reading. This is independent of the control power, hence temperature fluctuations (rapid increases above the target, on the arrival of mains hot water) should not be an issue in a well-designed control system.

Testing (Current Results)

- A number of tests have been undertaken so far. The current setup is using a single bank of 16 3000F supercapacitors, along with four 12 V, 12 Ah, lead-acid batteries. Additional supercapacitors will be used in future testing to achieve the targets with higher flow-rate and temperature rises.
- A test using the hybrid-series system, with the 3000 F supercapacitor bank, at a 90% duty cycle (Figure 3), shows the temperature output driving the capacitors with the entire power of the system. It can be seen that a temperature rise of approximately 30 degrees is obtained, but this cannot be sustained as the supercapcitors begin to run out of power.

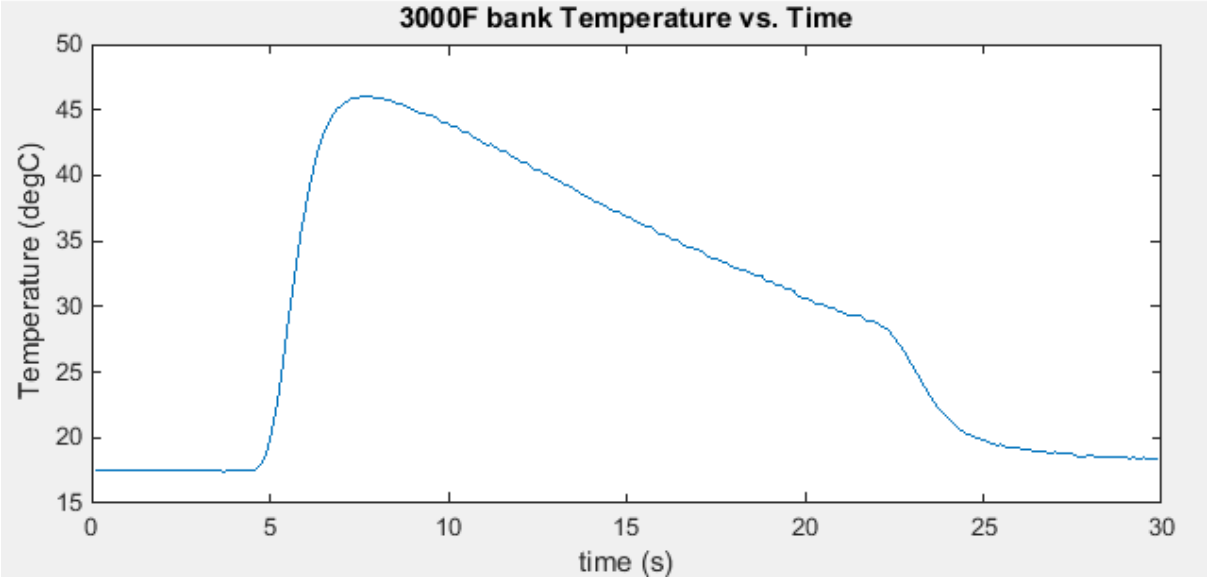

Figure 3: 90% Duty cycle full test, output temperature vs. time

- Implementing the control system discussed above, the PI controller was required to be tuned to meet the specifications. The following figures show some of the design process. The process is using a flow rate of 6 L/min, with a target temperature of 35 degrees. This is increased to 40 degrees in the final test.

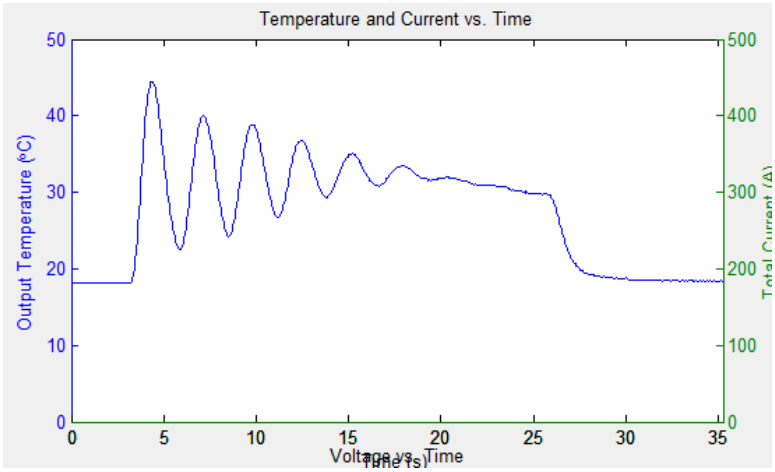

Figure 4: PI controller tuning. Attempt to sustain a temperature

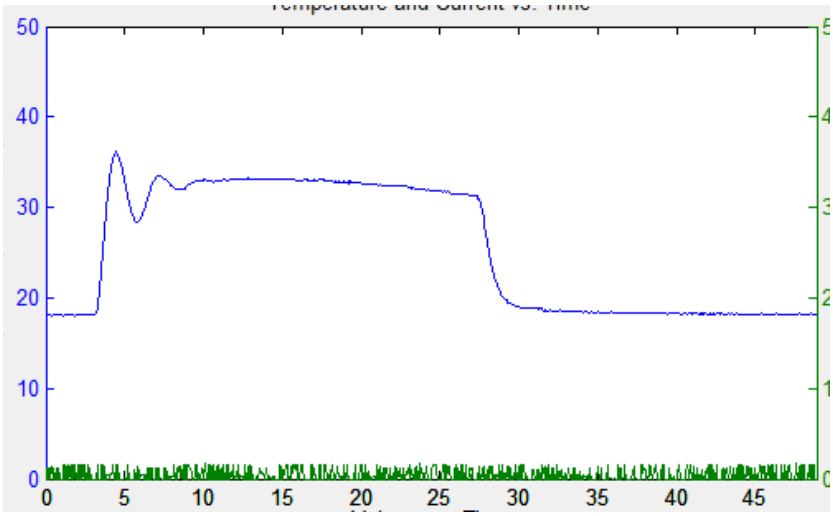

Figure 5: PI controller tuning. Improved attempt to sustain a temperature (the green lines can be ignored)

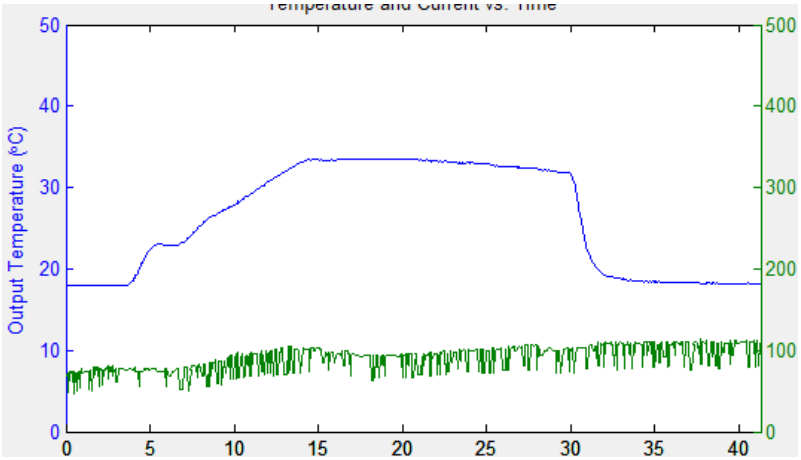

Figure 6: PI controller tuning. Added linear increase

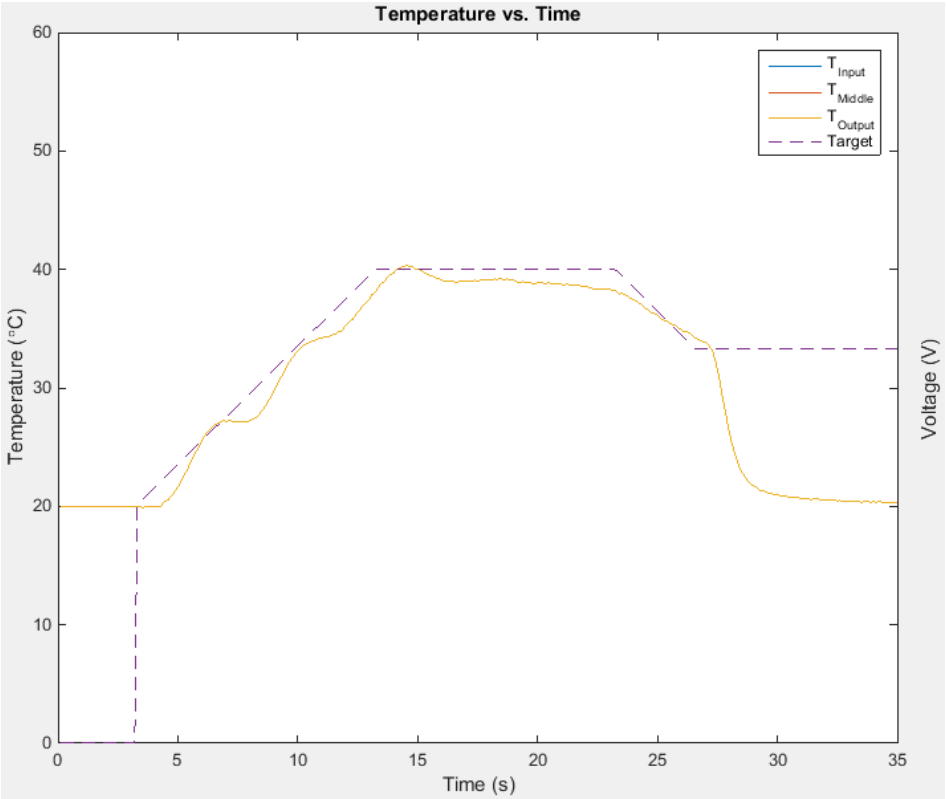

Figure 7: PI controller tuning. Increased target to 40 degrees, added linear decrease

- Figure 7 shows the current state of the system. It can be seen that the target temperature is being hit and sustained. The supercapacitors run out of energy on the linear decrease linear region and hence are switched off.
- More work is needed to achieve the full 30 seconds, however this could easily be done with this configuration with the addition of one or two supercapacitors.
- Some interesting results were seen when analysing the efficiency of the current system. Figure 8 shows that after the initial warm up period, the actual temperature exceeds the theoretical temperature. This is likely due to the fact that the coil is still heated, and there is heat transferred in the water even at a relatively high flow rate.

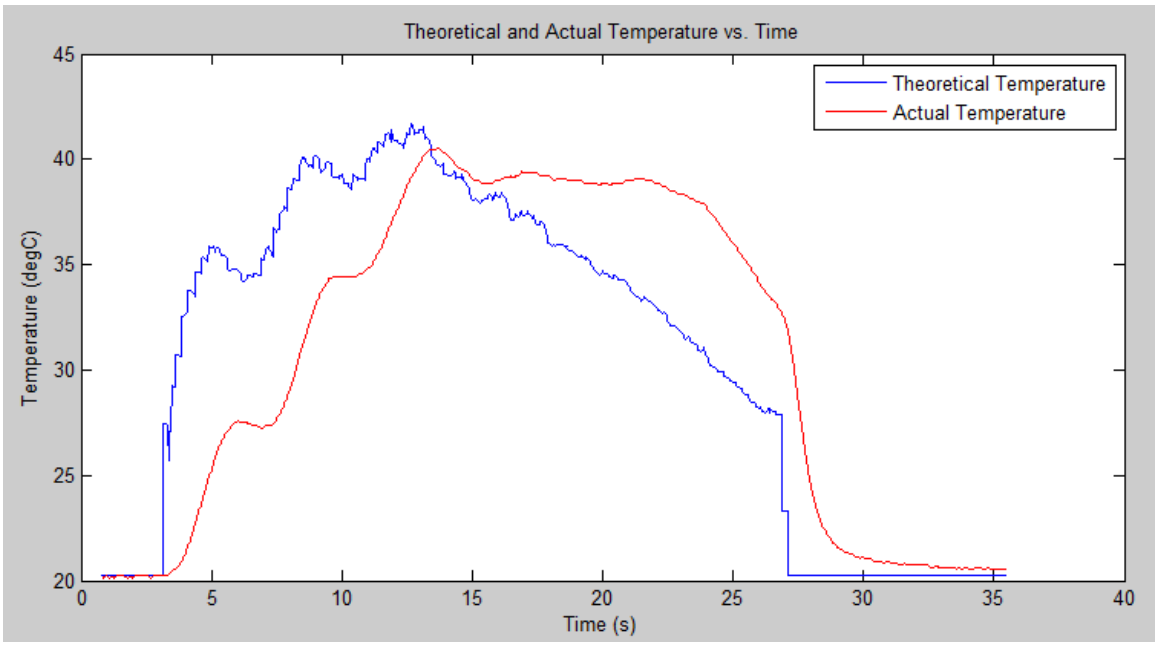

Future Work

- *Battery Storage Optimisation:
    - The battery storage configuration requires more investigation. Currently, four 12 V, 12 Ah batteries are being used in parallel to supply the current required. Tests need to be done to investigate how much energy is being used per battery, for each water heating cycle. The total drain per day can then be calculated, along with the depth of discharge.
        - The result of this optimisation is a potential reduction in number of batteries. Only three batteries might be required to meet the demands of the circuit, while not critically damaging the total battery lifetime.
- *Supercapacitor Optimisation:
    - The current system is showing that a number of the specifications are being reached, or are close to being reached. Additional supercapacitors will be introduced to the system, to hit all targets (including worst case scenarios). Because the first bank is getting close to the maximum allowed household DC voltage, a second bank will likely be the result. However, this bank may only have a small number of capacitors, in order to meet specifications.
- Coil/Element Optimisation:
    - As mentioned above, more research and investigation is required around the coil/element at the water interface. Optimising this could greatly reduce the initial inefficiencies in the circuit.
        - This would result in a lower energy requirement, as well as an inherent increase in the rise time of the temperature (moving from the current 10 seconds, to the target 2-4 seconds). The rise time could also be improved purely with the addition of supercapacitors; however this is a less desirable solution.
    - *This coil design ties closely with the theoretical vs. actual temperature output shown above. Further analysis should be done to improve on this, where it might be possible to minimise the amount of wasted power used to heat the coil to the required temperature.

Appendix C

Magnetics Design Guides

The two following tables are extracted from the Magnetics Inc 2013 ferrite catalogue (available online: https://www.mag-inc.com/.../MagneticsFerritePowerDesign2013.pdf)

Typical Power Handling Chart

Power in Watts				Pot, RS, DS	E Cores	RM, PQ, EP	UU, UI, UR	ETD, EER, EC	EFD, Planar	Toroid
20 kHz	50 kHz	100 kHz	250 kHz							
1000	1600	2250	4375		47228 EE		45917 UR	45959 ETD 47035 EC		46013 TC 46113 TC
1400	2500	3200	6240							
1600	2600	3700	7215				46420 UR			44932 TC 46019 TC
2000	3000	4500	8750		46527 EE 47133 EE 48020 EE					46325 TC 46326 TC 47313 TC
2800	4200	6500	12675				49316 UI 49316 UU		49938 EE	47325 TC 48613 TC 48625TC 48626 TC 49715 TC 49718 TC
11700	19000	26500	51500		49928 EE		49330 UU 49332 UU 49920 UU 49925 UI 49925 UU			49725 TC 49740 TC

Area Product Distribution (WaAc) Chart

WaAc (cm^4)	RS, DS, HS	E	EC, EER, EFD, ETD	EP, RM	ER	Planar	Pot	PQ	TC	U, UR
23		47133 EE								
24		46527 EE								
25									46019 TC 47313 TC	
32		48020 EE								

Appendix D

RLC Charging Matlab Codes

The MATLAB code shown below was used to simulate the characteristic behaviour of the RLC circuit.

simulation for a single 12 V battery charging a 310 F capacitor with varying m, L and fixed n, C, R. Observe the changes in time for the capacitor to reach V_c, total energy lost in the resistor, E_R and Energy stored in the inductor E_L.

```
clear all

n = 0.3;
VC = 2.7;      % V
R = 0.05;     % ohm
C = 310 ;      %
L_set = linspace (0.01, 0.2, 41); % H
m_set = linspace (1.1, 2, 40);
dt = .01;     % s
T = 150;        % s, total time
N = floor(T/dt); % maximun number of update steps

[v_R, v_L, v_C, i, h] = deal(NaN (length(m_set), length(L_set),
 N));
time = (0:N-1)*dt;
[w_R, w_R_RC, w_L, w_C, RLC_eff, RC_eff, T, TN] = deal(NaN
(length(m_set), length(L_set)));
```

loop through the range of inductor values, L and source factors, m

```
for k = 1 : length(L_set)
L = L_set(k);
for x = 1 : length(m_set)
m = m_set(x);
```

Initial conditions: starting current is zero, voltage across the resistor is zero, capacitor is having the start-up charge and the net voltage of the loop is acting across the inductor to cause the current rise

```
i(x,k,1) = 0;
h(x,k,1) = (m-n)*VC/L;
state = [ i(x,k,1) ; h(x,k,1)];
v_R(x,k,1) =  0;
v_C(x,k,1) =  n*VC;
params = [ R L C ];
```

The function for the derivatives

```
function [ deriv ]= RLC_dot( state, params )
i = state(1);
h = state(2); [ R l C ] = deal( params(1), params(2), params(3));

dh_dt = (-1/l)*(R*h + i/C);
deriv = [ h ; dh_dt];
end
```

Integration

```
for j = 2:N
reached_threshold = false;
state = state + RLC_dot( state, params )*dt;
[ i(x,k,j), h(x,k,j) ] = deal (state(1) , state(2));
v_R(x,k,j) = i(x,k,j)*R;
v_L(x,k,j) = h(x,k,j)*L;
v_C(x,k,j) = m*VC - v_R(x,k,j) -  v_L(x,k,j);

if v_C(x,k,j) > VC
reached_threshold = true;
break;
end

end % j loop
```

Find time, T, at which the capacitor is fully charged, for each m, L pair

```
v_C_k_x1 = v_C(x,k,:);
v_C_k_x = v_C_k_x1(:)-VC;
zc_set = find(v_C_k_x(1:end-1).*v_C_k_x(2:end)< 0);


% set up the time base for jj steps
time = [0:N-1]*dt;
roots = [];
% linear interpolation to find the first zero cross
for jj = 1 : length(zc_set)
zc = zc_set(jj);
t_zero = ((v_C_k_x(zc)*time(zc+1)) +...
v_C_k_x(zc+1)*time(zc))  /...
(v_C_k_x(zc)  +  v_C_k_x(zc+1));
roots = [roots; t_zero];
end % jj loop

% store value in T matrix (L_set X m_set)
T(x,k) = roots(1);
```

Find the enrgy lost in the resistor by calculating the area under the i^2R curve

```
i_k_x1 = i(x, k, :);
i_k_x = i_k_x1(:);
w_R1 = cumsum(R*(i_k_x.^2))*dt;
% ZC_1 is the first zero crossing
ZC_1 = zc_set(1);

w_R(x,k) = w_R1(ZC_1);
```

Calculate the enrgy stored in the inductor and the capacitor

```
w_L1 = 0.5*L*((i_k_x(ZC_1))^2);
w_L(x, k) = w_L1;
w_C(x, k) = 0.5*C*VC^2*(1-n^2);
```

Calculate the efficiency of the charging scheme assuming 75% of the stored inductor energy can be reused

```
RLC_eff(x, k) =  100*( 0.75*w_L(x, k) + w_C(x, k))/ ( w_L(x, k) +
w_C(x, k)+ w_R(x,k));


end % x loop for (m_set)

end % k loop for (L_set_)
```

Generate the 3-D plots

```
FS = 14;
figure(1); clf;
[L, M] = meshgrid (L_set, m_set);

subplot(3,1,1)
mesh(L, M,  T); colorbar
axis xy; axis tight;
xlabel('L (Inductor)', 'fontsize', FS);
ylabel('m (Source factor)', 'fontsize', FS);
zlabel('T (Time to charge)', 'fontsize', FS);

subplot(3,1,2)
mesh(L, M,  w_R); colorbar
axis xy; axis tight;
xlabel('L (Inductor)', 'fontsize', FS);
ylabel('m (Source factor)', 'fontsize', FS);
zlabel('E_R (Resistor energy loss)', 'fontsize', FS);

subplot(3,1,3)
mesh(L, M,  w_L);colorbar
axis xy; axis tight;
xlabel(' L (Inductor)', 'fontsize', FS);
ylabel('m (Source factor)', 'fontsize', FS);
zlabel('E_L (stored energy in the inductor)', 'fontsize', FS);
```

Appendix E

Microcontroller program

For the prototype fast SC charger, an 8-bit PIC 16F684 microcontroller was used. To avoid capacitor overcharging, both capacitor voltages need to be monitored. The microcontroller will control charging time by adjusting the duty cycle of the control signal. The control signal also maintain a voltage balance for the two halves of the SC bank when they are charging. This assumes the SC bank being charged is having a centre tap resulting in two equal sized SC banks.

Figure E.1 shows the pin assignment of the microcontroller. Pin 12 & 13 are analogue inputs used to monitor the two SC bank voltages. An analogue to digital converter processes the signal into digital form and controls the PWM output by using a simple compare function. The LED lights indicate the charging state. Some other analogue inputs are reserved for current and temperature monitoring in future work. The microcontroller code is given below.

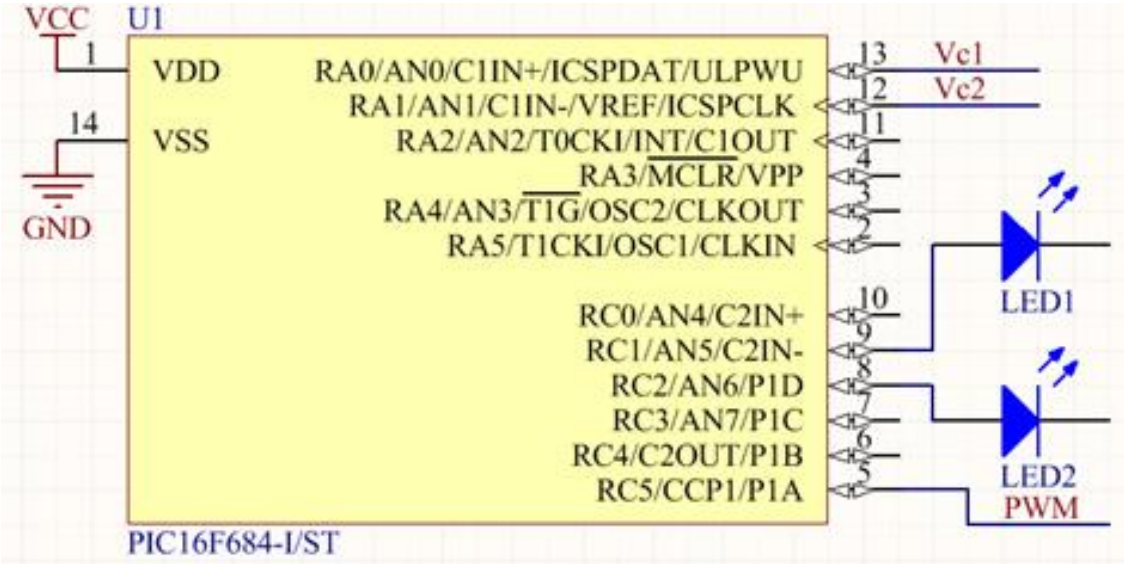

Figure E.1: Pin usage for the PIC microcontroller

```
#include<pic.h>
#include<stdlib.h>
#define u16 unsigned short int
#define clrwdt() asm("CLRWDT")
__CONFIG( INTIO & WDTDIS & MCLRDIS & BOREN&UNPROTECT&PWRTEN);
u16 val,v1,v2,mag,adch1,adcl1,SC1_vol,SC2_vol;
void init(void)
{
    PORTA = 0x00;
    TRISA = 0x03;
    PORTC = 0x00;
    TRISC = 0x00;
    CMCON0 = 0x07;
    ANSEL = 0x03;
    ADCON0 = 0b10000001; //pin3,4,5 (000 AN0) (001 AN1)
    T1CON = 0x15;
    T2CON = 0x1e;
    CCP1CON=0x3c;
    T2CON = 0b00000100; //00:1  01:4  10:16
    PR2 = 0xFe;
    CCPR1L=0;
}
//ADC read transfer the analog signal (SC voltage) to digital
void adc_read(void)
{
    GODONE = 1;
    while(GODONE ==1){;}  //Wait until ADC finished
    v1 = ADRESL + 256 * ADRESH;
    return;
}

void main()
{
    init();
    SC1_vol = SC2_vol = 0;
    while(1)
    {
        //change the ADC channel and read and store the SC voltage
        ADCON0 = 0b10000001;
```

```
        adc_read();
        SC1_vol = v1;
        ADCON0 = 0b10000101;
        adc_read();
        SC2_vol = v1;
        //Do the voltage comparison and control PWM duty cycle
        if((SC1_vol > 112) || (SC2_vol > 112) )
        {
            CCPR1L= 255;
            RC0 = 1;
            RC1 = 0;
        }
        else
        {
            CCPR1L = 127;
            RC0 = 0;
            RC1 = 1;
        }
    }
}
```

References

[1] N. Kularatna and L. Fernando, "High current voltage regulator," 15 2011, U.S. Patent 7 907 430.

[2] T. Wickramasinghe, N. Kularatna, and D. A. Steyn-Ross, "An extra-low-frequency RS-SCALDO technique: A new approach to design voltage regulator modules," in *Applied Power Electronics Conference and Exposition (APEC), 2015 IEEE*, March 2015, pp. 2039–2043.

[3] ——, "Supercapacitor-based DC-DC converter technique for DC-microgrids with UPS capability," in *DC Microgrids (ICDCM), 2015 IEEE First International Conference on*, June 2015, pp. 119–123.

[4] N. Kularatna and L. Fernando, "Power and telecommunication surge protection apparatus," 21 2014, N.Z. Patent 604332.

[5] J. Fernando, N. Kularatna, H. Round, and S. Talele, "Implementation of the supercapacitor-assisted surge absorber SCASA technique in a practical surge protector," in *Industrial Electronics Society, IECON 2014 - 40th Annual Conference of the IEEE*, Oct 2014, pp. 5191–5195.

[6] N. Kularatna, L. Tilakaratne, and P. Kumaran, "Design approaches to supercapacitor based surge resistant ups techniques," in *IECON 2011 - 37th Annual Conference on IEEE Industrial Electronics Society*, Nov 2011, pp. 4094 – 4099.

[7] N. Kularatna, A. Gattuso, N. Gurusinghe, and J. Du Toit, "Pre-stored supercapacitor energy as a solution for burst energy requirements in domestic in-line fast water heating systems," in *proc of IECON 2014, USA, NOV.* IEEE, 2014.

[8] N. Kularatna, K. Milani, and W. Round, "Supercapacitor energy storage in solar application: A design approach to minimize a fundamental loss issue by partitioning the load and the storage device," in *Industrial Electronics (ISIE), 2015 IEEE 24th International Symposium on*, June 2015, pp. 1308–1312.

[9] J. Permenter, "Insulated hot water storage tank for sink," Feb. 2 2004, U.S. Patent 10 788 150.

[10] D. Fazekasr, "Control means and process for domestic hot water recirculating," May 24 1984, U.S. Patent 06613452.

[11] O. Laing, "Water delivery system and method for making hot water available in domestic hot water installation," Apr. 11 2013, U.S. Patent 20130279891.

[12] "Seisco supercharger water heating models owners manual," http://media.wix.com/ugd/152e44_0b390d12ab584f7f96d2a9bbaf106a0e.pdf, p. 8, accessed: 2016-8-11.

[13] "Mini series point-of-use tankless electric water heaters," http://www.stiebel-eltron-usa.com/sites/default/files/pdf/brochure-mini.pdf, p. 4, accessed: 2016-8-11.

[14] "Rheem tankless electric water heaters," http://cdn.globalimageserver.com/fetchdocument-rh.aspx?name=rte-3-tankless-electric-brochure, p. 4, accessed: 2016-8-11.

[15] J. T. Salihi, "1974 energy requirements for electric cars and their impact on electric power generation and distribution systems," *Industry Applications, IEEE Transactions on*, vol. IA-20, no. 4, pp. 1095 – 1095, July 1984.

[16] "Residual current operated circuit breakers without integral overcurrent protection for household and similar uses RCCBs - part 1," 2011, AS/NZS 61008.1:2011.

[17] "Particular requirement for instantaneous water heaters," 2004, AS/NZS 60335.2.35:2004.

[18] D. Obey, *American Recovery and Reinvestment Act of 2009*. Public Law No: 111-5. [online]. Available: http://frwebgate.access.gpo.gov/cgi-bin/getdoc.cgi?dbname=111 cong public laws&docid=f:publ005.pdf, Feb 2009.

[19] D. Ragone, "Review of battery systems for electrically powered vehicles," in *SAE Technical Paper 680453*, Feb 1968, p. 9.

[20] M. Glavin, P. Chan, S. Armstrong, and W. Hurley, "A stand-alone photovoltaic supercapacitor battery hybrid energy storage system," in *13th Power Electronics and Motion Control Conference*, Sept 2008, pp. 1688–1695.

[21] D. Murray and J. Hayes, "Cycle testing of supercapacitors for long-life robust applications," *Power Electronics, IEEE Transactions on*, vol. 30, no. 5, pp. 2505–2516, May 2015.

[22] J. Fernando and N. Kularatna, "Supercapacitors for distributed energy storage in DC microgrids and loads," in *DC Microgrids (ICDCM), 2015 IEEE First International Conference on*, June 2015, pp. 339–342.

[23] J. Fernando, N. Kulatana, and K. Kankanamge, "Indirect applications of supercapacitor energy storage capabilities and characterisation required," in *Industrial Electronics (ISIE), 2013 IEEE International Symposium on*, May 2013, pp. 1–6.

[24] L. Shi and M. Crow, "Comparison of ultracapacitor electric circuit models," in *Power and Energy Society General Meeting - Conversion and Delivery of Electrical Energy in the 21st Century*, July 2008, pp. 1–6.

[25] R. de Levie, "On porous electrodes in electrolyte solutions," *Electrochemica Acta: Pergamon press Ltd.: Nothern Ireland*, vol. 8, pp. 751–780, 1963.

[26] S. Buller, E. Karden, D. Kok, and R. De Doncker, "Modeling the dynamic behavior of supercapacitors using impedance spectroscopy," *Industry Applications, IEEE Transactions on*, vol. 38, no. 6, pp. 1622–1626, Nov 2002.

[27] A. R. Hippel, "Dielectrics and waves," in *John Willey and Sons*, 1954.

[28] "IEEE recommended practice for the characterization and evaluation of emerging energy storage technologies in stationary applications," *IEEE Std 1679-2010*, pp. 1–38, Oct 2010.

[29] "IEEE recommended practice for sizing nickel-cadmium batteries for photovoltaic (pv) systems," *IEEE Std 1144-1996*, pp. i–, 1997.

[30] "Recommended charging equation and preventive maintenance procedures for rolls batteries," p. 28, 2015, Surrette Battery Co., Canada.

[31] "A white paper from the experts in business-critical continuity - capacitors age and capacitors have an end of life," http://www.emersonnetworkpower.com/documentation/en-US/Services/Market/Data-Center/Documents/LS%20Literature/White%20Paper/Capacitors-Age-and-Capacitors-Have-an-End-of-Life-WP-SL-24630.pdf, p. 12, accessed: 2016-8-11.

[32] W. Moungngam, R. Songprakorp, K. Chomsuwan, and T. Phatrapornnant, "Applied supercapacitor to energy storage during regenerative brake state in electric vehicle," in *Electrical Engineering/Electronics, Computer, Telecommunications and Information Technology (ECTI-CON), 2014 11th International Conference on*, May 2014, pp. 1–6.

[33] X. Shen, S. Chen, G. Li, Y. Zhang, X. Jiang, and T. T. Lie, "Configure methodology of onboard supercapacitor array for recycling regenerative braking energy of URT vehicles," *Industry Applications, IEEE Transactions on*, vol. 49, no. 4, pp. 1678–1686, July 2013.

[34] Y. Baghzouz, J. Fiene, J. Van Dam, L. Shi, E. Wilkinson, and R. Boehm, "Modifications to a hydrogen/electric hybrid bus," in *Energy Conversion Engineering Conference and Exhibit, 2000. (IECEC) 35th Intersociety*, vol. 1, 2000, pp. 363–370.

[35] S.-M. Kim and S.-K. Sul, "Control of rubber tyred gantry crane with energy storage based on supercapacitor bank," *Power Electronics, IEEE Transactions on*, vol. 21, no. 5, pp. 1420–1427, Sept 2006.

[36] Z. Yang, H. Xia, B. Wang, and F. Lin, "An overview on braking energy regeneration technologies in chinese urban railway transportation," in *Power Electronics Conference (IPEC-Hiroshima 2014 - ECCE-ASIA), 2014 International*, May 2014, pp. 2133–2139.

[37] G. Baoming, A. de Almeida, and F. Ferreira, "Supercapacitor-based optimum switched reluctance drive for advanced electric vehicles," in *Electrical Machines and*

Systems, 2005. ICEMS 2005. Proceedings of the Eighth International Conference on, vol. 1, Sept 2005, pp. 822–827.

[38] J. Wang, B. Taylor, Z. Sun, and D. Howe, "Experimental characterization of a supercapacitor-based electrical torque-boost system for downsized ICE vehicles," *Vehicular Technology, IEEE Transactions on*, vol. 56, no. 6, pp. 3674–3681, Nov 2007.

[39] R. Carter, A. Cruden, and P. Hall, "Optimizing for efficiency or battery life in a battery/supercapacitor electric vehicle," *Vehicular Technology, IEEE Transactions on*, vol. 61, no. 4, pp. 1526–1533, May 2012.

[40] A. Burke, "Ultracapacitor technologies and application in hybrid and electric vehicles," *International Journal of Energy Research*, 2009.

[41] A. Kuperman, I. Aharon, S. Malki, and A. Kara, "Design of a semiactive battery-ultracapacitor hybrid energy source," *IEEE Transactions on Power Electronics*, vol. 28, no. 2, pp. 806–815, Feb 2013.

[42] A. Pernia, S. Menendez, M. Prieto, J. Martinez, F. Nuno, I. Villar, and V. Ruiz, "Power supply based on carbon ultracapacitors for remote supervision systems," *Industrial Electronics, IEEE Transactions on*, vol. 57, no. 9, p. 31393147, Sep 2010.

[43] T. Ratniyomchai, S. Hillmansen, and P. Tricoli, "Recent developments and applications of energy storage devices in electrified railways," *Electrical Systems in Transportation, IET*, vol. 4, no. 1, pp. 9–20, March 2014.

[44] C. Tuck, "Modern battery technology," *Ellis Howard Limited, NewYork*, pp. 213 – 218, 1991.

[45] H. Catherino and F. Feres, "Sulfation as applied to lead-acid batteries: the myth and the reality, in: Proceedings of the fifth international conference on lead acid batteries," in *Proceedings of the Fifth International Conference on Lead Acid Batteries, Varna, Bulgaria, 1013 June*, 2002, pp. 197 –200.

[46] H. Catherino, F. Feres, and F. Trinidad, "Sulfation in lead acid batteries," *Journal of Power Sources*, vol. 129, no. 1, pp. 113 – 120, 2004.

[47] A. Kuperman and I. Aharon, "Batteryultracapacitor hybrids for pulsed current loads: A review," *Renew. Sust. Energy Rev.*, vol. 15, p. 981 992, Feb 2011.

[48] J. Zheng, T. Jow, and M. Ding, "Hybrid power sources for pulsed current applications," *IEEE Trans. Aerosp. Electron. Syst.*, vol. 37, no. 1, pp. 288 – 292, Jan 2001.

[49] M. Pagano and L. Piegari, "Hybrid electrochemical power sources for onboard applications," *IEEE. Trans. Energy Convers.*, vol. 22, no. 2, pp. 450 – 456, Jun 2007.

[50] J. Moreno, M. Ortuzar, and J. Dixon, "Energy management system for a hybrid electric vehicle using ultracapacitors and neural networks," *IEEE Trans. Ind. Electron.*, vol. 53, no. 2, pp. 614 – 623, Apr 2006.

[51] M. Camara, H. Gualous, F. Gustin, and A. Berthon, "Design and new control of DC/DC converters to share energy between supercapacitors and batteries in hybrid vehicles," *IEEE Trans. Veh. Technol.*, vol. 57, no. 5, pp. 2721 –2735, Sep 2008.

[52] ——, "DC/DC converter design for supercapacitor and battery power management in hybrid vehicle applications polynomial control strategy," *IEEE Trans. Ind. Electron.*, vol. 57, no. 2, pp. 587 –597, Jan 2010.

[53] N. Kularatna, *Energy Storage Devices for Electronic Systems: Rechargeable Batteries and Supercapacitors*. Elsevier Academic Press, 2014, pp. 165 - 168.

[54] A. Schneuwly and R. Gallay, "Properties and applications of supercapacitors from the state-of-the-art to future trends," in *Proc of PCIM, USA*, 2000.

[55] S. Lu, P. Weston, S. Hillmansen, H. Gooi, and C. Roberts, "Increasing the regenerative braking energy for railway vehicles," *Intelligent Transportation Systems, IEEE Transactions on*, vol. 15, no. 6, pp. 2506–2515, Dec 2014.

[56] T.-S. Kwon, S.-W. Lee, S.-K. Sul, C.-G. Park, N.-I. Kim, B. il Kang, and M. seok Hong, "Power control algorithm for hybrid excavator with supercapacitor," *Industry Applications, IEEE Transactions on*, vol. 46, no. 4, pp. 1447–1455, July 2010.

[57] S. Werkstetter, "Existing and future ultracapacitor-applications in the renewable energy market," in *PCIM Europe 2014; International Exhibition and Conference for Power Electronics, Intelligent Motion, Renewable Energy and Energy Management; Proceedings of*, May 2014, pp. 1–7.

[58] "ABB miniature circuitbreakers index 1sxu000023c0202 reva15," www.abb.us/lowvoltage, accessed: 2015-11-11.

[59] U. Madawala, D. Thrimawithana, and N. Kularatna, "An ICPT-supercapacitor hybrid system for surge-free power transfer," *Industrial Electronics, IEEE Transactions on*, vol. 54, no. 6, pp. 3287–3297, Dec 2007.

[60] N. Kularatna, J. Fernando, A. Pandey, and S. James, "Surge capability testing of supercapacitor families using a lightning surge simulator," *Industrial Electronics, IEEE Transactions on*, vol. 58, no. 10, pp. 4942 – 4949, Oct 2011.

[61] R. Bodnar and W. Redman-White, "An integrated ultracapacitor fast mains charger with combined power/current optimisation," in *ESSCIRC (ESSCIRC), 2013 Proceedings of the*, Sept 2013, pp. 161–164.

[62] ——, "A 250W/30A fast charger for ultracapacitors with direct mains connection," in *Circuit Theory and Design (ECCTD), 2011 20th European Conference on*, Aug 2011, pp. 813–816.

[63] G. Thrap, "Switching power supply," 2005, US Patent 6,912,136.

[64] H. Ryoo, S. Jang, Y. Jin, J. Kim, Y. Kim, S. Ahn, J. Gong, B. Lee, and D. Kim, "Design of high voltage capacitor charger with improved efficiency, power density and reliability," *Dielectrics and Electrical Insulation, IEEE Transactions on*, vol. 20, no. 4, pp. 1076–1084, August 2013.

[65] F. Musavi, M. Edington, W. Eberle, and W. Dunford, "Evaluation and efficiency comparison of front end AC-DC plug-in hybrid charger topologies," *Smart Grid, IEEE Transactions on*, vol. 3, no. 1, pp. 413–421, March 2012.

[66] F. Musavi, W. Eberle, and W. Dunford, "A high-performance single-phase bridgeless interleaved PFC converter for plug-in hybrid electric vehicle battery chargers," *Industry Applications, IEEE Transactions on*, vol. 47, no. 4, pp. 1833–1843, July 2011.

[67] *Design equations of high-power-factor flyback converters based on the L6561*, STMicroelectronics, Sep 2003.

[68] A. V. D. Bossche and V. C. Valchev, *Inductors and Transformers for Power Electronics*. CRC press, 2005.

[69] "Section 2: Magnetic core characteristics," www.ti.com/lit/ml/slup124/slup124.pdf, accessed: 2015-11-11.

[70] "Ferrite core material selection guide," www.mag-inc.com, accessed: 2015-11-11.

[71] S. Maniktala, *Switching Power Supply Design and Optimization*, 1st ed., 2005.

[72] "Application note AN-1024," www.irf.com/technical-info/appnotes/an-1024.pdf, accessed: 2015-11-11.

[73] "Magnetics ferrite cores 2013 catalogue," http://www.mag-inc.com, accessed: 2015-11-11.

[74] *How to deal with Leakage Elements in Flyback Converters*, ON Semiconductor, Sep 2005.

[75] K. Billings, *Switch Mode Power Supply Handbook*. New York:McGraw-Hill, 1989.

[76] "Reference design report for a 35 W power supply using $TOPSwitch^{TM}$ – $HXTOP258PN$," www.mouser.com/ds/2/328/rdr142-472704.pdf, accessed: 2015-11-11.

[77] J. Turchi, D. Dalal, P. Wang, and L. Jenk, *Power Factor Correction (PFC) Handbook*. ON Semiconductor, 2014.

[78] O. Garcia, J. Cobos, R. Prieto, P. Alou, and J. Uceda, "Single phase power factor correction: a survey," *Power Electronics, IEEE Transactions on*, vol. 18, no. 3, pp. 749–755, May 2003.

[79] S. Basu and M. Bollen, "A novel common power factor correction scheme for homes and offices," *Power Delivery, IEEE Transactions on*, vol. 20, no. 3, pp. 2257–2263, July 2005.

[80] "PFC boost converter design guide," www.infineon.com, accessed: 2015-11-11.

[81] "ESD-SCAP electric storage device-samwha capacitor," http://www.samwha.co.kr/SW_catalogue/ecatalog.asp?Dir=113, p. 7, accessed: 2016-8-11.